Synthesis, Characterisation and Cytotoxicity Evaluation of Novel Polymeric Carriers for Polymer Therapeutics: From Free Radical Polymerisation to Atom Transfer Radical Polymerisation

Lucile Dieudonné

A thesis submitted to Cardiff University in accordance with the requirements for the degree of Doctor of Philosophy

Centre for Polymer Therapeutics
Welsh School of Pharmacy
Cardiff University

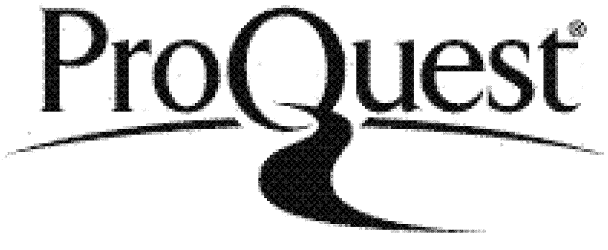

ProQuest LLC
789 East Eisenhower Parkway
P.O. Box 1346
Ann Arbor, MI 48106-1346

Signed ..... (candidate)

Date ..... 28/04/08 .....

STATEMENT 1

This thesis is being submitted in partial fulfillment of the requirements for th
of PhD.

Signed ..... (candidate)

Date ..... 28/04/08 .....

STATEMENT 2

This thesis is the result of my own independent work/investigation, excep
otherwise stated. Other sources are acknowledged by explicit references.

Signed ..... (candidate)

Date ..... 28/04/08 .....

STATEMENT 3

I hereby give consent for my thesis, if accepted, to be available for photocop
for inter-library loan, and for the title and summary to be made available to
organisations.

Signed ..... (candidate)

Date ..... 28/04/08 .....

À mon père

Acknowledgements

First, I would like to thank my supervisor Dr. Dirk Schmaljohann for his guidance and advice through these three years. All my gratitude goes to my deputy advisor, Prof. Ruth Duncan for her precious help, time, professionalism and support throughout my PhD and especially towards the end. Special thanks go to Dr. María Jesús Vicent who offered me all her support, time and energy for completing this thesis.

Thanks are due to the Centre for Polymer Therapeutics (CPT) and the Welsh School of Pharmacy for funding this study, to Elaine Ferguson for teaching me tissue culture, to James Rickard and Michael Rafael for their help in the copolymerisation with Chain Transfer Agent and linear Atom Transfer Radical Polymerisation studies.

I would also like to thank all my CPT colleagues. Thanks go to Janette for taking care of the labs and us, to little Wendy for being always helpful and available, to Neal, Michelle and Junior for their help with the labs, but also for always having listened and cheered me up. Many thanks are due to those who like me went through joyful and hard time: Helena, the sweet Sali, Zeena, Kerri, Cath and Sian, the repair-everything-Tom, the dynamic and cheerful Philipp, the always-hopeful-Kaz, the super efficient and energic Elaine and the reasurring and calming Sam*ish*. Many thanks to our hard-working and fun ex- and current post-docs: María Jesús, Nathalie, Maria Manunta, Lorella, Manuella, Alison, and Jing. Also, I would like to thank Arwyn for sharing his points of view on life, literature, "Welshitude", beer and rugby, as well as his international students who turned out to become great friends: Davide, Verena, Marjan and her other half, Emiel. I also had the chance to find support and make good friends outside work: many thanks to Felice, Shyam, Gian Luigi, Mireille and her African peaceful vibes. A huge thank you goes to my four special Cardiff men: Jacques, Jérome, Abdel and Dan with whom I shared so much, and to Fran for having from day one to the end, helped, listened, cried and laughed with me!

My list of thank you does not stop here as I had the fortune of finding support and friendship in Valencia, and all my gratitude goes to those who welcomed me, shared their time and shoulders, and accepted me with all my stress and discouragements here: "muchísimas gracias a" my dear María, fun Gonzalo, comforting Pili, tolerant Laura and brain-stimulating Juan. Thanks also go to all my new and sweet colleagues of Polimeros terapeuticos: Fabiana, Vanessa, Inma, Puri,

Amparo and Maria Helena and all the people I know from El Centro de Investigacion Principe Felipe and had to deal with my slow loss of sanity, in particular Carmen, Susana, Eliana, Ana, Mar, Ali, David, Béa, Imelda, Sergio, Pilar, Eva, Samuel, Alfredo, Léo, Jordi, Edu, François, Pau, Anita and Nuria.

Of course even if living abroad is invigorating and can broaden your mind, it can be very difficult and lonely especially if you loose the contact with your origins. I will always be grateful for the help and love of my French friends Choupinou, Maud, Blandine, Nicola, Nico B., La petite, Marie, and Mimile, and would like to apologise for being the cause of their new expensive phone bills...

And finally, the biggest thank you of all naturally goes to my family: my loving mum, my beautiful sisters, their patient partners and my adorable nephews. They have always backed me up in my choice of life, listened and encouraged and never doubted that I was able to put a final dot to this project. Thank you very much to all!

Abstract

Polymer therapeutics include water-soluble polymers designed as carriers for drugs, proteins or DNA. Over the last two decades, they have found increasing clinical use against cancer and other diseases. A growing number is in clinical trials or on the market. However, the polymers used so far have limitations including heterogeneity in structure, molecular weight, polydispersity, drug carrying capacity, lack of control of architecture and biodegradability of polymer backbone. Therefore, the aim of this study was to synthesise and characterise a library of linear/star homo/copolymers with potential for further development as second-generation polymer therapeutics.

Atom Transfer Radical Polymerisation (ATRP) and (chain transfer agent - CTA) Free Radical Polymerisation (FRP) techniques were used to synthesise water-soluble amine-based acrylamide and methacrylate homo/copolymers. Nuclear magnetic resonance, gel permeation chromatography, infrared and titration were used for characterisation. *In vitro* cytotoxicity studies of the polymers towards a murine melanoma cell line were performed using a cell viability evaluating colorimetric assay.

Molecular weights (from 3 000 to 550 000 $g.mol^{-1}$) were successfully adjusted by varying either the initiator or CTA to monomer ratios. Semitelechelic homo/copolymers with either carboxylic acid or hydroxyl termini were obtained using mercapto-based CTA. Either stable or degradable star-shaped poly(dimethylaminoethyl methacrylate) were obtained by copper-mediated ATRP using previously synthesised multifunctional initiators (4, 5 or 8 initiating moieties). A linear increase of predictable molecular weight with monomer conversion and narrow polydispersity (1.3) were observed. Amongst other molecular parameters systematically tested, the amount of cationic residues had the most striking effect on the cell viability.

To conclude, conditions were optimised for the synthesis of a library of water-soluble amine-based homo/copolymers with different molecular weight, composition, charge density and architecture using several polymerisation techniques. Preliminary evaluation of polymer cytotoxicity associated to molecular parameters is vital for intelligently designing future, novel, and biocompatible polymeric carriers.

Index

List of Figures & Schemes

Chapter 1:

Chapter 2:

Chapter 3:

Chapter 4:

Chapter 5:

Chapter 6:

Chapter 7:

Chapter 8:

List of Tables

Chapter 1:

Chapter 2:

Chapter 3:

Chapter 4:

Chapter 5:

Chapter 6:

Abbreviations and symbols

A-

Abs:	Absorbance
ACA:	4,4'-azobis(4-cyanopentanoic acid)
ACN:	Acetonitrile
AEM:	2-aminoethylmethacrylate
AFM:	Atomic Force Microscopy
AIBN:	2,2'-azobis(isobutyronitrile)
AIDS:	Acquired ImmunoDefficiency Syndrome
ANOVA:	Analysis of variance
atm:	Atmosphere
ATRA:	Atom Transfer Radical Addition
ATRP:	Atom Transfer Radical Polymerisation

B-

B16F10 cells:	Murine melanoma cell line
BHT:	2,6-di-*tert*-butyl-4-methylphenol
BOC-APAAm:	*N*-tert-butoxycarbonyl-*N'*-acryloyl-1,3-diaminopropane
bs:	Broad singlet (^{1}H-NMR)

C-

C_{tr}:	Chain transfer constant
Cat:	Catalyst
$CDCl_3$:	Deuterated chloroform
^{13}C-NMR:	Carbon nuclear magnetic resonance
CPT:	Centre for Polymer Therapeutics
CRP:	Controlled Radical Polymerisation
CTA:	Chain Transfer Agent
Cu(I)Br:	Copper (I) bromide
(Co)polymerisation:	Refers to both homo and copolymerisations
Copolymerisation:	Refers to the polymerisation of two monomers or comonomers

D-

d:	Doublet (^{1}H-NMR)
DAB:	Poly(propyleneimine) dendrimer with a diaminobutane core
DAB-Am-4:	Polypropylenimine tetraamine dendrimer, generation 1, 4-amino surface group
DAB-Am-8:	Polypropylenimine octaamine dendrimer, generation 2, 8-amino surface group
DAE:	Poly(propyleneimine) dendrimer with a diaminoethane core
DCC:	Dicyclohexylcarbodiimide
DCU:	*N,N'*-dicyclohexyl urea
ddH_2O:	Double distilled water
DMAEM:	*N,N'*-Dimethylaminoethyl methacrylate
DMAP:	4-(dimethylamino)pyridine
DMF:	*N,N*-Dimethylformamide
DMSO:	Dimethyl sulfoxide
DMSO-d_6:	Deuterated dimethyl sulfoxide
DNA:	Deoxyribonucleic acid
D_2O:	Deuterated water

E-

EA:	Elementary analysis
EDTA:	Ethylenediaminetetraacetic acid

EPR: Enhanced Permeability and Retention effect
EU: European Union
eq: Equivalent

F-
f: Functionality or function
FBS: Foetal bovine serum
FRP: Free Radical Polymerisation
FT-IR: Fourier Transform Infra-Red
FT-Raman: Fourier Transform Raman

G-
G0: Generation zero
G1: Generation one
G2: Generation two
Gly-Phe-Leu-Gly: Glycine-Phenylalanine-Leucine-Glycine
GPC: Gel Permeation Chromatography

H-
h: hour
HCl: Hydrochloric acid
HIV: Human Immunodefficiency Virus
HMTETA: 1,1,4,7,10,10-Hexamethyltriethylenetetramine
^{1}H-NMR: Proton nuclear magnetic resonance
Homopolymerisation: Strictly refers to the polymerisation of one monomer
HOSu: *N*-hydrosuccinimide
HPLC: High-performance liquid chromatography
HPMA: *N*-Hydroxypropylmethacrylamide

I-
I: Initiator
IC_{50}: Concentration of a drug required for 50% inhibition *in vitro*
INIFERTER: INItiator-transFER-agent-TERminator
IR: Infra-Red

J-
J: Coupling constant (^{1}H-NMR)

L-
LDH: Lactate dehydrogenase
Lig: Ligand
LOQ: Level of Quantification

M-
m: Multiplet (^{1}H-NMR)
M: Monomer
MaI: Macroinitiator
MALDI-TOF: Matrix-Assisted Laser Desorption/Ionization time of flight
ME: 2-Mercaptoethanol
min: Minutes
M_n: Number-average molecular weight
$M_{n,expected}$: Expected number-average molecular weight (ATRP)
$M_{n,experimental}$: Number-average molecular weight measured by GPC
$M_{n,theoretical}$: Theoretical number-average molecular weight (ATRP)
mol: Moles

m.p.: Melting point
MPA: 3-Mercaptopropionic acid
mPEG: monomethoxy poly(ethylene glycol)
MTT: 3-(4,5-dimethylthiazol-2-yl)-2,5-diphenyl-2H-tetrazolium bromide
MuI: Multifunctional initiator
MuI-DAB-4: DAB dendrimer-based multifunctional initiator with 4 functional moieties
MuI-DAB-8: DAB dendrimer-based multifunctional initiator with 8 functional moieties
MuI-ester-5: Alcohol-based multifunctional initiator with 4 functional moieties
MuI-ester-8: Alcohol-based multifunctional initiator with 4 functional moieties
M_w: Weight-average molecular weight
M_w/M_n: Polydispersity index

N-

N_2: Nitrogen
NA: Not applicable
NADH: Nicotinamide Adenine Dinucleotide
NADPH: Nicotinamide Adenosine Dinucleotide Phosphate
NaOH: Sodium Hydroxide
ND: Non-determined
NIPAAm: *N*-Isopropylacrylamide
NMP: Nitroxide mediated polymerisation
NMR: Nuclear magnetic resonance

P-

PAMAM: Polyamidoamine
PBS: Phosphate buffer saline
PDMAEM: Poly(dimethylamino)ethylmethacrylate
PEG: Poly(ethylene glycol)
PEI: Poly(ethyleneimine)
PEO: Poly(ethylene oxide)
PGA: Poly(glutamic acid)
PHPMA: Poly(*N*-hydroxypropylmethacrylamide)
PK1: HPMA-glycine-phenylalanine-leucine-glycine-doxorubicin copolymer
PK2: HPMA-glycine-phenylalanine-leucine-glycine-doxorubicin copolymer containing galactosamine residues
PLL Poly(lysine)
PMDETA: *N,N,N',N",N"*-pentamethyldiethylenetriamine
PNIPAAm: Poly(*N*-isopropylacrylamide)
ppm: Parts per million
PqAEM: Poly([2-(methacryloyloxy)ethyl] trimethylammonium chloride)
PS: Poly(styrene)
PVP: Poly(vinylpyridinium) salts

Q-

q: Quadruplet (^{1}H-NMR)
qAEM: 2-(methacryloyloxy)ethyl trimethylammonium chloride
qAPAAm: 3-acrylamidopropyl trimethylammonium chloride

R-

RAFT: Reversible Addition Fragmentation Transfer
R_g: Gyration radius
R_h: Hydrodynamic radius

RI:	Refractive index
RMPI:	Rose Park Memorial Institute
ROP:	Ring opening polymerisation
RT:	Room temperature
S-	
s:	Singlet (^{1}H-NMR)
SANS:	Small Angle Neutron Scattering
SCID:	Severe Combined ImmunoDeficiency
SEC:	Size exclusion chromatography
SEM:	Standard error of the mean
SMANCS:	Styrene-*co*-Maleic Anhydride-NeoCarzinoStatin
T-	
t:	Triplet (^{1}H-NMR)
T:	Temperature
THF:	Tetrahydrofuran
TMEDA:	*N,N,N',N'*- tetramethylethylenediamine
TNF:	Tumour Necrosis Factor
U-	
UK:	United Kingdom
UKCCCR:	United Kingdom co-ordinating committee on cancer research
UV:	Ultraviolet
V-	
V_h:	Hydrodynamic volume
X-	
XTT:	Sodium 3,3'-[1[(phenylamino)carbonyl]-3,4-tetrazolim]-*bis*-(4-methoxy-6-nitro) benzene sulfonic acid hydrate)
Symbols-	
[X]:	Concentration of compound X
Σ:	Sum
$\int$:	Integral
δ:	Bending vibrations (IR) or chemical shift (NMR)
$\bar{\nu}$:	Wavenumber (IR)
ν:	Stretching vibrations (IR)
~:	Approximately
μ:	Micro
λ:	Wavelength
3D:	Three-dimension
°C:	Celsius degree
v/v:	Volume per volume
w/v:	Weight per volume
%:	Percent
$X \leq Y$:	X is smaller or equal to Y
$X < Y$:	X is strictly smaller than Y
Δ:	Variation
≠:	Different
$Y = f(X)$	Y is a function of X

1

General Introduction

1.1. General introduction

Thanks to the work of Herman Staudinger in the 1920s, "Polymer Science" was first recognised as a discipline in its own right. Staudinger was later awarded the first Nobel Prize for polymer chemistry in 1953. He initially had to fight to convince others of the existence of polymers as macromolecules, whose monomer units are covalently bound to each other. Many argued that the proposed polymers were simply colloidal systems or aggregates of low molecular weight molecules. During the second half of the 20th century, the polymers found their place in every-day life in many diverse materials. Today they form an "indispensable contribution to the comfort, safety and expansion of our society from astronautic to medicine" (Ringsdorf 2004).

Polymers have become extensively used as biomedical materials such as sutures (Tomihata *et al.* 1998), hip prostheses (De Santis *et al.* 2000; Boesel and Reis 2007), contact lenses (Evans *et al.* 2001; Nicolson and Vogt 2001), and scaffolds for tissue engineering (Barnes *et al.* 2007; Ma 2008). In pharmaceutical industry, they are commonly used as excipients for formulation preparation (Baldrick 2000) and as controlled release systems such as matrices and gels (Sershen and West 2002; Lee and Yuk 2007).

One of the most prevailing subject in pharmaceutical and biomedical fields over the past few decades, has been the development of novel, water-soluble **Polymer Therapeutics** (as defined by Duncan *et al.* (1996)). This subclass of nanomedicines aims to improve existing chemotherapy and the delivery of more complex bioactive agents, which are limited by pharmacokinetics and pharmacological barriers (e.g. proteins and DNA). Polymer therapeutics (reviewed by Duncan (2003b)) are considered by the pharmaceutical community as new chemical entities and encompasses **polymeric drugs** (Gebelein and Carraher 1985; Dhal *et al.* 2002) (5 000-40 000 g.mol^{-1}), **polymer-drug conjugates** (Ringsdorf 1975; Duncan 2003b) (5-15 nm), **polymer-protein conjugates** (Davis 2002; Harris and Chess 2003) (10-20 nm), **polyplexes** (Wagner 2004) (40-60 nm) and **polymeric micelles** to which the drug is covalently bound (Kakizawa and Kataoka 2002) (60-100 nm) as depicted in Figure 1.1.

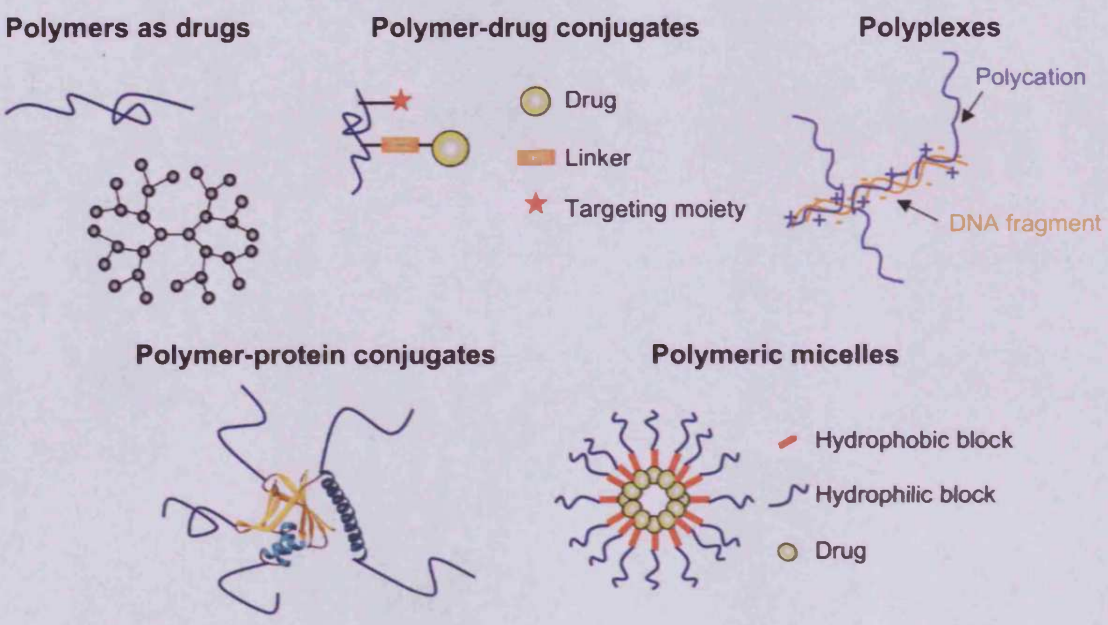

Figure 1.1: Schematic representation of polymer therapeutics (adapted from Duncan (2003b))

In this case, natural or synthetic polymers play an active role as drug delivery system, pro-drugs, drugs or imaging agent, amongst other functions.

Although, it has been criticised both by the scientific and non-scientific communities, and its development was delayed due to the reluctance of the pharmaceutical corporations to look beyond the difficulties involved in characterising polydisperse and macromolecular systems, the field of polymer therapeutics has become very popular in the last decades (Figure 1.2) and offers enormous therapeutic potential (reviewed by Duncan (2004) and Moghimi *et al.* (2005)).

As an attempt to improve the field of polymer therapeutics, this thesis will focus on the synthesis of a library of water-soluble polymers with potential as biocompatible carriers, where molecular weight, pK_a, composition, charge density and architecture are altered, using different polymer chemistry techniques.
This introduction deals with the historical facts of the emergence of the first polymer therapeutics in clinical use, the current understanding of the rationale for their design, as well as the mechanisms of the different synthetic techniques used here, to finally elaborate the aims of each Chapter.

1.2. Polymer therapeutics: the biological rationale

For many, the concept of using water-soluble and synthetic polymers for the delivery of therapeutics first appeared in the mid-70s with the theoretical model of targeted synthetic polymer-drug conjugate (Figure 1.3) developed by Ringsdorf (1975). However, in 1954, Jatzkewitz described the synthesis of a mescaline-*N*-vinylpyrrolidine conjugate attached via non-degradable or enzymatically degradable (glycyl-L-leucine) side chains (Jatzkewitz 1954).

Meanwhile, with the important studies using DNA as the carrier for the delivery of drugs, such as daunorubicin (Trouet *et al.* 1972), it was demonstrated that cellular uptake of macromolecules was limited to endocytosis, and this process could help to achieve "lysosomotropic" delivery of drug (reviewed by De Duve *et al.* (1974)).

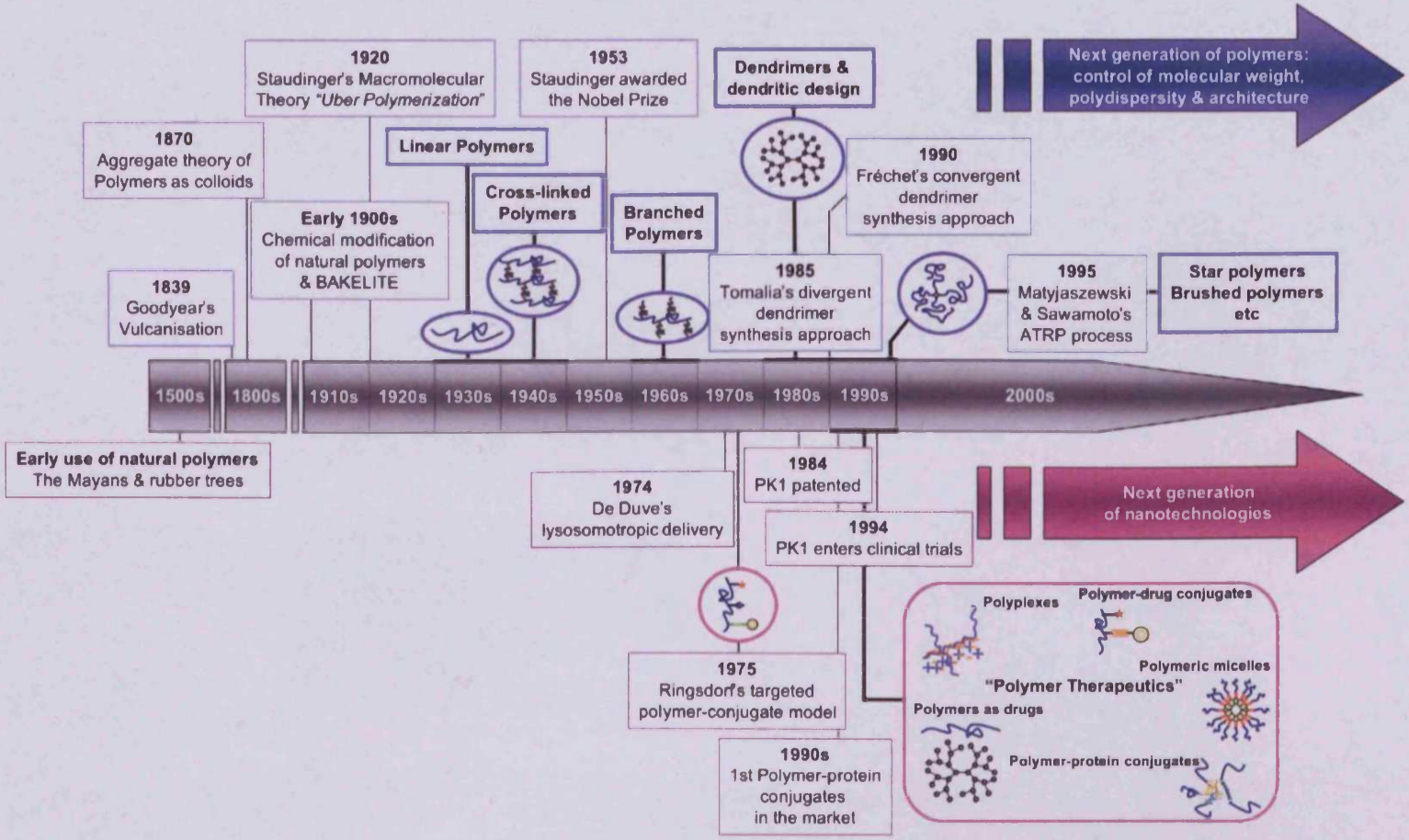

Figure 1.2: Time-scale tracking the developments of polymers and their uses in nanomedicines

Figure 1.3: Ringsdorf's model of polymer-drug conjugates (adapted from Ringsdorf (1975))

Where: is a water-soluble synthetic polymer, is the drug, is the degradable linker, is a targeting moiety and is a solubilizing moiety.

Whereas low molecular weight compounds can easily biodistribute via passive diffusion across cell membranes, cellular uptake of macromolecules is limited to the process of endocytosis. Endocytosis is an important process common to almost all cell types and involves cell membrane invagination for the capture and vesicular internalisation of extracellular molecules, such as proteins, which cannot cross through the hydrophobic plasma membrane (fluid phase endocytosis) (reviewed by Mellman (1996)). In the other hand, receptor-mediated endocytosis occurs when the macromolecule first binds to specific receptors on the cell membrane (e.g. via a targeting moiety) before being internalised in vesicles.

Once internalised, macromolecules are transferred via endosomes (pH ~ 6.0-6.5) to lysosomal compartments, which contain hydrolytic enzymes and a lower pH (pH ~ 5.0 and 5.5) (reviewed by Duncan (2003b)) as depicted in Figure 1.4. Conjugation of therapeutic agents to macromolecules through a linker that only degrades when exposed to these specific lysosomal conditions would allow intracellular release of the drug, which would then passively diffuse through the lysosomal membrane to reach its pharmacological target in the cell.

1.3. Polymer-drug conjugates and passive tumour targeting: the Enhanced Permeability and Retention (EPR) effect

In the late 80s, Maeda and colleagues (Matsumura and Maeda 1986) described the **Enhanced Permeability** and **Retention** (EPR) effect within tumours (also observed in inflammatory tissues). EPR is now used as a passive way of targeting solid tumours tissue for intravenously administered macromolecular drugs. Figure 1.5 schematically represents the EPR process.

Originally, tumours derive from one single genetically modified cell, which grows and multiplies by taking nutritive substances from the surrounding vasculatures. Rapidly, the cancerous mass requires a greater amount of nutrients and oxygen to promote its growth and to meet its needs; it starts producing its own vessels to support its significant growth. This process is known as **Angiogenesis**, a biological process regulated by many different growth factors (reviewed by Folkman and Shing (1992)). The new vessels created by the cancerous mass, possess unique characteristics, and are structurally and architecturally different from normal vessels (e.g. lack of smooth muscle layer cells, looser endothelial cell-cell junctions,

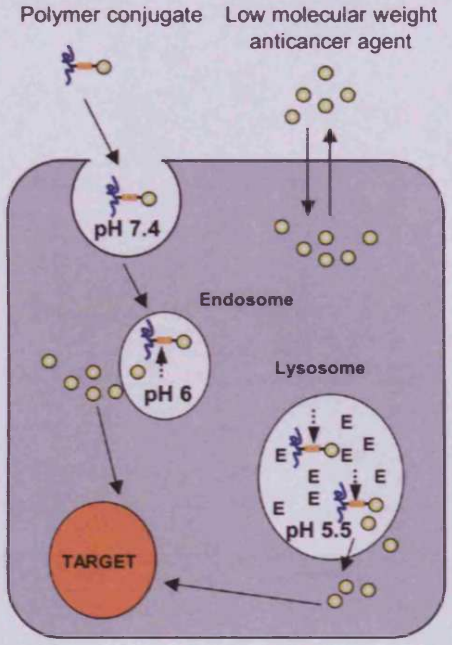

Figure 1.4: Lysosomotropic drug delivery of macromolecular polymer conjugates (adapted from Duncan *et al.* (1996))

Where E are the lysosomal enzymes (e.g. phosphotases, sulphatases, oxidases, hydrolases, peptidases (e.g. cathepsins)).

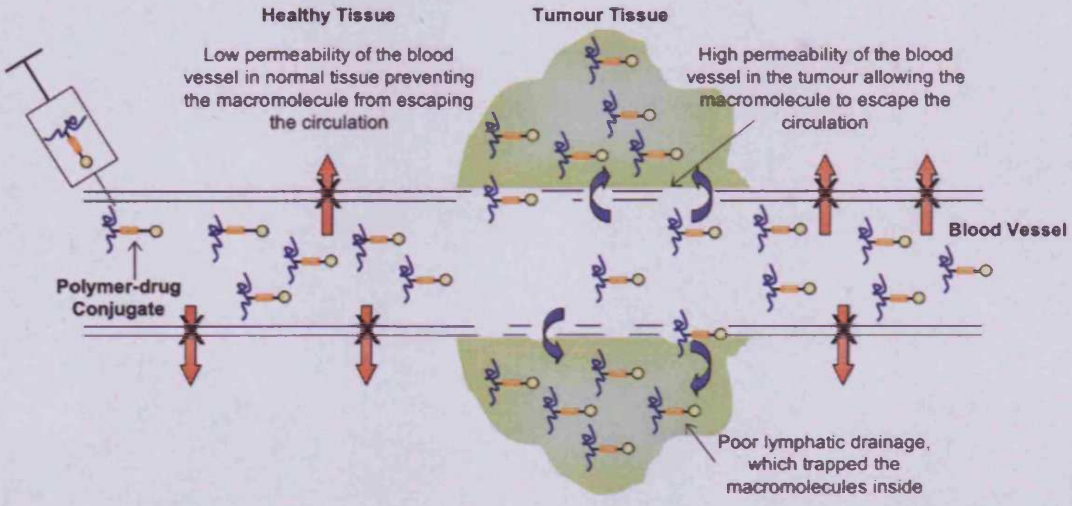

Figure 1.5: The EPR effect (adapted from Duncan (2003b))

Where:  is the macromolecular drug; and  represents the solid tumour.

incomplete basement membrane), which lead to an enhanced permeability of the cancerous capillaries for macromolecules (Duncan *et al.* 1987; Maeda 1994; Maeda 2001). Moreover, solid tumours lack effective lymphatic drainage, leading to lower clearance ability from the tumours, and consequently an enhanced retention of the macromolecular drugs within the tumour. Therefore, while low molecular weight molecules can diffuse evenly through normal and cancerous vessels; and distribute themselves randomly throughout the body, the EPR effect allows a discrimination of healthy tissues and this passive and selective targeting of solid tumour tissues allow an increased accumulation of the macromolecular medicine. Due to the new biodistribution of the macromolecular anticancer drug, disturbing and/or life-threatening side effects can be minimised. Once present in the tumour interstitium, polymer-drug conjugates can be active either extracellularly or after being uptaken by the cell via endocytosis (Duncan 2003b).

The following subsections briefly introduce some classes of polymer therapeutics relevant to this project. For more detailed information, the following reviews (Duncan 2003b; Twaites *et al.* 2005; Haag and Kratz 2006; Qiu and Bae 2006; Satchi-Fainaro *et al.* 2006; Vicent and Duncan 2006) and articles (Duncan 2004; Hoste *et al.* 2004) are advised to the reader.

1.4. Polymer-drug conjugates

Duncan, Kopeček and co-workers (Vasey *et al.* 1999 and reviewed by Duncan (2003b)) designed in the 80s, the first polymer-drug conjugate to be used in clinical trials: Prague-Keele 1, known as PK1 (or FCE 28068) (Figure 1.6), a *N*-(2-hydroxypropyl)methacrylamide (HPMA) copolymer containing the anticancer agent doxorubicin through a peptidyl linker glycine-phenylalanine-leucine-glycine or Gly-Phe-Leu-Gly. Later PK2 (or FCE 28069) (Figure 1.6), a HPMA-Gly-Phe-Leu-Gly-doxorubicin copolymer containing galactosamine residues as a targeting moiety, was designed and remained the only targeted polymer-anticancer drug conjugate to enter clinical trial to-date (Seymour *et al.* 2002).

After the design and introduction of PK1 and PK2 in clinical trials, a few more polymer-drug conjugates (Table 1.1) have entered clinical trials as potential

(a)

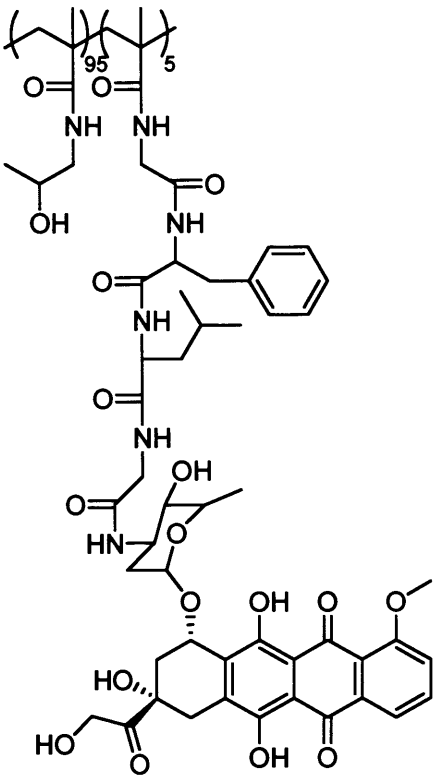

(b)

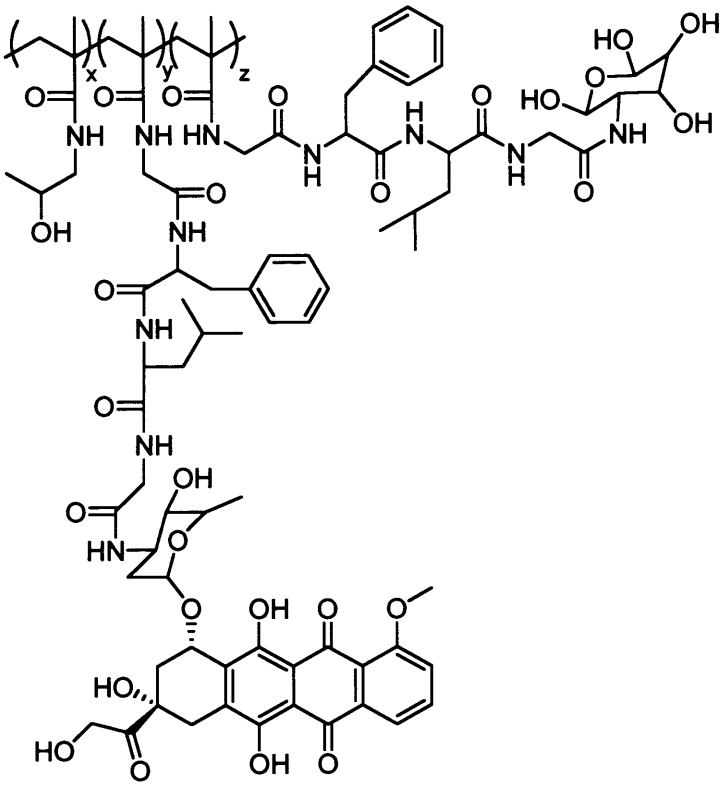

Figure 1.6: Structures of PK1 (a) and PK2 (b)

Table 1.1: Polymer-drug conjugates in clinical trials (Duncan and Kopeček 1984; Duncan 1992; Duncan 2003a; Thanou and Duncan 2003; Satchi-Fainaro *et al.* 2006)

Polymer-drug conjugate	Name	Linker	Status of Development	Reference
HPMA-doxorubicin copolymer	PK1	Amide	Phase II	Vasey *et al.* (1999); Huang and Oliff (2001)
HPMA-doxorubicin-galactosamine copolymer	PK2	Amide	Phase I/II	Duncan *et al.* (1986); Seymour *et al.* (2002)
HPMA-paclitaxel copolymer	PNU166945	Ester	Phase I	Terwogt *et al.* (2001)
HPMA-camptothecin copolymer	MAG-CPT/ PCNU 166148	Ester	Phase I	Schoemaker *et al.* (2002)
HPMA-platinate copolymer	AP5280	Malonate	Phase I/II	Gianasi *et al.* (2002)
PGA-paclitaxel	XYOTAX	Ester	Phase II/III	Li *et al.* (1998); De Vries *et al.* (2001); Sludden *et al.* (2001); Kudelka *et al.* (2002); Sabbatini *et al.* (2002); Schulz *et al.* (2002)
PGA-camptothecin	CT-2106	Ester	Phase I	De Vries *et al.* (2001)
PEG-camptothecin	PROTHECAN	Ester	Phase II	Shaffer *et al.* (2002)
PEG-paclitaxel		Carbamate	Phase I	Greenwald *et al.* (1996a); Greenwald (2001)
Dextran-doxorubicin	DOX-OXD	Schiff base	Phase I	Danhauser-Riedl *et al.* (1993)
Poly(saccharide) (carboxymethyldextran polyalcohol) -camptothecin	DE-310	Gly-Gly-Phe-Gly	Phase I	Kumazawa and Ochi (2004); Oguma *et al.* (2005)
Cyclodextrin-camptothecin	IT-101	Ester	Phase I	Schluep *et al.* (2006a); Schluep *et al.* (2006b)
Fleximer®*-camptothecin	XMT-1001	-	Phase I	Schwertschlag (2007); Yurkovetskiy *et al.* (2007)

*: Fleximer is hydrophilic polymer poly(1-hydroxymethylethylene hydroxyl-methyl formal)

anticancer agents (Duncan 2003b) and present promising results to date (Terwogt *et al.* 2001; Schoemaker *et al.* 2002; Duncan 2003b).

Components of polymer-drug conjugates

Polymer-drug conjugates are composed of three main parts and one optional one as seen in Figure 1.7: a polymer backbone (i), a linker (ii), a drug or several (combination therapy) (iii) and an optional targeting residue (iv).

i. The ***polymer backbone*** is a platform used to carry the molecules of drug. For the design of intravenously administered macromolecular conjugate, it should preferably be biococompatible (i.e. non-toxic and non-immunogenic), a water-soluble polymer capable of solubilising hydrophobic drugs, monodisperse or of low polydispersity. Also, it can be biodegradable or, if non-degradable, be of a size allowing future excretion via the porous glomerular membrane of the kidneys (Duncan 2003a). The presence of functional pendant groups or end groups on the polymer backbone is necessary to allow further conjugation to active molecules (e.g. drug, targeting moieties). The non-biodegradable polymers that are used to carry anticancer agents, and are being tested in clinical trials are poly(*N*-(2-hydroxypropyl)methacrylamide) (PHPMA) (Duncan *et al.* 1987; Duncan 1992), poly(ethylene glycol) (PEG) (Greenwald 2001; Veronese *et al.* 2005). Poly(glutamic acid) (PGA) and dextran (Mehvar 2000; Guu *et al.* 2002) are themselves biodegradable (Table 1.1 and Figure 1.8).

ii. The conjugated ***drug(s)*** could theoretically be any drug that is resistant to lysosomal pH (4.5, 5.5) and lysosomal enzymes for lysosomotropic delivery. An appropriate functional group on the drug to allow conjugation to the polymer backbone is needed. Polymer-based drugs of doxorubicin, paclitaxel, camptothecin and cisplatin are currently in clinical trials as polymer-anticancer drug conjugates (Duncan 2003b; Thanou and Duncan 2003). Also, a current interest in the field of polymer-drug conjugates is the development of combination treatments with the introduction of several drugs on the same polymer backbone (Vicent and Duncan 2006; Greco *et al.* 2007).

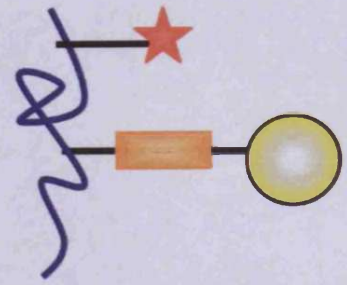

Figure 1.7: Polymer-drug conjugate

Where: is the polymeric backbone; is the drug; is the linker and is an optional targeting moiety.

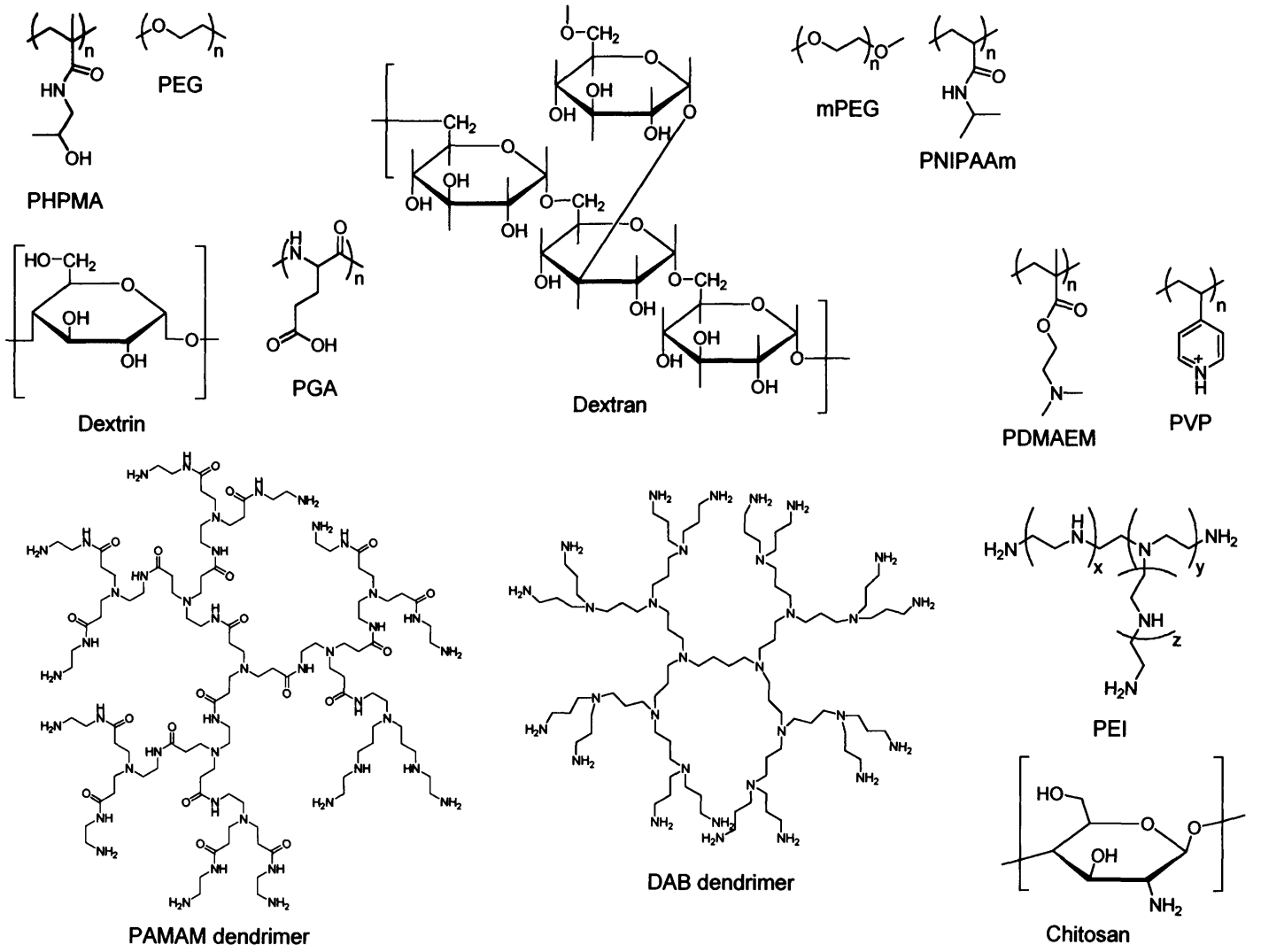

Figure 1.8: Polymers and dendrimers used or studied as potential macromolecular carriers in the field of polymer therapeutics

iii. The ***linker*** is a spacer connecting the drug to the polymer backbone and is a key feature of the macromolecular construct as its degradation should happen at cellular level and induce drug release at the desired cellular compartment. It can be designed and manifold so that the release of the drug occurs in specific intracellular compartments and at specific rates (Duncan 2002; 2003a). For instance, lysosomes can be targeted by lysosomotropic delivery where the polymer-drug conjugate is internalised into the cell before releasing the drug in the lysosomal compartment (De Duve *et al.* 1974). Most conjugates prepared to date are designated for lysosomotropic delivery. Two broad classes of pendent chain linkers have emerged as the most applicable types of linkers for this delivery pathway.

The first category encompasses the **peptidyl linkers**, which are designed to be stable in the bloodstream and other biological fluids and degraded when exposed to specific lysosomal enzymes (Brocchini and Duncan 1999). Studies *in vitro* using tritosomes (or lysosomal hepatic enzymes) and *in vivo* (Duncan *et al.* 1980; Kopeček *et al.* 1981; Brocchini and Duncan 1999) showed that the rate of release highly depends on the nature and chemical composition of the linker. Both steric factors (length of the linker) and structural factors (sequence of the amino acids) affect the cleavage of the drug from the polymer backbone.

Acid labile linkers form the second category of the spacers. In this case, they are pH-dependent linkers, stable in plasma at neutral pH (pH 7.4) and should only degrade by hydrolysis in the acidic environment of the endocytic pathway (pH 4-6.5) (Brocchini and Duncan 1999).

A number of linker chemistries have been proposed in the development of polymer-drug conjugates (Figure 1.9).

iv. The optional ***targeting residue*** is used to actively target and to directly and specifically deliver the macromolecular drug to the targeted cells or tissue. As previously mentioned, PK2 is the only polymer-drug conjugate containing a targeting ligand that is being clinically tested. Its galactosamine residues target the hepatocyte asialoglycoprotein receptors and PK2 was designed for the treatment of liver cancer (Seymour *et al.* 2002). The other anticancer polymer-drug conjugates tested in clinical trials passively target tumour tissues through the EPR effect (Figure 1.5).

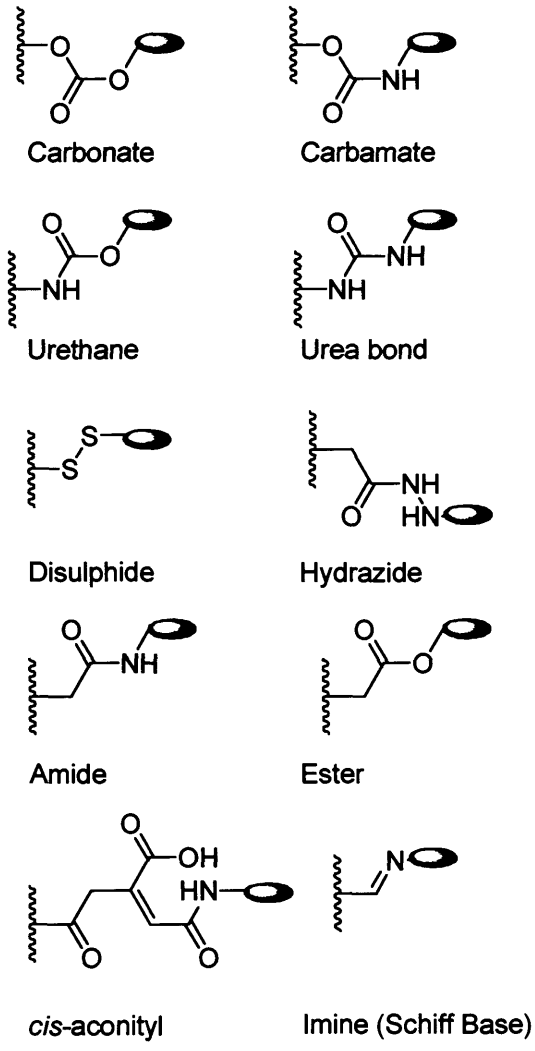

Figure 1.9: Acid labile linkers used to conjugate drugs to the polymer backbone (Brocchini and Duncan 1999)

Where: ⬭ represents the drug and ∿∿∿ the polymer backbone.

Synthetic methods for the design of polymer-drug conjugates

From a polymer chemistry point of view, the synthesis of linear polymer-drug conjugates can be designed using two main approaches, and Figure 1.10 schematically represents those. The first approach involves the copolymerisation of the three following components:

- a monomer
- a monomeric drug
- an optional monomer-targeting residue to directly form the desired polymer-drug conjugate.

The desired polymer-drug conjugate is therefore formed in a one-step process. The second approach relies on the use of ***polymer analogous chemistry***, where drugs and targeting molecules are successively conjugated to the previously synthesised polymeric backbone. In this case, the drug content of the conjugate can be modulated in an easier way, by varying the feed ratio of polymer to drug. Both approaches require careful synthesis and characterisation optimisations for successful control of molecular weight, polydispersity, purification, drug incorporation, and reproducibility.

1.5. Polymer-protein conjugates

Polymer-protein conjugates represent the most successful class of polymer therapeutic with several conjugates on the market for treatment of various cancer and hepatitis C (Table 1.2). Delivery of proteins is limited due to their immunogenicity and poor stability. Conjugation of a polymer to a protein (such as enzymes, cytokines, growth factors, and antibodies) is able to improve the solubility, stability, and half-life of the protein in plasma by decreasing its rapid renal clearance, and to reduce its immunogenicity, and to provide greater protection against degradative enzymes (Thanou and Duncan 2003). Also, it permits the reduction of injection frequency, therefore offers a better patient compliance.

Semitelechelic polymers (i.e. polymers with only one end group functionalised) are usually used to synthesise polymer-protein conjugates (Figure 1.11) and the conjugation of the protein is done through only one point attachment, avoiding any

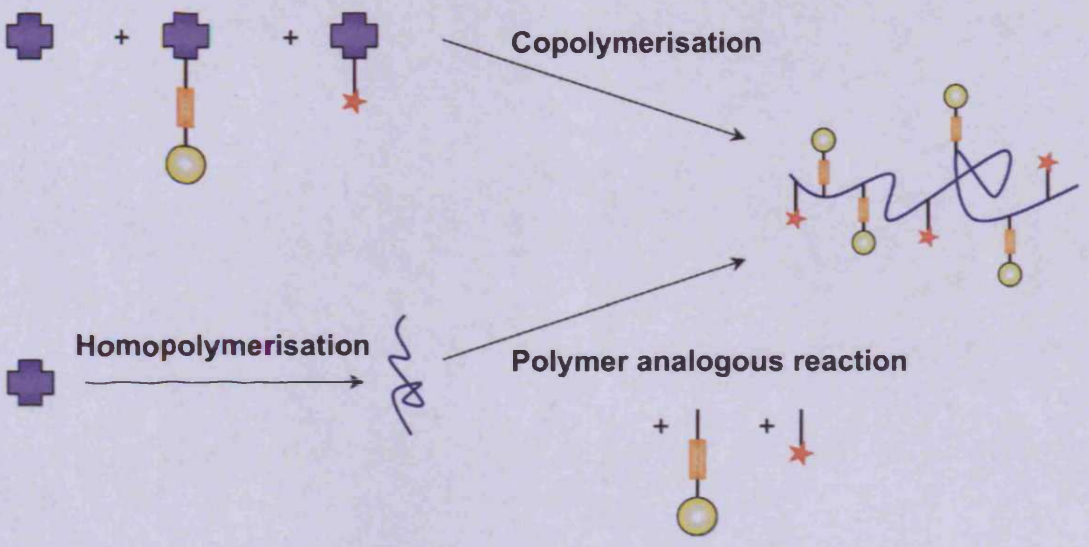

Figure 1.10: Schematic representation of the two main routes to synthesise polymer-drug conjugates

Where: represents the monomer, its polymer, is the drug; is the linker and is an optional targeting moiety.

Table 1.2: Polymer-protein conjugates on the market or in clinical development (adapted from Duncan 2003b and Satchi-Fainaro *et al.* 2006)

Polymer-protein conjugate	Name	Status (year to market)	Indication	References
PEG-adenosine deaminase	Adagen	1990	SCID syndrome	Levy *et al.* (1988)
SMANCS	Zinostatin, Stimalmer	1993 (Japan)	Hepatocellular carcinoma	Maeda and Konno (1997)
PEG-*L*-asparaginase	Oncaspar	1994	Acute lymphoblastic leukaemia	Graham (2003)
PEG-interferon-α 2b	PEGINTRON™	2000	Hepatitis C	Wang *et al.* (2002)
PEG-interferon-α 2b	PEGINTRON™	Various clinical trials	Cancer, multiple sclerosis, HIV/AIDS	Bukowski *et al.* (2002); Wang *et al.* (2002)
PEG-interferon-α 2a	PEGASYS	2002 (EU)	Hepatitis C	Rajender Reddy *et al.* (2002)
PEG-human growth hormone	Pegvisomant	2002	Acromegaly	Mukherjee *et al.* (2002)
PEG-granulocyte-colony stimulating factor	Neulasta™	2002	Prevention of chemotherapy-associated neutropaenia	Rajender Reddy *et al.* (2002)
PEG-anti-TNFα antibody fragment	Cimzia™	Phase II	Rheumatoid arthritis and Crohn's disease	Chapman *et al.* (1999)

Where SMANCS stands for Styrene-*co*-Maleic Anhydride-NeoCarzinoStatin, TNF for Tumour Necrosis Factor, SCID for Severe Combined ImmunoDeficiency, HIV/AIDS for Human Immunodefficiency Virus/Acquired ImmunoDefficiency Syndrome.

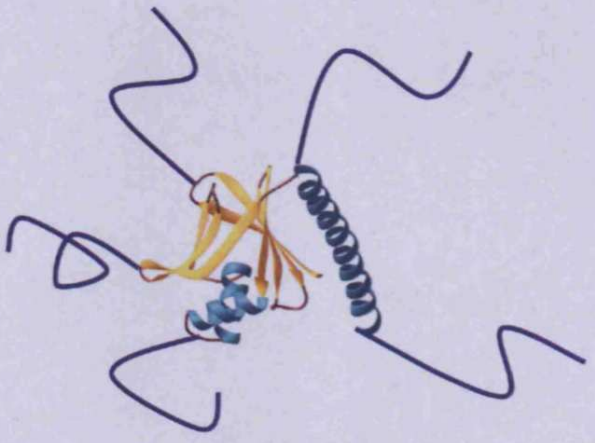

Figure 1.11: Polymer-protein conjugate

Where:  is the protein, and  is the semitelechelic polymer.

crosslinking. A linker must be introduced on the protein and should not induce toxic and immunogenic reactions, or loss of protein activity. Moreover, when designing a polymer-protein conjugates, particular care has to be taken regarding the reproducibility of the conjugation procedure (reviewed by Duncan (2003b)).
As an example, PEG is often used as a carrier for proteins, a procedure that is now known as the PEGylation of proteins (reviewed by Veronese (2001); Veronese and Pasut (2005)).

1.6. Polyplexes

As it is a field of great therapeutic potential (more than 4 000 human genetic-based diseases are known nowadays (Förster and Konrad 2003)), research on gene therapy has developed extensively (Figure 1.12). Gene delivery aims to introduce a specific DNA sequence into the targeted cells, transfect this sequence to efficiently express the gene that due to its deficiency or defectiveness, primarily caused the disease. Also, introducing synthetic fragments of DNA such as antisense oligonucleotides (Kabanov and Alakhov 1994; Kabanov *et al.* 1995b), allow the selective inhibition of the expression of faulty genes or the viral reproduction by interacting with the complementary intracellular nucleic acid. Currently, one of the challenges of gene therapy is the development of effective gene transfer vectors.

Viral vectors

As **viruses** have a natural need to integrate their genome into the host cell to live and reproduce themselves, they were the first types of vectors intensively studied (Förster and Konrad 2003). Viral vectors, such as genetically modified retroviruses and adenoviruses, presented promising results *in vitro* because of the high transfection efficiency they offered. Figure 1.13 summarises the different vectors used in gene therapy and under investigation in ongoing clinical trials. Nevertheless, viral vectors can cause immune or toxic reactions, and viral recombination when used *in vivo*, and therefore non-viral vectors perhaps offer a safer alternative, however, extensive work needs to be done before any compounds show similar transfection efficacy *in vivo*.

Non-viral vectors

The first generations of non-viral vectors primarily consisted in **naked DNA**, which was poorly transfected due to its substantial nuclease digestion, and DNA complexed to synthetic non-viral vectors such as **cationic liposomes** or **cationic polymers**. The

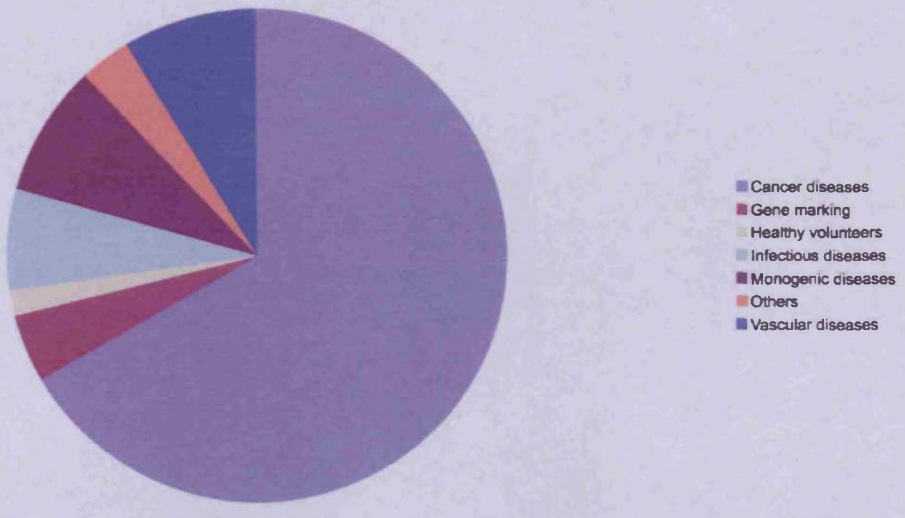

Figure 1.12: Indications addressed by Gene Therapy Clinical Trials (www.wiley.co.uk/genmed/clinical)

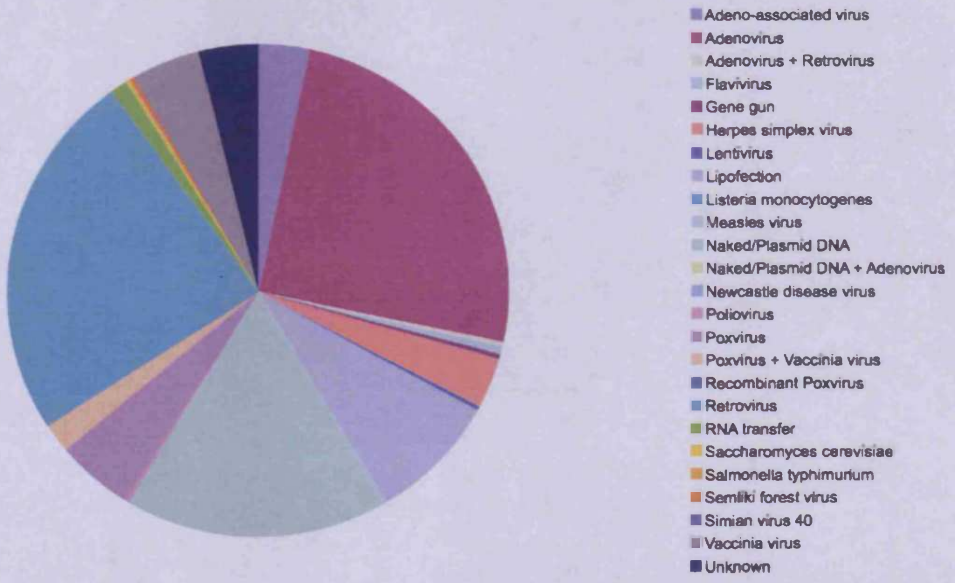

Figure 1.13: Vectors used in Gene Therapy Clinical Trials (www.wiley.co.uk/genmed/clinical)

complexes formed are called **lipoplexes** (Omidi *et al.* 2003) and **polyplexes** (Kabanov and Alakhov 1994; Kabanov and Kabanov 1995; Kabanov *et al.* 1995a; Kabanov *et al.* 1995b; MacLaughlin *et al.* 1998; Gebhart and Kabanov 2001; Richardson *et al.* 2001; Thanou *et al.* 2002), respectively.

Although their *in vivo* efficiency is still poor compared to viral vectors, they have the advantage of shielding the condensed DNA from nuclease digestion without introducing dangerous immune reactions. Plasmid DNA (small and circular extra-chromosomal DNA that can replicate independently in the host cell) is incorporated into a stable complex in both systems, as a result of electrostatic interactions between the positively charged groups of lipids or polycations and the negatively charged phosphate groups of the DNA (Kabanov and Alakhov 1994; Kabanov and Kabanov 1995).

In the case of polyplexes (Figure 1.14), also known as interpolyelectrolyte complexes (Kabanov and Kabanov 1995), the polymer used not only must be biocompatible, water soluble and capable of interacting with DNA, but also, they must be designed so they can promote intracellular delivery and bypass the degradative environment of the lysosomes towards their cargo. Many modifications can be made on the polymer to improve the gene delivery system. Composition of the multi-component construct (feed ratio of DNA/polycation), molecular weight and architecture of the polymer (linear, branched, block or graft copolymers, dendrimers) (Kabanov 1999; Gebhart and Kabanov 2001) and introduction of target-specific moieties can be taken into account (Guo and Lee 1999) for the design of efficient non-viral polymer-based gene vectors.

Several polycations have been studied so far to produce polyplexes for the delivery of polynucleotides. They include poly(vinylpyridinium) salts (PVP), polypeptides, such as poly(lysine) (PLL), poly(ethyleneimine) (PEI), poly(amidoamine) (PAMAM) (linear or dendrimers), chitosan and poly(methacrylic acid) derivatives such as poly(dimethylaminoethylmethacrylate) (PDMAEM) (MacLaughlin *et al.* 1998; Kabanov 1999; Richardson *et al.* 2001; Thanou *et al.* 2002; Förster and Konrad 2003) (Figure 1.8), but these often suffer from toxicity and rapid capture by the liver due to their cationic charge (Boussif *et al.* 1995; Malik *et al.* 2000).

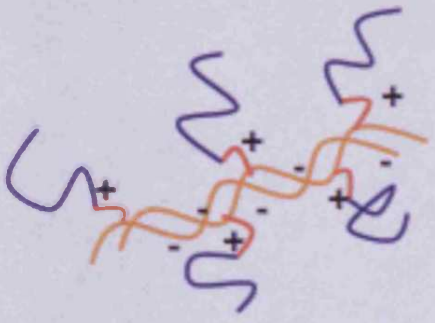

Figure 1.14: Schematic showing polyplex

Where:  represents the hydrophilic polymeric block,  the cationic polymeric block and  the DNA fragment.

As illustrated in Figure 1.13, mostly viral vectors (69 %), naked DNA (16.2 %) and lipofection (8.6 %), have been used in ongoing clinical trials. Thus, understanding the mechanism of gene transfection using polyplexes is crucial in order to increase their use and overcome the limitations of other vectors.

Transfection mechanism

The first stages of the mechanism of the transfection of mammalian cells by polyplexes are believed to occur as shown on Figure 1.15 (Kabanov and Kabanov 1995; Kabanov 1999; Twaites *et al.* 2005). After ***adsorption*** of the slightly positively charged polyplex on the negatively charged plasma membrane, some resultant ***changes in the properties*** of the plasma membrane constitute a signal for inducing an ***adsorptive endocytosis*** of the macromolecular construct. The next stages should involve the ***release of DNA*** from the polyplex and from the endocytosis compartment to the cytoplasm, and subsequently the ***migration of DNA*** to the nucleus, where transfection would occur. This last step is important, as its low efficacy severely reduces transfection. Nevertheless, its mechanism is not yet totally understood.

1.7. The next generation of polymer therapeutics

All the nano-sized polymer therapeutics are willing to enhance the delivery of drugs, proteins and genes by passively or actively targeting specific tissues and/or cell compartments, by protecting their active compounds from degradation, and by improving their pharmacokinetics and physico-chemical properties. As previously seen, several polymer-based medicines are already on the market or in clinical trials, proving the rationale of polymer therapeutics. Nevertheless, the polymers used so far have limitations including heterogeneity in structure, molecular weight, polydispersity, drug carrying capacity, lack of control of architecture and biodegradability of polymer backbone.

The experience gained in the field of polymer therapeutics and the knowledge acquired in polymer chemistry over the last few decades provide the basis for the development of a more sophisticated second-generation of polymer therapeutics, where carriers would gain for instance, more defined chemical composition and three-dimensional architecture.

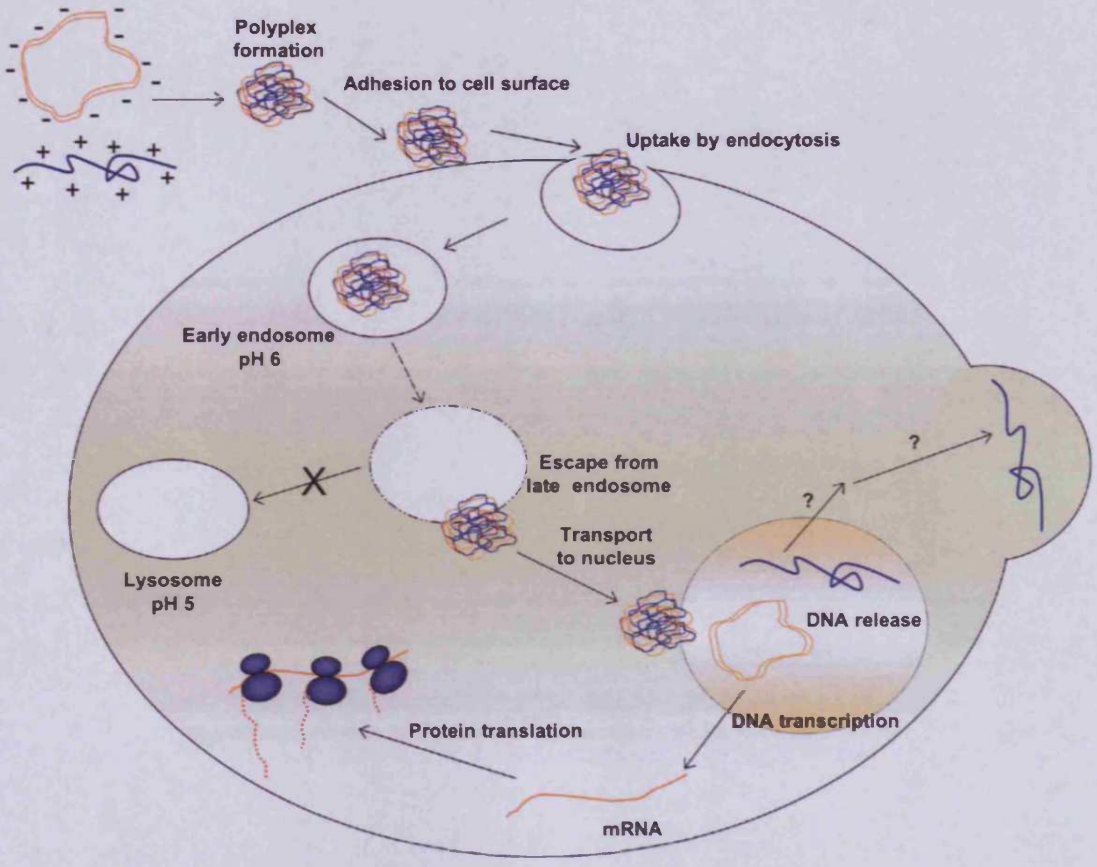

Figure 1.15: Schematic representation of the endocytosis of polyplexes (adapted from Twaites *et al.* (2005) and Haag and Kratz (2006))

The endocytic vesicles progressively mature from an early endosome (pH ~ 6), through a late endosome (pH dropping from 6 to 5) to a lysosome (pH ~ 5) (Watson *et al.* 2005).

As already demonstrated, non-linear polymers provide different cellular uptake efficiency and trafficking as they provide different pharmacological behaviour compared to their linear counterparts (Wang *et al.* 2000; Wiwattanapatapee *et al.* 2000; Xyloyiannis *et al.* 2003; Seib *et al.* 2007). Also, high polymer polydispersity leads to non-unique composition and distribution of molecular weight could affect the pharmacological behaviour of the polymer therapeutics (such as pharmacokinetics and pharmacodynamics). Moreover, more sophisticated constructs may provide improved opportunities for biorecognition, and three-dimensional biomimetic architectures (dendrimers and dendronized polymers): important key features for future polymer therapeutics (reviewed by Duncan (2003b)).

1.8. Polymeric architectures and their synthetic approaches

With the emergence of Controlled Radical Polymerisations techniques (CRP) (Matyjaszewski 1997; Matyjaszewski 2003) more complex polymeric architectures with more defined and controlled chemical compositions such as graft block copolymer or star-shaped copolymer systems can be designed, allowing the development of a second generation of polymer therapeutics.

The next Sections describe the different polymeric architectures that are being or may in the future be used for the design of polymer therapeutics, as well as the techniques used (also in this project) for their synthesis:

- Free Radical Polymerisation (FRP),
- Chain Transfer Agent (CTA) mediated FRP,
- Atom Transfer Radical Polymerisation (ATRP).

1.8.1. Synthesis of linear polymers by free radical polymerisation

FRP has many advantages. Many different solvents can be used, it tolerates small amounts of impurities and many functional groups can be carried by the monomers. These features allow the polymerisation of a wide range of styrenic, vinylic, and acrylic monomers. FRP proceeds by chain reactions and the polymer chain grows by addition of a monomer residue to the terminal free radical reactive site (or active centre). This induces the transfer of the active centre to the newly created chain end (Cowie 1991). The FRP mechanism (Cowie 1991; Elias 1997) can be divided into four different stages. These are referred to as: initiation, propagation, transfer and termination, and Figure 1.16 shows schematically these four steps.

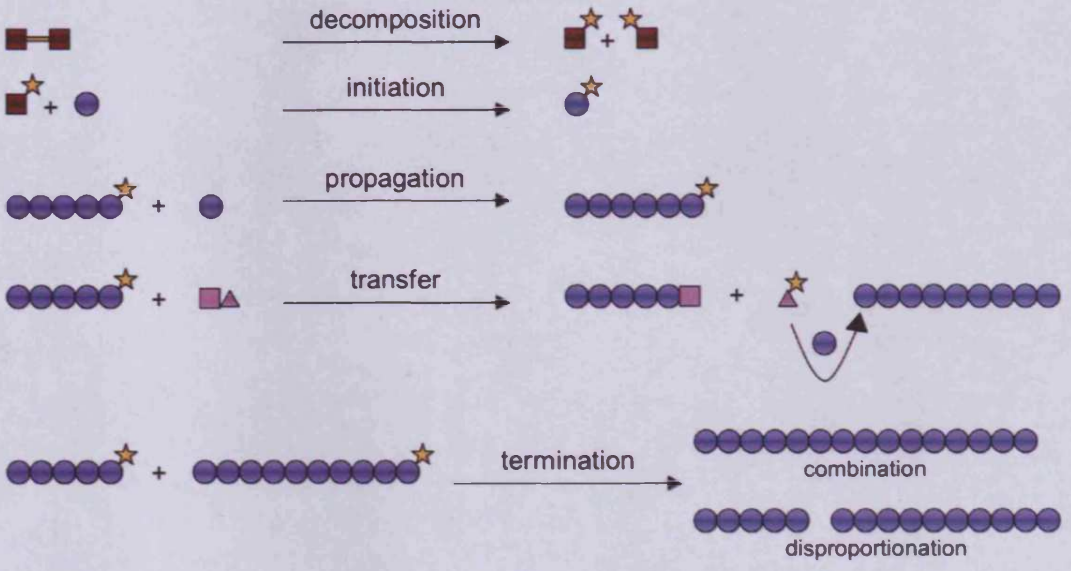

Figure 1.16: Schematic representation of the FRP mechanism

Where: ● represents the monomer, ▬▬ the initiator, ■★ the initiator radical, ★ the active centre, ■▲ the transfer agent, ▲★ the transfer agent radical, ●●●●●★ the growing radical and ●●●●●● the dead polymer chain.

Initiation involves two reactions to create an active centre (decomposition of the initiator and formation of a monomeric radical). First, primary free radicals are formed by thermal, redox, or photochemical decomposition of the initiator. As an example, 2,2'-azobis(isobutyronitrile) (AIBN) has been frequently used. AIBN decomposes on heating or when exposed to radiation of a wavelength of λ = 360 nm (Elias 1997). Usually, homolytic dissociation of the initiator molecule into two primary free radicals occurs. These then react with a monomer molecule to produce initial propagating radicals (Cowie 1991; Elias 1997).

The ***propagation*** step consists of successive additions of monomer molecules to the propagating radicals to form new propagating radicals of higher molecular weight.

Transfer reactions can occur between a growing radical (or macromolecular radical) and monomer, initiator, solvent molecules, impurities or polymer chains themselves. This leads to the deactivation of the growing polymer chain, and the formation of new free radicals, which can then initiate the propagation of other monomers. Normally seen as a side reaction of FRP, it is worth noting that chain transfer reactions can be introduced intentionally to control the molecular weight and/or to introduce end-group functionalities on the polymer backbone. This concept is further explained in Section 1.8.2.

Chain ***termination*** is the final step of FRP. It involves the reaction of two macroradicals via either **combination** or **disproportionation** reactions (Cowie 1991; Elias 1997). In the first case, two growing chains combine and form one single "dead" chain of higher molecular weight. In the case of disproportionation reactions, a hydrogen atom is extracted from one growing radical and it is transferred to the other macroradical. This leads to the termination of two polymer chains. One will have an unsaturated end-group, and the other will bear a saturated end-group. Normally during FRP, combination and disproportionation reactions prevail over transfer reactions.

Studies on the kinetics of FRP have developed an understanding of the limitations of this method.

They can be summarised as follows (Cowie 1991; Matyjaszewski 1997; Chiefari and Rizzardo 2002):

i. no defined functionalised end-group
ii. no control over architecture (e.g. no possible formation of block copolymer)
iii. little control over polydispersity
iv. little control over molecular weight

As the types of termination reactions (combination and disproportionation) can equally well occur, the polymer end groups are not strictly defined (Cowie 1991; Elias 1997). The end groups are also non-reactive. This means that there is no possibility of chain extension with addition of a new batch of monomers (Chiefari *et al.* 1998).

As the rate constant values for chain termination are greater than those for chain propagation, and as the termination steps inevitably lead to deactivated or "dead" polymers, it is impossible to increase polymer molecular weight or to form block copolymers by sequential addition of a new batch of monomer using FRP (Cowie 1991; Elias 1997).

From a kinetic point of view, polydispersity would theoretically be 1 in the case of termination by disproportionation, and it would be theoretically be 2 in the case of termination by combination. However, in practice polydispersity of polymers synthesised by FRP is in the range of 3 to 10. This is due to the fact that the concentrations of monomers and initiators are always changing during the reaction (Cowie 1991; Elias 1997).

As initiation and termination are continuous processes, the total concentration of radicals increases initially, but almost instantaneously reaches a constant value. The system is then in a steady state (Cowie 1991; Elias 1997). At this time, the initiation rate is equal to the termination rate resulting in steady state conditions that can be applied to the theoretical derivation of the kinetics of FRP. The propagation rate is much faster than the initiation rate, thus chain growth is much higher than the termination rate and so high molecular weight polymers are already obtained at low monomer conversion (Cowie 1991; Elias 1997).

Recently, many studies have tried to improve the method of radical polymerisation, especially to give better control of molecular weight and polydispersity, and also to

allow end-group functionalisation and synthesis of different polymer architecture. These techniques are discussed in the following Sections where the principles of CTA FRP and ATRP are introduced.

1.8.2. Chain transfer agent free radical polymerisation: control of molecular weight and end-group functionalisation

To overcome some of the limitations of FRP, CTA can be used to control molecular weight and polydispersity. This technique also enables the introduction of functional end groups to the polymer chain, allowing the synthesis of telechelic and/or semitelechelic polymers (Chiefari and Rizzardo 2002).

CTA (Figure 1.17) are compounds with labile hydrogen atom (such as allyl benzene and allyl phenyl ether), halomethanes, disulfides and thiols (Chiefari and Rizzardo 2002). The chemical structures of 3-mercaptopropionic acid (MPA) and 2-mercaptoethanol (ME) are also included in Figure 1.17 as those two thiol-based CTA were used in these studies.

The mechanism of action of CTA in FRP (Figure 1.18) is divided into three steps.

(i) In the first step, a propagating radical ($P_n^{\bullet}$) initiated by radicals formed through the decomposition of the initiator, reacts with a CTA (R-X). The R-X bond is homolytically cleaved to form two free radicals ($R^{\bullet}$ and $X^{\bullet}$) and the newly formed radical $X^{\bullet}$ can then react with a growing radical ($P_n^{\bullet}$) to form a "dead" polymer chain (P_n-X).

(ii) In step two, the CTA radical $R^{\bullet}$ can reinitiate the polymerisation of a monomer molecule (M) and form a new radical (R-$M^{\bullet}$).

(iii) After propagation, R-$M^{\bullet}$ produces, in step three, a new propagating chain ($RP_{m+1}^{\bullet}$) and then a semitelechelic polymer chain.

CTA efficiency is defined by its dimensionless chain transfer constant C_{tr} (Equation 1.1 and Table 1.3) (Chiefari and Rizzardo 2002).

H labile compounds

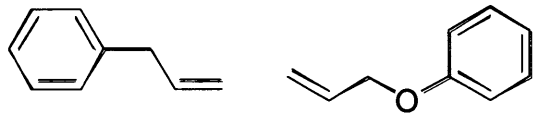

Halomethanes

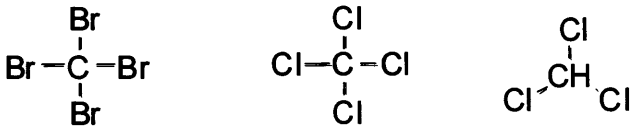

Thiols

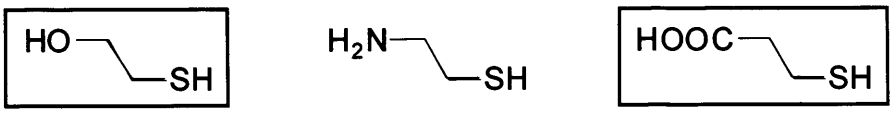

Disulfides

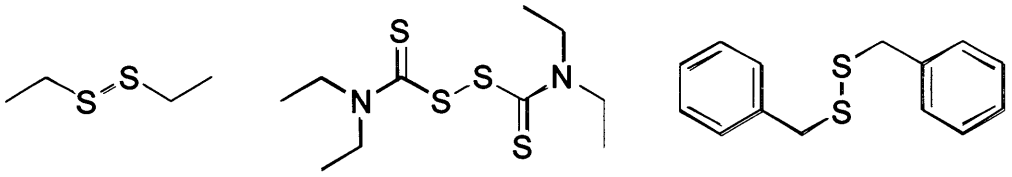

Figure 1.17: Several chemical structures of CTA (halomethanes, thiols and disulfides) including MPA and ME

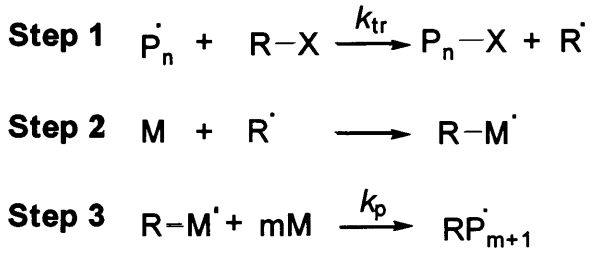

Figure 1.18: General chain transfer mechanism (taken from Chiefari and Rizzardo (2002))

Where k_{tr} and k_p are the rate constants of transfer and propagation steps, respectively.

$$C_{tr} = \frac{k_{tr}}{k_p} \qquad \text{(Eq 1.1)}$$

Where k_{tr} is the chain transfer rate constant, and k_p is the propagation rate constant.

Ideally C_{tr} is 1, which means that the transfer reactions are as fast as the propagation process, and the ratio of the molar concentration of CTA to monomer during the polymerisation is constant. Therefore, the average molecular weight of the polymer is approximately constant and will not change significantly from low to high conversions (Corner 1984). As seen in Table 1.3, for a given CTA, its C_{tr} is dependent on the monomer studied, on the temperature of the reaction, and also on the solvent used.

The reaction conditions for the CTA-mediated FRP must be chosen to ensure that the majority of the polymer chains synthesised have a CTA residue as an end-group. This can be achieved when the main chain terminating reaction is chain transfer to the CTA radical. The termination reactions between two propagating radicals (disproportionation and combination) cannot be completely eliminated. However, when these reactions occur in a much lower proportion compared to the termination reactions to the CTA radicals, most polymer chains will be telechelic and semitelechelic, and little unfunctionalised polymer will be found in the reaction mixture. These factors are important to consider, especially when the CTA is used not only to adjust molecular weight, but with the main aim of introducing functional polymer end groups. Synthesis of unfunctionalised polymer can be avoided using specific initiators that form radicals bearing the same functionality that is being introduced as the radicals of the CTA (as done for example by Wang *et al.* (2000)). In this case, any polymer chains initiated by an initiator radical would bear the required functionalised end-group. It is important to note that this method still does not avoid the synthesis of a mixture of telechelic and semitelechelic polymers (Kamei and Kopeček 1995; Wang *et al.* 2000).
Also important to note is that some solvents, e.g. chloroform or dichloromethane, can behave as CTA themselves. For all polymerisation reactions in solution, the choice of an appropriate solvent is crucial.

As semitelechelic polymers possess only one reactive functional end-group per

Table 1.3: Chain transfer constants (C_{tr}) of thiols, halomethanes and disulfides with various monomers at 60 °C (adapted from Chiefari and Rizzardo (2002))

CTA		R	Monomer		
			Methyl methacrylate	Styrene	Vinyl Acetate
Thiols RSH		n-C_4H_9	$6.70 \cdot 10^{-1}$	22.00	48.00
		n-$C_{12}H_{25}$	ND	19.00	ND
		$H_3N^+CH_2CH_2$	$1.10 \cdot 10^{-1}$	11.00	ND
		$HOCH_2CH_2$	$4.50 \cdot 10^{-1}$	ND	ND
		MeO_2CCH_2	$3.00 \cdot 10^{-1}$	1.40	$7.00 \cdot 10^{-2}$
Halomethanes	CBr_4	ND	$0.19 \cdot 10^{-4}$	$8.80 \cdot 10^{-4}$	$7.39 \cdot 10^{-2}$
	CCl_4	ND	$1.85 \cdot 10^{-3}$	$9.20 \cdot 10^{-3}$	$8.00 \cdot 10^{-2}$
	$CHCl_3$	ND	$1.77 \cdot 10^{-4}$	$3.40 \cdot 10^{-4}$	$1.60 \cdot 10^{-2}$
Disulfides RS-SR		C_2H_5	$1.30 \cdot 10^{-4}$	$4.50 \cdot 10^{-3}$ [(a)]	ND
		n-C_4H_9	ND	$2.40 \cdot 10^{-3}$	1.00
		$PhCH_2$	$6.30 \cdot 10^{-3}$	$1.00 \cdot 10^{-2}$	ND
		EtO_2CH_2	$6.50 \cdot 10^{-5}$	$1.50 \cdot 10^{-2}$	1.50
		Ph	$1.10 \cdot 10^{-2}$	$1.50 \cdot 10^{-1}$	ND
		PhC(=O)	10.00	36.00	ND
		$Et_2N(C=S)$	ND	$3.20 \cdot 10^{-1}$	ND

[(a)]: At 99 °C; ND: non-determined.

polymer chain, they are particularly useful for conjugation to biomaterial surfaces, and in the context of polymer therapeutics, to proteins, peptides, fluorophores, targeting moieties and drugs (Figure 1.19), avoiding cross-linking and loop formation (reviewed by Duncan 2003b). Semitelechelic polymers have been already extensively used to improve the properties of:

- surfaces (Lee *et al.* 1990; Gaertner and Offord 1996),
- therapeutic proteins (i.e. reduced biorecognition and protein adsorption) (Abuchowski *et al.* 1984; Zalipsky 1995; Gaertner and Offord 1996),
- enzymes (Takahashi *et al.* 1984; Wang *et al.* 1997) (i.e. increased resistance, reduction of antigenicity, prolongation of intravascular half-life, increased stability)
- and hydrophobic drugs (i.e. increased solubility and stability) (Greenwald *et al.* 1996b; Greenwald *et al.* 1996c).

Historically, monomethoxyPEG (mPEG) (Figure 1.8) was the first semitelechelic polymer to be used to modify the protein bovine serum albumin (Abuchowski *et al.* 1977b) and the enzyme bovine liver catalase (Abuchowski *et al.* 1977a). This procedure is referred to as PEGylation, and the evolution of PEGylation in chemistry has been extensively reviewed (Harris 1992; Veronese 2001; Harris and Chess 2003; Veronese and Pasut 2005). Initially, mPEG was chosen for protein modification due to its low immunogenicity, high chain flexibility, hydrophilicity, and its ability to prolong blood circulation time of the conjugated protein, and decrease protein immunogenicity. Since then, other water-soluble polymers have been used for this purpose including both synthetic polymers, such as PHPMA (Lu *et al.* 1998; 1999; Oupický *et al.* 1999a; Oupický *et al.* 2000a; Wang *et al.* 2000; Wang *et al.* 2004a; Subr *et al.* 2006) and the temperature-responsive polymer poly(*N*-isopropylacrylamide) (PNIPAAm) (Takei *et al.* 1993b; a; Takei *et al.* 1994; Takei *et al.* 1995; Matsukata *et al.* 1996), and natural polymers such as dextran (Suzuki *et al.* 1972; Fagnani *et al.* 1990; Takashina *et al.* 1991; Mehvar 2000) and dextrin (Ferguson *et al.* 2006; Hardwicke *et al.* 2007; Duncan *et al.* in press) (Figure 1.8).

1.8.3. Non-linear polymer architectures: the next generation of polymer therapeutics?

Recently, efforts in polymer chemistry have been focused on the design of novel

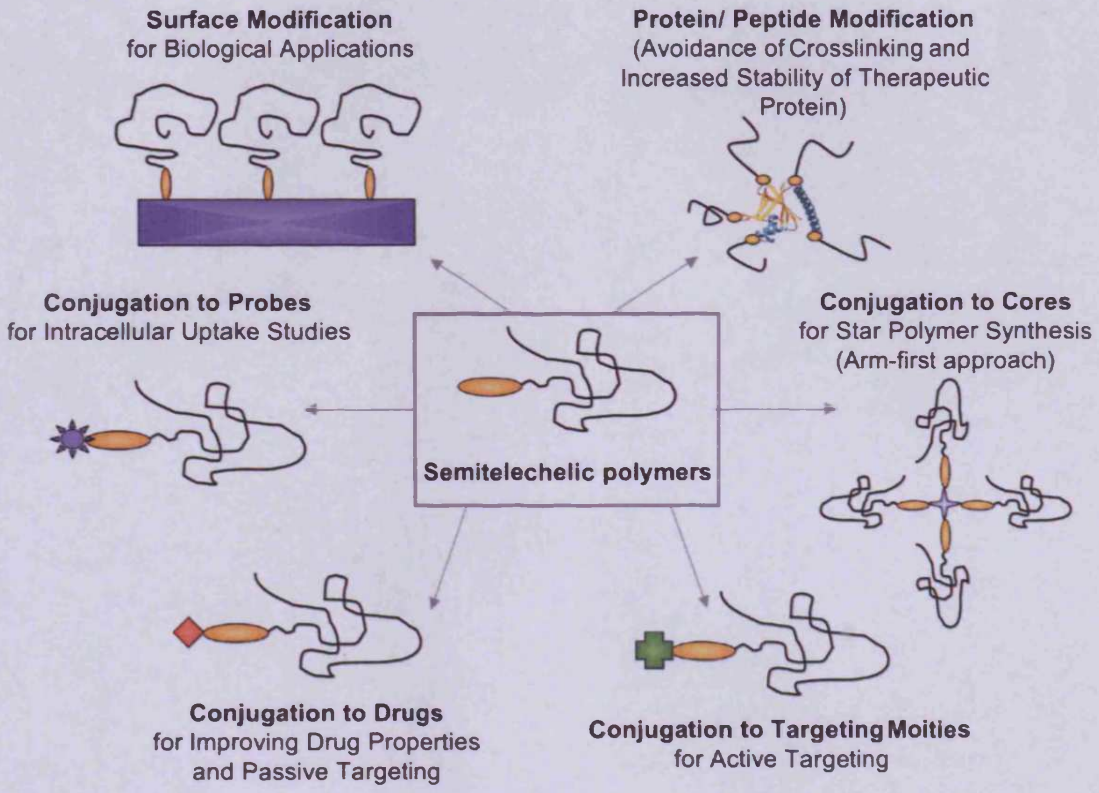

Figure 1.19: Potential uses of semitelechelic polymers

Where ⬭ represents a functional end-group (e.g. –COOH, -OH, $-NH_2$, etc); ✸ is a probe; ◆ is a drug and ✚ is a targeting moiety.

polymeric architectures (Figure 1.20). This chemistry was developed to improve the control of molecular weight, polydispersity and most importantly architecture of the polymer. In the context of polymer therapeutics, it is hoped that such structures will not only minimise heterogeneity but will also improve the biological and therapeutic properties of the macromolecular constructs produced.
As they are most relevant to this project, dendrimers and especially star polymers are described in more detail in the following Sections.

Dendrimers

Dendrimers (Figures 1.20 and 1.21) are highly branched synthetic macromolecules, having a unique three-dimensional structure with regular layers of branches extending from a central core (Tomalia *et al.* 1990). Although dendrimers are an important area at the state of the art of polymer chemistry, a comprehensive review on dendrimers is beyond the scope of this thesis. Detailed information can be found elsewhere (Tomalia *et al.* 1985; Hawker and Fréchet 1990; Tomalia *et al.* 1990; Vögtle 2000; Boas and Heegaard 2004; Dufès *et al.* 2005; Duncan and Izzo 2005; Svenson and Tomalia 2005; Qiu and Bae 2006; Wei *et al.* 2006; Tomalia *et al.* 2007).

As the synthetic approaches used to prepare star polymers show similarities with the routes to synthesise dendrimers, the following paragraphs will briefly introduce the pathways available for the synthesis of dendrimers, as well as the use of dendrimers in the field of polymer therapeutics.

The convergent and divergent synthetic approaches to dendrimers

Tomalia and Fréchet's groups were the pioneers of the dendrimer synthesis in the late 80s. Each of them described a method for the synthesis of well-defined, three-dimensional, globular dendrimers by either the divergent (Tomalia *et al.* 1985) or the convergent (Hawker and Fréchet 1990) synthetic strategies (Figure 1.21).
The divergent dendrimers are step wisely formed by growth of a monomeric unit from the inside (core) to the outwards (surface). The divergent method needs to employ very effective transformation reactions to avoid defects on the final dendrimer, as a high number of reactions have to be performed on a single molecule (reviewed by Boas and Heegaard (2004)).
In contrary, the convergent dendrimers are produced by an "outside-in" procedure, where "dendrons" are firstly formed, and then coupled to a core. In this case, the

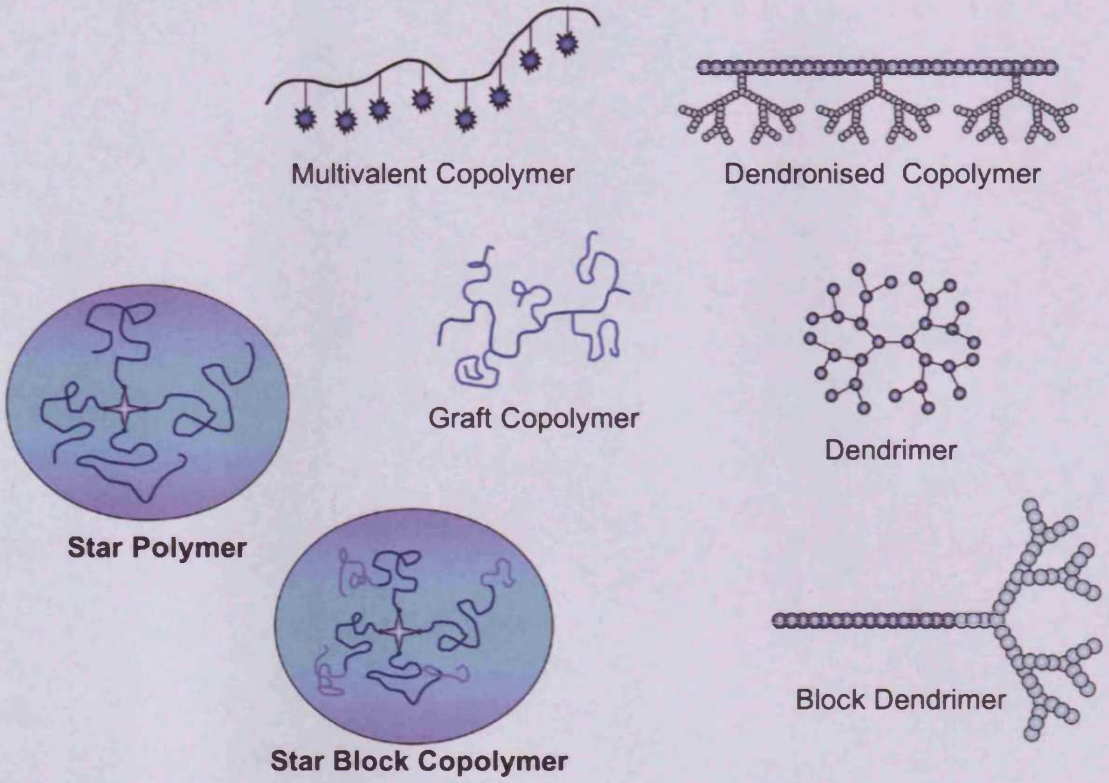

Figure 1.20: Novel polymeric architectures (adapted from Duncan (2003b))

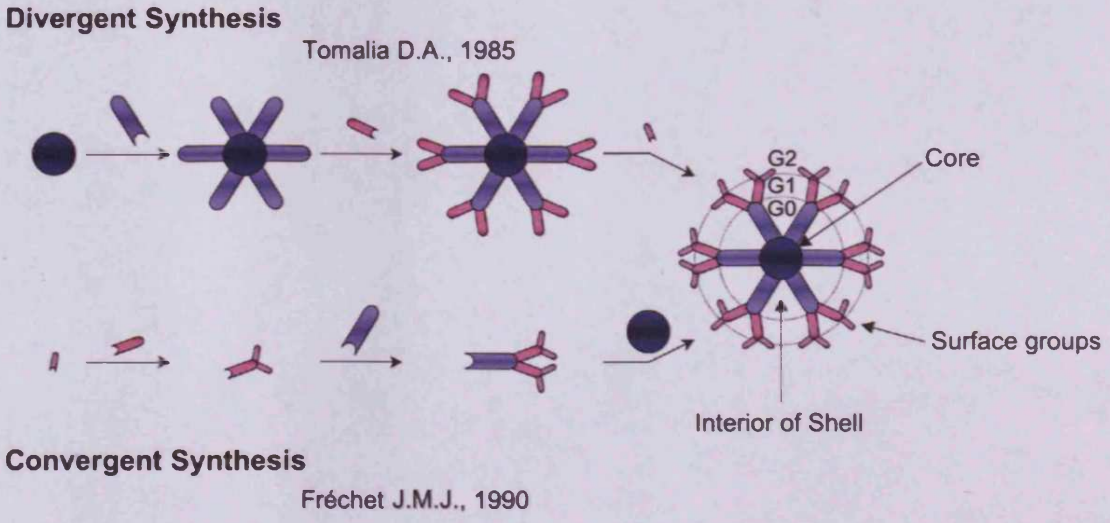

Figure 1.21: Dendrimer synthesis: divergent and convergent growth

difficulties come from the purification of the growing dendrons at each step, for the synthesis of dendrimers without defects (reviewed by Boas and Heegaard (2004)). Both methods consist of repeated synthetic steps and an additional layer of branches or dendrimer generation (G0, G1, G2, etc) is created at each cycle (Vögtle 2000) as depicted on Figure 1.21.

Dendrimers in the field of polymer therapeutics

Dendrimers provide many exciting opportunities for improving tissue targeting and intracellular delivery (Cloninger 2002; Dufès *et al.* 2005). The principal advantages of dendrimers over linear polymers are their monodispersity (which should provide reproducible pharmacokinetic behaviour), their precise 3D globular shape (which could affect their biological properties), their defined number of functional groups and their distinct inner (shell) and outer parts (surface) (Malmström and Hult 1997; Boas and Heegaard 2004). This last point is interesting as it allows the introduction of drugs in two different ways: they can either be hidden in the shell of the dendrimers (for non-covalent encapsulation of hydrophobic drugs); or can be covalently bound on the dendrimer surface (targeting and/or solubilising moieties, emergence of combination therapy).

Currently, several dendrimers such as PAMAM, poly(propyleneimine) (DAB), or poly(ethylene oxide) (PEO) grafted carbosilane are being studied and present research focuses on elucidating their structure-biological properties relationship (i.e. effect of dendrimers' generation and surface functionality on cytotoxicity and haemolytic compatibility) (Malik *et al.* 2000; Wiwattanapatapee *et al.* 2000; Cloninger 2002) (Figure 1.8). Dendrimers have been explored in the field of drug delivery as anticancer, antiviral, antibacterial drugs, magnetic resonance imaging contrast agent and as DNA transfection agents (Tack *et al.* 2006a; Tack *et al.* 2006c; b). Recently, the first dendrimer-based drug (PLL dendrimer, VivaGel™) entered clinical trials as a vaginal anti HIV virucide in the form of a gel (McCarthy *et al.* 2005). Nevertheless, many of these synthetic macromolecules are too toxic to be administered and used *in vivo*, thus further investigation is needed to establish if they are safe enough to move on to clinical studies (Duncan and Izzo 2005).

Star polymers

Star polymers (Figure 1.20) are also three-dimensional hyperbranched structures. However, in this case identical or distinct (in composition and/or molecular weight) linear arms emanate from one central body or core. Their physico-chemical properties (smaller hydrodynamic radius, lower solution viscosity, less flexibility compared to their linear counterparts) and their 3D shape and hyperbranched structure (increase of end-groups functionality and their distinct core and surface parts) make them perfect candidates for the design of novel polymer therapeutics, although research in this area is rather limited to date compared with the extensive work done with linear polymers and dendrimers (reviewed by Qiu and Bae (2006)).

Star polymers can be obtained by living ionic polymerisation (Hong *et al.* 1999; Hadjichristidis *et al.* 2001), group transfer polymerisation (Georgiou *et al.* 2004; Georgiou *et al.* 2006), and can be prepared with CRP (Matyjaszewski *et al.* 1999; Kamigaito *et al.* 2001; Matyjaszewski and Xia 2001; Mayadunne *et al.* 2003; Chen *et al.* 2006). The two former techniques will not be further discussed, as the scope of this project was narrowed to radical polymerisation processes.

Controlled Radical Polymerisation

CRP* (Darling 2000; Darling *et al.* 2000) is one of the most rapidly developing areas of polymer science with more than ten papers published per week. It provides living characteristics to radical polymerisation, allows the control of molecular weight and the synthesis of narrow dispersed polymers (below 1.1 with optimal conditions), with well-defined complex architecture (Matyjaszewski 2003). Figure 1.22 illustrates some of the possible structures that can be prepared by copolymerisation using CRP methods.

Four CRPs have been developed so far, namely ATRP (Kato *et al.* 1995; Wang and Matyjaszewski 1995a), Nitroxide Mediated Polymerisation (NMP) (Solomon *et al.* 1986; Georges *et al.* 1993), INItiator-transFER-agent-TERminator techniques (INIFERTER) (Otsu and Yoshida 1982; Otsu *et al.* 1982) and Reversible Addition

* In the literature, CRPs are also well known as **living/controlled polymerisation** and **living polymerisation** and despite the wide use of both terms, it will be referred to as CRP in this thesis.

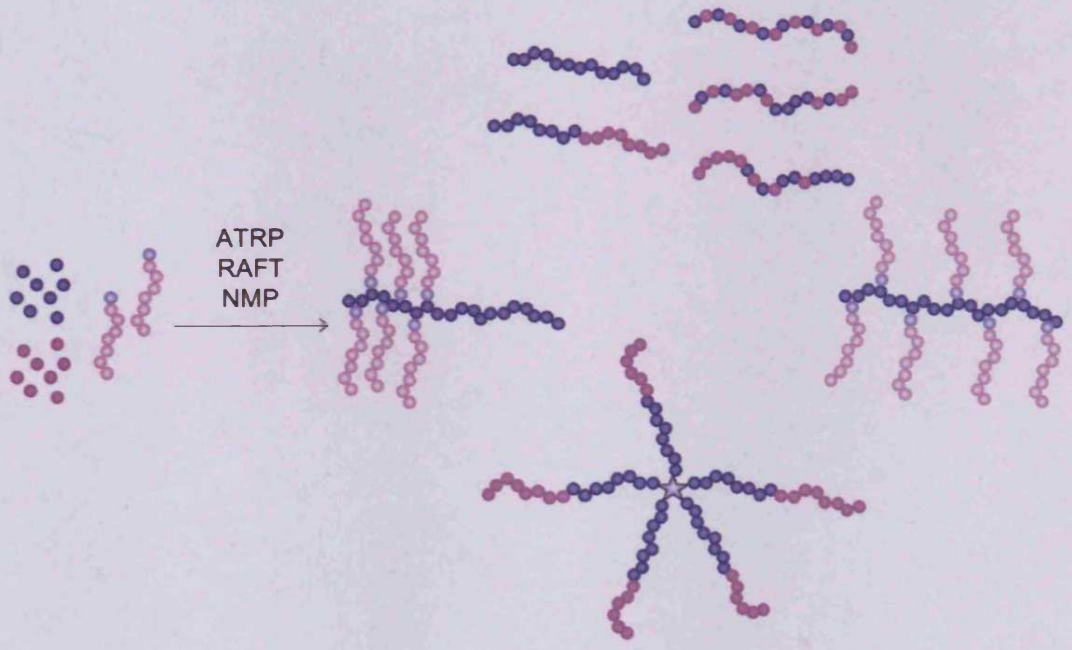

Figure 1.22: Examples of controlled topology and composition with CRP (adapted from Matyjaszewski (2003))

Fragmentation Transfer (RAFT) (Chiefari *et al.* 1998; Hawthorne *et al.* 1999; Goto *et al.* 2001; Quinn *et al.* 2001). They all involve the same strategy of mechanism (Kamigaito *et al.* 2001) (Figure 1.23), which aim to decrease the concentration of the growing radical species by introducing dormant species, and to reach a fast equilibrium between the active radicals and the dormant species, with the equilibrium being to a great extent on the side of the dormant species. This minimizes the probability of termination reactions and allows uniform growth of the polymer chains, thus narrowing polydispersity. As ATRP was used in this thesis, its mechanism is described below.

Atom Transfer Radical Polymerisation

ATRP was developed independently in 1995 by Matyjaszewski and co-workers (Wang and Matyjaszewski 1995a; Wang and Matyjaszewski 1995b; Patten and Matyjaszewski 1998) and Sawamoto's groups (Kato *et al.* 1995). The controlled synthesis of poly(styrene) (PS) in the presence of transition-metal complexes was then described by Matyjaszewski and co-workers (Wang and Matyjaszewski 1995a); and to date, ATRP is the most investigated CRP system due to its versatility (Matyjaszewski 2003).

It involves the use of transition metal complexes as catalysts to form adducts between organic halides and alkenes. This mechanism was formerly applied in organic chemistry with the Atom Transfer Radical Addition (ATRA) reactions to alkenes, thus leading to the analogy of names (Matyjaszewski 1997; 2002).

In short, the main goal of ATRP (Figure 1.24) is to create an equilibrium between dormant and propagating species, by reversibly activating:

1st) alkyl halides by redox reaction of a complexed metal with the terminal halogen group of the initiator and,

2nd) polymeric chains during the polymerisation.

As an initiating step, the oxidation of the metal M_t in the complex M_t^n-Y/ ligand leads to the homolytic cleavage of the carbon-halogen bond of the organic halide R-X. Consequently, the initiating radical species R$^{\bullet}$ and the oxidised metal complexed with the ligand (X-M_t^{n+1}-Y/ ligand) are formed. At this point, either chain propagation reactions or regeneration of dormant species R-X can occur by reaction of the radical R$^{\bullet}$ with either the monomer or the halogen on the oxidised metal, respectively.

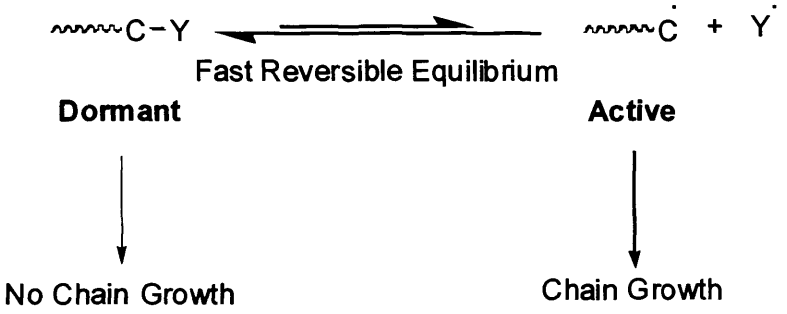

Figure 1.23: Controlled radical polymerisations strategy (adapted from Kamigaito *et al.* (2001))

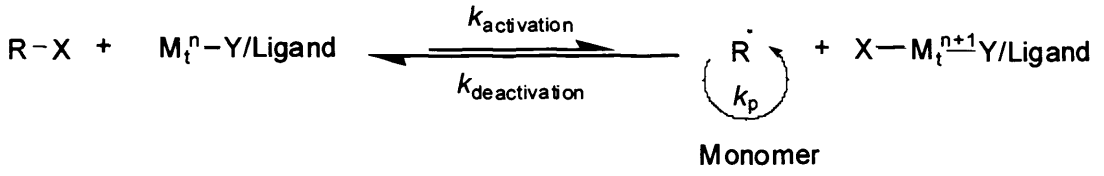

Figure 1.24: General Scheme of the ATRP mechanism (taken from Matyjaszewski and Xia (2001))

Where: R-X is an organic halide initiator, M_t^n a transition metal catalyst, Y a counterion or another ligand, R$^\bullet$ is a free radical or active species.

Maintaining a constantly low concentration of radicals in the reaction medium is the key feature of the ATRP mechanism as it reduces the number of termination reactions (radical coupling and disproportionation). It is achieved by attaining a constant reversible equilibrium weighted towards the dormant species.
Moreover, fast initiation and fast but reversible transformation of the radicals - into non-active species before addition of another monomer unit - lead to chain propagation and enable the uniform growth of all polymer chains, thus narrow polydispersity and functionalised end-groups are achieved.

The components of this complicated technique - an adequate initiator with transferable halogen, a suitable catalyst system composed of a transition metal species and an appropriate ligand or complexing agent - need to be carefully selected to obtain the desired polymers. Furthermore, solvent, temperature and reaction time can be altered to optimise the conditions of the process.
Several efficient ATRP systems have been developed for many monomers (such as styrene, (meth)acrylates, (meth)acrylamides, (meth)acrylic acids and acrylonitrile) as reviewed by Matyjaszewski and Xia (2001) and Kamigaito *et al.* (2001).
The typical and successful initiators used for ATRP are alkyl halides but many other types of halogenated compounds, such as benzylic halides, α-haloesters, α-haloketones, α-halonitriles and sulfonyl halides, can potentially be used as ATRP initiators.
A number of transition metal complexes have been applied to ATRP, and they can be classified following their periodic groups (Group 6: molybdenum and chromium; group 7: rhenium; group 8: ruthenium and iron; group 9: rhodium; group 10: nickel and palladium; group 11: copper).
The main role of the ligand is to solubilise the transition-metal in the solvent used and allow the metal centre to reach its appropriate redox potential to enable the atom transfer. They can be classified into two main groups: the nitrogen based ligands (for copper- and iron-mediated ATRP) and the phosphorus based ligands (efficient in complexing most of the transition metals studied in ATRP).

Star Polymer Synthesis: the Arm-first and Core-first Approaches

Similarly to some extend to the synthesis of dendrimers, star polymers can also be prepared by two main routes: the arm-first approach and the core-first approach.

The strategy of the *arm-first approach* is to first synthesise living or semitelechelic linear arms of the future star and then link them to one another. This can be achieved in radical polymerisation by (Figure 1.25):

(a)- the synthesis of the linear arms of the star in a first step, followed by their copolymerisation with a divinyl compound, which eventually form small crosslinkage (corresponding to the core of the star) (Quirk *et al.* 1999).

(b)- the synthesis of semitelechelic linear polymers in a first step with then their conjugation to the core. As an example, Kopeček and co-workers (Wang *et al.* 2000) described the synthesis of star PHPMA by the arm-first approach, where linear and semitelechelic PHPMA were conjugated to a PAMAM core.

The strategy of the *core first approach* is to first synthesise a multifunctional core, which is able, in a second step, to initiate the polymerisation of the monomer, and the arms of the star polymer are directly growing from the core (Figure 1.26). This can be achieved by ATRP using multifunctional initiators (i.e. initiators with more than two reactive carbon-halogen bonds) as reviewed by Matyjaszewski and Xia (2001). The first star polymer prepared by the core first approach ATRP was done in 1995 with the polymerisation of styrene using hexakis(bromoethyl)benzene as a multifunctional initiator (Wang *et al.* 1995).

Synthetic Challenges and Characterisation Issues

Both the core- and arm-first approaches raise some challenges in terms of uniformity of the produced stars and Figures 1.25 and 1.26 portray them.

In arm-first approach, where semi-functionalised polymeric arms are conjugated to a core (Figure 1.25, part (b)), the challenge is to achieve a full conjugation of the core. When using this method and after several conjugations, an increase in the steric hindrance, and consequently, a variation of the reactivity of the conjugation sites can occur. Also the removal of non-conjugated linear material is a challenging step. Futhermore, in the case of the formation of stars through propagation of a difunctional comonomer (Figure 1.25, part (a)), large and heterogeneous microgel are usually obtained. Finally, in the case of the core-first approach (Figure 1.26), the main drawbacks are the obtention of star polymers with non-uniformed arms, and the formation of star-star coupled materials.

In general, determining molecular weight of star polymer is more demanding than for linear polymers. Due to an increase of segment density and compactness, the

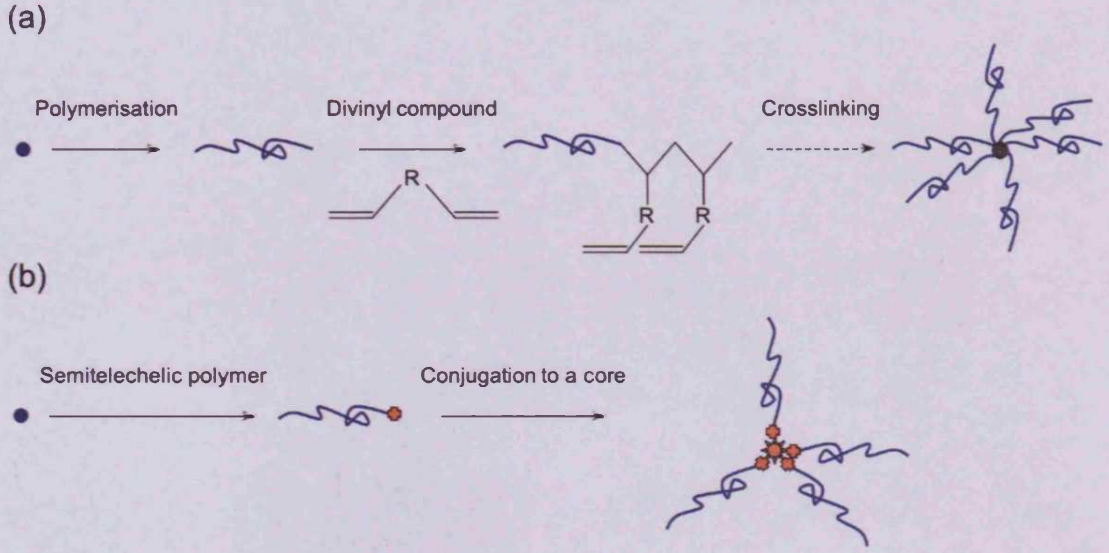

Figure 1.25: Synthesis of star polymers by the arm-first approach

Where ● represents the monomer, the linear polymer, the functionalised end-group of the semitelechelic linear polymer and the core.

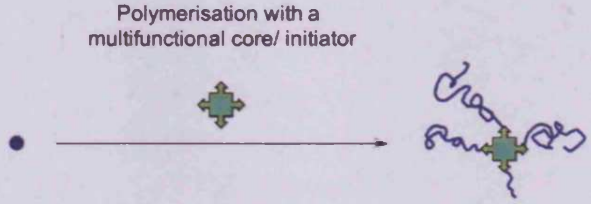

Figure 1.26: Synthesis of star polymer by the core-first approach

Where ● represents the monomer, the multifunctional initiator and the linear polymeric arms of the star.

hydrodynamic volume of star polymers can dramatically decrease compared to their linear homologues. Therefore, molecular weight will be underestimated when determined by conventional Gel Permeation Chromatography (GPC) calibrated with linear standards, as this technique is based on size exclusion (GPC principle and technique are described in detail in Chapter 2). Thus, the use of several techniques, such as Atomic Force Microscopy (AFM) (Antony *et al.* 2004), Nuclear Magnetic Resonance (NMR), light scattering (Themistou and Patrickios 2007) and triple detector GPC (light scattering, viscosimeter and reflective index) should be pursued to obtain relevant information on molecular weight and on the overall composition of stars (Angot *et al.* 1998; Matyjaszewski *et al.* 1999).

Star polymers in the field of polymer therapeutics

It is believed that the design of more complex architectures of the polymer carrier of therapeutic compounds would lead to a more elaborated second generation of polymer therapeutics. As star polymers offer many advantages (e.g. increase in end-group number, core/arm/surface groups domains, globular shape, rigidity, etc.) and as a lot of progress was recently made in polymer chemistry, various theoretical designs of star-based polymer therapeutics could be made (Figure 1.27). For instance, the formation of a biodegradable star polymer from its core, or from its polymer arms (with a biodegradable polymer such as PGA); or a biostable construct could be attractive. Also, variation of the molecular weight of the arms of the star polymer, or its number of arms can be modulated. Moreover, star homopolymer, star block copolymer or star polymer with miktoarms (i.e. star polymer that has its arms made of different homopolymers) would offer a no exhaustive library of constructs with potential for drug delivery.

Thus, determining their potential, efficiency and cytotoxicity as carriers in the field of polymer therapeutics is of great interest, and as an example, Kopeček and co-workers worked on the synthesis of star PHPMA with a PAMAM dendrimer core (Wang *et al.* 2000). They studied their potential as drug delivery systems after conjugation of doxorubicin. They showed that star-like polymer-doxorubicin conjugates were less cytotoxic than the linear conjugates and explained the differences as an influence of the architecture on both the rate of cell entry as well as the release rate of doxorubicin through lysosomal enzyme action.

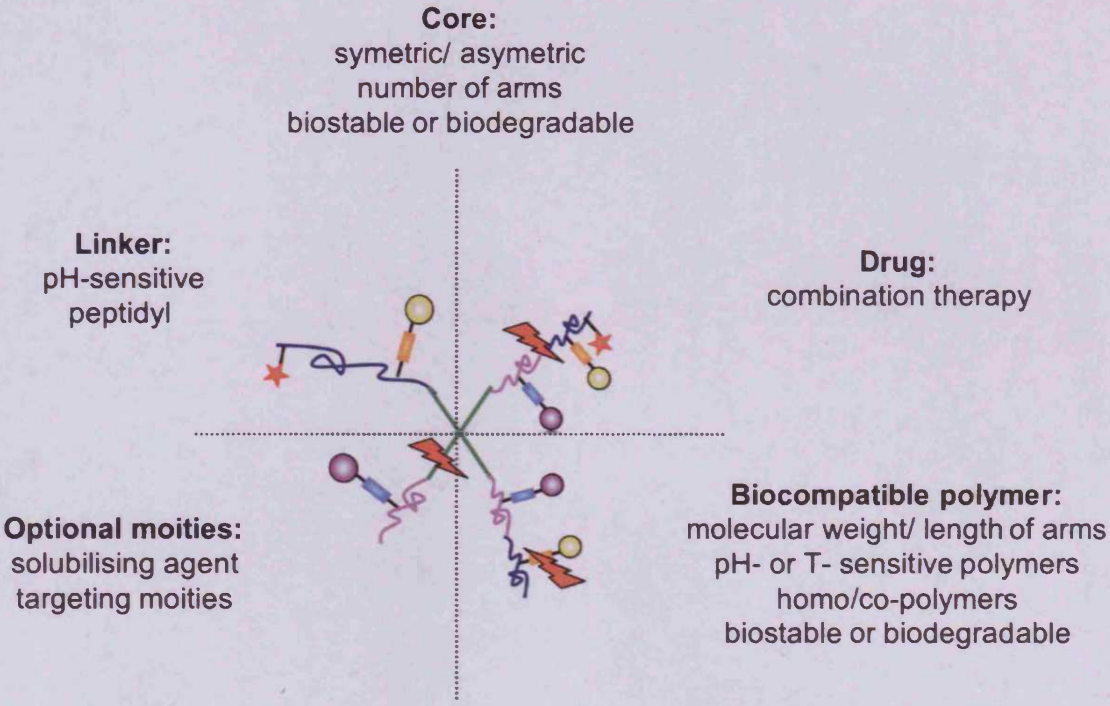

Figure 1.27: Schematic representation of theoretical star polymer-drug conjugates

Where and are the drugs, and the linkers, and the polymers, an optional moiety (targeting, solubilising), the core of the star polymer-drug conjugate and the cleavage possibility.

1.9. Aims of the project

As previous studies have shown that the cellular uptake (Xyloyiannis *et al.* 2003; Seib *et al.* 2007) and the intracellular release of a conjugated drug (Wang *et al.* 2000) are dependent on several parameters, such as molecular weight, composition, pK_a and architecture of the carrier studied, the idea of the development of a second generation of polymer therapeutics with non-linear carriers is attractive.
Also, non-unique structure, heterogeneity in composition and lack of control over polydispersity of the polymer carrier can affect the pharmacological behaviour and reproducibility of the therapeutic outcome of the polymer-based nanoconjugates.

Therefore, the onset aim of this thesis is the synthesis and characterisation of well-defined star polymers as carriers for the specific transport of drugs or oligonucleotide fragments. Additionally, the comparison of their biological properties, such as cytotoxicity, in relation to molecular parameters, such as, molecular weight, charge density, composition and architecture has also been studied. This project mainly focuses on seven monomers and their polymers, all introduced in the following Chapters. The selection process was carried out based on the principle that in the field of polymer therapeutics, there is a need and interest for water-soluble biocompatible polymers containing functional groups (for example: cationic groups for further condensation of DNA or for conjugation to drugs).

Chapter 2 describes the materials and methods used in this project. Chapter 3 introduces the synthesis of monomers and their linear water-soluble polymers by FRP. The effect of the molar ratio initiator to monomer on the molecular weight is also studied. In Chapter 4, the use of CTA in FRP is studied for the synthesis of semitelechelic polymers with control of molecular weight. ATRP was then optimised for the synthesis of water-soluble linear (Chapter 5) and star (Chapter 6) homopolymers with potential in polymer therapeutics. Chapter 7 deals with preliminary biological results obtained on the cytotoxicity of selected polymers with respect to molecular parameters (molecular weight, amine substitution, charge density). Finally, Chapter 8 provides a general conclusion/discussion on the main results achieved in this project.

2

Materials & General Methods

2.1. Equipment

2.1.1. Analytical

The manufacturer information and description of the analytical equipments used in this project are all listed in Table 2.1.

2.1.2. Cell culture

With the exception of the centrifugation steps, work with cells was performed in Bioair and Microflow Class II laminar flow hoods (Bioair Italy and Servicecare UK, respectively). For general tissue culture work, an inverted bright field microscope was used (Leica Germany). For routine cell counting, silver stained Neubauer haemocytometer (Marienfield Germany) was used. Tissue culture flasks (25, 75 and 150 cm^2) and tissue culture sterile 96-well plates were from Corning Inc USA. Sterile pipettes were from Elkay UK as well as 7 mL vials, universal containers and 60 mL pots.

2.2. Materials

Information of the materials and chemicals used in this thesis are summarised in Table 2.2 (general chemicals), Table 2.3 (chemicals used for the calibration of analytical instruments), Table 2.4 (chemicals used for purification and analysis experiments) and Table 2.5 (chemicals and materials used for the cell culture experiments).

2.3. General methods

The methods specified below describe the common procedures used in this thesis. In some cases, a more detailed description of specific technical or synthetic methods is given in the experimental chapters.

2.3.1. Elementary analysis

EA was carried out externally by MEDAC Ltd UK. The composition and purity of the products were confirmed using a static combustion system (CEC elemental analyser). The products (10 mg) were placed in eppendorf and sent off to MEDAC Ltd. EA of carbon, hydrogen and nitrogen elements were performed twice on each analysed sample. Results are presented as the average of both runs.

Table 2.1: Description and manufacturer information of the analytical equipment used

Analytical Equipment	Abbreviation	Model/ Description	Supplier/ Manufacturer
Aqueous Gel Permeation Chromatography System	Aqueous GPC	*Polymer Laboratories GPC system*	Polymer Laboratories UK
		Jasco PU-980 Intelligent High-Performance Liquid Chromatography pump	Jasco LtD UK
		TSK Progel PW_{XL} guard column (6 mm × 40 mm)	VISCOTEK UK
		2 ViscoGEL columns in series (both 7.5 mm x 300 mm): • TSK-gel G3000 PW_{XL}- particle size 6 µm • TSK-gel G4000 PW_{XL}- particle size 10 µm	
		Manual Injector (20 µL)	COTATI USA
		Differential Gilson 133 refractive index (detection)	Gilson Inc USA
		Caliber software (data analysis)	Polymer Laboratories UK
Organic Gel Permeation Chromatography System	Organic GPC	*Polymer Laboratories GPC 20 integrated system* Micro-volume doublepiston pump ResiPore guard column (50 mm x 4.6 mm) 2 ResiPore columns in series (particle size 3 μm, both 7.5 mm x 300 mm) Manual injector with integrated Rheodyne 7725i valve (100 µL) Deflection refractive index (detection) CIRRUS™ GPC software version 2.0 (data analysis)	Polymer Laboratories UK

Table 2.1: Description and manufacturer information of the analytical equipment used (Continued)

Analytical Equipment	Abbreviation	Model/ Description	Supplier/ Manufacturer
Ultraviolet	UV	Sunrise UV absorbance plate-reader	Tecan Austria
Fourier Transform Infra-Red	FT-IR or IR	Nicolet Avatar E.S.P. 360 FT-IR Spectrometer EZ OMNIC E.S.P 5.2 software (data analysis)	Thermo Scientific UK
Nuclear Magnetic Resonance	NMR	UltraShield™ 500 spectrometer	Bruker UK
Melting Points	m.p.	Griffin melting point apparatus Soda glass capillary tubes with sealed ends (100 mm)	Griffin Education USA Samco
Freeze drier	-	Flexi Dry FD-1.540 freeze dryer Vacuum pump	FTS Systems USA Javac Australia
Elementary Analysis*	EA	CEC elemental analyser	MEDAC Ltd UK
pH meter	pH	Checker pH meter	Hanna Instruments UK
Sonicator	-	Decon FS300b ultrasonic bath	York Glassware Services Ltd UK

*: experiments were carried out externally.

Table 2.2: List of general chemicals

Identification	Abbreviation	Supplier	Used for/ as
Acetic acid	-	Sigma-Aldrich UK	General use
Sodium bicarbonate	$NaHCO_3$	"	
Magnesium sulfate	$MgSO_4$	"	
Hydrochloric acid solution - 0.5 N	HCl	"	
Potassium hydroxide	KOH	"	
Sodium hydroxide	NaOH	Fisher UK	
Sodium chloride	NaCl	"	
***N,N*- dimethylformamide**	DMF	Fisher Scientific UK	Analytical grade solvents
Dimethyl sulfoxide	DMSO	"	(unless otherwise stated)
Dichloromethane	CH_2Cl_2	"	
Chloroform	$CHCl_3$	"	
Tetrahydrofuran	THF	"	
Acetone	-	"	
Methanol	-	"	
Ethanol	-	"	
Diethyl ether	-	"	
Acetonitrile	ACN	"	
Ethyl Acetate	-	"	
Dicyclohexylcarbodiimide	DCC	Lancaster UK	Dehydrating agent
***N*-hydrosuccinimide**	HOSu	"	Activating agent
Triethylamine	-	Lancaster UK	Bases
4-(dimethylamino)pyridine	DMAP	Sigma-Aldrich UK	

Table 2.2: List of general chemicals (Continued)

Identification	Abbreviation	Used after	Supplier	Used for/ as
Acryloyl chloride	-	distillation	Fluka UK	Monomer synthesis
Methacryloyl chloride	-	distillation	Acros Organics UK	
1-amino-2-propanol	-	-	"	
1,3-diaminopropane	-	-	"	
Di-*tert*-butyl dicarbonate	-	-	Sigma-Aldrich UK	
N*-(2-hydroxypropyl)methacrylamide	HPMA	-	MLS GmbH Leuna	Monomers
2-aminoethyl methacrylate hydrochloride	AEM	-	Acros Organics UK	
[2-(methacryloyloxy)ethyl] trimethylammonium chloride	quaternized AEM or qAEM	-	Sigma-Aldrich UK	
(3-acrylamidopropyl) trimethylammonium chloride	quaternized APAAm or qAPAAm	-	"	
***N,N'*-dimethylaminoethyl methacrylate**	DMAEM	distillation	Lancaster UK	
***N*-isopropylacrylamide**	NIPAAm	crystallisation in hexane	Acros Organics UK	
4,4'-azobis(4-cyanopentanoic acid)	ACA	-	Fluka UK	Azo-initiators
2,2'-azobis(isobutyronitrile)	AIBN	-	"	
3-mercaptopropionic acid	MPA	-	Acros Organics UK	Chain Transfer
2-mercaptoethanol	ME	-	"	Agents (CTA)
Ethyl α-bromoisobutyrate	-	-	Lancaster-Aldrich UK	ATRP initiators
Ethyl 2-bromopropionate	-	-	"	
Methyl α-bromophenylacetate	-	-	"	
Copper (I) bromide	Cu(I)Br	-	Sigma-Aldrich UK	Metal-based catalyst

*: HPMA was also synthesised in Chapter 3 according to the method described by Kopeček and Bazilova (1973).

Table 2.2: List of general chemicals (Continued)

Identification	Abbreviation	Used after	Supplier	Used for/ as
1,1,4,7,10,10-hexamethyl triethylenetetramine	HMTETA	-	Sigma-Aldrich UK	ATRP ligands
2,2'-bipyridyl or bipyridine	-	-	Lancaster UK	
Xylitol	-	-	Sigma-Aldrich UK	Cores of multifunctional ATRP initiator
Tripentaerythritol	-	-	Acros Organics UK	
Polypropylenimine tetraamine dendrimer generation 1	DAB-Am-4	-	Sigma-Aldrich UK	
Polypropylenimine octaamine dendrimer generation 2	DAB-Am-8	-	"	
α-bromoisobutyryl bromide	-	-	Sigma-Aldrich UK	Multifunctional ATRP initiator synthesis

Table 2.3: List of materials and chemicals used for calibrating the analytical instruments

Identification	Abbreviations	Supplier	Used for/ as
Phtalate buffer solution pH 4	-	Fisher Scientific UK	Calibration pH meter
Phosphate buffer solution pH 7	-	"	
Pullulan Poly(saccharide) Calibration Kit SAC-10 (molecular weight ranging from 738 to 112 000 g.mol^{-1})	-	Polymer Laboratories Ltd UK	Aqueous GPC monodisperse polymeric standard
Poly(styrene) EasiCal® Pre-prepared Calibration Kit (molecular weight ranging from 580 to 377 400 g.mol^{-1})	PS	Polymer Laboratories Ltd UK	Organic GPC monodisperse polymeric standards

Table 2.4: List of chemicals used for the analytical and purification experiments

Identification	Abbreviation	Technique	Supplier	Used for/ as
Phosphate buffer saline tablets	PBS	Aqueous GPC	Fluka UK	Aqueous GPC mobile phase
Sodium azide	NaN_3		Lancaster UK	Stabiliser of PBS mobile phase
Nylon membrane filters (0.2 µm)	-		Whatman International Ltd England	Filtration PBS *mobile phase*
High Performance Liquid Chromatography (HPLC) grade tetrahydrofuran	THF	Organic GPC	Fisher Scientific UK	Organic GPC mobile phase
Toluene	-		"	Internal flow marker for the organic GPC
2,6-di-*tert*-butyl-4-methylphenol	BHT		Sigma-Aldrich UK	Stabiliser of THF mobile phase
Single-use syringe filters (0.2 µm)	-	Aqueous and Organic GPC	Sartorius Germany	Filtration GPC samples
Deuterated dimethylsulfoxide	DMSO-d_6	NMR	Sigma-Aldrich UK	Solvents used for NMR analyses
Deuterated chloroform	$CDCl_3$		"	
Deuterated water	D_2O		Fluorochem UK	
Hydrochloric acid solution 5M	HCl	Titration	Fisher Scientific UK	Chemical used for titration
Sodium chloride	NaCl		"	
Sodium hydroxide anhydrous pellets	NaOH		Sigma-Aldrich UK	
Spectra/Pore 7 dialysis membranes (2 000 g.mol^{-1} cut-off)	-	Dialysis	Spectrum Laboratories Inc USA	Materials used for dialysis

Table 2.5: List of materials and chemicals used for cell culture

Identification	Abbreviation	Supplier
Murine melanoma cell line	B16F10	ATCC USA
Rose Park Memorial Institute 1640 medium with L-glutamine	RPMI	Invitrogen Life Technologies UK
0.05 % w/v trypsin with 0.53 mM sodium ethylenediaminetetraacetic acid	Trypsin-EDTA	"
Foetal bovine serum	FBS	"
3-(4,5-dimethylthiazol-2-yl)-2,5-diphenyl-2H-tetrazoliumbromide	MTT	Sigma-Aldrich UK
Trypan blue	-	"
Sterile optical grade DMSO	DMSO	"
Poly(ethyleneimine) (50 % w/v in water; M_w = 750 000 g.mol^{-1})	PEI	"
Dextran (Molecular weight from 64 000 to 76 000 g.mol^{-1})	-	"

2.3.2. Fourier Transform Infra-Red Spectroscopy

Dried and bulk samples (~ 5 mg) were scanned (128 scans) with wavenumbers ranging from 750 to 4000 cm^{-1}. Data were plotted as transmittance (%) in function of the wavenumber (cm^{-1}) and analysed using EZ OMNIC E.S.P 5.2 software.

2.3.3. Melting point

The products (~ 1 mg) were carefully placed in the bottom of a sealed capillary soda glass tube. The tube was then placed in the m.p. apparatus and the temperature was slowly and manually increased. At first sight of melting of the product, the temperature was noted and defined as the m.p..

2.3.4. Nuclear Magnetic Resonance Spectroscopy

For low molecular weight molecules (monomers and intermediate compounds of the synthesis of monomers), ~ 10 mg of compound was placed in a clean and dry NMR tube. In the case of high molecular weight compounds (polymers), at least 40 mg of the product was placed in the tube. The appropriate deuterated solvent (0.6 mL); depending on the sample solubility; was then added and the solution was allowed to homogenise for at least 0.5 h. NMR spectra were acquired with operating frequencies of 500 MHz (^{1}H-NMR, ~ 10 min) and 125 MHz (^{13}C-NMR, ~ 30 min for low molecular weight compounds and 4 h for polymers), processed and analysed by using the TopSpin® 2.0 software.

2.3.5. Characterisation of molecular weight and polydispersity using gel permeation chromatography

General principle

GPC, also known as Size Exclusion Chromatography (SEC), is an important analytical tool used to evaluate molecular weight characteristics of natural or synthetic polymers and proteins. Unlike HPLC, GPC relies, under ideal conditions, on a pure physical separation, where theoretically no chemical interactions of the sample with the GPC column (stationary phase) should be observed (Billingham and Jenkins 1972; Painter and Coleman 1997). To be more precise, GPC separates molecules upon their size **in solution**, which is directly proportional to their **hydrodynamic volume** (V_h).

Briefly, GPC involves size separation of the sample through a column packed with beads of a porous gel. Particularly large molecules cannot fit in the porous spheres and are washed out of the column first. These large molecules represent the ***exclusion limit*** of the column, and the volume of mobile phase required to elute them is called the ***void volume,*** V_V. Smaller molecules can permeate through the beads of gel; the smaller they are, the greater their retention is (Young and Lovell 1991) (Figure 2.1). Very small molecules behave in the same way as eluant (Young and Lovell 1991). The resulting separation reaches its limit and the volume required is known as the ***total permeation volume,*** V_T. The interstitial volume V_I is defined as followed (Equation 2.1):

$$V_I = V_T - V_V \qquad \text{(Eq 2.1)}$$

The most important pieces of information obtained from GPC are the number-average molecular weight (M_n), the weight-average molecular weight (M_w) and the polydispersity indices (M_w/M_n). Equations 2.2 to 2.4 define those numbers.

$$\overline{M_n} = \frac{\sum_i |N_i M_i|}{\sum_i N_i} \qquad \text{(Eq 2.2)}$$

$$\overline{M_w} = \frac{\sum_i |N_i M_i^2|}{\sum_i N_i M_i} \qquad \text{(Eq 2.3)}$$

$$PDI = \frac{\overline{M_w}}{\overline{M_n}} \qquad \text{(Eq 2.4)}$$

where N_i represents the number of polymer of a mass M_i.

V_h is not only dependent on the molecular weight of the analytes, but also on their conformation in solution, which is also directly linked to the solvent used as eluant. For example, the more effective the solvent - GOOD solvent - (or mobile phase), the higher the V_h of the dissolved molecule, thus the shorter its retention time and the higher its apparent molecular weight will be. The opposite will happen with a BAD solvent. Another important point is that the architecture of the analytes influences molecular weight characterisation. Indeed, the GPC systems used in this work were calibrated with linear narrow polydisperse pullulan (poly(saccharide)) and PS standards. These standards cannot give an absolute value for the characterisation of

Figure 2.1: Schematic representation of the GPC system and its separation principle

Molecules are separated on the basis of their size in solution (V_h) and are detected by a concentration detector (e.g. RI). The smaller V_h, the longer the molecules will take to permeate and hence the later the signal will appear on the chromatogram.

other non-linear polymers and other polymer chemistries, as they will have a different V_h. Hence, it is important to note that GPC gives a **relative** molecular weight.
Moreover, a protein of a given molecular weight will have a smaller V_h than a random coil polymer of the same molecular weight. Thus longer retention times will be observed for a globular-shaped protein, giving a smaller apparent molecular weight than seen for a random-coil polymer of the same molecular weight.
GPC is a very important tool for polymer characterisation and was widely used in this thesis, however, results should always be carefully considered and always related to the standards and eluant used; as well as the chemistry of the analytes.

In this project, two types of GPC were used, namely an aqueous-based system (mobile phase: PBS) and an organic-based (mobile phase: THF) system. The mobile phase preparation, column calibration, sample preparation and methods used for both systems are described more in detail in the following paragraphs.

Preparation of the mobile phase used*

Aqueous GPC

For 1 L of PBS eluent, 5 PBS tablets were dissolved up to 1 L with double distilled water. 1 mg of sodium azide was added to the solution to prevent bacterial growth in the buffer. The solution was then filtered through a nylon membrane filter (0.2 μm) and sonicated for 0.5 h before use.

Organic GPC

To a new HPLC grade THF bottle (2.5 L), 625 mg of BHT (250 ppm) was added as a solid to stabilise the mobile phase. The organic solution was then used without further preparation as the organic GPC system was equipped with a degasser.

Calibration of the GPC columns

Rationale for the choice of the GPC standards

Two sets of standards were selected, namely pullulan and PS standards. As mentioned above, the choice of the calibrating standards is very important to be able

* Taking into account the type of polymers analysed in these studies, addition of 5 % triethylamine in the mobile phases should have been considesered to compete with the possible chemical interaction from the amine-based polymers with the columns, and thus disminish the probabilities of having non Gaussian-bell shape chromatograms

to get correct information on the molecular weight of the analytes, and thus they should be as similar as possible (if not chemically identical) to the polymeric analytes to be characterised. As this was not possible in our case, pullulan and PS were chosen as GPC calibrating kits are commercially available, and as they allow a relative comparison of the molecular weight and polydispersity of our synthesised polymers between them. Those numbers were always considered carefully and when necessary, an explanation of surprising molecular weights is given considering the chemistry of the standards they are compared to and relative to the conformation and hydrodynamic volume the synthesised polymers are taking into the mobile phase used.

Aqueous GPC

A TSK Progel guard column and 2 ViscoGel columns were used in series (Table 2.1) and the system was calibrated using a pullulan poly(saccharide) calibration kit (6 samples of narrow-disperse pullulan standards with the molecular weight ranging from 738 to 112 000 $g.mol^{-1}$). Six pullulan standards were prepared in PBS mobile phase (3 mg/mL), and allowed to dissolve for 0.5 h before filtration through single-use syringe filters (0.2 μm). A sample (40 μL) was then injected into the GPC loop (20 μL). The elution time was 30 min using a flow rate of 1 mL/min and the Caliber software was used to prepare a calibration curve relating molecular weight ($g.mol^{-1}$) to retention time (min), as depicted in Figure 2.2.

Organic GPC

In this case, a ResiPore guard column and the 2 ResiPore columns were used in series (Table 2.1) and the system was calibrated using a PS EasiCal® pre-prepared calibration kit. This kit consists of two different combs (A and B), each having 10 detachable spatulas and supporting a mixture of 5 polymer standards per spatula. The molecular weight ranged from 580 to 377 400 $g.mol^{-1}$. One spatula of each type of comb was placed in vials and the appropriate volume of THF mobile phase (10 mL) was added to rapidly dissolve the thin film of polymers and to produce 2 GPC calibration solutions (1 mg/mL). After 0.5 h, samples were filtrated through single-use syringe filters (0.2 μm) and injected (110 μL) into the GPC loop (100 μL).

The standards were allowed to elute for 30 min at a flow rate of 1 mL/min. A calibration curve molecular weight = f(retention time) was automatically generated using CIRRUS™ GPC software version 2.0 (Figure 2.3).

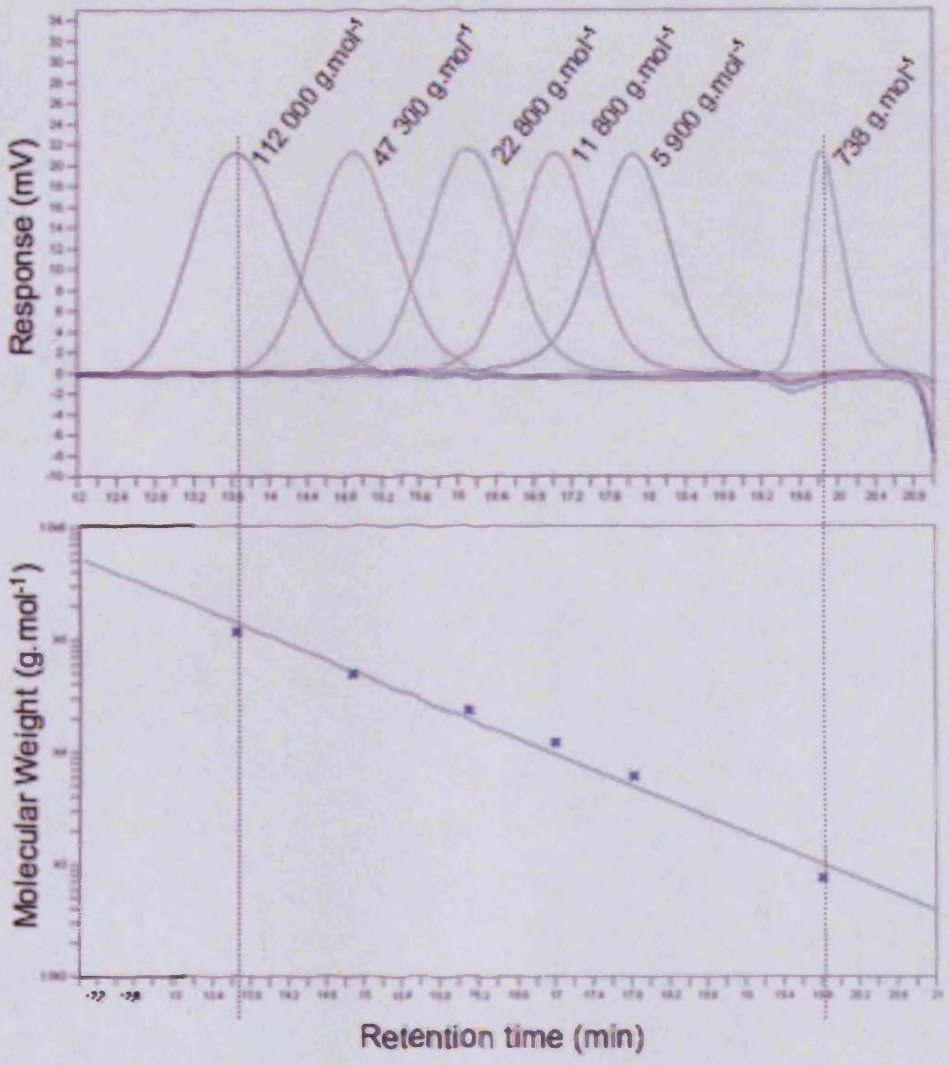

Figure 2.2: Chromatograms of monodisperse pullulan standards and the calibration curve for the aqueous GPC

Where the dotted lines indicate the limits of the calibration. PBS was used as the aqueous mobile phase

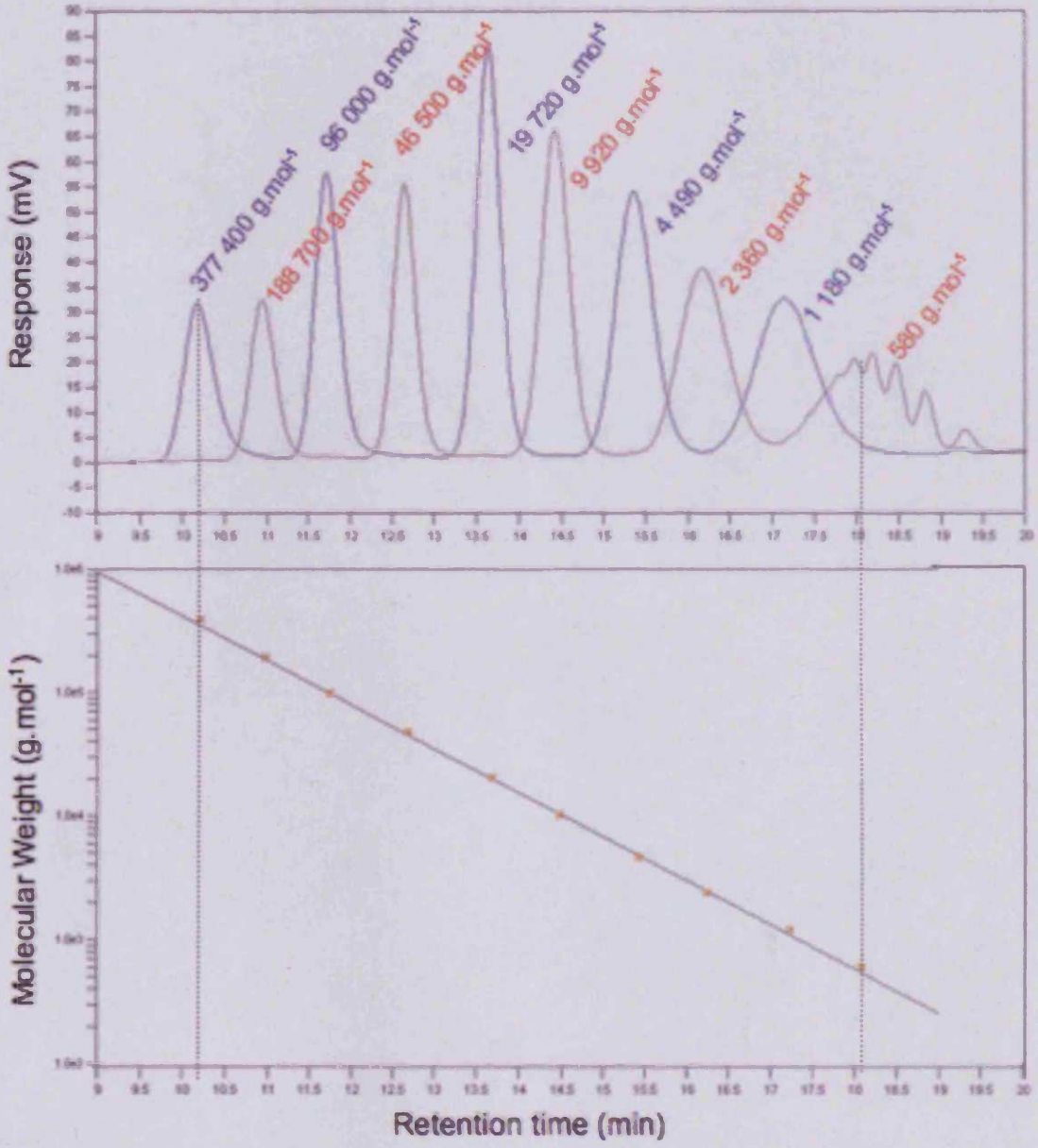

Figure 2.3: Chromatograms monodisperse PS standards and calibration curve for the organic GPC

Where the dotted lines indicate the limits of the calibration. THF was used as the mobile phase.

Sample preparations and running conditions

For both GPC systems, all polymer samples were prepared as follows: the analyte (~ 10 mg) were dissolved in 1 mL of the previously prepared and stabilised mobile phase (PBS or THF). In the case of organic GPC, toluene (20 µL) was added and was used as an internal flow marker. The analytes were allowed to fully dissolve for at least 0.5 h before filtration of the solutions through a single-use syringe filter (0.2 µm). Either 40 µL (aqueous GPC) or 110 µL (organic GPC) of the solutions were injected. A GPC flow rate of 1 mL/min was used and run for 30 min at 25 °C. The detection of the samples was done by differential refractive index, and as mentioned above, the data were analysed using the Caliber software (aqueous GPC) or the CIRRUS™ GPC software version 2.0 (organic GPC). The molecular weight characterisation of unknown samples was estimated from the calibration curves (Figures 2.2 and 2.3) and using manual integration.

2.3.6. Titration

The pK_a values of the monomers and polymers were determined by titration. The compound to be tested (30 mg) was dissolved in 30 mL of HCl solution (0.01 $mol.L^{-1}$) with a constant physiological NaCl environment (0.154 $mol.L^{-1}$). The solution was vigorously stirred while NaOH solution (0.01 $mol.L^{-1}$) in constant physiological NaCl environment was slowly added. The curves pH = f(volume of added NaOH solution) were plotted and the pK_a values were determined from either the first (strong base) or the second (weak base) inflexion point of the curve.

2.3.7. Cell culture

Cell culture was performed according to the guidelines given by The United Kingdom Co-ordinating Committee on Cancer Research (UKCCCR 2000). All cell work was carried out in a Class II laminar flow hood, pre-sterilised by Klericide® and 70 % v/v ethanol in double distilled water spray.

B16F10 cells were kept under aseptic conditions, without the addition of penicillin or streptomycin and they were micoplasma-free. PBS, double distilled water (both sterilised through autoclaving) and tissue culture medium containing 10 % FBS were used. Any disposable tissue culture equipment that came into contact with the hood was first sprayed with 70 % v/v ethanol in double distilled water. In addition, all

solutions that were added to cells were pre-warmed to 37 °C in a water bath containing 5 L of double distilled water and 1 mL Sigmaclean® water bath treatment.

Thawing of cryopreserved cells

Cryogenic vials of frozen cells were kept at -196 °C in liquid nitrogen until required. Upon use, the frozen vials were removed from liquid nitrogen and were defrosted in a 37 °C water bath. Cell suspensions were then added to a universal sterile container with 20 mL of media and were pelleted by centrifugation for 5 min at 1000 g. Supernatant was aspirated and cells were re-suspended in 5 mL of fresh media before being placed into 25 cm^2 flasks. Cells were then grown for 48 h in a 37 °C incubator. The growth of the cells was checked under the light microscope, the culture medium was then changed and the cells were allowed to grow and were passaged when confluency was reached.

Routine maintenance of cells and passaging

Cells were kept for less than 25 passages and were routinely viewed under a light microscope to check their growth. Cells were grown in vented 75 cm^2 tissue culture flasks in RPMI medium supplemented with 10 % FBS at 37 °C in humidified atmosphere with 5 % CO_2. The culture media was changed twice weekly to avoid depletion of essential nutrients. Only flasks with more than 70 % cell confluency were sub-cultured at a 1:10 split ratio, into 75 cm^2 flasks as described below.
Medium from confluent flasks was aspirated, leaving the adherent B16F10 cells on the bottom of the flask. The cells were then washed once with PBS and briefly incubated with 1 mL of trypsin-EDTA at 37 °C to cause cell detachment. Trypsin-EDTA was then inactivated by diluting it with 10 mL of tissue culture medium. Cell suspensions were centrifuged for 5 min at 243 g at room temperature. A 1 mL aliquot of cells re-suspended in fresh media was added to 9 mL of new medium inside new sterile 75 cm^2 flasks.

Cell counting and assessment of viability using trypan blue

Aliquots of suspended cells (100 µL) were mixed at a 1:1 v/v ratio with trypan blue (0.2 % trypan blue in PBS) in an eppendorf tube. Trypan blue is a blue dye able to penetrate dead cell membranes. Blue-stained cells are not viable, thus this method gives an indication of the number of viable cells in suspension after being placed in a haemocytometer slide.

Cells from ten × 0.1 mm^3 squares (five from the top and five from the bottom chamber of the haemocytometer) were counted using a light microscope. The average number of cells per mL of cell suspension was calculated as below (Equation 2.5):

$$Cells/mL = mean \times 2 \times 10^4 \quad \text{(Eq 2.5)}$$

Where the mean is the arithmetic mean of the ten values, 2 takes into account the trypan blue dilution and 10^4 accounts for the conversion from 0.1 mm^3 to mL.

The cell suspension was then diluted with the medium in order to obtain the appropriate seeding density required for the experiment.

Freezing cells for cryopreservation

Batches of cells were routinely frozen to maintain stocks. Cells were grown to confluency in 150 cm^2 flasks, trypsinised, centrifuged into pellets, re-suspended, counted as described above and diluted in the appropriate volume of freezing medium (90 % FBS + 10 % sterile DMSO) to give a 10^6 cells/mL suspension. Aliquots (1 mL) of this suspension were placed into 1 mL sterile and cryogenic vials, placed at -20 °C for 1 h, at -80 °C overnight and finally at -196 °C in liquid nitrogen the following day. They were stored until use.

2.3.8. MTT assay as a mean to assess cell viability: Growth curve

The MTT assay was initially introduced by Mosmann in 1983 as a method to assess cell viability (Mosmann 1983). Viable cells can reduce the yellow solution of the substrate (MTT, 5 mg/mL in PBS) into dark blue insoluble formazan crystals by a redox reaction mediated by the mitochondrial respiration products NADH and NADPH (Slater *et al.* 1963; Denizot and Lang 1986; Twentyman and Luscombe 1987; Sgouras and Duncan 1990; Vistica *et al.* 1991) (Scheme 2.1). The resulting formazan crystals readily dissolve in DMSO and the absorbance can be measured spectrophotometrically. Absorbance is proportional to the number of viable cells.

Determination of cell growth

On day 0, cells were seeded into sterile, flat-bottomed, 96-well plates (100 µL/well, seeding densities of $4 \cdot 10^4$ or 10^4 cells/mL) using a multi-channel pipette, and they were then allowed to settle for 24 h. The external well rows of the plate were filled with culture media to prevent surrounding wells from dehydrating.

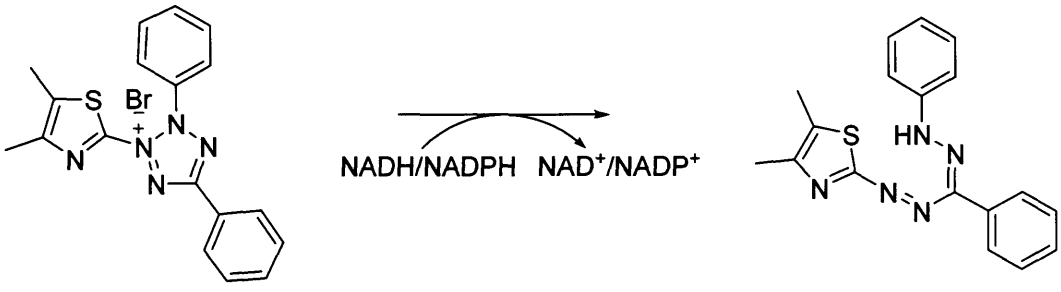

MTT (Yellow) **Formazan cyrstal** (Blue)

Scheme 2.1: Mechanism of action of MTT assay (taken from Mosmann (1983))

MTT stock solutions (5 mg/mL) were prepared by dissolving the compound in autoclaved PBS, before filtering them through a 0.2 μm filter. They were protected from light throughout and stored at 4 °C.

Each day, MTT stock solution (20 μL/well) was added to a row on the plate and the cells were incubated for a further 5 h. Then, the medium from the wells in this row (n = 6) was aspirated and replaced with optical-grade DMSO (100 μL/well) to solubilise the blue formazan crystals. The plates were then incubated for a further 30 min to allow the crystals to dissolve.

Absorbance was then read with a UV plate-reader (with an emission wavelength of λ = 550 nm). The formazan-DMSO mixture was then removed from the wells under local exhaust, and replaced with PBS (100 μL/well). Plates were returned to the incubator and this process was continued daily over a period of 7 days.

Growth curves were produced plotting the absorbance against time (Figure 2.4) and doubling times of ~ 10 h and ~ 48 h were measured for seeding densities of $4 \cdot 10^4$ and 10^4 cells/mL, respectively.

2.3.9. Evaluation of polymer cytotoxicity using the MTT assay

The MTT assay, as described in Section 2.3.8, was also used to establish the cytotoxicity of several synthesised polymers. Cells were used in their exponential phase of growth. Considering Figure 2.4, B16F10 cells were seeded on day 0 into a 96-well plate at a seeding density of 10^4 cells/mL (100 μL cell suspension/well in RPMI medium supplemented with 10 % FBS) and allowed to adhere for 24 h. On day 1, the medium was replaced by polymers in medium (from 0.001 to 10 mg/mL). Fresh medium alone was used as control. On day 4 (after a 72 h incubation), MTT solution (20 μL; 5 mg/mL in PBS) was added and the plates were incubated for a further 5 h. The media was then removed, and the formazan crystals dissolved in optical grade DMSO (100 μL). After incubation at 37 °C for 30 min, the plates were analysed by UV absorbance at λ = 550 nm. The results were expressed as a percentage of viable cells and as follows (Equation 2.6).

$$\text{Cell Viability (\%)} = \frac{Abs_{550x} \times 100}{Abs_{550Control}} \qquad \text{(Eq 2.6)}$$

Where: Abs_{550x} is the absorbance measured for the compound at a polymer concentration x

$Abs_{550Control}$ is the absorbance measured for control cells

(a)

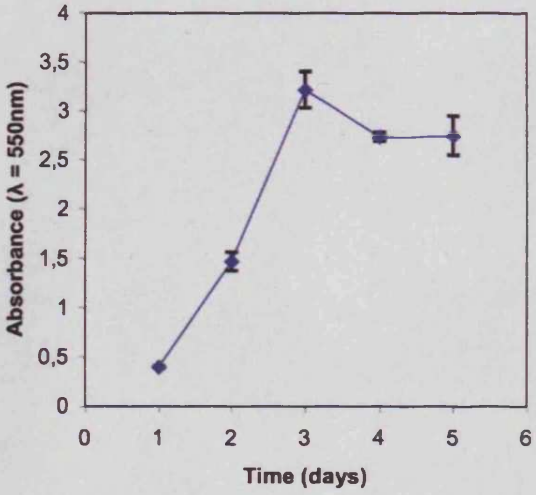

(b)

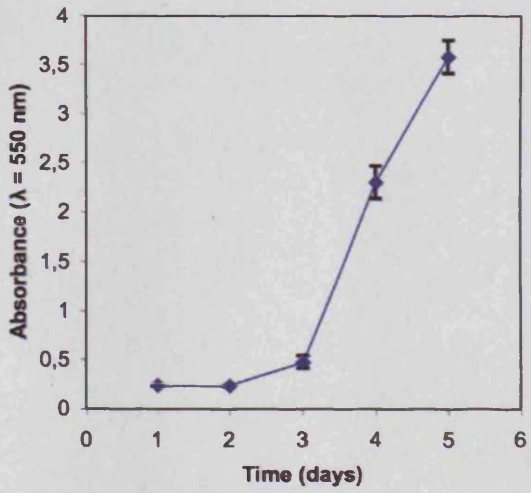

Figure 2.4: Growth curves of B16F10 cells

Panel (a): seeding density = $4 \cdot 10^4$ cells/mL, with a doubling time of ~ 10 h and panel (b): seeding density = 10^4 cells/mL, with a doubling time of ~ 48 h. Data show mean ± SEM, n= 6. When error bars are not visible they are hidden by the symbol.

The concentration-response curves generated from this data were then fit to the logarithmic function derived from the Hill Equation (Equation 2.7).

$$y = R_{min} + (R_{max} - R_{min})/(1 + (x/IC_{50})^{P}) \quad \text{(Eq 2.7)}$$

Where R_{max} was fixed at 100 and R_{min} was fixed at 0 (Kean *et al.* 2005).

The IC_{50} value is defined as the polymer concentration at which cell growth is inhibited by 50 % and computer generated IC_{50} values were compared with the values directly read on the graphs at 50 % of cell viability.

PEI (50 % w/v in water; M_w = 750 000 $g.mol^{-1}$) and dextran (from leuconostoc mesenteroides bacteria; molecular weight ranging from 64 000 to 76 000 $g.mol^{-1}$) were used as positive and negative controls, respectively.

Data were expressed as mean ± SEM. Statistical significance was set at $p < 0.05$ (indicated with * on the graphs in Chapter 7). When only two groups were compared, Student's t test for small sample size was used. If more than two groups were compared evaluation of significance was performed using one way Analysis Of Variance (ANOVA) followed by Bonferroni *post hoc* test.

3

Synthesis of Monomers & Polymers by Free Radical Polymerisation

3.1. Introduction

The purpose of these studies was to synthesise and characterise in depth a library of linear homo- and copolymers with different molecular weight, composition and pK_a value that might have potential to be used in the field of polymer therapeutics as carriers for drug, protein or oligonucleotide.

A goal of this thesis was to systematically assess the effect of each molecular parameter of the polymer (composition, molecular weight, architecture, pK_a and charge density) on polymer cytotoxicity (as further explained in Chapter 7) in comparison with the cytotoxicity of well-studied commercially available polymers (e.g. PEI). It was hoped to identify polymers suitable for future use in the design of biocompatible and efficient polymeric carriers.

3.1.1. Rationale for the choice of the polymerisation technique: FRP

As seen in Chapter 1 Section 1.8, several radical polymerisation techniques are available to polymer chemists for the synthesis of polymers of different composition, architecture, and with different molecular weight characteristics. Each technique gives a different level of control over these parameters. At the beginning of this study, FRP was chosen, as it is a versatile radical polymerisation technique that can easily be used to copolymerise several vinylic monomers, and thus it offers the opportunity to design linear polymers with different composition, pK_a and charge density. Moreover, even though FRP does not allow total control over molecular weight and polydispersity, by varying the reaction conditions (and more precisely, the initiator to monomer molar ratios), linear polymers of distinct molecular weight characteristics can be produced. Other polymerisation techniques, namely FRP with CTA (Chapter 4) and ATRP (Chapters 5 and 6) were later used to synthesise polymers with the same or different architectures in a more controlled manner.

3.1.2. Rationale for the choice of the monomers and their polymers to be studied

Figure 3.1 schematically represents the rationale for the choice of these monomers used in these studies.

The monomers used for these studies were chosen because:

(i) It was hoped that the polymers prepared would offer the opportunity of being used in the field of polymer therapeutics, i.e. they would be

Figure 3.1: Rationale for the selection of the monomers used in these studies

biocompatible, for gene therapy be able to condense genetic material (polycations), and/or for further conjugation to drugs or proteins have appropriate functional groups.

(ii) The polymers obtained would provide a library offering the possibility of studying systematically effects of charge and molecular weight on the cell viability (Chapter 7).

These studies mainly used six monomers for polymer synthesis, namely: AEM, DMAEM, qAEM, qAPAAm, HPMA and a protected *N*-tert-butoxycarbonyl-*N'*-acryloyl-1,3-diaminopropane (BOC-APAAm).

The first three are commercially available monomers (AEM, DMAEM, qAEM) and they have already been used by other research groups to synthesise amino-based methacrylate polymers as gene delivery vectors (Cherng *et al.* 1996; van de Wetering *et al.* 1998a; De Smedt *et al.* 2000; Rungsardthong *et al.* 2001); (Oupicky *et al.* 1999a; Oupicky *et al.* 1999b; Howard *et al.* 2000; Oupicky *et al.* 2000a; Oupicky *et al.* 2000b). They were selected here as they offer the possibility to study the influence of the substitution pattern of amine and polymer charge density on biological properties, without altering the chemistry of the whole polymer.

The monomers from the APAAm family (BOC-APAAm and qAPAAm) also form polymers that could theoretically be used for gene delivery after deprotection of the BOC residues, thanks to the charged pendant groups along the polymeric main chain. However, they give rise to amino-based polyacrylamides with different amine substitutions (primary or quaternized). In this case, degradation studies and comparison of the effects on biological properties with their homologous amino-based methacrylate polymers, PAEM and PqAEM, were used to study the potential of structure optimisation.

HPMA is a methacrylamide monomer that when homo- and copolymerised can give biocompatible polymers. These polymers have already been extensively studied in the fields of drug delivery and other biomedical applications (Morgan *et al.* 1996; Vasey *et al.* 1999; Duncan 2003).

One of the common features of cationic polymers is their cytotoxicity. An important need is to improve cationic vectors and decrease their side effects. A reduction in polycation charge density can be helpful and combination with hydrophilic polymers such as PEG (Rungsardthong *et al.* 2001; Petersen *et al.* 2002; Tang *et al.* 2003) and PHPMA (Oupicky *et al.* 1999a; Oupicky *et al.* 1999b; Howard *et al.* 2000; Oupicky *et al.* 2000a; Oupicky *et al.* 2000b) have been already employed for the synthesis of block and graft copolymeric DNA vectors.

Here, the synthesis of a library of statistical cationic copolymers was undertaken. When copolymerised with the aforementioned monomers (for instance AEM and DMAEM), HPMA would be expected to influence molecular parameters such as the charge density, the composition, and the molecular weight.

3.1.3. Technical aims

It was first necessary to synthesise HPMA monomer and the protected acrylamide monomer BOC-APAAm. This was done following the procedure previously described by (Kopeček and Bazilova 1973) and (Hobson and Feast 1999), respectively. The other monomers were all commercially available and used as received (except for DMAEM that was distilled before use).

To synthesise linear homopolymers with a range of molecular weight, composition, pK_a, and charge density and to establish the effect of the [I]/[M] ratios on the molecular weight, FRP of AEM, DMAEM, HPMA, qAEM, qAPAAm and BOC-APAAm was undertaken using different [I]/[M] ratios (from 0.58 to 3 %). Also, the cationic amino-based monomers AEM or DMAEM were copolymerised with HPMA and at different comonomer molar ratios ($[M_{cationic}]/\Sigma[M]$ = 0, 25, 50, 75, 100 %) in order to synthesise copolymers with a wide range of composition, pK_a, charge density and molecular weight.

In all studies, polymerisation parameters and characteristics of the synthesised polymers were investigated in-depth and GPC, ^{1}H- and ^{13}C-NMR, and titration were used for polymer characterisation.

3.2. Methods

3.2.1. General methods

The monomers and polymers synthesised were characterised using the techniques and methods previously described in Chapter 2, Section 2.3, e.g. m.p., IR, EA, ^{1}H-NMR, ^{13}C-NMR, GPC and titration studies were undertaken.

3.2.2. Monomer synthesis

Synthesis and characterisation of HPMA

HPMA was synthesised as previously described by (Kopeček and Bazilova 1973) (Scheme 3.1). Briefly, 1-amino-2-propanol (14.4 g, 0.192 mol) was dissolved in ACN (55 mL) and the solution was cooled down to 0 °C. A solution of methacryloyl chloride (10.0 g, 0.096 mol) in ACN (40 mL) was then added dropwise. The solution was stirred for 2 h at 0 °C and for 1 h more at room temperature. At the end of the reaction, the precipitate formed was filtered off, and the filtrate was concentrated. White crystals were isolated (30 % yield) by recrystallisation from THF and dried under vacuum at 30 °C. The product was analysed by m.p., IR, EA, ^{1}H- and ^{13}C-NMR.

The results obtained are summarised as follows. Key: the red letters are assigned to the protons and the blue numbers designate the carbon atoms. Wavenumbers $\bar{\nu}$ are expressed in cm^{-1}; ν represents the stretching vibrations and δ, the bending vibrations. For NMR data, δ are expressed in ppm and s is a singlet, bs a broad singlet, d a doublet, t a triplet, m a multiplet and J represents a coupling constant.

m.p.: 65°C ($m.p._{Theoretical}$ = 67°C).

EA: $N_{Experimental}$ = 9.78 % ($N_{Theoretical}$ = 9.78 %); $H_{Experimental}$ = 9.15 % ($H_{Theoretical}$ = 9.15 %); $C_{Experimental}$ = 57.78 % ($C_{Theoretical}$ = 58.72 %).

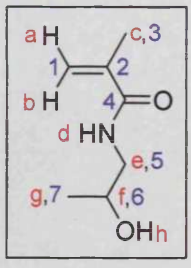

IR: $\bar{\nu}$ (cm^{-1}) = 1 655, strong band, $\nu_{C=O}$ (amide I); 1 617, strong band, $\nu_{C=C}$; 1 550, ν_{CN} (amide II); 1 330-1 200, δ_{NH} and δ_{OCN}.

^{1}H-NMR (DMSO-d_6, ppm): δ = 1.05, d, 3H, H_g, $^{3}J_{gf}$ = 6.24 Hz; 1.85, s, 3H, H_c; 3.05, t, 2H, H_e, $^{3}J_{ef}$ = 5.5 Hz; 3.7, m, 1H, H_f, $^{3}J_{fh}$ = 4.74 and $^{3}J_{fg}$ = 6.24 Hz; 4.7, d, 1H, H_h, $^{3}J_{hf}$ = 4.74 Hz; 5.3 and 5.6, 2 s, 2H, H_a and H_b;

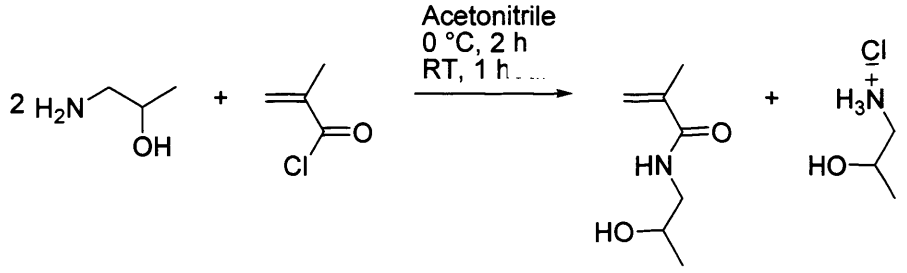

Scheme 3.1: Synthesis of HPMA monomer

7.8, bs, 1H, H_d.

^{13}C-NMR (DMSO-d_6, ppm): δ = 19, C_7; 22, C_3; 46, C_5; 65, C_6; 120 and 140, C_1 and C_2; 168, C_4.

Synthesis and characterisation of *N*-tert-Butoxycarbonyl-*N'*-acryloyl-1,3-diaminopropane

BOC-APAAm was synthesised by a two-step procedure as previously described by (Hobson and Feast 1999). The method is briefly summarised below and depicted in Schemes 3.2 and 3.3.

Step 1: N-tert-Butoxycarbonyl-1,3-diaminopropane (Scheme 3.2)

A solution of 1,3-diaminopropane (5.00 g, 0.0670 mol) in dichloromethane (35 mL) was placed in a round-bottom flask and cooled down to 0 °C. A solution of di-*tert*-butyl dicarbonate (3.67 g, 0.0168 mol) in dichloromethane (20 mL) was added dropwise over 2 h with good magnetic stirring. The mixture was then allowed to warm up to room temperature and left to react overnight. The white solid formed during the reaction was filtered off, and the filtrate was concentrated on the rotavapor. Deionised water (20 mL) was then added to the residue and the solution was saturated with sodium chloride before being extracted with ethyl acetate (3 x 25 mL). After evaporation of ethyl acetate under reduced pressure, a pale oil was isolated. It was then dissolved in chloroform (10 mL), and the residual sodium chloride was removed by filtration through a porosity 3-sinter funnel. The solvent was removed under reduced pressure and the product dried under vacuum at 30 °C to produce *N-tert*-butoxycarbonyl-1,3-diaminopropane (65 % yield). The product was analysed by m.p., IR, EA, ^{1}H- and ^{13}C-NMR.

Characteristics of the product are summarised below (key as above):

m.p.: 88°C ($m.p._{Theoretical}$ not available).

EA: $N_{Experimental}$ = 14.11 % ($N_{Theoretical}$ = 16.07 %); $H_{Experimental}$ = 9.42 % ($H_{Theoretical}$ = 10.41 %); $C_{Experimental}$ = 52.12 % ($C_{Theoretical}$ = 55.15 %).

IR: $\bar{\nu}$ (cm^{-1}) = 1 677, strong band, $\nu_{C=O}$ (amide I); 1 526, strong band, ν_{CN} (amide II); 1 365-1 200; δ_{NH} and δ_{OCN}.

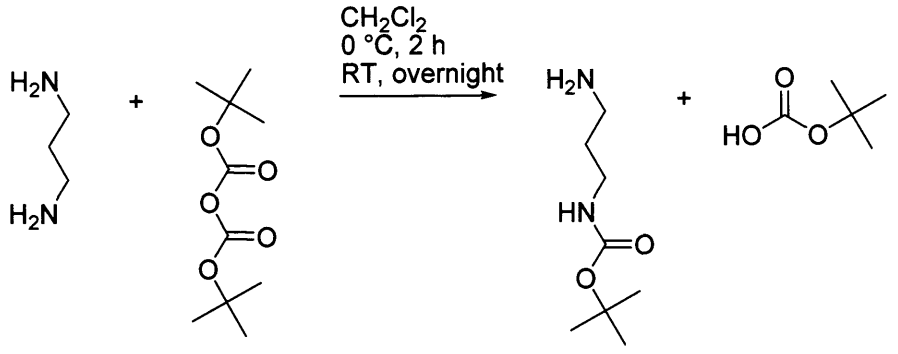

Scheme 3.2: Step 1 of the synthesis of BOC-APAAm

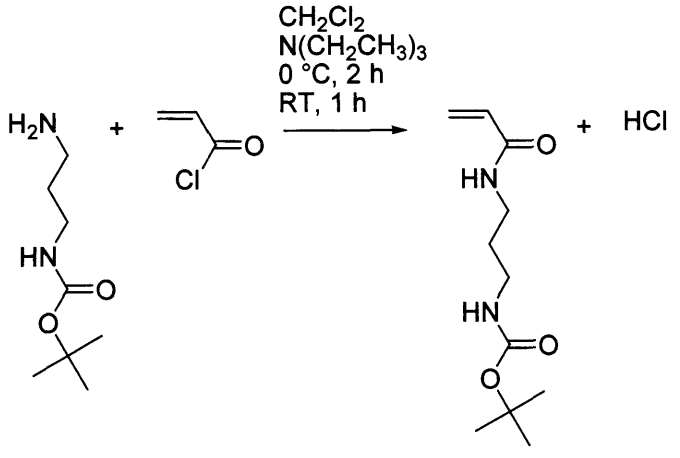

Scheme 3.3: Step 2 of the synthesis of BOC-APAAm

^{1}H-NMR ($CDCl_3$, ppm): δ = 1.33, s, 2H, H_a; 1.37, s, 9H, H_f; 1.55, m, 2H, H_c; 2.69, t, 2H, H_b, $^3J_{bc}$ = 7 Hz; 3.15, t, 2H, H_d, $^3J_{dc}$ = 6.52 Hz; 4.85, bs, 1H, H_e. The signals from the amine and the amide protons are not seen when the spectra is done in D_2O.

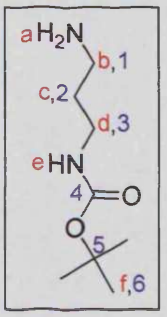

^{13}C-NMR ($CDCl_3$, ppm): δ = 27.67, C_6; 32.16, C_2; 37.50, C_1; 39.05, C_3; 78.20, C_5; 154.60, C_4.

Step 2: N-*tert Butoxycarbonyl*-N'-*acryloyl-1,3-diaminopropane (Scheme 3.3)*

A solution of triethylamine (372 mg, 3.68 mmol) and *N-tert*-butoxycarbonyl-1,3-diaminopropane (640 mg, 3.68 mmol) in anhydrous dichloromethane (10 mL) was added dropwise over 1 h to a well stirred and cooled to 0°C solution of acryloyl chloride (400 mg, 4.42 mmol) in anhydrous dichloromethane (10 mL). After addition, the reaction took place over 1 h more at room temperature. The solvent was then removed under reduced pressure, and the residue was washed with deionised water and extracted with chloroform (3 x 25 mL). The combined organic fractions were then concentrated under reduced pressure and the resultant white solid dried under vacuum at 30 °C to produce *N-tert*-butoxycarbonyl-*N'*-acryloyl-1,3-diaminopropane (60 % yield). The product was analysed by m.p., IR, EA, ^{1}H- and ^{13}C-NMR.

The characteristics of the product are summarised below (key as above):

m.p.: 58°C ($m.p._{Theoretical}$ not available).

EA: $N_{Experimental}$ = 11.88 % ($N_{Theoretical}$ = 12.27 %); $H_{Experimental}$ = 8.81 % ($H_{Theoretical}$ = 8.83 %); $C_{Experimental}$ = 56.96 % ($C_{Theoretical}$ = 57.87 %).

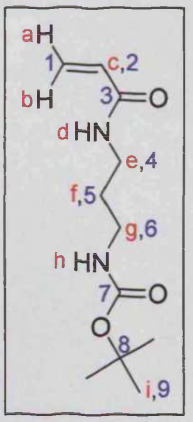

IR: $\bar{\nu}$ (cm^{-1}) = 1 687 and 1 658, strong bands, $\nu_{C=O}$ protecting group and amide I band; 1 625, $\nu_{C=C}$; 1 554 and 1 530, strong bands, ν_{CN} and δ_{CN} (Amide II band); 1 365-1 200; ν_{C-O}, δ_{NH} and δ_{OCN} (Amide III band).

^{1}H-NMR ($CDCl_3$, ppm): δ = 1.45, s, 9H, H_i; 1.65, m, 2H, H_f; 3.17, m, 2H, H_e, $^3J_{ef}$ = 6 Hz; 3.39, m, 2H, H_g, $^3J_{gf}$ = 6.23 Hz; 4.95, bs, 1H, H_d; 5.65- 6.15 and 6.25, m, 3H, H_a- H_c and H_b, $J_{GEM\ a\text{-}b}$ = 1.31 Hz; $J_{TRANS\ b\text{-}c}$ = 15.6 Hz; $J_{CIS\ a\text{-}c}$ = 9.05 Hz; 6.50, bs, 1H, H_h.

^{13}C-NMR ($CDCl_3$, ppm): δ = 28.40, C_9; 30.18, C_5; 35.80, C_4; 37.01, C_6; 79.48, C_8; 126.14, C_1; 131.11, C_2; 156.84, C_3; 165.91, C_7.

3.2.3. Synthesis and characterisation of homopolymers

Homopolymers were synthesised from AEM, DMAEM, HPMA, the quaternized monomers (qAEM and qAPAAm) and BOC-APAAm by FRP using thermal azo-based initiators. The initiator to monomer molar ratios ([I]/[M]) were varied from 0.58 % to 3 %. The following paragraphs describe the general methods used. Full characterisation of the products by IR, ^{1}H- and ^{13}C-NMR, GPC is given for selected samples.

Table 3.1 summarises the conditions used to prepare homopolymers P 1- P 18.

Synthesis and characterisation of homopolymers of AEM, HPMA, qAEM and qAPAAm in water

Homopolymers were synthesised in deionised water at 60 °C, in a nitrogen atmosphere, and using ACA as the initiator as shown in Schemes 3.4 to 3.6. The synthesis and characterisation of PAEM (P 3) is given as an example, and all other reactions were carried out in the same way but using different [I]/Σ[M] ratios (Table 3.1).

Synthesis of the PAEM homopolymer P 3 (Table 3.1)

Typical reaction conditions were as follows. AEM (2.0 g, 12 mmol), ACA (33.8 mg, 120 μmol, [I]/[M] = 1 %) were dissolved in deionised water (20 mL), at room temperature, in a round-bottom flask with a magnetic stirrer. The mixture was then degassed for 0.5 h with nitrogen before the flask was sealed and placed in an oil bath at 60 °C for 12 h. The reaction was stopped by cooling to room temperature and the polymer isolated and purified by 3 precipitations from deionised water into cold acetone and dried under vacuum at 40 °C.

This reaction was repeated using different [I]/Σ[M] ratios (1 to 3 %), and also for each monomer AEM, HPMA, qAEM or qAPAAm.

The following paragraphs summarise the characteristics of the PAEM, PHPMA, PqAEM and PqAPAAm homopolymers synthesised (IR, ^{1}H- and ^{13}C-NMR).

Key: the red letters are assigned to the protons of the chemical entities, carbon

Table 3.1: Summary of the reaction conditions used to prepare the homopolymers from HPMA, AEM, DMAEM, qAEM, qAPAAm and BOC-APAAm

Identification	Monomers	[I]/Σ[M] (%)
P 1	AEM[a]	2.00
P 2	"	1.50
P 3	"	1.00
P 4	HPMA[a]	1.00
P 5	DMAEM[b]	2.00
P 6	"	1.50
P 7	"	1.00
P 8	"	0.58
P 9	HPMA[b]	1.00
P 10	qAEM[a]	3.00
P 11	"	2.00
P 12	"	1.00
P 13	qAPAAm[a]	3.00
P 14	"	2.00
P 15	"	1.00
P 16	BOC-APAAm[c]	3.00
P 17	"	2.00
P 18	"	1.00

[a]: Polymerisations carried out in deionised water at 60 °C under N_2 atm with ACA; [b]: Polymerisations carried out in ethanol at 65 °C under N_2 atm with AIBN; [c]: Polymerisations carried out in DMF at 100 °C under N_2 atm with AIBN.

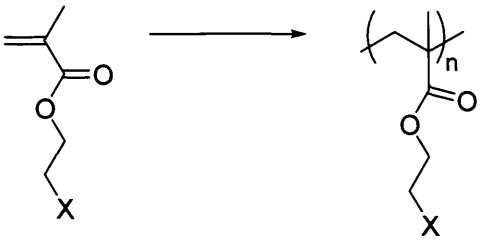

Scheme 3.4: Free radical homopolymerisations of the monomers AEM, DMAEM or qAEM

With: For AEM: X = $NH_3^+Cl^-$ and for qAEM: X = $N^+(CH_3)_3Cl^-$, both homopolymerisations carried out with ACA as the initiator, in deionised water, at 60 °C, under N_2 atm, [ACA]/[M] varying from 1 to 3 %.

For DMAEM: X = $N(CH_3)_2$, homopolymerisation carried out with AIBN as the initiator, in ethanol, at 65 °C, under N_2 atm; [AIBN]/[DMAEM] = 0.58, 1, 1.5 and 2 %.

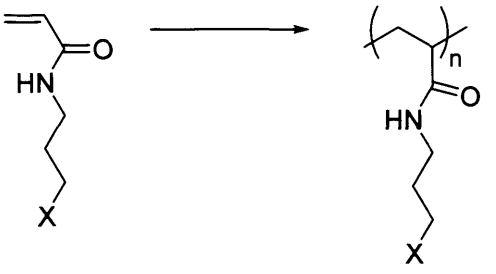

Scheme 3.5: Free radical homopolymerisations of the monomers qAPAAm and BOC-APAAm

With: For qAPAAm: X = $N^+(CH_3)_3Cl^-$, homopolymerisation carried out with ACA as the initiator, in deionised water, at 60 °C, under N_2 atm, [ACA]/[qAPAAm] = 1, 2 and 3 %.

For BOC-APAAm: X = $NHCOOC(CH_3)_3$, homopolymerisation carried out with AIBN as the initiator, in DMF, at 100 °C, under N_2 atm; [AIBN]/[BOC-APAAm] = 1, 2 and 3 %.

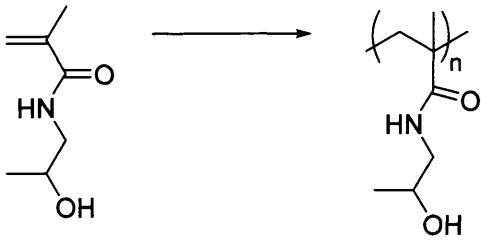

Scheme 3.6: Free radical homopolymerisations of HPMA monomer

Both under N_2 atm with [I]/[HPMA] = 1 % and initiated either with ACA in deionised water, at 60 °C or with AIBN in ethanol, at 65 °C.

elements are labeled by the blue numbers.

Characterisation of the PAEM samples P 1- P 3 (Table 3.1)

Yield: 70 %.

IR: $\bar{\nu}$ (cm^{-1}) = 2 915, ν_{C-H} and vibration of $^{+}$N-H group (absorbing between 3 300 and 2 000); 1 721, $\nu_{C=O}$; 1 601, ν^{+}_{NH3}; 1 481, δ_{CH}; 1 255, ν_{C-O}; 1 350-800, δ_{C-C} and δ_{CH}.

^{1}H-NMR (DMSO-d_6, ppm): δ = 0.8 to 1.8, broad peaks, 3H, H_b; 2.1, broad peak, 2H, H_a; 3.1, bs, 2H, H_d; 4.3, bs, 2H, H_c; 8.6, bs, 3H, H_e.

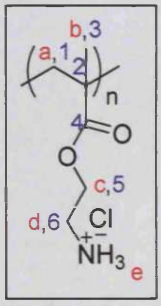

^{13}C-NMR (DMSO-d_6, ppm): δ = 15, C_3; 17, C_1; 44, C_2; 60, C_6; 65, C_5; 175, C_4.

GPC (PBS, flow rate 1 mL/min, columns calibrated with narrow pullulan standards): M_n and M_w/M_n ranging from 12 720 g.mol^{-1}, 2.10 to 40 670 g.mol^{-1}, 1.10.

Characterisation of the PHPMA samples P 4 and P 9 (Table 3.1)

Yield: 75 %.

IR: $\bar{\nu}$ (cm^{-1}) = 3 343, ν_{O-H}; 2 972, ν_{C-H}; 1 639, $\nu_{C=O}$ (Amide I band); 1 522, ν_{C-N} and δ_{CNH} (Amide II band); 1 451, δ_{COH}; 1 330-1 200, δ_{NH} and δ_{OCN} (Amide III band) and 1 350-800, δ_{C-C} and δ_{CH}.

^{1}H-NMR (DMSO-d_6, ppm): δ = 0.8, bs, 3H, H_b; 0.9, ss, 3H, H_f; 1.7, bs, 2H, H_a; 2.9, bs, 2H, H_d; 3.7, bs, 1H, H_e; 4.7, bs, 1H, H_g; 7.2, bs, 1H, H_c.

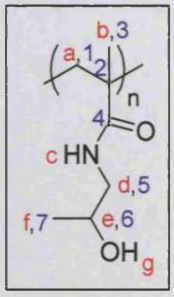

^{13}C-NMR (DMSO- d_6, ppm): δ = 15, C_3; 17, C_1; 22, C_7; 45, C_2; 48, C_5; 65, C_6; 177, C_4.

GPC: P 4: M_n = 75 090 g.mol^{-1} and M_w/M_n = 2.77 (PBS, flow rate 1 mL/min, columns calibrated with narrow pullulan standards). P 9: M_n = 27 850 g.mol^{-1} and M_w/M_n = 2.51 (THF, flow rate 1 mL/min, column calibrated with narrow PS standards).

Characterisation of the PqAEM samples P 10- P 12 (Table 3.1)

Yield: 95 %.

IR: $\bar{\nu}$ (cm^{-1}) = wide band around 2 945, ν_{C-H}; 2 852, vibration of $^{+}$N-H group (absorbing between 3 300 and 2 000 cm^{-1}); 1 729, $\nu_{C=O}$; 1 477, δ_{CH}; 1 239, ν_{C-O}; 1 350-800, δ_{C-C} and δ_{CH}.

^{1}H-NMR (D_2O, ppm): δ = 1, broad peaks, 3H, H_b; 2, broad peaks, 2H, H_a; 3.2, bs, 9H, H_e; 3.8, bs, 2H, H_d; 4.4, bs, 2H, H_c.

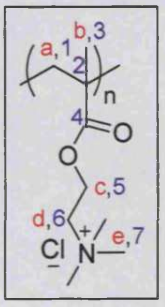

^{13}C-NMR (D_2O, ppm): δ = 19, C_3; 45, C_1; 52, C_2; 54, C_7; 59, C_6; 64, C_5; 178, C_4.

GPC (PBS, flow rate 1 mL/min, columns calibrated with narrow pullulan standards): M_n and M_w/M_n ranging from 75 620 $g.mol^{-1}$, 3.87 to 224 350 $g.mol^{-1}$, 2.44.

Characterisation of the PqAPAAm samples P 13- P 15 (Table 3.1)

Yield: 90 %.

IR: $\bar{\nu}$ (cm^{-1}) = wide band around 2 973, ν_{C-H}; 2 857, vibration of $^{+}$N-H group (absorbing between 3 300 and 2 000 cm^{-1}); 1 641, $\nu_{C=O}$ (Amide I band); 1 552, ν_{C-N} and δ_{CNH} (Amide II band); 1 467, δ_{CH}; 1 330-1 200, δ_{NH} and δ_{OCN} (Amide III band) and 1 350-800, δ_{C-C} and δ_{CH}.

^{1}H-NMR (D_2O, ppm): δ = 1.1 to 2.2, broad peaks, 5H, H_a, H_b and H_e; 3.1, bs, 9H, H_g; 3.2, bs, 2H, H_f; 3.4, bs, 2H, H_d; H_c is not seen as experiment done in D_2O.

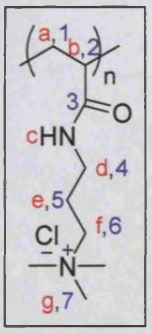

^{13}C-NMR (D_2O, ppm): δ = 22, C_5; 35, C_1; 36, C_6; 42, C_2; 53, C_7; 64, C_4; 176, C_3.

GPC (PBS, flow rate 1 mL/min, columns calibrated with narrow pullulan standards): M_n and M_w/M_n ranging from 91 100 $g.mol^{-1}$, 2.69 to 349 580 $g.mol^{-1}$, 1.48.

Synthesis of DMAEM and HPMA homopolymers in ethanol

The DMAEM and HPMA homopolymer synthesis was carried out in ethanol at 65 °C, in a nitrogen atmosphere, and using AIBN as the initiator (Schemes 3.4 and 3.6). The synthesis and characterisation of PDMAEM P 7 is given as an example, and all other homopolymers were prepared in the same way but using different [I]/Σ[M] ratios (Table 3.1).

Synthesis of the PDMAEM P 7 (Table 3.1)

Typical reaction conditions were as follows. DMAEM (2.0 g, 12.7 mmol), AIBN (20.9 mg, 127.0 μmol, [I]/[M] = 1 %) were dissolved in ethanol (20 mL), at room temperature, in a round-bottom flask with a magnetic stirrer. The mixture was then degassed for 0.5 h with nitrogen before the flask was sealed and placed in an oil bath at 65 °C for 12 h. The reaction was then stopped by cooling the mixture down to room temperature. The polymers were then isolated and purified by 3 precipitations from ethanol into cold diethyl ether and dried under vacuum at 40 °C.

This synthesis was repeated at different [I]/Σ[M] ratios (0.58 to 2.00 %) to prepare the DMAEM and HPMA homopolymers.

Characterisation of the PHPMA sample P 9 (Table 3.1)

The results obtained were previously summarised in Section 3.2.3.

Characterisation of the PDMAEM samples P 5- P 8 (Table 3.1)

Yield: 65 %.

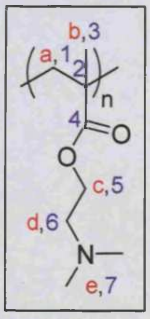

IR: $\bar{\nu}$ (cm^{-1}) = 2 939, ν_{C-H}; 1 722, $\nu_{C=O}$; 1 451, δ_{CH}; 1 270, ν_{C-O}; 1 350-800, δ_{C-C} and δ_{CH}.

^{1}H-NMR ($CDCl_3$, ppm): δ = 0.7 to 2.1, broad peaks, 5H, H_a and H_b; 2.2, bs, 6H, H_e; 2.6, bs, 2H, H_d; 4.1, bs, 2H, H_c.

^{13}C-NMR ($CDCl_3$, ppm): δ = 15, C_3; 17, C_1; 44, C_2; 45, C_7; 56, C_6; 62, C_5; 175, C_4.

GPC (THF, flow rate 1 mL/min, column calibrated with narrow PS standards): M_n and M_w/M_n ranging from 19 050 g.mol^{-1}, 2.10 to 30 140 g.mol^{-1}, 2.00.

Synthesis of BOC-APAAm homopolymers in DMF

The homopolymerisation of BOC-APAAm was carried out in DMF at 100 °C in a nitrogen atmosphere using AIBN as the initiator (Scheme 3.5). The synthesis and characterisation of PBOC-APAAm (P 18) is given as an example. All other syntheses were carried out in the same way, but using different [I]/Σ[M] ratios (Table 3.1).

Synthesis of the PBOC-APAAm P 18 (Table 3.1)

Typical reaction conditions were as follows. BOC-APAAm (2.0 g, 8.76 mmol), AIBN (14.4 mg, 87.60 µmol, [I]/[M] = 1 %) were dissolved in DMF (20 mL) at room temperature in a round-bottom flask containing a magnetic stirrer. The mixture was then degassed for 0.5 h with nitrogen before the flask was sealed and placed in an oil bath at 100 °C for 12 h. The reaction was stopped by cooling to room temperature. The polymers were then isolated in a 75 % average yield, and purified by 3 precipitations from DMF into cold acetone and dried under vacuum at 40 °C.

This procedure was repeated at [I]/Σ[M] ratios of 1 to 3 %.

Characterisation of the PBOC-APAAm samples P 16- P 18 (Table 3.1)

Yield: 75 %.

IR: $\bar{\nu}$ (cm^{-1}) = wide band around 2 970, ν_{C-H}; 1 700, $\nu_{C=O}$ of the protecting group; 1 650, $\nu_{C=O}$ (Amide I band); 1 520, ν_{C-N} and δ_{CNH} (Amide II band); 1 330-1 200, δ_{NH} and δ_{OCN} (Amide III band); 1 200, ν_{C-O} and 1 350-800, δ_{C-C} and δ_{CH}.

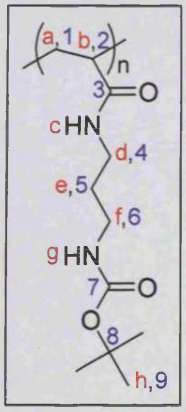

^{1}H-NMR ($CDCl_3$, ppm): δ = 1.4, bs, 9H, H_h; 1.6, broad peaks, 3H, H_a and H_b; 2.1, bs, 2H, H_e; 3.1, bs, 2H, H_d; 3.2, bs, 2H, H_f; 5.4, bs, 1H, H_c; 7.2, bs, 1H, H_g.

^{13}C-NMR ($CDCl_3$, ppm): δ = 27, C_9; 28, C_1; 30, C_5; 35, C_2; 37, C_4; 40, C_6; 78, C_8; 155, C_3; 174, C_7.

GPC (THF, flow rate 1 mL/min, column calibrated with narrow PS standards): M_n and M_w/M_n ranging from 55 840 g.mol^{-1}, 2.40 to 87 510 g.mol^{-1}, 2.00.

3.2.4. Synthesis and characterisation of amine-based HPMA copolymers

AEM (M_1)/HPMA (M_3) and DMAEM (M_2)/HPMA (M_3) copolymers were synthesised by FRP using thermal azo-based initiators. The [I]/Σ[M] ratio was fixed to 1 % and the [M_x]/Σ[M] ratios were adjusted to give 0, 25, 50, 75 or 100 % with x being either 1 or 2.

The general methods used are described below and the products were characterised by IR, ^{1}H- and ^{13}C-NMR, GPC. Table 3.2 summarises the conditions used for each copolymerisation reaction (P 19- P 24).

Synthesis of AEM/HPMA copolymers

AEM (M_1) and HPMA (M_3) were copolymerised in deionised water, under nitrogen, at 60 °C using ACA as a thermal the initiator (Scheme 3.7). [I]/Σ[M] was always 1 % and [M_1]/Σ[M] was being 0, 25, 50, 75 or 100 % (Table 3.2). As an example, the synthesis of the $PAEM_{50}HPMA_{50}$ copolymer P 20 is described in details below.

Synthesis of the $PAEM_{50}HPMA_{50}$ copolymer P 20 (Table 3.2)

Typical reaction conditions were as follows. M_1 (2.00 g, 12 mmol), M_3 (1.73 g, 12 mmol, [M_1]/Σ[M] = 50 %) and ACA (67.30 mg, 240 µmol, [I]/Σ[M] = 1 %) were dissolved in deionised water (40 mL) in a round-bottom flask containing a magnetic stirrer. The mixture was then degassed for 0.5 h with nitrogen before the flask was sealed and placed in an oil bath at 60 °C for 12 h. The reaction was then cooled to room temperature. The polymer was isolated in a 55 % average yield, and purified by 3 precipitations from deionised water into cold acetone, and finally dried under vacuum at 40 °C.

This synthesis was repeated at [M_1]/Σ[M] ratios of 0, 25, 75 and 100 %.

Table 3.2: Summary of the reaction conditions for the copolymerisations of HPMA with either AEM or DMAEM

Identification	Comonomers	[I]/Σ[M] (%)	$[M_x]/\Sigma[M]^{(c)}$ (%)
P 19	AEM (M_1) /HPMA (M_3)[(a)]	1.00	25
P 20	"		50
P 21	"		75
P 22	DMAEM (M_2) /HPMA (M_3)[(b)]	1.00	25
P 23	"		50
P 24	"		75

[(a)]: Polymerisations carried out in deionised water at 60 °C under N_2 atm with ACA; [(b)]: Polymerisations carried out in ethanol at 65 °C under N_2 atm with AIBN; [(c)]: Where x is either 1 or 2.

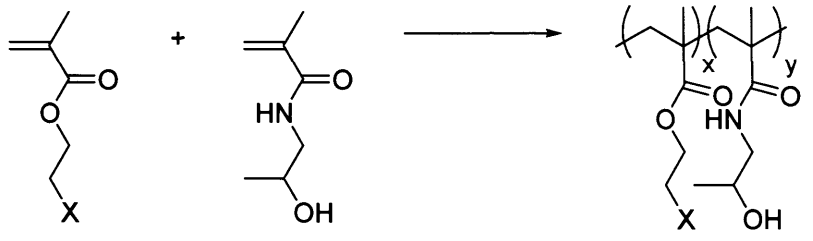

Scheme 3.7: Free radical copolymerisation of HPMA (M_3) with either AEM (M_1) or DMAEM (M_2)

For AEM (M_1): X = $NH_3^+Cl^-$, copolymerisation carried out with ACA as the initiator, in deionised water, at 60 °C, under N_2 atm; [ACA]/∑[M] = 1 %, [M_1]/∑[M] = 25, 50 or 75 %.

For DMAEM (M_2): X = $N(CH_3)_2$, copolymerisation carried out with AIBN as the initiator, in ethanol, at 65 °C, under N_2 atm; [AIBN]/∑[M] = 1 %, [M_3]/∑[M] = 25, 50 or 75 %.

Characterisation of the $PAEM_xHPMA_y$ copolymer samples P 19- P 21 (Table 3.2)

IR: $\bar{\nu}$ (cm^{-1}) = 3 378, ν_{O-H}; 2 924, ν_{C-H} and vibration of $^{+}$N-H group (absorbing between 3300 and 2000 cm^{-1}); 1 725, $\nu_{C=O}$ of the ester bonds of the AEM residues; 1 629, $\nu_{C=O}$ (Amide I band); 1 529, ν_{C-N} and δ_{CNH} (Amide II band); 1 457, δ_{COH} and δ_{CH}; 1 232, ν_{C-O}; 1 330-1 200, δ_{NH} and δ_{OCN} (Amide III band) and 1 350-800, δ_{C-C} and δ_{CH}.

^{1}H-NMR (D_2O, ppm): δ = 0.8 to 1.8, bs, 5H, H_a and H_b; 2.1, bs, 3H, H_e; 2.5, bs, 2H, H_d; 4.3, bs, 2H, H_c; 1, bs, 6H, H_g and H_k; 1.7, bs, 2H, H_f; 3, bs, 2H, H_i; 3.8, bs, 1H, H_j.

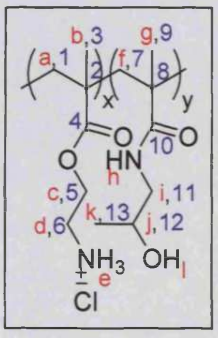

^{13}C-NMR (D_2O, ppm): δ = 15, C_3; 17, C_1; 4, C_2; 60, C_6; 65, C_5; 175, C_4; 15, C_9; 17, C_7; 22, C_{13}; 45, C_8; 48, C_{11}; 65, C_{12}; 177, C_{10}.

GPC (PBS, flow rate 1 mL/min, columns calibrated with narrow pullulan standards): M_n and M_w/M_n ranging from 35 180 $g.mol^{-1}$, 1.20 to 55 200 $g.mol^{-1}$, 3.43.

Synthesis of DMAEM/HPMA copolymers

DMAEM (M_2) and HPMA (M_3) were copolymerised in ethanol, under a nitrogen atmosphere, at 65 °C using AIBN as a thermal the initiator (Scheme 3.7). In each case, [I]/∑[M] was 1 % and [M_2]/∑[M] was 0, 25, 50, 75 or 100 % (Table 3.2).

Synthesis of the $PDMAEM_{50}HPMA_{50}$ copolymer P 23 (Table 3.2)

Typical reaction conditions were as follows. Freshly distilled M_2 (2.00 g, 12.7 mmol), M_3 (1.82 g, 12.7 mmol, [M_2]/∑[M] = 50 %) and AIBN (41.80 mg, 254.0 µmol, [I]/∑[M] = 1 %) were dissolved in ethanol (40 mL) in a round-bottom flask containing a magnetic stirrer. The mixture was then degassed for 0.5 h with nitrogen before the flask was sealed and placed in an oil bath at 65 °C for 12 h. The reaction was then cooled down to room temperature. The polymer was isolated in a 50 % average yield, and purified by 3 precipitations from ethanol into diethyl ether, and finally dried under vacuum at 40 °C.

This synthesis was repeated at different [M_2]/Σ[M] ratios (0, 25, 75 and 100 %).

Characterisation of the $PDMAEM_xHPMA_y$ copolymer samples P 22- P 24 (Table 3.2)

IR: $\bar{\nu}$ (cm^{-1}) = 3 300, ν_{O-H}; 2 971, ν_{C-H}; 1 728, $\nu_{C=O}$ of the ester bonds of the DMAEM residues; 1 622, $\nu_{C=O}$ (Amide I band); 1 525, ν_{C-N} and δ_{CNH} (Amide II band); 1 467, δ_{COH} and δ_{CH}; 1 265, ν_{C-O}; 1 330-1 200, δ_{NH} and δ_{OCN} (Amide III band) and 1 350-800, δ_{C-C} and δ_{CH}.

^{1}H-NMR (DMSO-d_6, ppm): δ = 0.7 to 2.1, broad peaks, 5H, H_a and H_b; 2.2, bs, 6H, H_e; 2.6, bs, 2H, H_d; 4.1, bs, 2H, H_c; 0.8, bs, 3H, H_g; 0.9, ss, 3H, H_k; 1.7, broad peak, 2H, H_f; 2.9, bs, 2H, H_i; 3.7, bs, 1H, H_j; 4.7, bs, 1H, H_l; 7.2, bs, 1H, H_h.

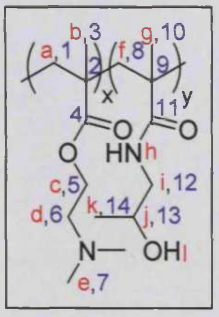

^{13}C-NMR (DMSO-d_6, ppm): δ = 15, C_3 and C_{10}; 17, C_1 and C_8; 44, C_2; 45, C_7; 56, C_6; 62, C_5; 175, C_4; 22, C_{14}; 45, C_9; 48, C_{12}; 65, C_{13}; 177, C_{11}.

GPC (THF, flow rate 1 mL/min, column calibrated with narrow PS standards): M_n and M_w/M_n ranging from 12 290 g.mol^{-1}, 1.44 to 27 830 g.mol^{-1}, 2.85.

3.3. Results

3.3.1. Synthesis of monomers

HPMA monomer (Scheme 3.1) was obtained as a white solid with a 30 % yield and its composition and purity were confirmed by m.p., IR, ^{1}H- and ^{13}C-NMR and EA (Section 3.2.2). The measured EA of the carbon, hydrogen and nitrogen elements were consistent with the expected theoretical percentages.

The protected monomer BOC-APAAm was prepared by a two-step reaction (Schemes 3.2 and 3.3) and obtained in a 39 % total yield (65 % yield for step 1 and 60 % yield for step 2). Both the intermediate and the final products were analysed by ^{1}H- and ^{13}C-NMR, IR, m.p. and EA (Section 3.2.2). The EA for the intermediate *N-tert*-Butoxycarbonyl-1,3-diaminopropane showed a higher percentage of carbon, hydrogen and nitrogen than expected giving ~ 12.5 % of error in some cases. However, the EA of BOC-APAAm had a good correlation between the theoretical and measured values, confirming the purity of the final product. Despite, the differences found in the EA of the intermediate compound, all other analyses (IR,

m.p., ^{1}H- and ^{13}C-NMR) confirmed the structure of both the intermediate and the final products.

3.3.2. AEM, DMAEM, qAEM, qAPAAm, BOC-APAAm and HPMA homopolymers

Homopolymerisations of the methacrylate monomers (AEM, DMAEM, qAEM) and the acrylamide monomers (HPMA, qAPAAm, BOC-APAAm) (Schemes 3.4 to 3.6) were successfully performed at different [I]/[M] ratios. The purity and composition of all the products were confirmed by IR, ^{1}H- and ^{13}C-NMR (Section 3.2.3) and the homopolymers were obtained in average yield of 65 % to 95 % (Table 3.3). The molecular weight and polydispersity of the synthesised polymers were determined by GPC and Table 3.3 shows that high to really high molecular weight polymers were obtained (M_n from 12 720 to 349 580 g.mol^{-1}), with polydispersity ranging from 1.10 to 3.87. Figure 3.2 shows the molecular weight of the homopolymers as a function of the [I]/[M] ratios. There is a general trend towards a decrease of the molecular weight with an increase of the [I]/[M] ratio.

3.3.3. AEM (or DMAEM)/HPMA copolymers

Copolymerisation of the cationic amino-based monomers (AEM or DMAEM) with HPMA was successfully achieved at 60 °C in deionised water for the AEM/HPMA copolymers and at 65 °C in ethanol for DMAEM/HPMA copolymers (Scheme 3.7). These copolymers were obtained in an average yield of 55 % and 50 %, for PAEM-*co*-HPMA and PDMAEM-*co*-HPMA, respectively.

The final composition of the synthesised copolymers was determined by ^{1}H-NMR, by comparing the integral of the methine protons (H_a) of the HPMA residues against the integral of the methylene protons (H_b) in alpha position of the ester group of the amino-based methacrylate residue (Equation 3.1).

$$y = \frac{\int H_b}{\int H_b + 2\int H_a} \times 100 \qquad \text{(Eq 3.1)}$$

where y corresponds to the percentage of AEM or DMAEM residue in the copolymers.

As seen in Figures 3.3 and 3.4, as the feed ratio of the cationic-based methacrylate monomer was increased, the peak corresponding to the cationic residue in the copolymer also increased leading to a higher proportion of the cationic residues in the

Table 3.3: Summary of the molecular weight, polydisperisty and yield obtained for the homopolymerisation of AEM, DMAEM, HPMA, qAEM, qAPAAm and BOC-APAAm

Identification	Homopolymer	[I]/[M] ratio (%)	M_n (g.mol^{-1})	M_w/M_n	Yield[f] (%)
P 1	PAEM[a]	2.00	12 720[d]	2.10[d]	70
P 2	"	1.50	32 900[d]	1.10[d]	"
P 3	"	1.00	40 670[d]	1.20[d]	"
P 5	PDMAEM[b]	2.00	19 050[e]	2.10[e]	65
P 6	"	1.50	22 900[e]	2.00[e]	"
P 7	"	1.00	27 830[e]	2.00[e]	"
P 8	"	0.58	30 140[e]	2.00[e]	"
P 10	PqAEM[a]	3.00	105 790[d]	2.86[d]	95
P 11	"	2.00	75 620[d]	3.87[d]	"
P 12	"	1.00	224 350[d]	2.44[d]	"
P 13	PqAPAAm[a]	3.00	91 100[d]	2.69[d]	90
P 14	"	2.00	295 025[d]	1.76[d]	"
P 15	"	1.00	349 580[d]	1.48[d]	"
P 16	PBOC-APAAm[c]	3.00	55 840[e]	2.40[e]	75
P 17	"	2.00	82 660[e]	2.10[e]	"
P 18	"	1.00	87 510[e]	2.00[e]	"
P 4[a]	PHPMA	1.00	75 090	2.77	75
P 9[b]	"	1.00	27 850	2.51	"

[a]: Homopolymerisation carried out in deionised water under N_2 atm at 60°C with ACA as the initiator; [b]: Homopolymerisation carried out in ethanol under N_2 atm at 65°C with AIBN as the initiator; [c]: Homopolymerisation carried out in DMF under N_2 atm at 100°C with AIBN as the initiator; [d]: Mobile phase PBS, column calibrated with narrow pullulan standards, flow rate 1 mL/min. [e]: Mobile phase THF, column calibrated with narrow PS standards, flow rate 1 mL/min. [f]: Yield measured gravimetrically at the end of the polymerisation.

(a)

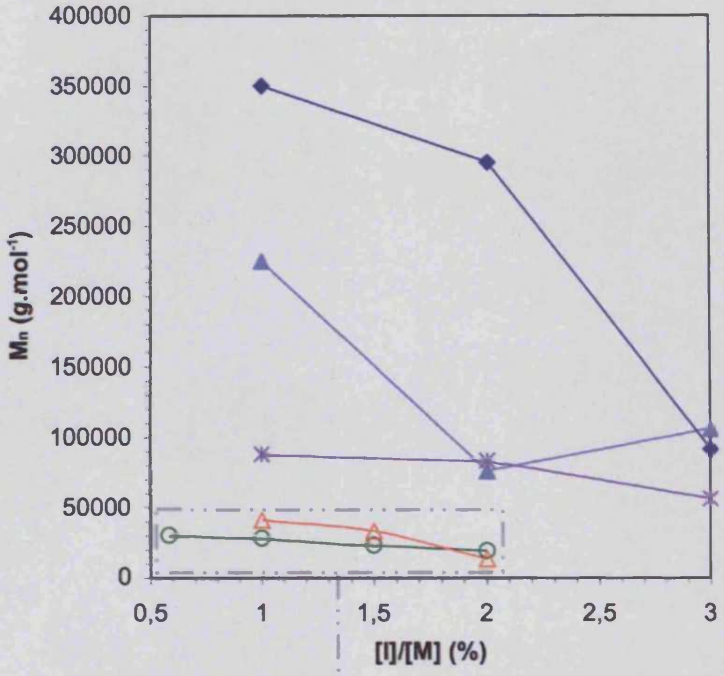

(b)

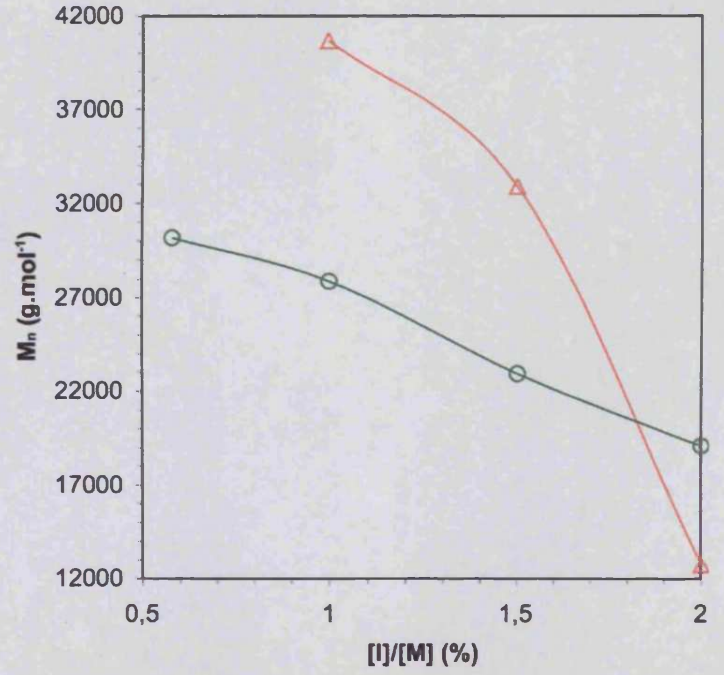

Figure 3.2: Free radical homopolymerisation studies: Effect of [I]/[M] molar ratio on number-average molecular weight

Panel (a) shows all studied polymers: ◆ PqAPAAm; ▲ PqAEM; △ PAEM; ○ PDMAEM; ✳ PBOC-APAAm; panel (b) zooms in on △ PAEM and ○ PDMAEM.

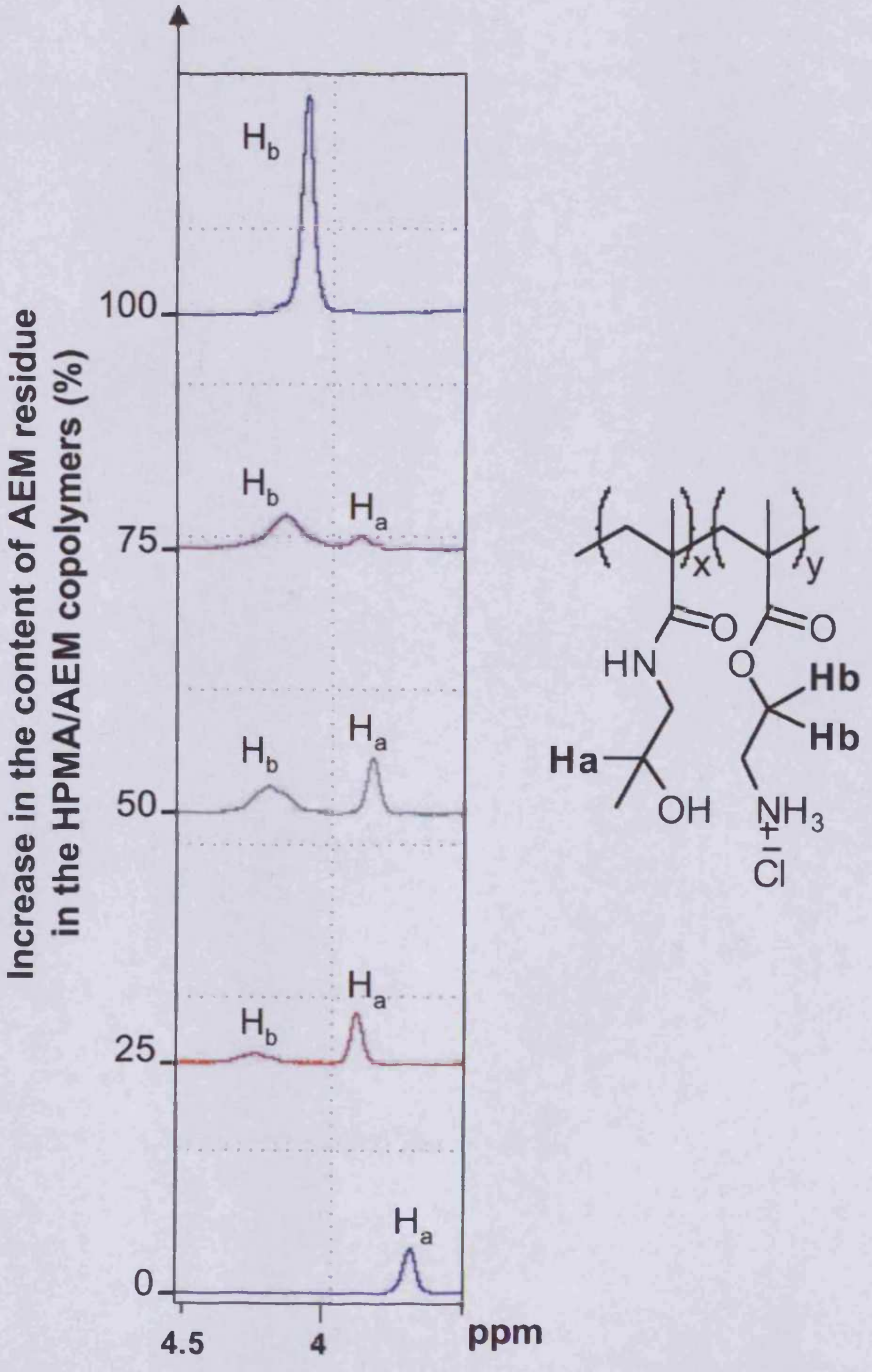

Figure 3.3: **Expanded region of the ^{1}H-NMR spectra obtained for the HPMA/AEM copolymers in D_2O**

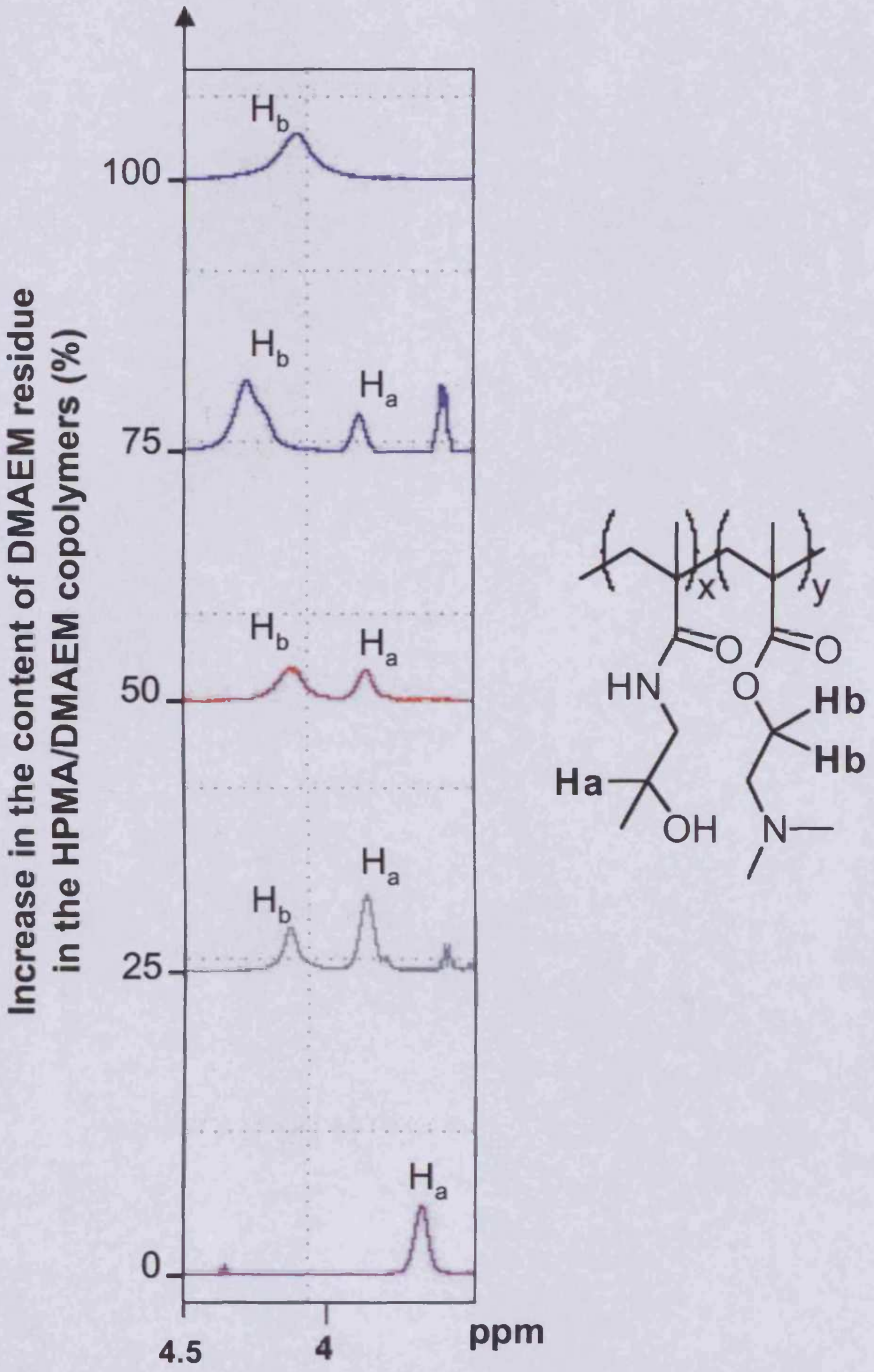

Figure 3.4: Expanded region of the ^{1}H-NMR spectra obtained for the HPMA/DMAEM copolymers in D_2O*

---

* *The multiplet observed at 3.6 ppm for PDMAEM$_{25}$-co-HPMA$_{75}$ and PDMAEM$_{75}$-co-HPMA$_{25}$ was attributed to the residual ethanol from the reaction.*

final copolymer composition.

The final composition of all the copolymers are summarised in Table 3.4. It can be seen that the ratios calculated from the ^{1}H-NMR spectra were similar to the expected theoretical values.

The M_n and polydispersity M_w/M_n of all the copolymers are also summarised in Table 3.4. It can be seen that high molecular weight copolymers were successfully synthesised, with a M_n as high as 75 090 g.mol^{-1}, and a polydispersity ranging from 1.20 to 3.43.

The pK_a of the copolymers (Table 3.5) was read at the inflexion point of the titration curves (Figures 3.5 and 3.6). In both families of copolymer, a lower pK_a value was seen for the monomers compared to their HPMA copolymers. Moreover, there was an increase in the buffering capacity of the copolymer as indicated by the width of the step in the titration curves (Figures 3.5 and 3.6) as the content in cationic repeating unit within the copolymer increased.

3.4. Discussion

3.4.1. Monomer synthesis

Acylation of amines by acyl halides is a general procedure for the preparation of amides (March 1992). In a so-called Schotten-Baumann reaction, a base is added to neutralise the HX formed during the reaction. For the synthesis of HPMA (Scheme 3.1), 1-amino-2-propanol was used in excess to trap the forming of the hydrochloride acid leading to the formation of the salt 1-amino-2-propanol hydrochloride. The synthesis of HPMA was previously described by (Kopeček and Bazilova 1973) and this method was used in these studies with some minor modifications. The final product was isolated by recrystallisation from THF here, whereas methanol was used by Kopeček and co-workers (Kopeček and Bazilova 1973). They obtained a chromatographically pure compound with a m.p. of 67 °C (no yield was given). Here, the monomer was obtained in a 30 % yield and as a pure product (proven by E.A., ^{1}H- and ^{13}C-NMR, IR) with a m.p. of 65 °C. Although the final yield for the synthesis of HPMA monomer was low in these studies, recrystallisation from methanol as described by (Kopeček and Bazilova 1973) was not successful.

Table 3.4: Summary of the composition, the molecular weight characteristics and the yield of the AEM/HPMA and DMAEM/HPMA copolymers synthesised

Polymer	Feeding composition (%)	Final composition (%)[e]	[I]/Σ[M] ratios (%)	M_n (g.mol^{-1})	M_w/M_n	Yield[f] (%)
P 4	HPMA (100)[a]	HPMA (100)	1	75 090[c]	2.77[c]	75
P 19	AEM (25), HPMA (75)[a]	AEM (22), HPMA (78)	1	55 200[c]	2.75[c]	55
P 20	AEM (50), HPMA (50)[a]	AEM (42), HPMA (58)	"	35 180[c]	2.80[c]	"
P 21	AEM (75), HPMA (25)[a]	AEM (67), HPMA (33)	"	47 090[c]	3.43[c]	"
P 3	AEM (100)[a]	AEM (100)	"	40 670[c]	1.20[c]	70
P 9	HPMA (100)[b]	HPMA (100)	1	27 850[d]	2.51[d]	75
P 22	DMAEM (25), HPMA (75)[b]	DMAEM (25), HPMA (75)	1	21 020[d]	2.85[d]	50
P 23	DMAEM (50), HPMA (50)[b]	DMAEM (47), HPMA (53)	"	12 290[d]	2.09[d]	"
P 24	DMAEM (75), HPMA (25)[b]	DMAEM (67), HPMA (33)	"	18 510[d]	1.44[d]	"
P 7	DMAEM (100)[b]	DMAEM (100)	"	27 830[d]	2.00[d]	65

[a]: Copolymerisation carried out at 60 °C in deionised water with ACA as the initiator under N_2 atm; [b]: Copolymerisation carried out at 65 °C in ethanol with AIBN as the initiator under N_2 atm; [c]: Mobile phase PBS, column calibrated with narrow pullulan standards, flow rate 1 mL/min. [d]: Mobile phase THF, column calibrated with narrow PS standards, flow rate 1 mL/min; [e]: Percentages calculated using ^{1}H-NMR spectrometry and equation 3.1. [f]: Yield measured gravimetrically at the end of the polymerisation.

Table 3.5: The pK_a values determined by titration for AEM and DMAEM monomers and their HPMA copolymers

Polymer	Composition	Approximate % of cationic residue in the copolymer	pK_a [(a)]
P 3	**AEM/HPMA**	100	8.0
P 21	**copolymers**	75	8.0
P 20		50	8.5
P 19		25	8.5
-	**AEM monomer**	NA	9.0
P 7	**DMAEM/HPMA**	100	7.6
P 24	**copolymers**	75	8.0
P 23		50	7.6
P 22		25	7.8
-	**DMAEM monomer**	NA	8.8

[(a)]: read at the inflexion point of the buffering capacity on the titration curves (Figures 3.5 and 3.6); NA: non applicable.

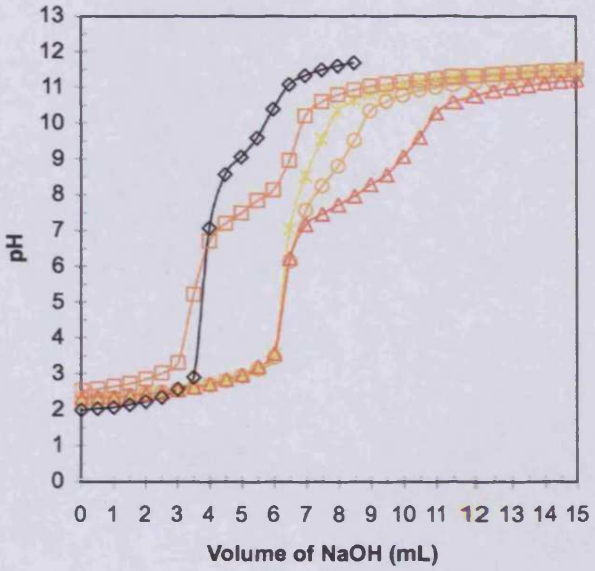

Figure 3.5: Titration curves for the AEM/HPMA copolymers and AEM monomer with NaOH in physiological NaCl

Legend: △ PAEM; □ $PAEM_{75}$-*co*-$HPMA_{25}$; ○ $PAEM_{50}$-*co*-$HPMA_{50}$; ✳ $PAEM_{25}$-*co*-$HPMA_{75}$; ◇ AEM monomer.

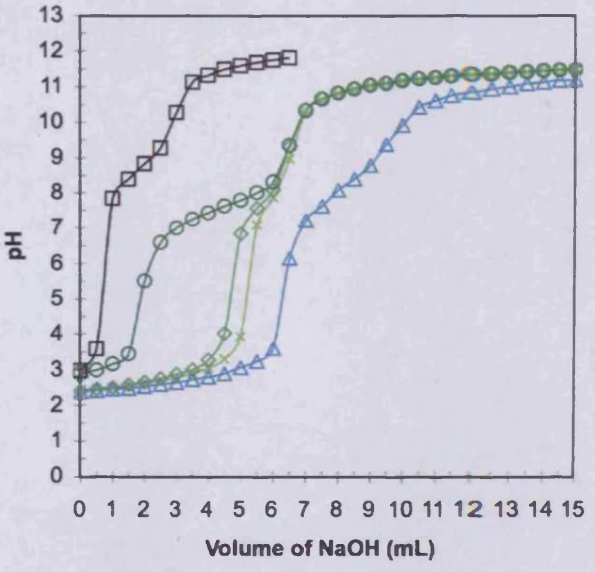

Figure 3.6: Titration curves for the DMAEM/HPMA copolymers and DMAEM monomer with NaOH in physiological NaCl

Legend: ○ PDMAEM; △ $PDMAEM_{75}$-*co*-$HPMA_{25}$; ◇ $PDMAEM_{50}$-*co*-$HPMA_{50}$; × $PDMAEM_{25}$-*co*-$HPMA_{75}$; □ DMAEM monomer.

Considering the purity of the HPMA produced here, it could be used for polymerisation studies without further purification. No further optimisation of the synthetic method was undertaken.

The protected monomer BOC-APAAm was prepared in a two-step reaction (Schemes 3.2 and 3.3), following the procedure of (Hobson and Feast 1999). In this case, the final product was obtained in a 39 % yield (65 % step 1 and 60 % step 2) whereas Hobson *et al.* described a 70 % yield (89 % step 1 and 80 % step 2). The difference is difficult to explain. Although the BOC-APAAm monomer was isolated in a poorer yield here, the IR and NMR spectra were in good agreement with data from the literature (Hobson and Feast 1999). Also, m.p. of both the intermediate (88°C) and final products (58°C) were assigned here, but no data was available in the literature allowing full comparison. EA of the intermediate compound indicated impurities (12.5 % error here, and Hobson and co-workers found up to 6.5 % of error). In contrast, the final compound had an error that was lower than 3.2 % in both cases. BOC-APAAm was then used without further purification for the homopolymerisation studies, although recrystallisation of both the product could have help to reduce these discrepancies and to optimise their yield.

3.4.2. Homopolymerisation studies

Homopolymers of DMAEM, AEM, HPMA, qAEM, qAPAAm, and BOC-APAAm were synthesised in high yield and the polymers had a high to really high molecular weight (Table 3.3). Comparison of the results described here with the literature on radical homopolymerisation of the same monomers was relatively difficult, as these monomers have been usually used in more complex systems being designed as polycation vectors or drug carriers. Nevertheless, the yield and molecular weight characteristics found here (Table 3.3) were in agreement with that expected when using FRP. The really high molecular weight and polydispersity obtained can be explained by considering the GPC system used (comment later explained). For example, Hennink and co-workers synthesised homopolymers of DMAEM by FRP in toluene (19 to 83 v/v %) at 60 °C with AIBN as a thermo-initiator ([I]/[M] = 1 %) (van de Wetering *et al.* 1998a). They obtained pure homopolymers in 80 % yield on average, with a M_n ranging from 20 000 to 75 000 g.mol^{-1} and a M_w/M_n of 3.15 to 4.12. Thus, even though the synthetic method they used seemed to be more

advantageous from a pure polymer chemistry point of view, the FPR of DMAEM in ethanol used here could be preferable for the synthesis of homopolycations to be used in the field of polymer therapeutics as it provides the advantage of nondegradable polymers having relatively low molecular weight (under 40 000 $g.mol^{-1}$) and low polydispersity. Both are important parameters for a polymer to be used as a therapeutic carrier.

Comments on hydrolytic stability

A mechanistic study of the hydrolytic stability of PDMAEM and its monomer was undertaken in Hennink's laboratory (van de Wetering *et al.* 1998b). They showed that the ester in DMAEM monomer is rather unstable toward hydrolysis in an aqueous solution at pH 7.4 and 37°C. They claimed that a coordination effect occurs between the protonated dimethylamino group of the monomer and its ester carbonyl, rendering the ester more susceptible to nucleophilic attack of a hydroxyl ion. At the conditions mentioned above, they evaluated the half time of formation of the resulting methacrylic acid to be 17 h. In the same study, they showed in the case of PDMAEM, the ester groups in the polymer are quite insensitive towards hydrolysis even at pH 1 and 7, and 80°C.

In the other hand, S. Armes' group claimed that qAEM was undergoing a transesterification when polymerised by ATRP in pure aqueous media or methanol/water mixtures, leading to the formation of a statistical copolymer qAEM/methyl methacrylate (Li *et al.* 2003), not considering results published earlier in the same journal. We believe that the hydrolysis of the ester of the quaternized monomer is more susceptible to occur in these protic media than a transesterification. In our case, the amino-based methacrylate monomers and its corresponding quaternized monomer were polymerised either in water or ethanol, and partial hydrolysis of the monomer during their 12 h polymerisation has to be taken into account as presented by Hennink's group. If happening, the final polymers should be statistical copolymers of AEM, qAEM or DMAEM with methacrylic acid. Although the hydrolysis effect has been proven, no peaks corresponding to the unwanted repeating unit of methacrylic acid were observed neither in proton nor in carbon NMR, suggesting that the synthesised polymers here were not hydrolysed into methacrylic acid.

Comments on aqueous GPC methodology used

It is important to discuss the methodology used to estimate molecular weight, as the values obtained are only relative ones. The high molecular weights determined here can be easily explained as the aqueous GPC system used was calibrated using pullulan standards. These non-charged poly(saccharide) standards will adopt a random coil conformation in PBS. Thus, they are not the best standards for determination of the molecular weight of the studied polymers due to their lack of chemical similarities. In contrast, the quaternized polymers, when dissolved in PBS, will form an extended coil due to the repulsion of the positive charges along the polymer backbone. Thus, it is expected that their molecular weight will be overestimated when compared with the more compact pullulan standards. Similarly, considering that the pK_a of PAEM is between 7 to 9 (Table 3.5), these polymers will be approximately half protonated in PBS at pH = 7.4, also leading to an overestimation of their molecular weight.

Ideally, as discussed in Chapter 2 (Section 2.3.5), the calibration of GPC columns should be done with narrow polystandards of identical or very similar chemical composition to that of the analytes. However, this was unfortunately not possible here as a matter of laboratory procedure. GPC calibrated with pullulans was used here as it provides a relative molecular weight, and it enables the comparison of the molecular weight of the libraries of polymers prepared.

Effect of [I]/[M] ratios on molecular weight obtained

As seen in Equation 3.2, the average kinetic chain length $\bar{\nu}$ (defined as the number of monomer molecules added to an initiator radical before termination of the macroradical) decreases as the initiator concentration increases (Elias 1997). Increasing the initiator concentration directly increases the number of growing chains, and therefore the probability of termination is also increased. Thus, varying the initiator concentration is one way of controlling the molecular weight and allows synthesis of polymers of lower molecular weight.

$$\bar{\nu} = \frac{k_p[M]}{2(f \times k_t k_d[I])^{1/2}} \qquad \text{(Eq 3.2)}$$

The effect of the [I]/Σ[M] molar ratio seen in the different polymerisation systems studied here showed a general decrease in the apparent molecular weight with an

increase in the [I]/Σ[M] molar ratio (Figure 3.2) and this is consistent with Equation 3.2.

Nevertheless, this method of molecular weight control during FRP can encounter a deviation known as the "Trommsdorff effect" (Elias 1997) when used for bulk polymerisations (which does not apply here in these studies). This occurs when the overall concentration of radicals in the medium is too high, leading to an autoacceleration of the polymerisation reaction with potential lack of control over the exothermic reaction. Dilution of the radical species with solvents enables the control over the occurrence of this side-reaction.

In our cases, other methods to control polymer molecular weight including the use of CTA are alternatively being employed and this is discussed further in Chapter 4.

3.4.3. Copolymerisation studies

High molecular weight cationic copolymers of HPMA were also successfully synthesised (Table 3.4). As discussed previously, the values of molecular weight given can only be relative due to the use of a conventional aqueous GPC system here.

Composition of HPMA copolymers

During statistical copolymer synthesis, ^{1}H-NMR spectroscopy is usually used to determine the final composition of the copolymers prepared. For example, Hennink and co-workers used ^{1}H-NMR spectroscopy to determine the final composition of their DMAEM copolymers which included the hydrophobic methyl methacrylate monomer, the amphiphilic ethoxytriethylene glycol methacrylate monomer or the hydrophilic *N*-vinyl-pyrrolidone monomer (van de Wetering *et al.* 1998a). Here, ^{1}H-NMR was also used to determine of the final composition of the AEM/HPMA or DMAEM/HPMA copolymers and the experimental composition was similar to that of the expected theoretical composition (Table 3.4). As the reaction conditions were selected to reach full conversion of the monomers into polymers (12 h reaction time), this result was expected. Nevertheless, it should be noted that reactivity ratios for the methacrylamide/methacrylate co-systems studied here could have been evaluated if the polymerisations were stopped before full completion and followed kinetically. Data from literature (Greenley 1989) suggests that in these kinds of co-system kinetically followed, the methacrylamide monomer (M_A) is less reactive than the methacrylate one (M_B), and thus the reactivity ratio $r_A = k_{AA}/k_{AB}$ is smaller than r_B =

k_{BB}/k_{BA} (Figure 3.7). As an example, in the co-system methacrylamide/ethyl 2-methacrylate, the reactivity ratios were calculated to be r_A = 0.46 and r_B = 0.83 (Greenley 1989). In the case of methyl methacrylate/acrylamide, r_A was evaluated to be 0.14 and r_B, 1.3 (Greenley 1989).

Determination of pK_a values

The pK_a value of the weak cationic polyelectrolyte DMAEM homopolymer (Table 3.5) determined here corroborated the values presented in the literature (pK_a ~ 7.5) (van de Wetering *et al.* 1999; Vamvakaki *et al.* 2001). Moreover, as the AEM/HPMA and DMAEM/HPMA copolymers have a lower degree of freedom in solution than their respective monomers (AEM or DMAEM), it was expected that the pK_a values of the copolymers would be lower than those of the cationic monomers. This was clearly observed to be true (Table 3.5 and Figures 3.5 and 3.6). In addition, it was found, as expected, that increasing the content of cationic residues along the HPMA copolymer chain led to an increase in the buffering capacity of the copolymers, as HPMA residues give non-ionic hydrophilic polymers.

3.5. Conclusions

These first studies synthesised a library of linear water-soluble homo- and copolymers with different molecular weight, composition and charge density using FRP. It was demonstrated that altering the [I]/Σ[M] molar ratios could, to a certain extent, control the final molecular weight of the polymer. Copolymerisation by FRP was easily used to synthesise copolymers of different composition, pK_a values and molecular weight.

However, FRP did not allow full control over molecular weight and polydispersity. Therefore, the next studies explored other polymerisation techniques to better control molecular weight, composition, charge density and polydispersity. Next studies (Chapter 4) used CTA and FRP, to control the molecular weight and allow the synthesis of a wider range of polymers. As the use of CTA allows the introduction of functionality to the end-group of the polymer backbone it can be used to synthesise semitelechelic homo- and copolymers.

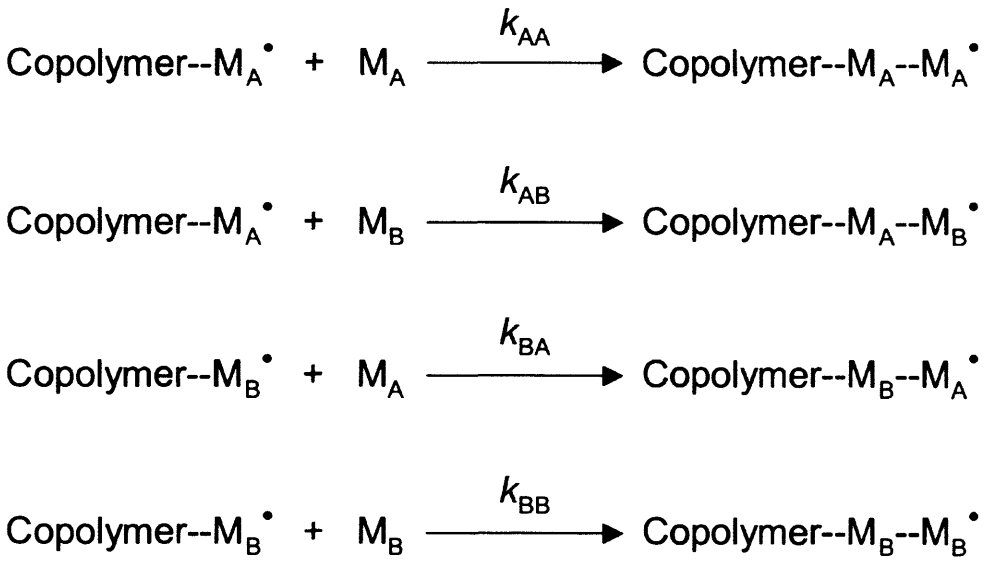

Figure 3.7: Schematic representation of the possible propagation reactions for the free radical copolymerisation of methacrylamide (M_A) with methylmethacrylate (M_B)

4

Synthesis & Characterisation of Semitelechelic Polymers by Chain Transfer Agent Free Radical Polymerisation: Effect of Chain Transfer Agent on Molecular Weight and Determination of 3-Mercaptopropionic Acid Transfer Constants

4.1. Introduction

As discussed in Chapter 1 (Section 1.8.1) and Chapter 3, FRP is a versatile technique easily used for the polymerisation of vinylic monomers (Cowie 1991; Elias 1997). However, one of the drawbacks of FRP is the lack of control over polymer molecular weight (Colombani and Chaumont 1996). It has been shown that the CTA used in FRP can help the control of molecular weight and also enable the introduction of end-group functionality to the polymer chain. More specifically, this allows the synthesis of semitelechelic polymers (Chiefari and Rizzardo 2002). As discussed in the general introduction (Chapter 1, Section 1.8.2), biocompatible, semitelechelic and water-soluble polymers can have many interesting applications (Chapter 1, Figure 1.19) especially in relation to the conjugation to bioactive agents and proteins in the field of polymer therapeutics.

As the overall aim of this thesis was the synthesis of a well-characterised polymer library with various composition, charge density, molecular weight, pK_a and architecture, CTA-mediated FRP was used here to synthesise water-soluble semitelechelic and linear polymers with the hope of having a better control over molecular weight.

4.1.1. Rationale for the choice of the monomers and the polymers studied

As explained in Chapter 3 (Section 3.1.2), the two main factors influencing the choice of the monomers used in these studies were that their semitelechelic polymers have potential for further development as polymer therapeutics. Also, the choice of the monomers was made keeping in mind that an objective of these studies was to later investigate and compare the effect of individual molecular parameters, such as molecular weight, charge density, pK_a, and composition on cytotoxicity (Chapter 7).

These studies mainly focused on the six monomers, namely AEM, DMAEM, qAEM, qAPAAm, HPMA and NIPAAm, and the synthesis of their semitelechelic homopolymers or HPMA copolymers (Figure 4.1). As already explained (Chapter 3, Section 3.1.2), the amino-based methacrylate monomers (AEM, DMAEM, qAEM) were chosen to prepare semitelechelic polymers as they can potentially be used to condense DNA by electrostatic attraction and thus be used as gene delivery vectors

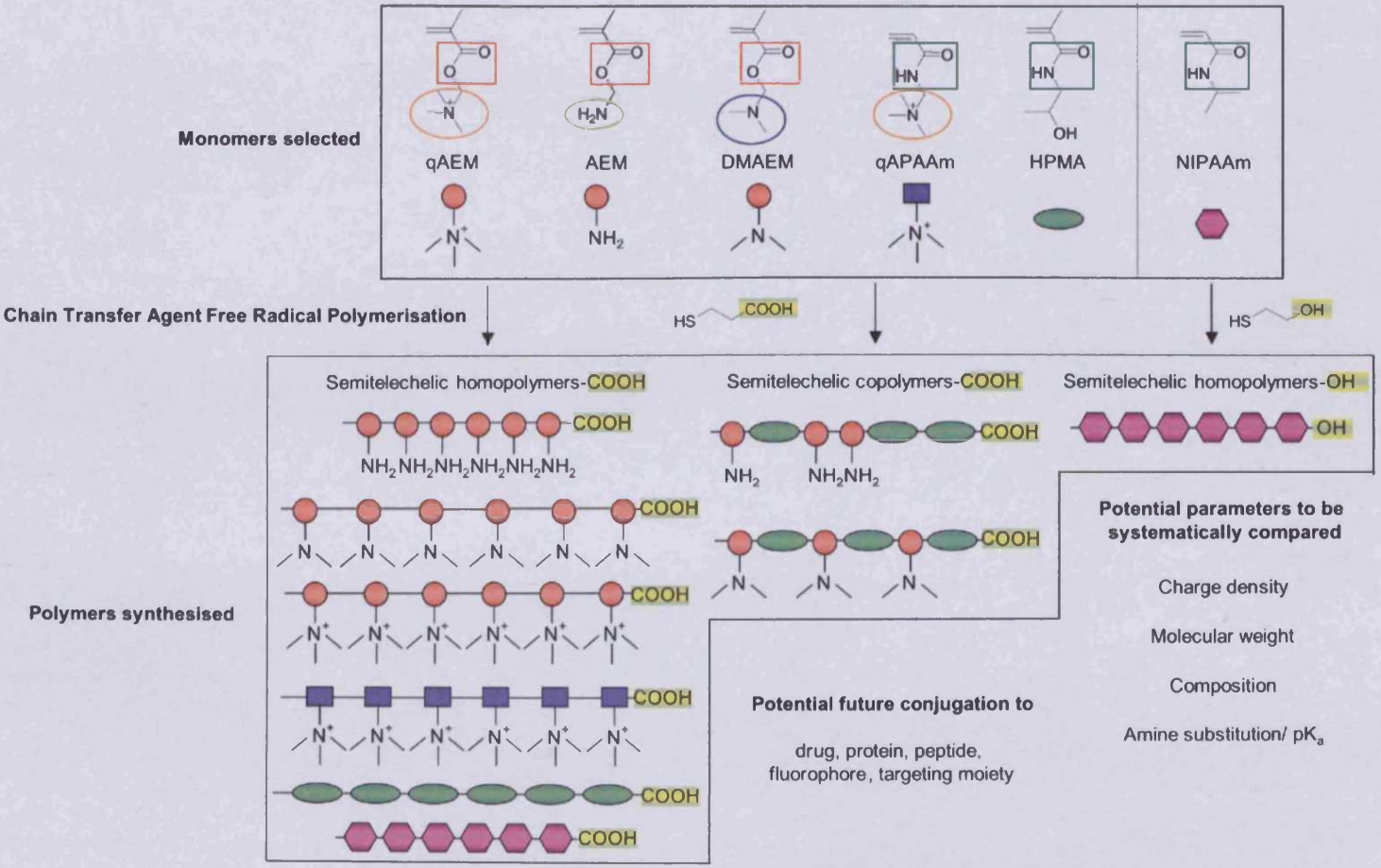

Figure 4.1: Rationale for the selection of the monomers used in these studies

(Cherng *et al.* 1996; van de Wetering *et al.* 1998; De Smedt *et al.* 2000; Rungsardthong *et al.* 2001). Also, conjugation through the amino group of their repeating units, or through their functionalised end-group, to drug, protein or targeting moiety would enable the design of novel polymer therapeutics. Moreover, the influence of the amine substitution and the charge density on biological properties may be studied without altering the overall chemistry of the polymer.

The monomer qAPAAm was chosen as it offers the possibility to obtain semitelechelic polymers with potential for gene delivery due to its charged pendant groups on the backbone. As it forms amino-based polyacrylamides, it is possible to compare its rate of degradation and other biological properties with amino-based polymethacrylate PqAEM, will allow further selection of the optimum biocompatible polymer structure for design of gene delivery vectors.

Finally, the acrylamide monomers used, HPMA and NIPAAm produce well-known biocompatible polymers that have been extensively studied in the fields of drug delivery and for other biomedical applications (Cole *et al.* 1987; Takei *et al.* 1994; Takei *et al.* 1995; Morgan *et al.* 1996; Vasey *et al.* 1999; Duncan 2003; Liu *et al.* 2003; Schmaljohann *et al.* 2003).
The semitelechelic homopolymers of HPMA and NIPAAm offer great opportunities for conjugation to peptides, proteins and/or drugs (Hoffman 1987; Monji and Hoffman 1987; Shoemaker *et al.* 1987; Hoffman 1995; Bulmus *et al.* 2000; Bulmus *et al.* 2003; Duncan 2003; Hoffman and Stayton 2007). They can in theory provide similar advantages to those obtained when using PEGylation of protein: prolongation of blood circulation time, decrease of immunogenicity and decrease of degradation of the conjugated protein (Harris 1992; Veronese 2001; Harris and Chess 2003; Veronese and Pasut 2005). Moreover, copolymerisation of HPMA with the amino-based methacrylate monomers (AEM or DMAEM) can be used to control the charge density and the composition of the semitelechelic copolymers synthesised. These polymers can then be compared with their cationic homopolymers, and consequently the influence of molecular parameters on biological properties evaluated.

4.1.2. Rationale for the choice of the CTA

As discussed in Chapter 1 (Section 1.8.2, Figure 1.17) CTA are compounds with labile hydrogen atoms such as halomethanes, disulfides and thiols. Several thiols have been extensively used for the synthesis of semitelechelic polymers, namely methyl 3-mercaptopropionate (Lu *et al.* 1998; Lu *et al.* 1999), 2-mercaptoethylamine (Lu *et al.* 1998; Lu *et al.* 1999), MPA (Takei *et al.* 1993b; a; Takei *et al.* 1995; Lu *et al.* 1998; Dvorak *et al.* 1999; Tsunoda *et al.* 2000; Wang *et al.* 2000), 2-aminoethanethiol (Kamei and Kopecek 1995), 3-mercaptopropionic hydrazide (Lu *et al.* 1998), 1-dodecanethiol (Hacioglu *et al.* 2002) and ME (van de Wetering *et al.* 1997; van de Wetering *et al.* 1998; Bos *et al.* 2000; Bos *et al.* 2004).
These studies used either MPA or ME as CTA to enable the introduction of either carboxylic acid or hydroxylic end-groups into the polymeric chain.

4.1.3. Technical aims

The main aims of these studies were the following:

- To synthesise and characterise a library of linear semitelechelic water-soluble homo- and copolymers with potential for further conjugation to bioactive agents, cores, or fluorophores, with different molecular weight and end-group functionality,
- To determine the effect of the CTA concentration on molecular weight and polydispersity of the synthesised semitelechelic polymer,
- To determine the efficiency of MPA as CTA with its apparent chain transfer constant (C^*_{tr}) in different systems (either one or two monomers) at complete monomer conversion.

Thus, to synthesise semitelechelic homopolymers with adjusted molecular weight, the monomers HPMA, AEM, DMAEM, NIPAAm, qAEM and qAPAAm were homopolymerised by FRP in the presence of either MPA or ME as CTA. Moreover, AEM and DMAEM were copolymerised with HPMA by FRP using MPA as CTA, to form linear semitelechelic copolymers of various composition (25 and 75 % of HPMA residue) and molecular weight characteristics. Overall, the CTA to monomer molar ratios ([CTA]/Σ[M]) were varied from 0.00 % to 14.49 %, while the [I]/Σ[M] ratios were fixed to 1.00, 2.00 or 4.30 %.

4.2. Methods

4.2.1. General methods

The semitelechelic homo- and copolymers synthesised were characterised using the techniques and methods previously described in Chapter 2, Section 2.3, i.e. IR, ^{1}H-NMR, ^{13}C-NMR and GPC.

4.2.2. Synthetic methods

The following Sections describe the synthetic methods used and Table 4.1 summarises the specific conditions used during polymerisation. The experiments described for the synthesis of the AEM/HPMA and DMAEM/HPMA copolymers were done in the Centre for Polymer Therapeutics in part by James Rickard, under my supervision.

Synthesis and characterisation of the semitelechelic PAEM-*co*-HPMA and the quaternized polymers

All polymerisations of AEM/HPMA and the quaternized monomers were carried out in deionised water at 60 °C, in a nitrogen atmosphere, using ACA as the initiator ([I]/Σ[M] = 1 %) and MPA as the CTA. A [CTA]/Σ[M] ratio of 0 to 3 % was used. The synthesis and characterisation of semitelechelic $PAEM_{25}HPMA_{75}$ with carboxylic end-group (P 25) is described as an example. All other polymerisations were carried out in the same way using different [CTA]/Σ[M] and comonomer ratios in case of PAEM-*co*-HPMA, as depicted on Schemes 4.1 and 4.2.

Synthesis of the semitelechelic $PAEM_{25}HPMA_{75}$ P 25 (Table 4.1)

AEM (778 mg, 4.690 mmol), HPMA (2 g, 14.000 mmol), ACA (52 mg, 0.186 mmol, [I]/Σ[M] = 1.0 %) and MPA (8 μL, 91.200 μmol, [CTA]/Σ[M] = 0.5 %) were dissolved in deionised water (20 mL) in a round-bottom flask at room temperature. The solution was continuously stirred with a magnetic stirrer and was degassed for 0.5 h with nitrogen before the flask was sealed and placed in an oil bath at 60 °C for 12 h. The reaction was then stopped by cooling the mixture to room temperature. The polymer was then isolated and purified by precipitation (3 times) from deionised water into cold acetone and dried under vacuum at 40 °C.

This whole procedure was repeated using different [CTA]/Σ[M] ratios (0 to 3 %) and

Table 4.1: Summary of the initial conditions for the synthesis of semitelechelic polymers

Identification	Monomers	[I]/Σ[M] (%)	[CTA]/Σ[M] (%)
P 19	$AEM_{25}HPMA_{75}$[a]	1.0	0.00
P 25	"		0.50[c]
P 26	"		1.00[c]
P 27	"		2.00[c]
P 28	"		3.00[c]
P 21	$AEM_{75}HPMA_{25}$[a]	1.0	0.00
P 29	"		0.50[c]
P 30	"		1.00[c]
P 31	"		2.00[c]
P 32	"		3.00[c]
P 3	AEM[a]	1.0	0.00
P 33	"		1.00[c]
P 34	"		2.00[c]
P 35	"		3.00[c]
P 22	$DMAEM_{25}HPMA_{75}$[b]	1.0	0.00
P 36	"		0.50[c]
P 37	"		1.00[c]
P 38	"		2.00[c]
P 39	"		3.00[c]
P 5	DMAEM[b]	2.0	0.00
P 40	"		1.00[c]
P 41	"		2.00[c]
P 42	"		3.00[c]

[a]: Polymerisation was carried out in deionised water/60 °C/ACA/N_2 atm; [b]: Polymerisation was carried out in ethanol/65 °C/AIBN/N_2 atm; [c]: MPA was used as CTA.

Table 4.1: Summary of the initial conditions for the synthesis of semitelechelic polymers (Continued)

Identification	Monomers	[I]/Σ[M] (%)	[CTA]/Σ[M] (%)
P 12	qAEM[a]	1.0	0.00
P 43	"		1.00[c]
P 44	"		2.00[c]
P 45	"		3.00[c]
P 15	qAPAAm[a]	1.0	0.00
P 46	"		1.00[c]
P 47	"		2.00[c]
P 48	"		3.00[c]
P 49	HPMA[d]	4.3	0.00
P 50	"		0.62[c]
P 51	"		1.20[c]
P 52	"		1.77[c]
P 53	"		2.39[c]
P 54	"		3.14[c]
P 55	"		3.89[c]
P 56	"		7.22[c]
P 57	"		10.14[c]
P 58	"		14.49[c]
P 59	NIPAAm[e]	1.0	0.00
P 60	"		4.00[c]
P 59	"		0.00
P 61	"		1.00[f]
P 62	"		4.00[f]

[a]: Polymerisation was carried out in deionised water/60 °C/ACA/N_2 atm; [c]: MPA was used as CTA; [d]: Polymerisations was carried out in methanol/50 °C/ACA/N_2 atm; [e]: Polymerisations was carried out in DMF/60 °C/AIBN/N_2 atm; [f]: ME was used as CTA.

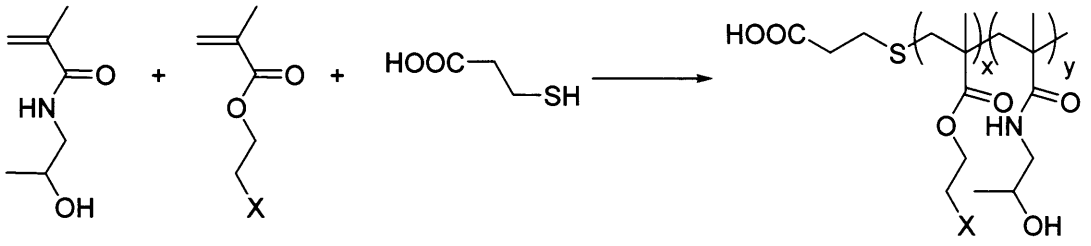

Scheme 4.1: Free radical copolymerisation of the cosystems HPMA/AEM or HPMA/DMAEM using MPA as CTA

With: For AEM: X = NH_3^+ Cl^-, polymerisation with ACA as the initiator, in deionised water, at 60 °C, under N_2 atm; [ACA]/Σ[M] = 1 %

For DMAEM: X = $N(CH_3)_2$, polymerisation with AIBN as the initiator, in ethanol, at 65 °C, under N_2 atm; [AIBN]/Σ[M] = 1 or 2 %.

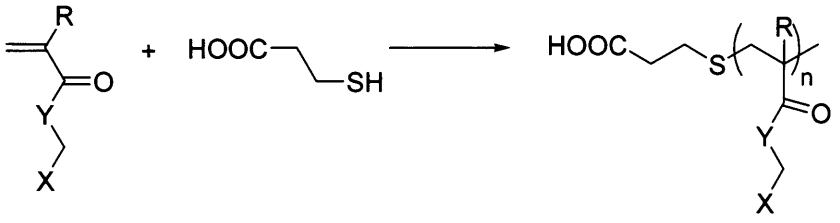

Scheme 4.2: Free radical homopolymerisation of the quaternized monomers and HPMA using MPA as CTA

With: For qAEM: R = CH_3, Y = O, X = $CH_2N^+(CH_3)_3Cl^-$; polymerisation with ACA as the initiator, in deionised water, at 60 °C, under N_2 atm; [ACA]/[qAEM] = 1.0 %

For qAPAAm: R = H, Y = NH, X = $(CH_2)_2N^+(CH_3)_3Cl^-$; polymerisation with ACA as the initiator, in deionised water, at 60 °C, under N_2 atm; [ACA]/Σ[qAPAAm] = 1.0 %

For HPMA: R = CH_3, Y = NH, X = $CHCH_3OH$; polymerisation with ACA as the initiator, in methanol, at 50 °C, under N_2 atm; [ACA]/[HPMA] = 4.3 %.

for different systems: either $AEM_{25}HPMA_{75}$, $AEM_{75}HPMA_{75}$, qAEM or qAPAAm (Table 4.1).

Characterisation of the semitelechelic PAEM-*co*-HPMA, PqAEM and PqAPAAm by IR, ^{1}H- and ^{13}C-NMR is described below.

The key is as follows: the red letters are assigned to the protons of the chemical entities; carbon elements are labelled by the blue numbers. Wavenumbers $\bar{\nu}$ are expressed in cm^{-1}; ν represents the stretching vibrations and δ, the bending vibrations. In NMR, δ are expressed in ppm and s is a singlet, bs a broad singlet, d a doublet, t a triplet, m a multiplet and J represents a coupling constant.

Characterisation of the semitelechelic PAEM-co-HPMA samples P 3, P 19, P 21 and P 25-P 35 (Table 4.1)

Yield: 50 % on average

IR: $\bar{\nu}$ (cm^{-1}) = 3 300, ν_{O-H}; 2 959, ν_{C-H} and vibration of $^{+}N-H$ group (absorbing between 3 300 and 2 000 cm^{-1}); 1 721, $\nu_{C=O}$ of the ester bonds; 1 634, $\nu_{C=O}$ (Amide I band); 1 529, ν_{C-N} and δ_{CNH} (Amide II band); 1 451, δ_{COH} and δ_{CH}; 1 242, ν_{C-O}; 1 330-1 200, δ_{NH} and δ_{OCN} (Amide III band) and 1 350-800, δ_{C-C} and δ_{CH}.

^{1}H-NMR (D_2O, ppm): δ = 0.8 to 1.8, bs, 5H, H_a and H_b; 2.1, bs, 3H, H_e; 2.5, bs, 2H, H_d; 4.3, bs, 2H, H_c; 1, bs, 6H, H_g and H_k; 1.7, bs, 2H, H_f; 3, bs, 2H, H_i; 3.8, bs, 1H, H_j.

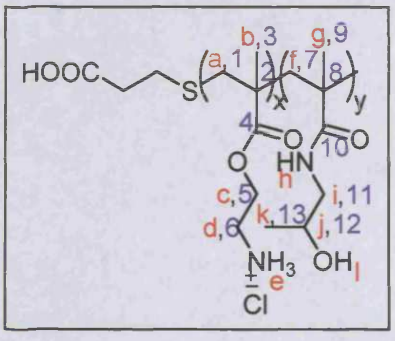

^{13}C-NMR (D_2O, ppm): δ = 15, C_3; 17, C_1; 44, C_2; 60, C_6; 65, C_5; 175, C_4; 15, C_9; 17, C_7; 22, C_{13}; 45, C_8; 48, C_{11}; 65, C_{12}; 177, C_{10}.

GPC (PBS, flow rate 1 mL/min, columns calibrated with narrow pullulan standards): M_n, M_w/M_n ranging from 55 200 $g.mol^{-1}$, 2.75 to 4 600 $g.mol^{-1}$, 1.14 for $PAEM_{25}$-*co*-$HPMA_{75}$; from 47 090 $g.mol^{-1}$, 3.43 to 3 480 $g.mol^{-1}$, 1.02 for $PAEM_{75}$-*co*-$HPMA_{25}$; and from 40 670 $g.mol^{-1}$, 2.60 to 6 330 $g.mol^{-1}$, 1.50 for PAEM.

Characterisation of the semitelechelic PqAEM samples P 12 and P 43-P 45 (Table 4.1)

Yield: 90 %

IR: $\bar{\nu}$ (cm^{-1}) = wide band around 2 957, ν_{C-H}; 2 857, vibration of $^{+}$N-H group (absorbing between 3 300 and 2 000 cm^{-1}); 1 725, $\nu_{C=O}$; 1 470, δ_{CH}; 1 230, ν_{C-O}; 1 350-800, δ_{C-C} and δ_{CH}.

^{1}H-NMR (D_2O, ppm): δ = 1, bs, 3H, H_b; 2, bs, 2H, H_a; 3.2, bs, 9H, H_e; 3.8, bs, 2H, H_d; 4.4, bs, 2H, H_c.

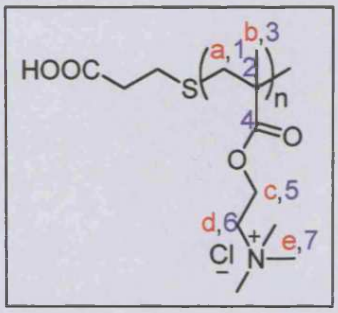

^{13}C-NMR (D_2O, ppm): δ = 19, C_3; 45, C_1; 52, C_2; 54, C_7; 59, C_6; 64, C_5; 178, C_4.

GPC (PBS, flow rate 1 mL/min, columns calibrated with narrow pullulan standards): M_n, M_w/M_n ranging from 224 350 g.mol^{-1}, 4.36 to 10 900 g.mol^{-1}, 2.13.

Characterisation of the semitelechelic PqAPAAm samples P 15 and P 46-P 48 (Table 4.1)

Yield: 85 %

IR: $\bar{\nu}$ (cm^{-1}) = wide band around 2 941, ν_{C-H}; 2 861, vibration of $^{+}$N-H group (absorbing between 3 300 and 2 000 cm^{-1}); 1 646, $\nu_{C=O}$ (Amide I band); 1 542, ν_{C-N} and δ_{CNH} (Amide II band); 1 486, δ_{CH}; 1 330-1 200, δ_{NH} and δ_{OCN} (Amide III band) and 1 350-800 δ_{C-C} and δ_{CH}.

^{1}H-NMR (D_2O, ppm): δ = 1.1 to 2.2, 5H, H_a, H_b and H_e; 3.1, bs, 9H, H_g; 3.2, bs, 2H, H_f; 3.4, bs, 2H, H_d.

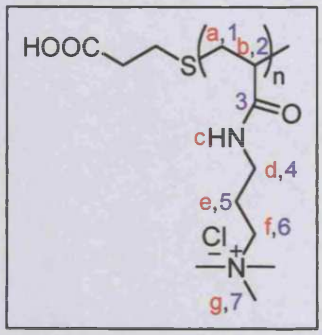

^{13}C-NMR (D_2O, ppm): δ = 22, C_5; 35, C_1; 36, C_6; 42, C_2; 53, C_7; 64, C_4; 176, C_3.

GPC (PBS, flow rate 1 mL/min, columns calibrated with narrow pullulan standards): M_n, M_w/M_n ranging from 349 580 g.mol^{-1}, 8.88 to 7 030 g.mol^{-1}, 8.53.

Synthesis and characterisation of the semitelechelic PDMAEM-*co*-HPMA

The DMAEM/HPMA polymerisation reactions were carried out in ethanol at 65 °C in a nitrogen atmosphere using AIBN as the initiator (where [I]/Σ[M] was 1 or 2 %) and MPA was used as the CTA (Scheme 4.1). The [CTA]/Σ[M] ratio was varied from 0 to 3 % (Table 4.1). The synthesis and characterisation of the semitelechelic $PDMAEM_{25}HPMA_{75}$ with carboxylic end-group P 36 is given as an example. All other polymerisations were carried out in the same way at different [CTA]/Σ[M] and comonomer ratios.

Synthesis of the semitelechelic $PDMAEM_{25}HPMA_{75}$ P 36 (Table 4.1)

DMAEM (790 µL, 4.670 mmol), HPMA (2.0 g, 14.000 mmol), AIBN (30.2 mg, 0.184 mmol, [I]/Σ[M] = 1.0 %) and MPA (8 µL, 91.200 µmol, [CTA]/Σ[M] = 0.5 %) were dissolved in ethanol (20 mL) in a round-bottom flask, with a magnetic stirrer and at room temperature. The mixture was then degassed with nitrogen for 0.5 h before the flask was sealed and placed in an oil bath at 65 °C for 12 h. The reaction was stopped by cooling the mixture to room temperature and the polymer was isolated and purified by precipitation (3 times) from ethanol into cold diethyl ether, dried under vacuum at 40 °C and characterised by IR, ^{1}H- and ^{13}C-NMR.

Characterisation of the semitelechelic PDMAEM-co-HPMA samples P 5, P 22 and P 36-P 42 (Table 4.1)

Yield: 40 % on average

IR: $\bar{\nu}$ (cm^{-1}) = 3 344 cm^{-1}, ν_{O-H}; 2 923, ν_{C-H}; 1 721, $\nu_{C=O}$ of the ester bonds; 1 627, $\nu_{C=O}$ (Amide I band); 1 525, ν_{C-N} and δ_{CNH} (Amide II band); 1 477, δ_{COH} and δ_{CH}; 1 268, ν_{C-O}; 1 330-1 200, δ_{NH} and δ_{OCN} (Amide III band) and 1 350-800 δ_{C-C} and δ_{CH}.

^{1}H-NMR (DMSO-d_6, ppm): δ = 0.7 to 2.1, broad peaks, 5H, H_a and H_b; 2.2, bs, 6H, H_e; 2.6, bs, 2H, H_d; 4.1, bs, 2H, H_c; 0.8, bs, 3H, H_g; 0.9, ss, 3H, H_k; 1.7, broad peak, 2H, H_f; 2.9, bs, 2H, H_i; 3.7, bs, 1H, H_j; 4.7, bs, 1H, H_l; 7.2, bs, 1H, H_h.

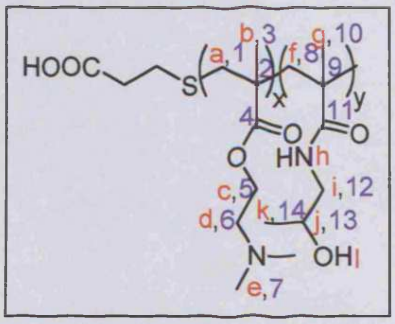

^{13}C-NMR (DMSO-d_6, ppm): δ = 15, C_3 and C_{10}; 17, C_1 and C_8; 44, C_2; 45, C_7; 56, C_6; 62, C_5; 175, C_4; 22, C_{14}; 45, C_9; 48, C_{12}; 65, C_{13}; 177, C_{11}.

GPC (THF, flow rate 1 mL/min column calibrated with narrow PS standards): M_n, M_w/M_n ranging from 21 020 g.mol^{-1}, 2.85 to 3 000 g.mol^{-1}, 1.50 for $PDMAEM_{25}$-*co*-$HPMA_{75}$; and from 19 050 g.mol^{-1}, 2.60 to 6 500 g.mol^{-1}, 1.50 for PDMAEM.

Synthesis and characterisation of the semitelechelic PHPMA

All polymerisations were carried out using the method described by Kopeček and co-workers (Wang *et al.* 2000) using different [CTA]/[M] and comonomer ratios. Semitelechelic PHPMA homopolymer was synthesised in methanol at 50 °C under a nitrogen atmosphere using ACA as the initiator ([I]/[M] = 4.3 %) and MPA as the CTA (Scheme 4.2). The [CTA]/[M] ratio was varied from 0.00 to 14.49 % (Table 4.1). The synthesis of the semitelechelic PHPMA with carboxylic end-group P 55 is given as an example. All other HPMA homopolymers were synthesised in the same way using different [CTA]/[M] (Table 4.1).

Synthesis of the semitelechelic PHPMA P 55 (Table 4.1)

HPMA (2.0 g, 14.0 mmol), ACA (168.2 mg, 0.6 mmol, [I]/[M] = 4.30 %), MPA (87.5 µL, 1.0 mmol, [CTA]/[M] = 7.22 %) were dissolved in methanol (20 mL) at room temperature in a round-bottom flask with a magnetic stirrer. The mixture was then degassed for 0.5 h with nitrogen before the flask was sealed and placed in an oil bath at 50 °C for 12 h. The reaction was stopped by cooling the mixture to room temperature and the homopolymer was then isolated and purified by precipitation (3 times) from methanol into cold acetone, dried under vacuum at 40 °C and characterised by IR, ^{1}H- and ^{13}C-NMR.

Characterisation of the semitelechelic PHPMA samples P 49-P 58 (Table 4.1)

Yield: 70 %.

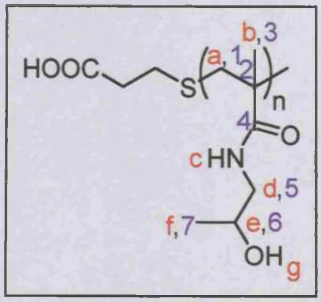

IR: $\bar{\nu}$ (cm^{-1}) = 3 352, ν_{O-H}; 2 972, ν_{C-H}; 2 900, ν_{CH-O}; 1 660, $\nu_{C=O}$ (Amide I band); 1 530, ν_{C-N} and δ_{CNH} (Amide II band); 1 388, δ_{CH}; 1 330-1 200, δ_{NH} and δ_{OCN} (Amide III band) and 1 210-800 δ_{C-C} and δ_{CH}.

^{1}H-NMR (DMSO-d_6, ppm): δ = 0.8, bs, 3H, H_b; 0.9, ss, 3H, H_f; 1.7, bs, 2H, H_a; 2.9, bs, 2H, H_d; 3.7, bs, 1H, H_e; 4.7, bs, 1H, H_g; 7.2, bs, 1H, H_c.

^{13}C-NMR (DMSO- d_6, ppm): δ = 15, C_3; 17, C_1; 22, C_7; 45, C_2; 48, C_5; 65, C_6; 177, C_4.

GPC (PBS, flow rate 1 mL/min, columns calibrated with narrow pullulan standards): M_n, M_w/M_n ranging from 24 500 g.mol^{-1}, 2.00 to 1 440 g.mol^{-1}, 1.40.

Synthesis and characterisation of the semitelechelic PNIPAAm

To synthesise semitelechelic NIPAAm-based homopolymers with hydroxylic or carboxylic end-groups, ME or MPA were used as the CTA, respectively. The homopolymerisation was carried out in DMF at 60 °C under a nitrogen atmosphere using AIBN as the initiator ([I]/[M] = 1 %) (Scheme 4.3). The ratio of [CTA]/[M] was varied from 0 to 4 % (Table 4.1). The synthesis of semitelechelic PNIPAAm with hydroxylic end-group P 62 is given as an example (Table 4.1). All other NIPAAm homopolymers were synthesised in the same way using either ME or MPA as CTA and different [CTA]/[M] ratios were used (Table 4.1).

Synthesis of the semitelechelic PNIPAAm P 62 (Table 4.1)

NIPAAm (5.65 g, 50.0 mmol), AIBN (82.10 mg, 0.5 mmol, [I]/[M] = 1 %) and ME (143.60 μL, 2.0 mmol, [CTA]/[M] = 4 %) were dissolved in DMF (40 mL) at room temperature in a round-bottom flask with a magnetic stirrer. The mixture was then degassed for 0.5 h with nitrogen before the flask was sealed and placed in an oil bath at 60 °C for 12 h. The reaction was stopped by cooling the mixture to room temperature. The homopolymer was then isolated and purified by precipitation (3 times) from DMF into cold diethyl ether, dried under vacuum at 40 °C and characterised by IR, ^{1}H- and ^{13}C-NMR.

Characterisation of the semitelechelic PNIPAAm samples P 59-P 62 (Table 4.1)

Yield: 60 % for hydroxylic end-group PNIPAAm
77 % for carboxylic end-group PNIPAAm

IR: $\bar{\nu}$ (cm^{-1}) = 3 302, ν_{O-H}; 2 970, ν_{C-H}; 1 645, $\nu_{C=O}$ (Amide I band); 1 534, ν_{C-N} and δ_{CNH} (Amide II band); 1 450, δ_{CH}; 1 330-1 200, δ_{NH} and δ_{OCN} (Amide III

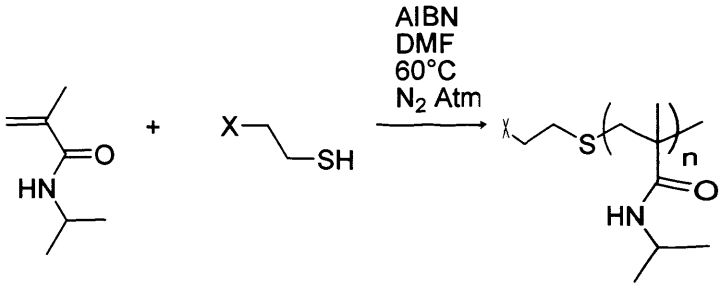

Scheme 4.3: Free radical homopolymerisation of NIPAAm using MPA or ME as CTA

With: X = COOH when MPA is used as the CTA

X = OH when ME is used as the CTA

band) and 1 350-800 δ_{C-C} and δ_{CH}.

^{1}H-NMR ($CDCl_3$, ppm): δ = 1.1, ss, 6H, H_e; 1.5 to 3.0, broad peaks, 5H, H_a and H_b; 4.0, ss, 1H, H_d; 6.4, bs, 1H, H_c.

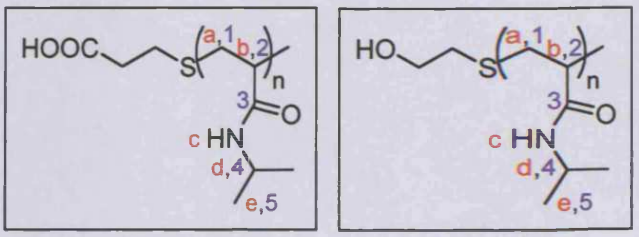

^{13}C-NMR ($CDCl_3$, ppm): δ = 23, C_5; 36, bs, C_1; 42, s, C_4; 43, bs, C_2; 175, C_3.

GPC (THF, flow rate 1 mL/min column calibrated with narrow PS standards): M_n, M_w/M_n ranging from 71 430 g.mol^{-1}, 2.10 to 515 g.mol^{-1}, 1.10 when MPA was used as CTA; and M_n and M_w/M_n ranging from 71 430 g.mol^{-1}, 2.10 to 450 g.mol^{-1}, 1.10 when ME was used as CTA.

Esterification of the semitelechelic PHPMA P 54 bearing a carboxylic end-group with *N*-hydroxysuccinimide to form an activated ester

Esterification of the semitelechelic PHPMA bearing a carboxylic acid end-group P 54 (Table 4.1) was undertaken using HOSu as described by Kopeček and co-workers (Lu *et al.* 1998) (Scheme 4.4). Briefly, P 54 (150 mg, M_n = 3 450 g.mol^{-1}, M_w/M_n = 1.90, $2.30 \cdot 10^{-2}$ mmol) and HOSu (45 mg, 0.39 mmol) were dissolved in DMF (2.5 mL), and cooled to 0 °C. DCC (81 mg, 0.39 mmol) was dissolved in DMF (0.5 mL) and added dropwise. The solution was stirred for 48 h at 4 °C, warmed to room temperature and then stirred for a further 12 h. Acetic acid (21 µL, 0.35 mmol) was then added and the mixture was stirred for a further 2 h. The white precipitate formed, *N,N'*-dicyclohexyl urea (DCU), was then filtered off. The product (P 63) was isolated and purified by precipitation (3 times) from DMF into cold diethyl ether and dried under vacuum at 40 °C. P 63 was obtained as a white powder in a 75 % yield, and was analysed by IR, ^{1}H- and ^{13}C-NMR.

Characterisation of the activated semitelechelic PHPMA sample P 63

IR: $\bar{\nu}$ (cm^{-1}) = 3 323, ν_{O-H}; 2 927, ν_{C-H}; 2 847, ν_{O-H} and ν_{CH-O}; 1 732, $\nu_{C=O}$ of the lactam end-group; 1 625, $\nu_{C=O}$ (Amide I band); 1 570, ν_{C-N} and δ_{CNH} (Amide II band); 1 534, ν_{N-H}; 1 460-1 370, δ_{CH}; 1 330-1 200, δ_{NH} and δ_{OCN} (Amide III band) and 1 350-800, δ_{C-C} and δ_{CH}.

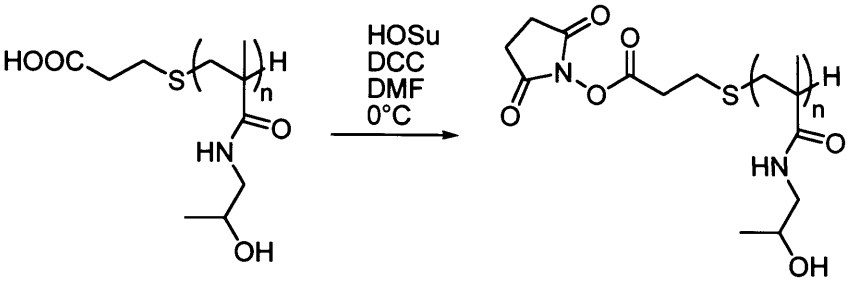

Scheme 4.4: Activation of the carboxylic end group of semitelechelic PHPMA (P 54)

^{1}H-NMR (DMSO-d_6, ppm): δ = 0.8, bs, 3H, H_b; 1.0, s, 3H, H_f; 1.7, bs, 2H, H_a; 2.37, small s, 2H, H_h; 2.43, small s, 2H, H_i; 2.9, bs, 2H, H_d; 3.7, bs, 1H, H_e; 4.7, bs, 1H, H_g; 7.2, bs, 1H, H_c.

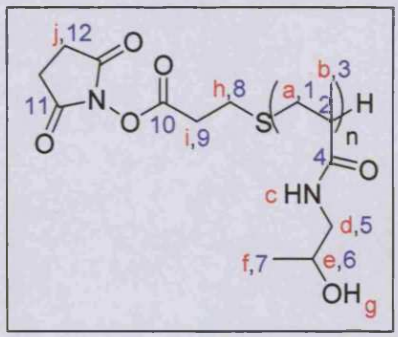

^{13}C-NMR (DMSO- d_6, ppm): δ = 15, C_3; 17, C_1; 22, C_7; 25, C_8; 32, C_{12}; 34, C_9; 45, C_2; 48, C_5; 65, C_6; 170, C_{10}; 174, C_{11}; 177, C_4.

GPC (PBS, flow rate 1 mL/min, columns calibrated with narrow pullulan standards): M_n = 4 810 g.mol^{-1} and M_w/M_n = 1.60.

4.3. Results

4.3.1. Synthesis and characterisation of semitelechelic PHPMA, PqAEM, PqAPAAm, PNIPAAm, PAEM-co-HPMA and PDMAEM-co-HPMA

Synthesis of semitelechelic PHPMA, PNIPAAm, PqAEM, PqAPAAm, PAEM-*co*-HPMA and PDMAEM-*co*-HPMA was successfully achieved using MPA or ME as the CTA. Analysis by IR, ^{1}H-, ^{13}C-NMR and GPC (Section 4.2) showed that pure polymers (i.e. without traces of residual solvent and/or unreacted monomers) were obtained in the form of a white powder. The yield ranged from 40 to 80 % and Tables 4.2 - 4.4 summarise the results obtained.

^{1}H-NMR was used to determine the final composition of the copolymers comparing the integral of the methine protons of the HPMA repeating unit against the integral of the methylene protons in alpha position of the ester group of the amino-based methacrylate repeating unit. As can be seen in Tables 4.2 and 4.3, the calculated final composition of the semitelechelic copolymers of HPMA were similar to the expected values and very close to the feeding ratios of HPMA and amino-based methacrylate monomers.

Characterisation of the end-group of the homo- and copolymers using IR and NMR proved difficult. No bands or peaks were observed from the end-groups of P 25-P 48, P 50-P 58, P 60-P 62. Therefore, alternative techniques had to be sought in order to verify these functionalisations (see Section 4.3.4. for detailed explanation).

Table 4.2: Final composition, number-average molecular weight and polydispersity of the semitelechelic AEM/HPMA polymers

Identification	Initial Composition (%)	Final Composition (%)		[CTA]/Σ[M] (%)	M_n (g.mol^{-1})	M_w/M_n	Average yield (%)[(d)]
P 19	AEM (25), HPMA (75)[(a)]	AEM	(22)	0.00	55 200[(c)]	2.75[(c)]	
P 25	"	"	(21)	0.50[(b)]	9 380[(c)]	2.40[(c)]	
P 26	"	"	(21)	1.00[(b)]	10 070[(c)]	1.67[(c)]	50
P 27	"	"	(22)	2.00[(b)]	5 660[(c)]	1.22[(c)]	
P 28	"	"	(23)	3.00[(b)]	4 600[(c)]	1.14[(c)]	
P 21	AEM (75), HPMA (25)[(a)]	AEM	(67)	0.00	47 090[(c)]	3.43[(c)]	
P 29	"	"	(67)	0.50[(b)]	20 550[(c)]	1.68[(c)]	
P 30	"	"	(67)	1.00[(b)]	3 990[(c)]	1.05[(c)]	50
P 31	"	"	(70)	2.00[(b)]	3 480[(c)]	1.02[(c)]	
P 32	"	"	(70)	3.00[(b)]	3 510[(c)]	1.02[(c)]	
P 3	AEM (100)[(a)]	AEM	(100)	0.00	40 670[(c)]	1.20[(c)]	
P 33	"	"	"	1.00[(b)]	12 460[(c)]	2.60[(c)]	50
P 34	"	"	"	2.00[(b)]	8 580[(c)]	1.80[(c)]	
P 35	"	"	"	3.00[(b)]	6 330[(c)]	1.50[(c)]	

[(a)]: Polymerisation was carried out in deionised water at 60 °C under N_2 atm with [I]/Σ[M] = 1 % and ACA as the initiator; [(b)]: MPA was used as the CTA; [(c)]: Mobile phase PBS, flow rate 1 mL/min, column calibrated with narrow pullulan standards; [(d)]: Yield measured gravimetrically at the end of the polymerisation.

Table 4.3: Final composition, number-average molecular weight and polydispersity of the semitelechelic DMAEM/HPMA polymers

Identification	Initial Composition (%)	Final Composition (%)		[CTA]/Σ[M] (%)	M_n (g.mol^{-1})	M_w/M_n	Average yield (%)[e]
P 22	DMAEM (25), HPMA (75)[a]	DMAEM	(25)	0.00	21 020[d]	2.85	
P 36	"	"	(25)	0.50[c]	7 220[d]	2.70	
P 37	"	"	(28)	1.00[c]	3 610[d]	2.60	40
P 38	"	"	(26)	2.00[c]	3 000[d]	1.80	
P 39	"	"	(32)	3.00[c]	4 430[d]	1.50	
P 5	DMAEM (100)[b]	DMAEM	(100)	0.00	19 050[d]	2.10	
P 40	"	"		1.00[c]	7 350[d]	2.60	40
P 41	"	"		2.00[c]	6 810[d]	1.80	
P 42	"	"		3.00[c]	6 500[d]	1.50	

[a]: Polymerisation was carried out in ethanol at 65 °C under N_2 atm with [I]/Σ[M] = 1 % and AIBN as the initiator; [b]: Polymerisation was carried out in ethanol at 65 °C under N_2 atm with [I]/Σ[M] = 2 % and AIBN as the initiator; [c]: MPA was used as the CTA; [d]: Mobile phase THF, flow rate 1 mL/min; column calibrated with narrow PS standards; [e]: Yield measured gravimetrically at the end of the polymerisation.

Table 4.4: Final composition, M_n and polydispersity of the semitelechelic qAEM, qAPAAm, HPMA and NIPAAm homopolymers

Identification	Initial Composition (%)	Final Composition (%)	[CTA]/Σ[M] (%)	M_n (g.mol^{-1})	M_w/M_n	Yield (%)[h]
P 12	qAEM (100)[a]	qAEM (100)	0.00	224 350[f]	2.44[f]	
P 43	"	"	1.00[d]	68 760[f]	2.13[f]	90
P 44	"	"	2.00[d]	13 660[f]	4.36[f]	
P 45	"	"	3.00[d]	10 900[f]	3.35[f]	
P 15	qAPAAm (100)[a]	qAPAAm (100)	0.00	349 580[f]	1.48[f]	
P 46	"	"	1.00[d]	17 480[f]	6.71[f]	85
P 47	"	"	2.00[d]	7 030[f]	8.53[f]	
P 48	"	"	3.00[d]	7 140[f]	8.88[f]	
P 49	HPMA (100)[b]	HPMA (100)	0.00	24 500[f]	2.00[f]	
P 50	"	"	0.62[d]	9 050[f]	2.00[f]	
P 51	"	"	1.20[d]	6 150[f]	2.00[f]	
P 52	"	"	1.77[d]	5 000[f]	1.80[f]	
P 53	"	"	2.39[d]	3 530[f]	1.70[f]	70
P 54	"	"	3.14[d]	3 450[f]	1.90[f]	
P 55	"	"	3.89[d]	3 190[f]	1.60[f]	
P 56	"	"	7.22[d]	1 890[f]	1.80[f]	
P 57	"	"	10.14[d]	2 110[f]	1.40[f]	
P 58	"	"	14.49[d]	1 440[f]	1.80[f]	
P 59	NIPAAm (100)[c]	NIPAAm (100)	0.00	71 430[g]	2.10[g]	77
P 60	"	"	4.00[d]	515[g]	1.10[g]	
P 59	"	"	0.00	71 430[g]	2.10[g]	
P 61	"	"	1.00[e]	470[g]	1.10[g]	60
P 62	"	"	4.00[e]	450[g]	1.20[g]	

Polymerisations were carried out in [a]: Deionised water/ACA/60 °C/N_2 atm with [I]/Σ[M] = 1 %, [b]: Methanol/ACA/50 °C/N_2 atm with [I]/Σ[M] = 4.3 %, [c]: DMF/AIBN/60 °C/N_2 atm with [I]/Σ[M] = 1 %; [d]: MPA was used as the CTA; [e]: ME was used as the CTA; [f]: PBS as mobile phase, flow rate 1 mL/min, column calibrated with narrow pullulan standards; [g]: THF as mobile phase, flow rate 1 mL/min, column calibrated with narrow PS standards; [h]: Yield measured gravimetrically at the end of the polymerisation.

4.3.2. Molecular weight and polydispersity

Tables 4.2 to 4.4 show that in all cases, except qPAEM and qPAPAAm, the polydispersity decreased with increasing amounts of CTA. On average, the polydispersity was ~ 2 or lower.

When M_n was plotted as a function of molar ratio [CTA]/Σ[M] (Figure 4.2), it could be seen that M_n decreased when high amounts of CTA were used in the reaction. Eventually a plateau was reached when the molar ratio of [CTA]/Σ[M] reached 2 to 4 %.

The quaternized homopolymers had a very high M_n (as high as 349 580 g.mol^{-1}, Table 4.4). However for PqAEM, the M_n fell from 224 350 to 10 900 g.mol^{-1} when the [MPA]/[qAEM] ratio was increased from 1 to 3 %. The polydispersity of PqAEM was high, being up to 3.28 in average (from P 43 to P 45). In the case of PqAPAAm, the M_n decreased from 349 580 to 7 030 g.mol^{-1} with an increase of [MPA]/[qAPAAm] ratio from 1 to 3 % and with a high average polydispersity of 8.04 (from P 46 to P 48). The NIPAAm-based polymers (Table 4.4) had a very low M_n (450 g.mol^{-1}) according to the GPC results when CTA was used. Nevertheless, even though GPC indicated a very low M_n, ^{1}H-NMR confirmed the existence of PNIPAAm as the signals obtained were characteristic of a polymer structure, i.e. wide and broad peaks.

4.3.3. Determination of C^*_{tr} for 3-mercaptopropionic acid in different polymerisation systems

When chain transfer reactions occur to an added compound (e.g. CTA) in FRP, the Mayo equation becomes as defined in Equations 4.1 and 4.2 (Berger and Brandrup 1989; Odian 1991).

$$\frac{1}{\overline{DP_n}} = \left(\frac{1}{\overline{DP_n}}\right)_0 + C_{tr} \times \frac{[CTA]}{[M]} \qquad \text{(Eq 4.1)}$$

$$\frac{1}{\overline{DP_n}} = \left(\frac{1}{\overline{DP_n}}\right)_0 + \frac{k_{tr}}{k_p} \times \frac{[CTA]}{\sum[M]} \qquad \text{(Eq 4.2)}$$

where $(1/DP_n)_0$ is the value of $1/DP_n$ in the absence of the CTA and sums the transfers to monomer, initiator, polymer and solvent.

(a)

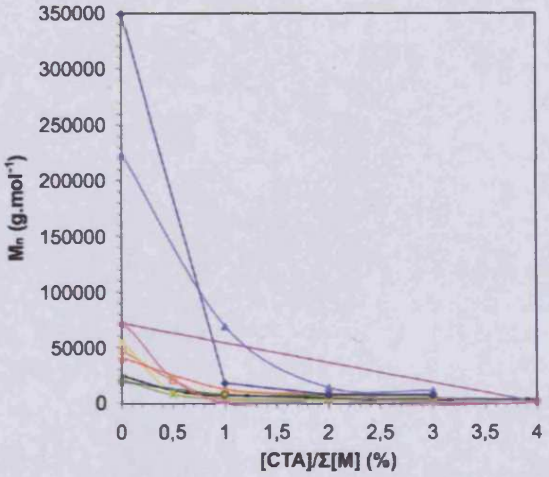

(b)

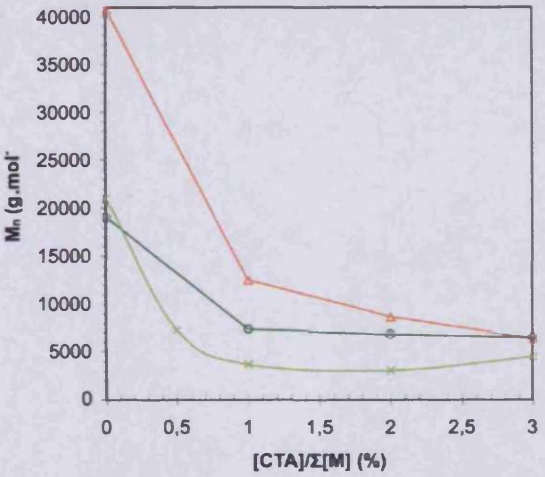

(c)

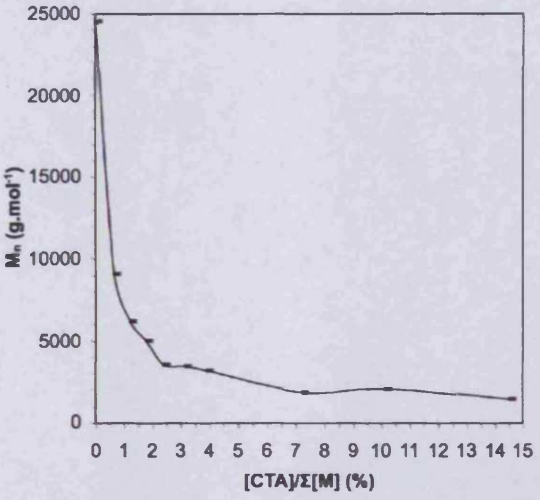

Figure 4.2: Effect of the [CTA]/Σ[M] ratio on number-average molecular weight

Panel (a) plots all polymers studied: ◆ PqAPAAm; ▲ PqAEM; △ PAEM; □ $PAEM_{75}$-*co*-$HPMA_{25}$; ✳ $PAEM_{25}$-*co*-$HPMA_{75}$; ○ PDMAEM; × $PDMAEM_{25}$-*co*-$HPMA_{75}$; - PHPMA; ◇ PNIPAAm with MPA; – PNIPAAm with ME; panel (b) zooms in on △ PAEM; ○ PDMAEM; × $PDMAEM_{25}$-*co*-$HPMA_{75}$ and panel (c) plots - PHPMA.

The C_{tr} (Chapter 1, Section 1.8.2) or its apparent value C^*_{tr} (determined at complete monomer conversion) for a specific CTA is obtained from the slope of the plot of the inverse of the number-average degree of polymerisation ($1/DP_n$) against the mercaptan to monomer molar ratio ([CTA]/Σ[M]) when this relationship is linear.

In the case of homopolymers, the DP_n can be calculated from the ratio of the M_n to the molecular weight of the repeating unit of the homopolymer M_0 (Equation 4.3):

$$\overline{DP_n} = \frac{\overline{M_n}}{M_0} \qquad \text{(Eq 4.3)}$$

In the case of copolymers, the DP_n is as follows (Equation 4.4):

$$\overline{DP_n} = \frac{\overline{M_n}}{\alpha \times M_{1,0} + \beta \times M_{2,0}} \qquad \text{(Eq 4.4)}$$

where $M_{1,0}$ and $M_{2,0}$ are the molecular weight of the comonomers; α and β the proportion of each monomer in the final copolymer and where $[M] = [M_1]+[M_2]$.

Following calculation of DP_n, plots of $1/DP_n = f([CTA]/\Sigma[M])$ were made for each system (Figure 4.3). C^*_{tr} was determined as the slope of each equation obtained by linear regression. The C^*_{tr} values for MPA in several polymerisation reactions and the correlation coefficient R (a dimensionless measure of the reliability of the linear relationship between $1/DP_n$ (the ordinates) and [CTA]/Σ[M] (the abscissas)) are listed in Table 4.5. It can be seen that R values were greater or equal to 95 %, except for the DMAEM, qAPAAm monomers, and the AEM (75 %)/HPMA (25 %) and DMAEM (25 %)/HPMA (75 %) comonomer systems. Table 4.5 also shows that the C^*_{tr} of MPA used as CTA for the polymerisation of methacrylate-based monomers (AEM, qAEM, and comonomers $AEM_{25}/HPMA_{75}$) ranged from 0.66 to 0.91. In the case of the methacrylamide-based HPMA monomer, the C^*_{tr} of MPA was 0.59.

4.3.4. Activation of the carboxylic acid end-group of semitelechelic PHPMA

Transformation of the carboxylic end groups of a low molecular weight semitelechelic PHPMA (P 54) into an activated ester was attempted by esterification with HOSu using DCC as the dehydrating agent in DMF (Wang *et al.* 2000), to form P 63 (Scheme 4.4). This polymer was obtained in the form of a white powder in a 75 % yield, the molecular weight and polydispersity of P 63 was not significantly different from that of the starting polymer P 54 (Table 4.6). The IR spectra of P 54

(a)

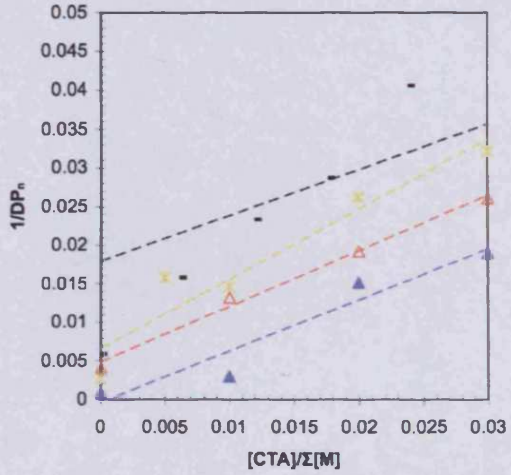

(b)

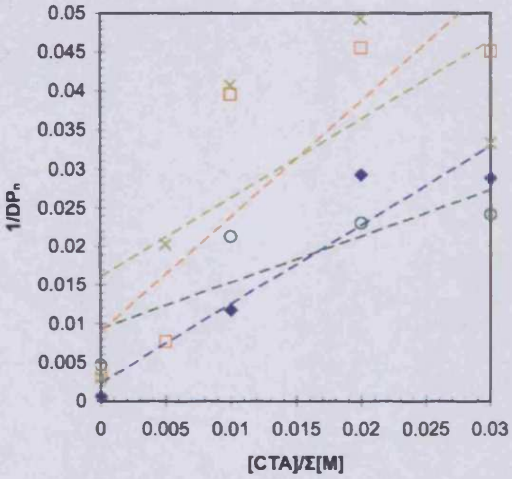

(c)

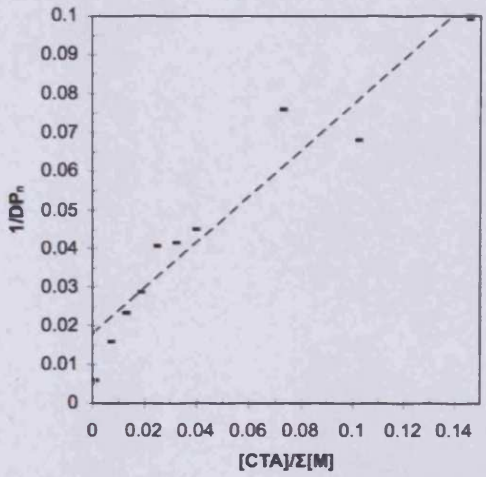

Figure 4.3: Effect of the concentration of the CTA MPA, on the number-average degree of polymerisation (DP_n) for several polymerisation reactions

Panel (a): ▲ PqAEM; △ PAEM; ✳ $PAEM_{25}$-*co*-$HPMA_{75}$; - PHPMA; panel (b): ◆ PqAPAAm; □ $PAEM_{75}$-*co*-$HPMA_{25}$; ○ PDMAEM; × $PDMAEM_{25}$-*co*-$HPMA_{75}$; panel (c) expands the case of PHPMA. The dashed lines correspond to the regression trend lines of each system.

Table 4.5: Calculated Apparent Chain Transfer Constants (C^*_{tr}) for MPA

Systems	C^*_{tr} for MPA	R[(d)]
AEM	0.72[(a)]	0.99
DMAEM	0.60[(b)]	0.85
HPMA	0.59[(c)]	0.96
AEM_{25} $HPMA_{75}$	0.91[(a)]	0.96
AEM_{75} $HPMA_{25}$	1.49[(a)]	0.86
$DMAEM_{25}$ $HPMA_{75}$	1.01[(b)]	0.67
qAEM	0.66[(a)]	0.96
qAPAAm	1.02[(a)]	0.94

[(a)]: Polymerisation was carried out in deionised water at 60 °C with ACA as the initiator; [(b)]: Polymerisation was carried out in ethanol at 65 °C with AIBN as the initiator; [(c)]: Polymerisation was carried out in methanol at 50 °C with AIBN as the initiator; [(d)]: Correlation coefficient of linear regression.

Table 4.6: Summary of the molecular weight and polydispersity of the semitelechelic polymer P 54 and its semitelechelic ester derivative polymer P 63

Polymer Identification	M_n (g.mol^{-1}) [(a)]	M_w/M_n [(a)]
P 54 (starting material)	3 450	1.90
P 63	4 810	1.60

[(a)]: Mobile phase PBS, column calibrated with narrow pullulan standards.

and P 63 in bulk are shown in Figure 4.4 and the band assignment is summarised in Table 4.7.

The usual bands corresponding to PHPMA can be seen as well as a new band at 1 732 cm^{-1} that could correspond to an ester functionality of the ring of the terminal groups. The ^{1}H-NMR spectrum of P 63 in deuterated DMSO is shown in Figure 4.5. Peaks corresponding to the PHPMA backbone can be seen, with two additional small peaks at 2.37 and 2.43 ppm, which could represent the aliphatic moiety of HOSu. The ^{13}C-NMR of P 63 in DMSO-d_6 (Figure 4.6) showed five additional peaks (δ = 25, 32, 34, 170 and 174 ppm) not attributed to the carbon atoms of the polymer backbone.

4.4. Discussion

Polymers of DMAEM, AEM, HPMA, qAEM, qAPAAm, and NIPAAm were successfully synthesised in good yield (40 to 90 %) with a range of molecular weight (349 580 - 450 $g.mol^{-1}$). These results were in good agreement with data described in the literature. For example, the synthesis of semitelechelic PDMAEM with carboxylic acid end-group using either MPA or mercaptoacetic acid as CTA, AIBN as initiator ([I]/[M] = 1 %) was previously studied by FRP in either THF or toluene at 60 °C, respectively (van de Wetering 1999). In the studies mentioned, semitelechelic PDMAEM with M_n of 6 810 and 3 400 $g.mol^{-1}$ with mercaptoacetic acid as CTA ([CTA]/[M] ratios of 2 and 4 %), and having a M_w/M_n of 2.35 and 2.15 were obtained. The semitelechelic PDMAEM synthesised with MPA using a [MPA]/[M] ratios of 15 % and AIBN ([I]/[M] = 1 %) had a M_n of 1 500 $g.mol^{-1}$ and M_w/M_n = 2.67. These values are in good agreement with those obtained in the current studies.

As expected and as seen in Chapter 3, at full monomer conversion, the composition of the AEM/HPMA or DMAEM/HPMA copolymers, synthesised by FRP using MPA as CTA, was very similar to the comonomer feed ratio introduced.

CTA are used in FRP to control molecular weight and polydispersity, and/or to introduce functional end groups into the polymer backbone giving telechelic and/or semitelechelic polymers (Chiefari and Rizzardo 2002). For all ten monomer systems, the M_n of the synthesised polymers was expected to decrease with an increase in the added content of CTA. Similarly, the polydispersity, on average around 2 (Tables 4.2

(a)

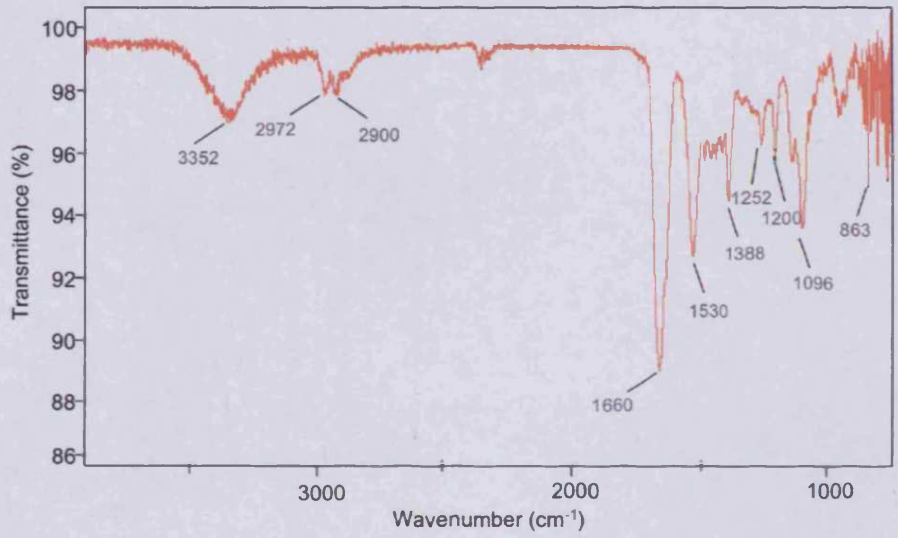

(b)

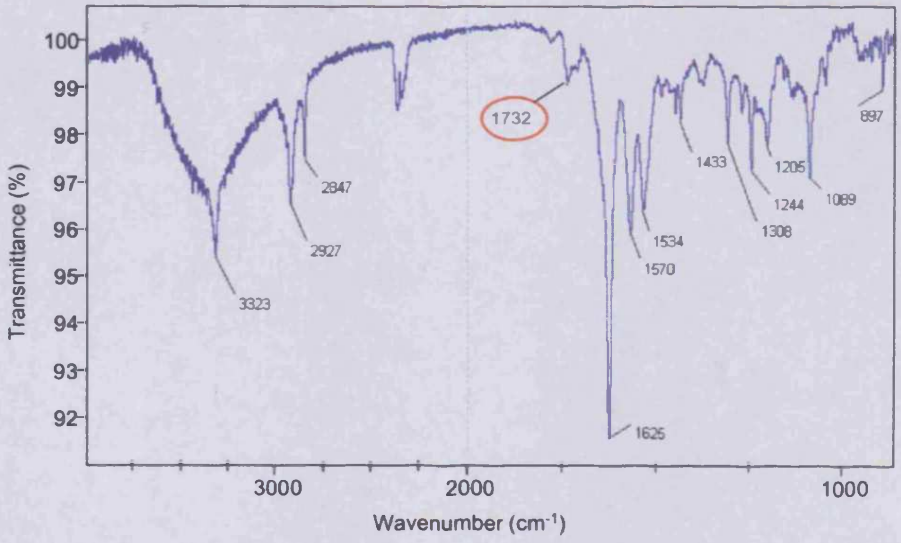

Figure 4.4: IR spectra of the carboxylic acid semitelechelic PHPMA P 54 panel (a) and the activated carboxylic acid semitelechelic PHPMA P 63 panel (b) in bulk*

* A surprising relative change in the stretching vibration frequency of the amide I band was observed from the P 54 (1 660 cm^{-1}) to P 63 (1 625 cm^{-1}). Data from the literature (Gunzler and Gremlich 2002) show that stretching vibrations of amide I band are often found from 1 680 to 1 630 cm^{-1}.

Table 4.7: Identification of the IR bands of P 63

Wavenumber (cm^{-1})	**Frequency (cm^{-1})**	**Vibration type**
3 323	3 600- 3 250	ν_{OH}
2 927	2 960- 2 850	ν_{CH}
2 847	2 900- 2 700	ν_{CH-O}
2 360		$\nu_{C=O}$ of CO_2
1 732	1 850- 1 670 depending on the ring size (5-atom ring ~ 1 720)	$\nu_{C=O}$ of the lactam's end-group
1 625	1 680- 1 630	$\nu_{C=O}$ (Amide I band)
1 570	1 570- 1 515	$\nu_{CN} + \delta_{CNH}$ (Amide II band)
1 534	1 580- 1 490	ν_{NH}
1 433	1 460- 1 370	δ_{CH}
1 308	1 330- 1 200	$\delta_{NH} + \delta_{OCN}$ (Amide III band)
1 244		
1 205		
1 089	1 210- 800	$\delta_{C-C} + \delta_{CH}$
897		

Where ν is the stretching vibration and δ is the bending vibration of the specified bond.

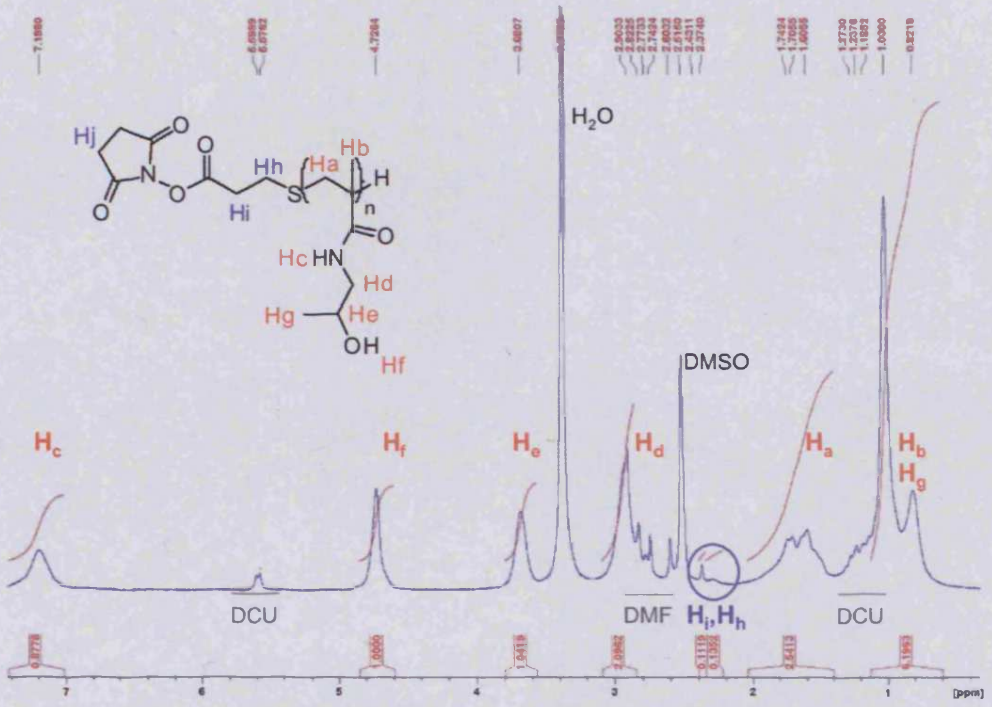

Figure 4.5: **^{1}H-NMR spectrum of the activated carboxylic acid semitelechelic PHPMA P 63 in DMSO-d_6**

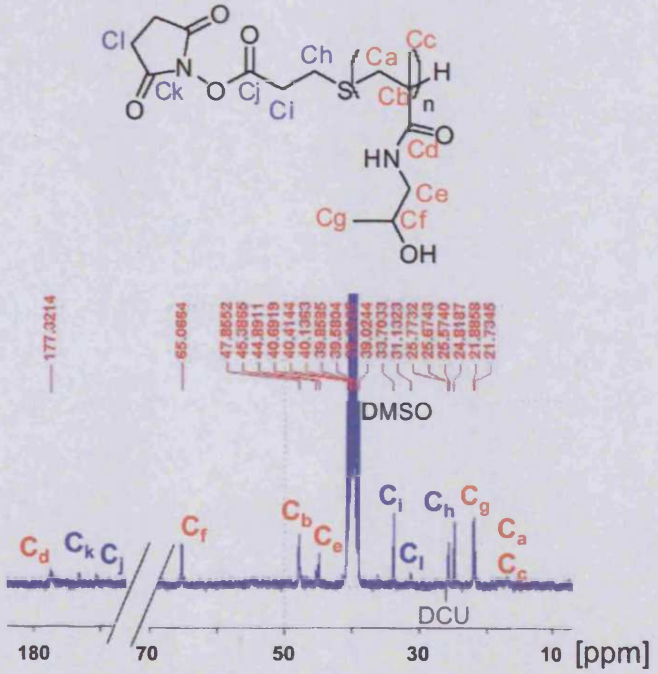

Figure 4.6: **^{13}C-NMR spectrum of the activated carboxylic acid semitelechelic PHPMA P 63 in DMSO-d_6**

to 4.4) was expected to be lower than the usual reported polydispersity in conventional FRP (2 to 5 with a theoretical limit of 1.5) (Georges *et al.* 1993).

4.4.1. Direct end-group characterisation

End-group characterisation of the semitelechelic homo- and copolymers proved difficult using IR and NMR. It was impossible to find the expected bands/peaks in the spectra obtained, although the percentage of end-groups compared to the number of repeating unit reached up to 25 % in some cases (percentages calculated following Equation 4.5 and increasing from 0.5 % to 25 % with a decrease in the M_n).

$$\% = \frac{100}{\overline{DP_n}} = \frac{100 \times MW_{RU}}{\overline{M_n}} \qquad \text{(Eq 4.5)}$$

Where DP_n is the number-average degree of polymerisation and MW_{RU} the molecular weight of the repeating unit of the polymer.

Nevertheless, the absence of the signals did not mean that the polymer was not end-group functionalised. Temperature-dependent NMR, and variation of the relaxation time of the NMR machine could be used to try and improve the NMR resolution but these experiments were not undertaken here. Table 4.8 summarises the expected values for the signals from the functionalised end-group on IR, ^{1}H and ^{13}C-NMR (Silverstein *et al.* 1981b; a; Gunzler and Gremlich 2002).

Other methods might have been used to determine end group functionality. They were not carried out here due to lack of time. These methods include MALDI-TOF MS, FT-Raman spectroscopy, titration of the end-group (carboxylic acid or hydroxylic group). Polymer derivatisation using a fluorescent probe to covalently conjugate to the polymer end-group can also be used to quantify functional end-group. The synthesis of semitelechelic oligomers (i.e. low molecular weight polymers) could also have helped to define end-group as in this case, the end-group signals in NMR or IR would not be hidden by the strong signals from the polymer backbone. In Section 4.4.4, the activation of end-group of semitelechelic polymers is introduced and discussed as a potential method for indirect proof of existence of functionalised termini.

Table 4.8: Expected signals of the functionalised end-group of the polymers

	Polymer-S-CH_2-CH_2-COOH	**Polymer-S-CH_2-CH_2-OH**
IR (cm^{-1})	Stretching vibrations of C=O: 1 705 Bending vibrations of S-C: 730 to 570	Bending vibrations of S-C: 730 to 570
^{1}H-NMR (ppm)	-COO**H**: singlet, 12 -S-C**H_2**-: triplet, 2.25 HOOC-C**H_2**-: triplet, 2.35	-O**H**: singlet, 5.35 -S-C**H_2**-: triplet, 2.60 HO-C**H_2**-: triplet, 3.40
^{13}C-NMR (ppm)	**C**=O: 165 to 185 -S-**C**H_2-: 30 HOOC-**C**H_2-: 34	-S-**C**H_2-: 36 HO-**C**H_2-: 61

4.4.2. Effect of CTA on molecular weight and polydispersity

Kopeček *et al.* (Lu *et al.* 1998; Lu *et al.* 1999; Lu *et al.* 2000) studied the synthesis of semitelechelic PHPMA by radical polymerisation in the presence of alkyl mercaptans with different functional groups, namely: amino, carboxy, hydrazo and methyl ester end groups.

Semitelechelic PHPMA with a carboxylic end-group was synthesised in methanol at 50 °C using MPA as the CTA and AIBN as the initiator (Lu *et al.* 1998; Lu *et al.* 2000). These authors also discussed the effect of the molar ratio [CTA]/Σ[M] (varied from 0 to 30 %) on molecular weight and similar conclusions to those obtained in the present studies were drawn. The M_w ranged from 2 000 to more than 15 000 $g.mol^{-1}$ when the [CTA]/Σ[M] decreased from 30 to 0 % (no polydispersity index were given). So, although the initiator used by Kopeček and co-workers was different from the one used here, it can be seen in Table 4.9 that very similar data were obtained in both cases.

Of all the monomers studied, the quaternized monomers and NIPAAm produced unexpectedly high molecular weight polymers when characterised by GPC (Table 4.4). The limitations of GPC described in Chapter 3 (Section 3.4.2) also apply here.

The quaternized homopolymers PqAEM and PqAPAAm are polycations. It was therefore expected that very high apparent molecular weight ranges would be obtained when characterised by aqueous GPC. This is because they adopt a highly extended conformation in aqueous solution due to charge-charge repulsion and thus have increased hydrodynamic volumes.

Moreover, GPC characterisation of PNIPAAm (P 60 to P 62) gave very low M_n (~ 450 $g.mol^{-1}$) (Table 4.4).

It has been shown in the literature (Wu *et al.* 1993; Ganachaud *et al.* 2000) that surprising molecular weight information for NIPAAm-based polymers can be obtained when using GPC methodology without care. This particular polymer undergoes a coil-to-globule transition in water at 33 °C (Schild 1992), and therefore tends to interact with the stationary phase of the GPC column, resulting in a very high retention time and consequently low apparent molecular weight.

Table 4.9: Comparison of M_n obtained by Kopeček *et al.* (Lu *et al.* 2000) and in these studies for the FRP of HPMA using MPA as CTA

Kopeček *et al.*		**This study**[(a)]		
[CTA]/Σ[M](%)	**M_w (g.mol^{-1})**	**[CTA]/Σ[M](%)**	**M_n (g.mol^{-1})**	**M_w (g.mol^{-1})**
1.25	11 250	1.20	6 150	12 300
2.50	6 250	2.39	3 530	6 000

[(a)]: mobile phase PBS, column calibrated with narrow pullulan standards.

One solution for overpassing this problem and as mentioned in Chapter 2, is the addition of 5 % triethylamine in the mobile phase. This should help for breaking the polymer/stationary phase chemical interaction by introducing competing chemical interactions triethylamine/stationary phase. Therefore, a more accurate molecular weight information should be obtained.

Other methods (membrane and vapour pressure osmometries or light scattering), which give an absolute molecular weight of polymer solutions, could be used to verify these data.

4.4.3. 3-Mercaptopropionic acid efficiency (C^*_{tr}) for different polymerisation systems

As seen in Chapter 1, Section 1.8.2, C_{tr} is a measure of the efficiency of the CTA; the closer to 1, the more efficient the CTA. For any given CTA, several C_{tr} can be measured, as it is specific to a particular system and depends upon the monomer studied, the temperature of the reaction, and the solvent used. When the polymerisation reactions are complete and the monomer species fully converted, chain transfer constant measured is therefore an apparent one (C^*_{tr}).

As described in Section 4.3.3, C^*_{tr} is defined as the slope of the plot $1/DP_n = f([CTA]/\Sigma[M])$ if a linear relationship can be determined (Equation 4.2). When calculating linear regression for the plots presented in Figure 4.2, it was important to consider the correlation coefficient R. Indeed, R is an indicator of the reliability of linear regression, and values close to 1 (or 100 %) indicate excellent linear reliability. Only in the case of the systems AEM, HPMA, $AEM_{25}HPMA_{75}$ and qAEM with MPA as CTA, was R higher than 95 % (Table 4.5). C^*_{tr} values of MPA calculated for the other systems (namely DMAEM, $AEM_{75}HPMA_{25}$, $DMAEM_{25}HPMA_{75}$ and qAPAAm) should be discussed with caution, and further studies should be undertaken before drawing firm conclusions.

In the four remaining systems (AEM, HPMA, $AEM_{25}HPMA_{75}$ and qAEM), the C^*_{tr} calculated were in good agreement with published data.

When mercapto compounds were used as CTA for the FRP of methyl methacrylate the C_{tr} was 0.62 for ME (Berger and Brandrup 1989); and 0.63 for ethyl mercaptoacetate (O'Brien and Gornick 1955). For the CTA FRP of AEM, qAEM, or

$AEM_{25}/HPMA_{75}$, which all give methacrylate-based polymers, the C^*_{tr} of MPA ranged from 0.66 to 0.91, which were in agreement with those published figures.
Moreover, when 1-dodecanethiol was used as CTA in the polymerisation of *N*-octadecylacrylamide initiated by peroxide (in butyl alcohol), its C_{tr} was found to be 0.54 (Berger and Brandrup 1989). In this study, the C^*_{tr} for MPA in the homopolymerisation of the methacrylamide monomer HPMA was 0.59, in contrast to the value of 0.34 determined by Kopeček *et al.* (Lu *et al.* 2000) using the same polymerisation conditions, except that AIBN was used as the initiator instead of ACA.

MPA was found to be more efficient when used with methacrylate-based monomers (AEM: $C^*_{tr} = 0.72$; qAEM: $C^*_{tr} = 0.66$; $AEM_{25}/HPMA_{75}$: $C^*_{tr} = 0.91$) than when used with methacrylamide-based monomers (HPMA: $C^*_{tr} = 0.59$). This might be explained in part by the easier proton transfer from methacrylate-based radicals to MPA (compared with methacrylamide-based radicals) due to more electronegative pendant groups on methacrylate-based monomers. Similar conclusions were drawn when comparing efficiencies of thiols used as CTA in polymerisations of styrene or methyl methacrylate (O'Brien and Gornick 1955; Chiefari and Rizzardo 2002) (Table 1.3, Chapter 1, Section 1.8.2).

4.4.4. End-group characterisation by activation of the functionalised termini

Due to the unexpected difficulties of end-group characterisation (Section 4.3.1), an indirect approach to reveal end-group functionalisation was used. The experimental procedure described by Kopeček and co-workers (Wang *et al.* 2000) was followed to activate semitelechelic PHPMA containing carboxylic end-groups (P 54). The rationale for this experiment was to obtain a semitelechelic PHPMA with an activated ester end-group that would give characteristic signals in regions different from those coming from the PHPMA backbone, thus, proving the existence of the carboxylic acid end-group of PHPMA.

End-group activation was achieved using a great excess of DCC and HOSu without leading to intra- and inter-molecular side reactions between the hydroxylic group of PHPMA and the carboxylic termini, as no alteration on molecular weight was observed (Table 4.6). Activating the end-group of polymers should not alter the

overall molecular weight of the polymer, unless side reactions, such as inter- and intra- conjugations occur. The activated ester semitelechelic PHPMA was obtained in 75 % yield of polymer and this was in good agreement with published data (Lu *et al.* 1998), where semitelechelic PHPMA with activated ester end-group was synthesised in 54 to 90 % yield of polymer. Data obtained from IR, ^{1}H-NMR and ^{13}C-NMR seem to confirm that activation of the carboxylic acid end groups of semitelechelic PHPMA was possible. Indeed, the additional band seen at 1 732 cm^{-1} in the IR spectrum of P 63 (Figure 4.3) could correspond to the stretching vibrations of the carbonyl group ($\nu_{C=O}$) from a 5-atom cycle (Gunzler and Gremlich 2002), which matched the lactam functionalised end-group of polymer P 63. Moreover, the two additional small peaks (2.37 and 2.43 ppm) observed in the ^{1}H-NMR spectrum of P 63 in DMSO-d_6 (Figure 4.4) could be assigned to the protons of the methylene groups in alpha position to the sulphur atom (Figure 4.4: H_h) (expected at 2.25 ppm by calculation (Silverstein *et al.* 1981b)) and the protons of the methylene groups in beta position to the sulphur atom (Figure 4.4: H_i) (expected at 2.35 ppm by calculation (Silverstein *et al.* 1981b)), respectively. Methylene protons of the ring (Figure 4.4: H_j) are expected at 3 ppm (Silverstein *et al.* 1981b) and are thought to appear under the broad peak of H_d from the pendant group of PHPMA.
Finally, considering the ^{13}C-NMR spectrum in DMSO-d_6 (Figure 4.5), the five additional peaks observed at 25, 32, 34 170 and 174 ppm could be assigned to the carbons from the activated ester end-group (Figure 4.5: C_l, C_h, C_i, C_j, C_k), respectively as they were similar to the calculated chemical shifts (Silverstein *et al.* 1981a).

Although these analyses seem to be positive, it should not be forgotten than with a 500 MHz NMR, and considering the molecular weight of P 54 and P 63, the signals from the end-groups are expected to be observed much more easily, as they represent 4 % of the polymer (calculated with Eq 4.5).

In summary, activation of functionalised end-group is usually a reliable method for detecting their existence. Nevertheless, direct proof of existence of the end-group of semitelechelic polymers is the ideal scenario and, thus should always be sought for full confirmation of their existence.

4.5. Conclusions

In conclusion, the synthesis of a library of linear water-soluble homo- and copolymers with different molecular weight, composition, charge density and potential end-group functionality, was achieved in these studies by FRP using CTA. It is now possible to work out the [CTA]/Σ[M] molar ratio needed to reach a specific and desired molecular weight for a desired polymer composition. Semitelechelic polymers are attractive starting materials for further conjugation to cores (to form star polymers through the arm-first approach). In addition their conjugation to protein, peptide and drugs would enable the synthesis of new polymer therapeutics.

The next chapter examines the use of a CRP technique for the synthesis of well-defined linear polymer with controlled molecular weight and narrow polydispersity. The optimisation of this technique and the synthesis of a library of linear PDMAEM using commercially available initiators were studied in Chapter 5.

5

Optimisation of the Synthesis of Linear PDMAEM by Atom Transfer Radical Polymerisation

5.1. Introduction

To better control the synthesis of linear cationic polymers and to optimise the conditions for future synthesis of star-shaped cationic polymers as described in Chapter 6 (using the core-first approach and multifunctional initiators), a library of linear homopolymers of DMAEM was synthesised in these studies using ATRP.

5.1.1. Rationale for the choice of ATRP technique

As discussed in Chapter 1 (Section 1.8.3), ATRP is an especially successful CRP technique, and it has been widely used. Since 1993, over 7 000 papers have been published on CRP, and there are more than 4 000 papers describing ATRP methods since 1995 (http://www.chem.cmu.edu/groups/maty/about/research/02.html; Matyjaszewski 2003)). It can be said that ATRP is probably the most robust and efficient CRP techniques (as reviewed by Kamigaito *et al.* (2001)). This method offers the opportunity to synthesise a wide range of well-defined polymers with controlled composition, functionality and architecture. It uses a straightforward experimental setup, simple initiators (alkyl halides for instance), together with easily accessible and inexpensive catalysts, for example, copper-based compounds, which form complexes by coordination with commercially available aliphatic amines (http://www.chem.cmu.edu/groups/maty/about/research/02.html; Matyjaszewski 2003)).

As previously mentioned in Chapter 1 (Section 1.8.3), most ATRP reactions require four components:

- an initiator with at least one transferable atom,
- a transition metal that can participate in a one electron redox process,
- a ligand that forms a solubilising complex with the transition metal, and
- one or more radically homo and copolymerisable monomers.

Also, these reactions can be run under homogeneous or heterogeneous conditions. The former generally give better control of the ATRP characteristics. Scheme 5.1 shows, as an example, the ATRP synthesis of DMAEM using Cu(I)Br as catalyst and alkyl bromides as initiators. ATRP has been widely used to synthesise PDMAEM using several initiators, catalytic systems, and reaction conditions (polar, non polar organic or aqueous solvents and temperature, see Table 5.1).

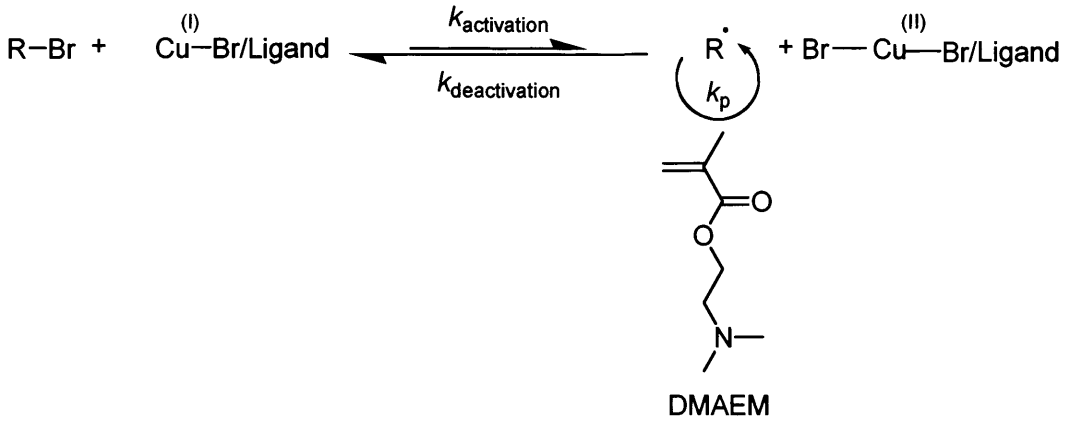

Scheme 5.1: ATRP of DMAEM using Cu(I)Br as catalyst and alkyl bromides as initiators

Table 5.1: Summary of the reaction conditions of the Cu(I)Br-based ATRP of DMAEM from selected articles

Initiator	Ligand	Solvent	T (° C)	Reference
2-bromopropionitrile	HMTETA	dichlorobenzene	50.0	(Zhang *et al.* 1998)
p-toluenesulfonyl chloride	"	"	"	
ethyl α-bromoisobutyrate	HMTETA	dichlorobenzene	"	
	bipyridine	anisole	90.0	
	TMEDA*	"	"	
	PMDETA**	"	"	
	HMTETA	anisole	"	
	"	dichlorobenzene	"	
	"	toluene	"	
	"	ethylene carbonate	"	
	"	dichlorobenzene	70.0	
	"	"	22.8	
vinyloxyethyl 2-bromoisobutyrate	HMTETA	bulk	60.0	(Shen *et al.* 2000)
vinyloxypropyl trichloroacetamide	"	"	"	
methyl α-bromophenylacetate	bipyridine	water	20.0	(Zeng *et al.* 2000a)
allyl 2-bromoisobutyrate	"	"	"	
vinyloxyethyl 2-bromoisobutyrate	"	"	"	
ethyl α-bromoisobutyrate	"	"	"	
α-bromo r-butyrolactone	"	"	"	
methyl α-bromophenylacetate	HMTETA	"	"	
allyl 2-bromoisobutyrate	"	"	"	
vinyloxyethyl 2-bromoisobutyrate	"	"	"	
ethyl α-bromoisobutyrate	"	"	"	
α-bromo r-butyrolactone	"	"	"	

*: TMEDA: *N,N,N',N'*-tetramethylethylenediamine; **: PMDETA: *N,N,N',N'',N''*-pentamethyldiethylenetriamine

Table 5.1: Summary of the reaction conditions of ATRP of DMAEM from selected articles (Continued)

Initiator	Ligand	Solvent	T (° C)	Reference
vinyl chloroacetate	tris(2-di (butylacrylate) aminoethyl)amine	bulk	60.0	(Zeng *et al.* 2000b)
allyl bromide	〃	〃	〃	
vinyl benzyl chloride	〃	〃	〃	
allyl 2-bromoisobutyrate	〃	〃	〃	
(2-methylbutenyl) 2-bromopropionate	〃	〃	〃	
allyl trichloroacetamide	〃	〃	〃	
vinyl chloroacetate	HMTETA	〃	〃	
allyl bromide	〃	〃	〃	
vinyl benzyl chloride	〃	〃	〃	
allyl 2-bromoisobutyrate	〃	〃	〃	
(2-methylbutenyl) 2-bromopropionate	〃	〃	〃	
allyl trichloroacetamide	〃	〃	〃	
vinyl benzyl chloride	PMDETA**	〃	〃	
allyl 2-bromoisobutyrate	PMDETA**	〃	〃	
	tris(2-di (methylacrylate) aminoethyl)amine	〃	〃	
	18-crown-6	〃	〃	
ethyl α-bromoisobutyrate	HMTETA	THF	60.0	(Ydens *et al.* 2005)
		toluene	85.0	
		bulk	25.0	
		THF	〃	

**: PMDETA: *N,N,N',N",N"*-pentamethyldiethylenetriamine

5.1.2. Rationale for the choice of initiators, catalyst and ligands

Matyjaszewski stated that "a basic requirement for a good ATRP initiator is that it should have a reactivity at least comparable to that of the subsequently growing chains" (Matyjaszewski and Xia 2001). Therefore, when selecting an ATRP initiator, a good start is to select a compound whom radicals have similar chemical structure compared to that of the monomer to be polymerised. Thus, here, 3 alkyl bromide compounds were chosen as initiators for the ATRP of the DMAEM monomer. In particular, ethyl 2-bromopropionate, ethyl α-bromoisobutyrate, and methyl α-bromophenylacetate (Figure 5.1) were used.

Cu(I)Br was chosen as it is known to be a robust ATRP catalyst and it has been used for a wide range of monomers (reviewed by (Matyjaszewski and Xia 2001) and (Kamigaito *et al.* 2001)) and especially for ATRP of DMAEM (Zhang *et al.* 1998; Shen *et al.* 2000; Zeng *et al.* 2000a; b; Ydens *et al.* 2005) (Table 5.1).

Two nitrogen-based ligands were chosen to complex Cu(I)Br, namely, 2,2'-bipyridine, a bidentate ligand, and HMTETA, a multidentate ligand (Figure 5.1). Both had previously shown good efficiency in copper-mediated ATRP (in contrast with sulphur, oxygen and phosphorous ligands) (reviewed by (Matyjaszewski and Xia 2001)), and also given good results for the ATRP of DMAEM (Zhang *et al.* 1998; Shen *et al.* 2000; Zeng *et al.* 2000a; b; Ydens *et al.* 2005).

5.1.4. Technical aims

The technical aims of these studies are summarised in Figure 5.2. They were to:

- synthesise linear PDMAEM by ATRP and study the efficiency of different initiators (ethyl 2-bromopropionate, ethyl α-bromoisobutyrate, methyl α-bromophenylacetate), ligands of the catalyst copper (I) bromide (HMTETA, bipyridine), solvents (water, DMF, DMSO, bulk), reaction temperatures (from RT to 90 °C), applying a variation of initiator, catalyst or ligand to monomer molar ratio ([I]/[M], [Cat]/[M], [Lig]/[M] from 0.5 to 3 %),
- follow the kinetics of ATRP, using ^{1}H-NMR and GPC, and to define the degree of conversion with time, and to correlate of molecular weight and polydispersity with conversion in order to determine the factors controlling

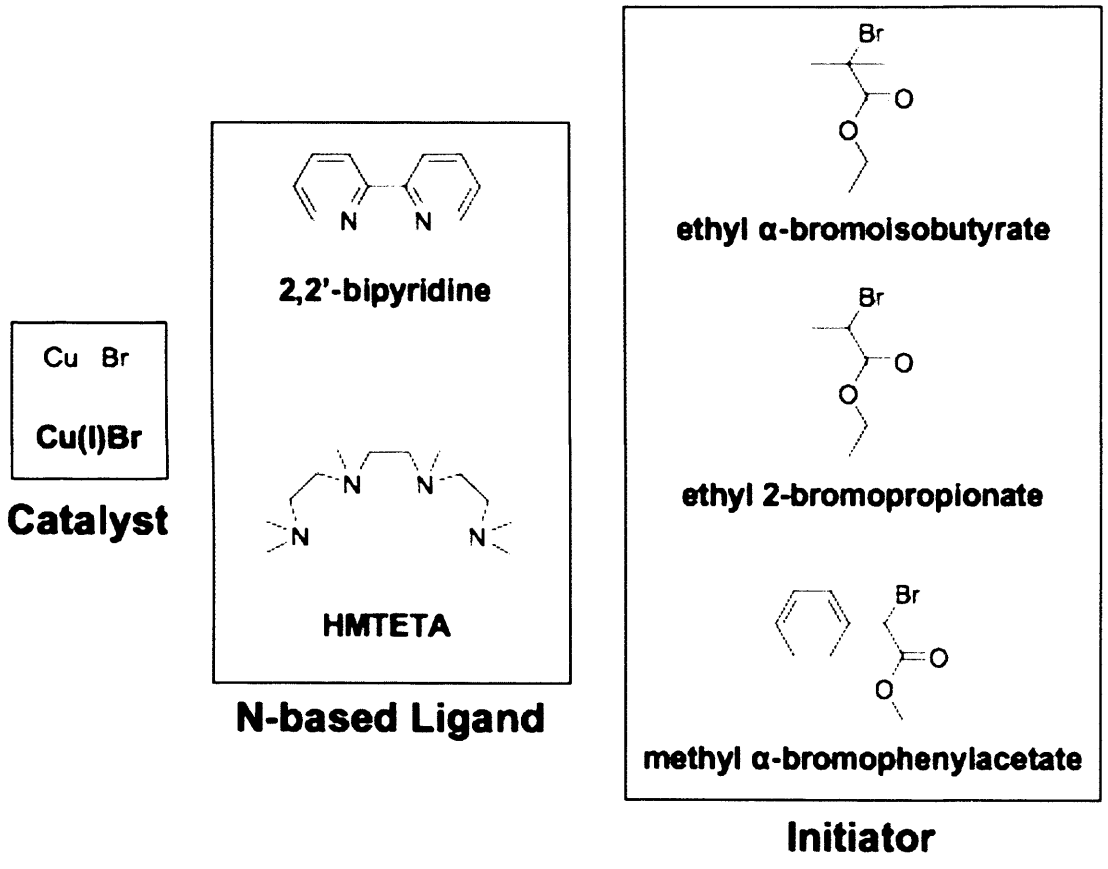

Figure 5.1: **Chemical structures of the catalyst, ligands and initiators used in these experiments**

Figure 5.2: Schematic representation of the aims of these studies

ATRP in each set of experiments,

- verify the living character of the linear homopolymers of DMAEM by using them as macroinitiators for the ATRP of new batches of DMAEM monomer, and for chain extension of linear cationic polymers.

All these experiments were carried out, keeping in mind the ATRP conditions that would be needed for the optimisation of future synthesis of star-shaped PDMAEM by ATRP using multifunctional ATRP initiators (Chapter 6). Also, it was borne in mind that the linear PDMAEMs synthesised would be studied for basic biological properties in Chapter 7 and their properties compared with their linear homologues synthesised by FRP (with or without CTA, Chapters 3 and 4, respectively).
Finally, it was hoped that these polymers might be useful as drug, protein or oligonucleotide carriers. Therefore, the [I]/[M] ratios were chosen so that at complete monomeric conversion, the molecular weight of the linear PDMAEM synthesised would not be higher than 40 000 $g.mol^{-1}$, to ensure excretion via the kidneys (Duncan 2003a).

5.2. Methods

5.2.1. Kinetic studies relating to the synthesis of linear PDMAEM by ATRP

ATRP polymerisation of DMAEM was studied using different initiators, ligands and also by varying the polymerisation conditions. Copper (I) bromide was always used as catalyst. The reaction conditions used are summarised in detail in Table 5.2. Scheme 5.2 shows ATRP of DMAEM using ethyl α-bromoisobutyrate, Cu(I)Br, HMTETA in DMF. The temperature was varied from 60 to 90 °C. A typical reaction procedure is described below. These experiments were in part undertaken by Michael Rafael in the Centre for Polymer Therapeutics and under my supervision.

Synthesis of the linear homopolymer of DMAEM P 70 by ATRP (Table 5.2)
DMAEM (3 mL, 17.75 mmol), Cu(I)Br (13.4 mg, 93.4 μmol, [Cu(I)Br]/[DMAEM] = 0.5 %) and HMTETA (24 μL, 88.5 μmol, [HMTETA]/[DMAEM] = 0.5 %) were mixed in a round bottom-flask with a magnetic stirrer and purged with N_2 for 40 min. Ethyl α-bromoisobutyrate (26 μL, 177 μmol, [I]/[M] = 1 %) was dissolved in double

Table 5.2: Reaction conditions for the synthesis of the linear PDMAEM by ATRP

Polymer	[I]/[M] (%)	[Cat]/[M] (%)	[Lig]/[M] (%)	Solvent (v/v %)	T (°C)	Time (h)
P 64[a]	1.6	1.6	1.6	Bulk	60	1.50
P 65[a]	1.0	1.0	1.0	Bulk	60	1.50
P 66[b]	1.0	1.0	3.0	Bulk	80	16.00
P 67[a]	0.8	0.8	0.8	ddH_20, 50	RT	0.08
P 68[c]	1.0	1.0	2.0	ddH_20, 52	RT	16.00
P 69[d]	1.0	1.0	1.0	ddH_20, 50	RT	1.50
P 70[a]	1.0	0.5	0.5	ddH_20, 20	RT	1.00
P 71[e]	1.0	0.5	0.5	ddH_20, 20	RT	1.00
P 72[a]	2.0	1.6	1.6	DMF, 20	60	44.00
P 73[a]	2.0	1.6	1.6	DMF, 50	60	21.40
P 74[a]	2.0	1.6	1.6	DMF, 20	90	46.50
P 75[a]	1.0	1.0	1.0	DMSO, 50	50	2.00
P 76[a]	1.0	1.0	1.0	DMSO, 50	RT	1.50
P 77[a]	1.0	1.0	1.0	DMSO, 25	50	3.40

[a]: Reactions initiated with ethyl α-bromoisobutyrate/Cu(I)Br/HMTETA complex; [b]: Reactions initiated with ethyl 2-bromopropionate/Cu(I)Br/Bipyridine complex; [c]: Reactions initiated with methyl α-bromophenylacetate/Cu(I)Br/Bipyridine complex; [d]: Reactions initiated with methyl α-bromophenylacetate/Cu(I)Br/HMTETA complex; [e]: Reactions initiated with ethyl α-bromoisobutyrate/Cu(I)Br/Bipyridine complex.

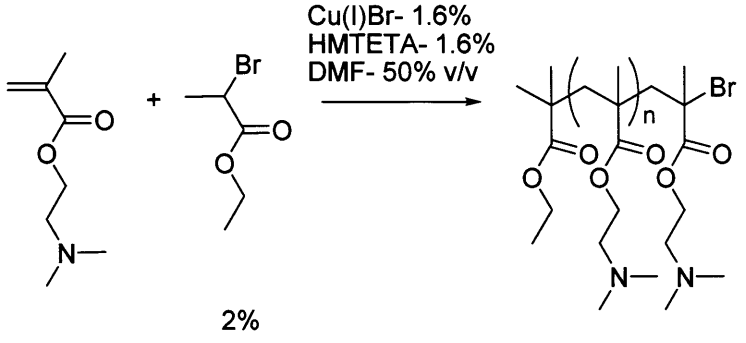

Scheme 5.2: Scheme for the synthesis of PDMAEM by ATRP in DMF (P 72 - P 74)

distilled water (15 mL, 20 % v/v) in a conical flask and purged with N_2 for 40 min. At the end of the purge, the initiator solution was carefully transferred to the rest of the reagents, using a syringe previously purged with N_2. The reaction was continued at room temperature. Samples (0.3 mL) of the reaction mixture were carefully taken (using a N_2-purged syringe) throughout the reaction period and placed in eppendorf tubes and immediately frozen in liquid nitrogen to quickly stop the reaction.

Each sample was subsequently analysed by ^{1}H-NMR and GPC to determine the conversion and the M_n, respectively. Once the reaction was finished (after 1 h), the polymer was purified from unreacted monomer, residual catalyst and ligand by extensive dialysis (molecular weight cut-off 2 000 g.mol^{-1}) against double distilled water for 48 h. The aqueous polymer solution was then lyophilised to yield a white solid.

When reactions were undertaken in bulk, all the chemicals were mixed together in the round-bottom flask and the reaction mixture purged with N_2 for 40 min, and for the reactions undertaken at temperatures higher than room temperature, the flask was placed in an oil bath immediately after addition of the initiator solution.

For both the ATRP reactions carried out in bulk and organic solvents, at the end of the reaction the mixture was dissolved in distilled water (20 mL) and then dialysed. All polymers were characterised by ^{1}H-NMR, ^{13}C-NMR and GPC as described in Chapter 2, Section 2.3. The results obtained are summarised below and the key is as follows: the red letters are assigned to the protons of DMAEM and carbon elements are labeled by the blue numbers.

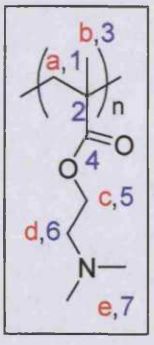

Characterisation of the linear PDMAEM samples P 64 - P 77 (Table 5.2)

^{1}H-NMR (D_2O, ppm)*: δ = 0.7 to 1, broad peaks, 5H, H_a and H_b; 2.2, bs, 6H, H_e; 2.5, bs, 2H, H_d; 4.1, bs, 2H, H_c.

^{13}C-NMR (D_2O, ppm): δ = 15, C_3; 17, C_1; 43.5, C_7; 53, C_2;

* *The chemical shifts δ are expressed in ppm, and bs stands for broad singlet.*

56, C_6; 62, C_5; 177, C_4.

GPC (THF, flow rate 1 mL/min, columns calibrated with narrow PS standards): M_n ranging from 3 800 to 85 660 g.mol^{-1} and M_w/M_n ranging from 1.18 to 3.65.

5.2.2. Chain extension reactions using previously synthesised linear PDMAEM as macroinitiators

In these studies, the monomer DMAEM was polymerised by ATRP initiated by linear PDMAEM macroinitiators (MaI) using either P 72 or P 73. The reaction was catalysed by the Cu(I)Br/HMTETA complex in DMF (Scheme 5.3). The reaction conditions used are summarised in detail in Table 5.3, and a typical reaction is described below. The reaction conditions were then varied as described in Table 5.3.

Synthesis of the extended linear PDMAEM P 79 by ATRP (Table 5.3)

DMAEM (1.50 mL, 8.87 mmol), Cu(I)Br (20.35 mg, 142.00 µmol, [Cu(I)Br]/[DMAEM] = 1.6 %) and HMTETA (38.60 µL, 142.00 µmol, [HMTETA]/[DMAEM] = 1.6 %) were mixed in a round-bottom flask with a magnetic stirrer and purged with N_2 for 40 min. The linear PDMAEM MaI (sample P 73, 975.00 mg, M_n = 5 500 g.mol^{-1}, 177.40 µmol, [MaI]/[M] = 2.0 %) was dissolved in DMF (1.50 mL, 50 % v/v) in a conical flask and purged with N_2 for 40 min. At the end of the purge, the initiator solution was carefully transferred to the rest of the reagents, using a N_2-purged syringe and the flask was immediately placed at 60 °C in an oil-bath. Samples (0.10 mL) of the reaction mixture were carefully taken throughout the reaction, using a N_2-purged syringe. They were immediately frozen in liquid nitrogen to quickly stop the reaction, and ^{1}H-NMR and GPC were used to determine conversion and M_n, respectively. At the end of the reaction the mixture was allowed to cool to room temperature and 20 mL of double distilled water was added. The polymer was then purified from unreacted monomer, residual catalyst, ligand, and solvent, by extensive dialysis (molecular weight cut-off 2 000 g.mol^{-1}) against double distilled water for 48 h. The aqueous polymer solution was then lyophilised for 2 days to yield a white solid.

Characterisation of the extended linear PDMAEM samples P 78 - P 79 (Table 5.3)

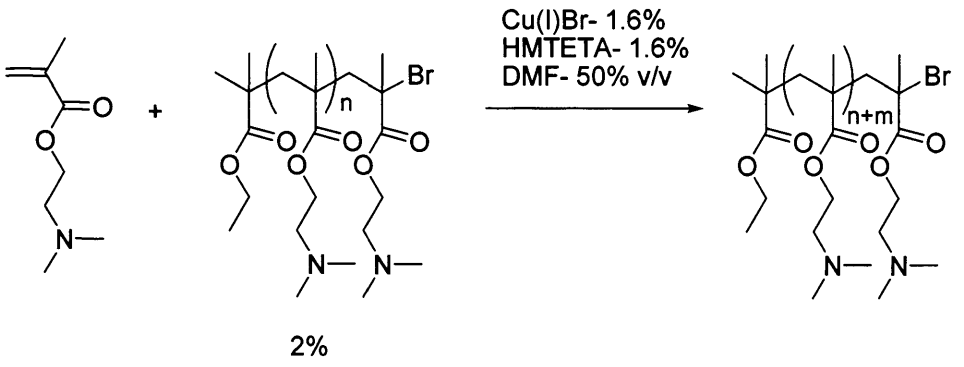

Scheme 5.3: Chain extension of linear PDMAEM by ATRP in DMF

Table 5.3: Reaction conditions of the chain extension of PDMAEM by linear ATRP in DMF

Polymer	Identification of MaI used	M_n of MaI used ($g.mol^{-1}$) [c]	M_w/M_n of MaI used[c]	[MaI]/[M] (%)	[Cat]/[M] (%)	[Lig]/[M] (%)	Concentration of the solvent (v/v %)	Time (days)
P 78	P 72	3 800	1.30	1	1.6	1.6	33	3
P 79	P 73	5 500	1.18	2	1.6	1.6	50	6

Both reactions catalysed with a Cu(I)Br/HMTETA complex in DMF at 60 °C.

These extended, linear polymers were analysed by ^{1}H- and ^{13}C-NMR in D_2O. The chemical shifts are summarised in Section 5.2.1. Polymers were injected onto a GPC column calibrated with narrow PS standards (THF as mobile phase). M_n values of the polymers obtained (P 78 - P 79) were of 5 330 g.mol^{-1} and 7 100 g.mol^{-1} with polydispersity of 1.26 and 1.24, respectively.

5.3. Results

5.3.1. Kinetic studies

For the kinetic studies, the conversion was estimated at each point in time using ^{1}H-NMR and Equations 5.1 and 5.2. Theoretically, the conversion can be estimated using Equation 5.1.

$$Conversion = \left(\frac{\Delta[M]}{[M]_0}\right) = \frac{[M]_0 - [M]_{residual}}{[M]_0} \qquad \text{(Eq.5.1)}$$

where $\Delta[M]$ is the concentration of the consumed monomer during the reaction, $[M]_0$ is the initial monomer concentration and $[M]_{residual}$ is the final monomer concentration in the reaction mixture at the end of the reaction.

However, experimentally, the percentage conversion can be calculated using Equation 5.2, where the integrals of the polymeric methylene H_d are compared with the integrals of the monomeric methines H_a and H_b, and the monomeric methylene H_c (Figure 5.3).

$$Conversion = \frac{\int H_d}{\frac{\left(\int H_a + \int H_b + \int H_c\right)}{2} + \int H_d} \times 100 \qquad \text{(Eq.5.2)}$$

Once the conversion is determined, the theoretical number-average molecular weight ($M_{n,\,theoretical}$) can be predicted using Equations 5.3 and 5.4, as in the case of a living polymerisation (adapted from (Matyjaszewski and Xia 2001), (Wang and Matyjaszewski 1995), and (Zhang *et al.* 1998)).

$$M_{n,theoretical} = \left(\frac{\Delta[M]}{[I]_0}\right) \times MW_{Monomer} + MW_{Initiator} \qquad \text{(Eq.5.3)}$$

and

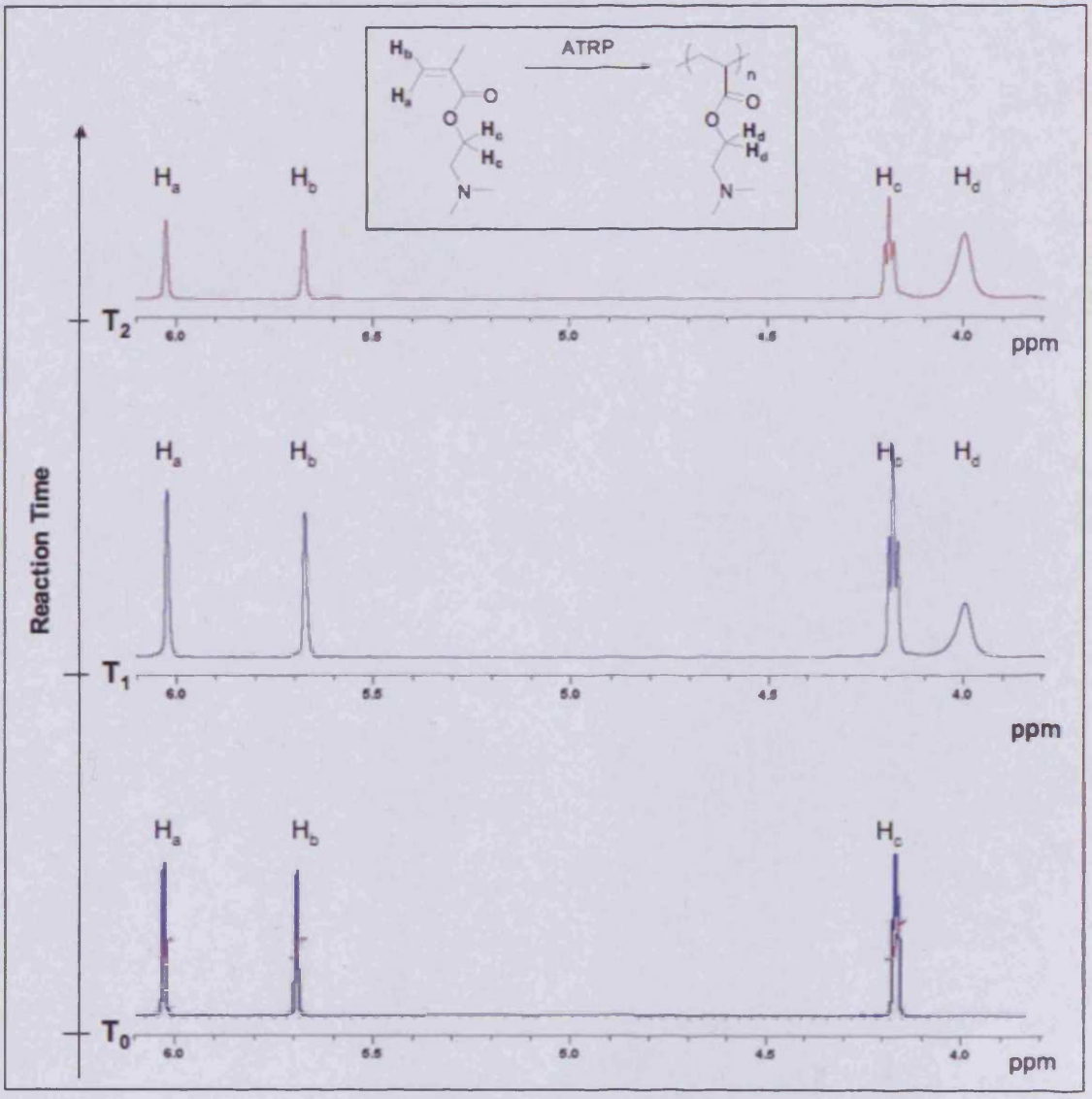

Figure 5.3: Representation of the monomer to polymer conversion by ^{1}H-NMR spectra of ATRP of DMAEM (P 72, Table 5.2)

With T_0 = 0 min, T_1 = 7 min, T_2 = 20 min. The areas under the monomeric proton peaks decrease while the ones relating to the polymeric proton increase with time, confirming the conversion of monomer into polymer.

$$M_{n,theoretical} = \left(\frac{Conversion \times [M]_0}{[I]_0} \right) \times MW_{Monomer} + MW_{Initiator} \quad \text{(Eq 5.4)}$$

where $M_{n,theoretical}$ is the number-average molecular weight expected for the polymer, $[I]_0$ and $MW_{Initiator}$ are the initial concentration and molecular weight of the initiator, respectively, and $MW_{Monomer}$ is the molecular weight of the monomer (157.21 $g.mol^{-1}$ for DMAEM monomer).

Table 5.4 summarises the estimated conversion, the theoretical and experimental molecular weight obtained for each ATRP reaction.

5.3.2. Effect of solvent, initiator and ligand on the ATRP characteristics of DMAEM

Effect of solvent

In general, the reactions done in bulk or in double distilled water (samples P 64 – P 71) showed an increase in viscosity very soon after the reaction started. This resulted in the measurement of high conversions (around 90 %) at short reaction times for samples P 64, P 65, P 69, and P 71 (Table 5.4). The high viscosity of these reaction mixtures made it impossible to collect samples during the reaction period so no kinetic data could be obtained. Moreover, apart from sample P 65, which was prepared in bulk and sample P 69 prepared in double distilled water, the experimental molecular weight obtained in these studies did not correlate with the theoretical ones (see discussion).

The reactions carried out in DMF or DMSO seemed to improve the control of the ATRP, at least from the conversion point of view. A good conversion was obtained after longer reaction times. Also, polymers that had an experimental molecular weight closer to the theoretical values were obtained. For example, the reactions performed in DMF (samples P 72 – P 74) showed a good correlation of molecular weight and also had a narrow polydispersity of 1.18 to 2.88. This polydispersity was lower than seen for reactions undertaken in bulk or in water (M_w/M_n = 1.28 – 3.65).

Effect of initiator

Of the three initiators studied, ethyl α-bromoisobutyrate gave better control of molecular weight and polydispersity (except for the reactions carried out in water: P 67 and P 70). This can be clearly seen when comparing the characteristics of samples

Table 5.4: Summary of the conversion, and the theoretical and experimental molecular weight characteristics of the linear PDMAEM synthesised by ATRP

Identification	Time (h)	Solvent	v/v (%)	Temperature (° C)	Conversion (%)[m]	$M_{n,\ theoretical}$ ($g.mol^{-1}$)[n]	$M_{n,\ experimental}$ ($g.mol^{-1}$)[o]	M_w/M_n[o]
P 64[a],[f]	1.50			60	99.0	9 920	12 035	1.28
P 65[a],[g]	1.50	Bulk	-	60	92.0	14 660	13 630	1.41
P 66[b],[h]	16.00			80	80.0	12 760	30 935	3.65
P 67[a],[i]	0.08		50	RT	90.5	17 980	60 000	1.63
P 68[c],[j]	16.00		52	RT	83.0	13 280	26 100	1.50
P 69[d],[g]	1.50	ddH_2O	50	RT	90.0	14 380	17 620	1.68
P 70[a],[k]	1.00		20	RT	51.0	8 210	85 660	2.30
P 71[e],[k]	1.00		20	RT	78.0	12 460	63 460	1.96
P 72[a],[l]	44.00		20	60	48.5	4 000	3 800	1.30
P 73[a],[l]	21.40	DMF	50	60	65.3	5 330	5 500	1.18
P 74[a],[l]	46.50		20	90	45.2	3 750	5 540	1.26
P 75[a],[g]	2.00		50	50	18.0	3 025	6 600	1.23
P 76[a],[g]	1.50	DMSO	50	RT	38.8	6 295	11 750	1.40
P 77[a],[g]	3.40		25	50	16.2	2 740	12 040	2.88

[a]: Reactions initiated with ethyl α-bromoisobutyrate/ Cu(I)Br/ HMTETA complex; [b]: Reactions initiated with ethyl 2-bromopropionate/ Cu(I)Br/ Bipyridine complex; [c]: Reactions initiated with methyl α-bromophenylacetate/ Cu(I)Br/ Bipyridine complex; [d]: Reactions initiated with methyl α-bromophenylacetate/ Cu(I)Br/ HMTETA complex; [e]: Reactions initiated with ethyl α-bromoisobutyrate/ Cu(I)Br/ Bipyridine complex; [f]: [I]/[M]-[Cat]/[M]-[Lig]/[M] = 1.6-1.6-1.6 (%); [g]: [I]/[M]-[Cat]/[M]-[Lig]/[M] = 1-1-1 (%); [h]: [I]/[M]-[Cat]/[M]-[Lig]/[M] = 1-1-3 (%); [i]: [I]/[M]-[Cat]/[M]-[Lig]/[M] = 0.8-0.8-0.8 (%); [j]: [I]/[M]-[Cat]/[M]-[Lig]/[M] = 1-1-2 (%); [k]: [I]/[M]-[Cat]/[M]-[Lig]/[M] = 1-0.5-0.5 (%); [l]: [I]/[M]-[Cat]/[M]-[Lig]/[M] = 2-1.6-1.6 (%); [m]: Determined by ^{1}H-NMR spectroscopy and Eq.5.2; [n]: Calculated with Eq.5.4; [o]: Determined by GPC, mobile phase THF, columns calibrated with narrow PS standards, after extensive dialysis of the final polymer at the end of the reaction.

P 64 and P 65 with sample P 66 (Table 5.4). Ethyl α-bromoisobutyrate was therefore used as initiator for all further ATRP experiments of DMAEM.

Effect of ligand

Comparison of the results obtained for reactions conducted in bulk and in water, using the same conditions but different ligands, showed that in general reactions carried out using HMTETA as the ligand gave better control of molecular weight and polydispersity. Higher conversion was also reached in a shorter reaction time. This can be seen by comparing the results obtained for samples P 64 and P 65 with sample P 66; sample P 69 with sample P 68; and also sample P 67 with sample P 71.
Therefore, in following experiments using DMF or DMSO as solvents, the reactions used HMTETA as the ligand with ethyl α-bromoisobutyrate as the initiator.

5.3.3. Effect of organic solvent: DMF and DMSO

The ATRP reactions involving the monomer DMAEM, ethyl α-bromoisobutyrate as the initiator, Cu(I)Br as the catalyst and HMTETA as the ligand was studied kinetically using either DMF or DMSO as solvent and at several temperatures and dilutions (Table 5.4). Figures 5.4 - 5.5 show plots of the evolution of the conversion and M_n against time and conversion, respectively, for two experiments carried out in DMF.
At first glance, it appears that reactions in DMF gave better control of polymer characteristics (conversion, similarity of experimental and theoretical M_n, and polydispersity) than those for the DMSO. Indeed, in DMF as a general trend, even though the conversion did not increase linearly with time for any of the reactions, the experimental M_n did increase proportionally with the conversion. Additionally, the polydispersity remained relatively low for the experiments carried out in DMF compared with those done in DMSO (Table 5.4).

5.3.4. Chain extension reactions: livingness of this ATRP system

The linear PDMAEM samples (P 72 and P 73) were used as macroinitiators for further ATRP experiment of DMAEM in DMF using the Cu(I)Br/HMTETA catalytic system (Scheme 5.3, Section 5.2.2). The results obtained for these two linear chain extension reactions are summarised in Table 5.5. It can be seen that samples P 78 and P 79 displayed an small increase in the final molecular weight of approximately 1 500

(a)

(b)

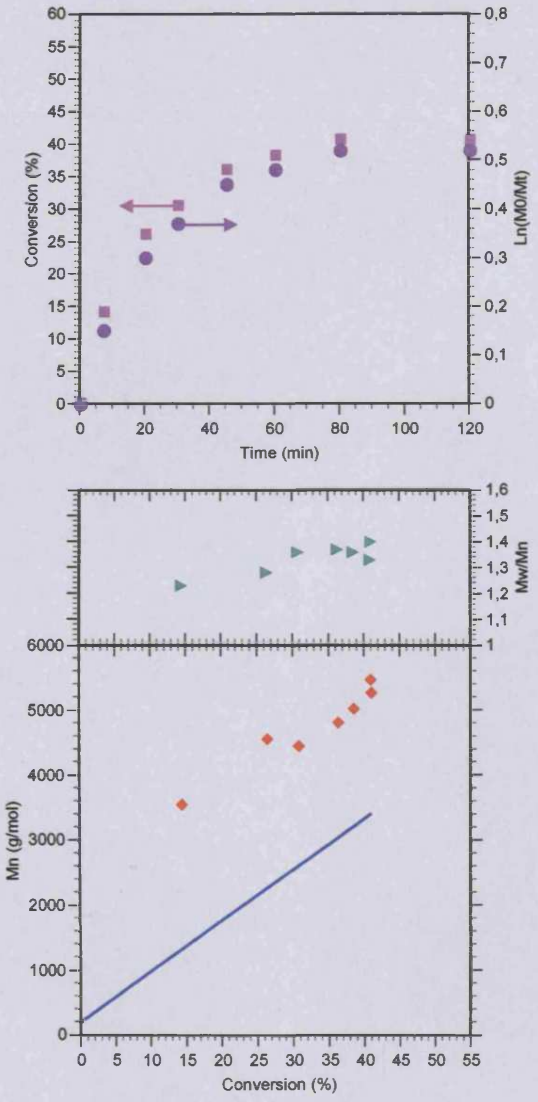

Figure 5.4*: Kinetic plots for the synthesis of PDMAEM in DMF (20 v/v %, 60 °C, P 72)

Reaction initiated by ethyl α-bromoisobutyrate ([I]/[M] = 2 %), catalysed by Cu(I)Br/HMTETA ([Cat]/[M] = 1.6 %, [Lig]/[M] = 1.6 %) at 60 °C. Panel (a) plots the conversion (■) and Ln(M0/Mt)** (●) against time (min), while on panel (b) theoretical (—) and experimental (◆) M_n and M_w/M_n (▶) are plotted against the conversion (%).

---

* The experimental M_n used for plotting part (b) of this Figure are the one measured during the experiment before dialysis of the final product, and thus does not correlate with figures presented in Table 5.4. ** Where Mt represents the concentration of monomer M in the reaction at the time t

(a)

(b)

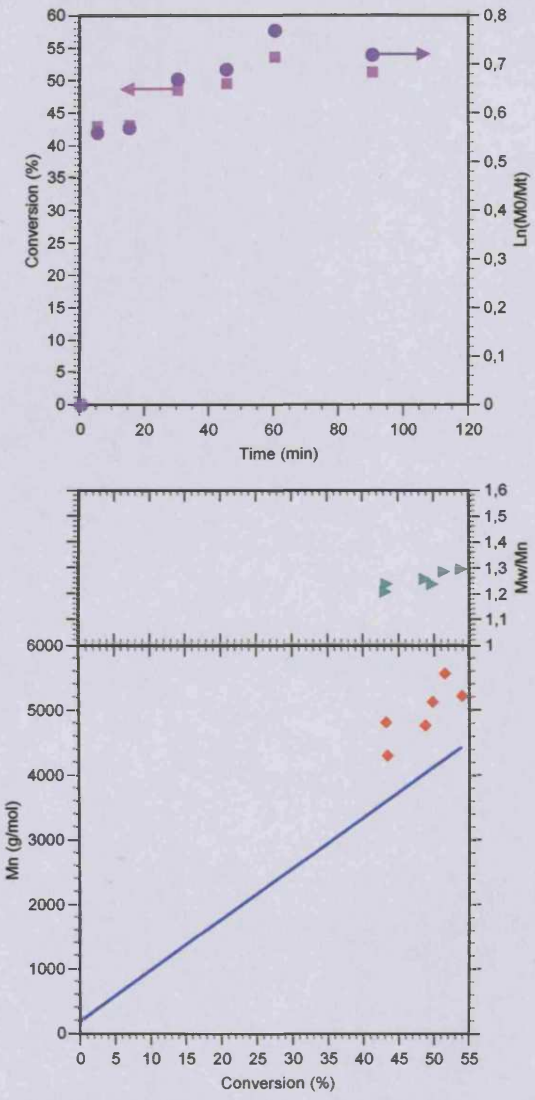

Figure 5.5*: Kinetic plots for the synthesis of PDMAEM in DMF (50 v/v %, 60 °C, P 73)

Reaction initiated by ethyl α-bromoisobutyrate ([I]/[M] = 2 %), catalysed by Cu(I)Br/HMTETA ([Cat]/[M] = 1.6 %, [Lig]/[M] = 1.6 %) at 60 °C. Panel (a) plots the conversion (■) and Ln(M0/Mt)** (●) against time (min), while on panel (b) theoretical (—) and experimental (◆) M_n and M_w/M_n (▶) are plotted against the conversion (%).

---

* The experimental M_n used for plotting part (b) of this Figure are the one measured during the experiment before dialysis of the final product, and thus does not correlate with figures presented in Table 5.4. ** Where Mt represents the concentration of monomer M in the reaction at the time t

Table 5.5: Summary of the conversion, and the theoretical and experimental molecular weight characteristics of the linear chain extension reactions

Polymer	MaI			Time (days)	Conversion (%)[d]	$M_{n,theoretical}$ (g.mol^{-1})[e]	$M_{n,experimental}$ (g.mol^{-1})[c]	M_w/M_n [c]
	Identification	M_n (g.mol^{-1}) [c]	M_w/M_n [c]					
P 78[a]	P 72	3 800	1.30	3	20	7 000	5 330	1.26
P 79[b]	P 73	5 500	1.18	6	38	8 500	7 100	1.24

[a]: in DMF (33 % v/v) with [MaI]/[M] = 1 %, [Cu(I)Br]/[M] = 1.6 %, [HMTETA]/[M] = 1.6 % at 60 °C; [b]: in DMF (50 % v/v) with [MaI]/[M] = 2 %, [Cu(I)Br]/[M] = 1.6 %, [HMTETA]/[M] = 1.6 % at 60 °C; [c]: determined by GPC, mobile phase THF, columns calibrated with narrow PS standards; [d]: determined by ^{1}H-NMR spectroscopy; [e]: calculated with Eq.5.4.

$g.mol^{-1}$ compared to the macroinitiators, and the polydispersity remained in the range of the starting macroinitiators (≤ 1.30).

5.4. Discussion

Before the synthesis of star-based PDMAEM using the core-first approach with multifunctional initiators (introduced and explained in Chapter 6) it was important to study, and optimise, the ATRP of DMAEM using simple and commercially available initiators. It was hoped to define optimal conditions for the more complex reactions to follow. Several reaction conditions were studied and the polymerisations followed kinetically in an attempt to gain understanding of the mechanism of polymerisation. Also, further polymerisation using PDMAEM as a macroinitiator was studied to verify the "living" character expected with controlled radical polymerisation techniques.

In general, when using ATRP several factors must be verified in order to meet the definition of CRP. These factors (reviewed by Matyjaszewski and Xia (2001)) can be summarised as follows:

1. there should be a linear increase in conversion with time in semi logarithmic coordinates: $Ln(M_0/M_t)= f(time)$ (indicating a constant concentration of active species, first-order kinetics with respect to monomer and non significant presence of termination reactions)
2. there should be a linear increase in M_n with conversion and a good correlation with the theoretical M_n (indicating a small contribution of irreversible terminating reactions and a good initiator efficiency)
3. the resulting polymer should have a narrow molecular weight distribution ($1.0 < M_w/M_n < 1.5$)
4. for chain extension reactions, there should be an increase in molecular weight of the product compared to that of the macroinitiator.

Even though the products P 65 (prepared in bulk) and P 69 (prepared in water) gave a high conversion at low reaction time, and displayed both molecular weights similar to the theoretical expected values and relatively low polydispersity, these reaction conditions did not result in polymerisation with a total control due to their fast rate of polymerisation and the high viscosity generated (see samples P 64 - P 71 in Table

5.4). For samples P 64 to P 71 (Table 5.4), the M_n values measured were different and higher than the theoretical. In most cases there was clear evidence of a poor control of polymerisation. When Pelton and co-workers (Zeng *et al.* 2000a) studied the ATRP of DMAEM in water, they reported similar results. They found that only methyl α-bromophenylacetate was soluble in water and able to initiate the ATRP of DMAEM in a controlled manner. Also, as DMAEM forms thermosensitive polymers with a lower critical solution temperature around 50 °C (Chen and Min 2001; Heijl and Du Prez 2004), they observed that for the fast and poorly controlled polymerisations, the heat released caused phase-separation of the PDMAEM. They obtained polymers with high molecular weight and broad polydispersity. Finally another important point to take into consideration is that the hydrolytic stability of the DMAEM monomer in water, as mentioned in Chapter 3. It was shown that the ester in DMAEM monomer is rather unstable toward hydrolysis in an aqueous solution at pH 7.4 and 37°C (van de Wetering *et al.* 1998b). Thus polymerisation of this monomer undertaken in water will lead to the synthesis of statistical copolymer of DMAEM with methyl(acrylic acid), rendering the system more complicated and making the polymerisation process less controllable.

Considering these preliminary results, and the low solubility of Cu(I)Br in non-polar solvents (Zhang *et al.* 1998), the use of organic solvents such as DMF and DMSO was explored in an attempt to improve the homogeneity of the system. Furthermore, DMF and DMSO gave a better solubilisation of the reactants present and therefore helped to maintain a low concentration of the growing radicals.

As showed previously (Zhang *et al.* 1998; Shen *et al.* 2000; Zeng *et al.* 2000b) Cu(I)Br combined with multidentate amines proved to be a good catalyst system for the ATRP of DMAEM. It has been shown previously that the efficiency of *N*-based ligands increases with the number of coordinating sites. A tetradentate ligand is more active than a bidentate (reviewed by (Matyjaszewski and Xia 2001)) and this could explain the differences observed here. It was found that reactions carried out using HMTETA as the ligand gave better control of the molecular weight and polydispersity of the products compared with those prepared using bipyridine.

Consequently most studies were focused on the optimisation of the ATRP of DMAEM using Cu(I)Br, HMTETA, ethyl α-bromoisobutyrate in polar organic solvents. For the reactions carried out in DMF and DMSO (samples P 72 to P 77 in Table 5.4), the relationship between the logarithm of monomer conversion with time was not linear indicating non-conservation of radicals throughout the reaction. Also, the tailing seen in GPC traces at higher conversions (data not shown) suggested the occurrence of termination events and/or catalyst deactivation. The latter could occur through the sampling process even if it was done with great care (Matyjaszewski *et al.* 1999; Bontempo *et al.* 2005). Irreversible termination reactions would lead to an increase of the concentration of Cu(II) species resulting in an activation/deactivation equilibrium shift and it would favour the formation of dormant species. This effect was noticeable on the plots M_n = f(conversion) where the measured molecular weights were all greater than those expected (Figures 5.4 and 5.5 compared to non-presented data).

Nonetheless, when DMF was used as solvent a linear increase of the experimental M_n with conversion was observed (see sample P 73). Therefore, although the polar organic solvent DMF was not considered optimal for ATRP due to possible competitive chelation of copper ions (Godwin *et al.* 2001), it did produce the best results here. Others have previously shown that ATRP of DMAEM is also possible in polar organic solvents such as THF, dichlorobenzene, anisole, and butylacetate (Zhang *et al.* 1998; Zeng *et al.* 2000a). However, in high polar solvents such as DMSO, the polymerisation rate was fast and the polydispersity of the synthesised polymer was broad (Zeng *et al.* 2000b). In these studies comparison of DMSO with DMF showed that DMF was clearly the best solvent and thus, it was used for the synthesis of star-based polymers by ATRP with the following system: Cu(I)Br as catalyst, HMTETA as ligand, and ethyl α-bromoisobutyrate as initiator, at 60°C (Chapter 6).

One theoretical characteristic of ATRP is the possibility to create polymers bearing the halide at their end-groups. This halide can then, in theory, be transferred to the catalyst/ligand complex, leading to the formation of a macroradical that could potentially initiate again the polymerisation of a fresh batch of either the same or another monomer. NMR is usually used to identify and quantify the halide-

functionalised end-groups of the synthesised polymer. Nevertheless, in these studies, it was difficult to observe those functionalised end-groups by NMR, thus the use of another method, known as chain extension reactions was employed to prove their existence.

The little increase in molecular weight produce by chain extension of PDMAEM using ATRP and previously synthesised PDMAEM as macroinitiator, indicates a loss in the bromine end-groups needed for reinitiating the polymerisation of DMAEM. As explained by Teodorescu and Matyjaszewski (1999, 2000) and reviewed by Matyjaszewski and Xia (2001), who studied the ATRP of amine and amide containing monomers, a displacement of the terminal bromine groups by substitution reaction with the amines of the pendant groups of the repeating unit can occur. This side reaction leads to the loss of the bromine-based initiating units needed for the subsequent chain extension attempted, and in our case, the quaternization of the amine atoms on the pendant groups of the PDMAEM polymers.

5.5. Conclusions

These studies synthesised a library of linear homopolymers of DMAEM using ATRP. The reaction conditions were optimised and it was found that Cu(I)Br, HMTETA, ethyl α-bromoisobutyrate and DMF gave the best results, with a linear increase of molecular weight with conversion, low polydispersity ($M_w/M_n \leq 1.30$), good correlation between theoretical and experimental molecular weight, and an increase of molecular weight of the polymer with addition of a new batch of monomers. Optimisation was done to allow subsequent synthesis of star-based PDMAEM using the core-first approach ATRP, multifunctional initiators and optimised ATRP conditions (Chapter 6).

Furthermore, this library was also used together with the other linear PDMAEMs previously synthesised by conventional FRP with (Chapter 3) or without CTA (Chapter 4) to study the biological properties of these polymers (Chapter 7).

6

Synthesis & Characterisation of Multifunctional ATRP Initiators & Star Polymers of DMAEM by ATRP

6.1. Introduction

The goal of these studies was the design of novel star shaped polymers of DMAEM keeping in mind their potential future application in the field of polymer therapeutics. As mentioned in Chapter 1 (Section 1.3.3) star polymers can be prepared using multifunctional initiators (i.e. compounds bearing more than one initiating unit) to provide a core as a basis for ATRP. Historically, hexakis(bromoethyl)benzene was the first multifunctional initiator used in this way for the synthesis of star shaped PS by ATRP (Wang *et al.* 1995). Since then research has been focusing on the design of other well-defined star polymers by ATRP. For example, 3-arm (Kasko *et al.* 1998; Matyjaszewski *et al.* 1999), 4-arm (Matyjaszewski *et al.* 1999; Jiang *et al.* 2000) and up to 12-arm (Heise *et al.* 1999; Heise *et al.* 2000) star polymers were synthesised by ATRP using multifunctional initiators. Star polymers of n-butyl acrylate, styrene, methyl methacrylate and 11-(4'-cyanophenyl-4"-phenoxy)undecyl acrylate with a molecular weight as high as 85 000 $g.mol^{-1}$ and polydispersity as low as 1.08 were successfully synthesised using the core-first approach ATRP and multifunctional, dendrimer-like initiators.

Moreover, by definition of CRP the arm length of a star polymer can be varied by altering the initial molar ratio [I]/[M] (Kamigaito *et al.* 2001). This can, in theory, provide an attractive control over molecular weight. The synthesis of DMAEM star polymers has been widely reported and Table 6.1 briefly summarises several DMAEM-based star polymers that have already been developed. They have had molecular weights ranging from 10 000 to 230 000 $g.mol^{-1}$, and a narrow polydispersity ranging from 1.09 to 1.50.

For these studies, synthesis of star polymers that focused on DMAEM was appealing as this enabled the study of polymer architecture on properties by comparison with the respective linear homologues. The star polymers would be expected to have lower hydrodynamic volume, lower flexibility, and a more compact 3-dimensional structure. Thus it might be expected that their biological properties (e.g. cell binding, endocytosis and exocytosis rate, and degradation in the case of biodegradable star polymers) would also be different compared to linear polymers.

Table 6.1: Summary of the reaction conditions for the synthesis of DMAEM-based star polymers by ATRP and core-first approach from selected articles

Initiator	Number of arms	Catalyst	Ligand	Solvent	T (° C)	Reference
1,3,5-Tri-*O*-isobutyryl bromide benzene	3	Cu(I)Br	*n*-propyl-2-pyridinylmethyleneamine	toluene	85	Limer *et al.* 2006
1,2,3,4,6-Penta-*O*-isobutyryl bromide-α-D-glucose	5	Cu(I)Br	*n*-propyl-2-pyridinylmethyleneamine	toluene	85	"
ND	8	Cu(I)Br	*n*-propyl-2-pyridinylmethyleneamine	toluene	85	"
Tris-(2-aminoethyl)amine	3	Cu(I)Br	bipyridine	methanol	RT	Li *et al.* 2005
Triethanolamine	3	Cu(I)Br	bipyridine	methanol	RT	
1,1,1,1-Tetrakis(2'-bromo-2'-methylpropionyloxymethyl)methane	4	Cu(I)Br	*N*-(n-propyl)-2-pyridylmethaneimine	toluene	100	Lecolley *et al.* 2003
ND	3	Cu(I)Br	*N*-(n-propyl)-2-pyridylmethaneimine	toluene	100	"
ND	2	Cu(I)Br	*N*-(n-propyl)-2-pyridylmethaneimine	toluene	100	"
PAMAM-Cl generation 1 to 5 (dendrimer-based initiators with peripheral alkyl chlorine)	from 8 to 128	Cu(I)Cl	PMDETA*	water	80	Hui *et al.* 2005
1,4-(2'-bromo-2'-methyl-propionate)-benzene macroinitiator	2	Cu(I)Br	*N*-(n-propyl)-2-pyridylmethanimine	toluene	90	Narrainen *et al.* 2002
1,3,5-(2'-bromo-2'-methyl-propionate)-benzene macroinitiator	3	Cu(I)Br	*N*-(n-propyl)-2-pyridylmethanimine	toluene	90	"

ND: not defined; *: PMDETA: *N,N,N',N",N"*-pentamethyldiethylenetriamine.

Using ATRP, a wide range of multifunctional cores has been employed for the synthesis of star polymers. These encompass for example: polyols, cyclotriphosphazines, cyclosiloxanes (Matyjaszewski *et al.* 1999), modified calixarenes (Angot *et al.* 1998; Ueda *et al.* 1998), multisulfonyl chloride (Percec *et al.* 2000), aromatic alcohols (Narrainen *et al.* 2002), sugar (Haddleton *et al.* 1999), cycodextrin (Ohno *et al.* 2001), metallo-based compounds (Viau *et al.* 2005), dendritic cores (Angot *et al.* 1998; Hawker *et al.* 1998; Nakagawa *et al.* 1998; Heise *et al.* 1999; Wang *et al.* 1999; Yoo *et al.* 2003).

In these studies, the synthesis of hydrotically stable (dendritic-based) and degradable (alcohol-based) cores was attempted. The rationale for the choice of these cores was the belief that the star polymers derived from them by ATRP would be either stable or hydrolytically labile under specific conditions. The development of biodegradable and stable star polymers would, in the future, offer the possibility of designing a variety of constructs for use as polymer therapeutics. Also, low and high numbers of initiating moieties were chosen so that the star polymers synthesised would have different physicochemical properties including 3D conformation, hydrodynamic volume and flexibility. By varying the number of arms on the star polymers, it should later be possible to control the drug loading capacity, and/or the number of targeting moieties conjugated.

Technical aims

Figure 6.1 shows schematically the aims of these studies. It was first necessary to synthesise multifunctional cores. Commercially available DAB dendrimers of generation 1 and 2 (4 and 8 functionable amine groups, respectively) were chosen and they were functionalised with alkyl bromide groups (as ATRP initiating moieties) through hydrolytically stable amide-based linkers. In addition, two alcohol-based cores, namely xylitol and tripentaerythritol (5 and 8 functionable hydroxyl groups), were chosen and also functionalised with alkyl bromide groups through hydrolytically degradable ester linkers. Figure 6.2 shows the structures of the four ATRP initiators designed here.

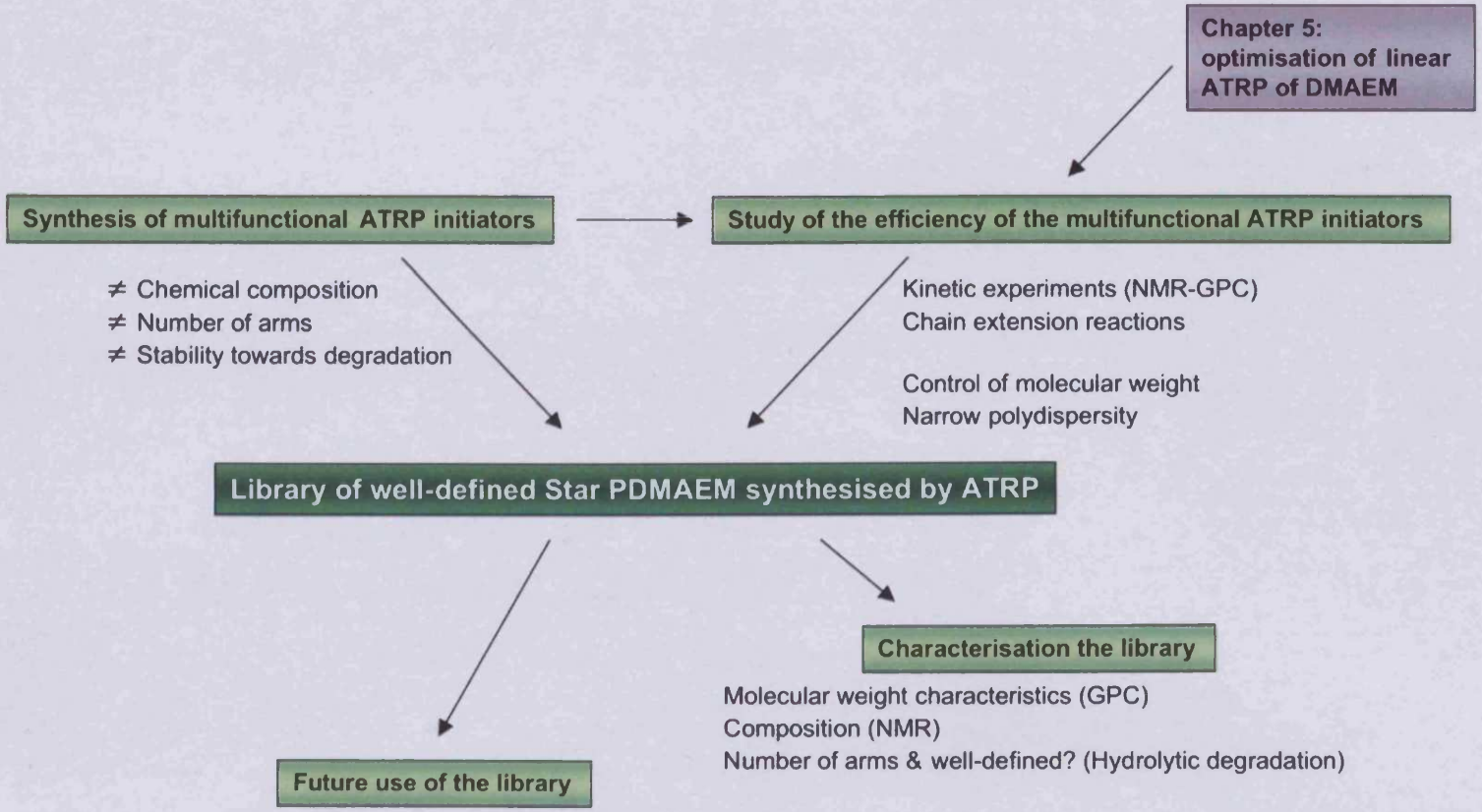

Figure 6.1: Schematic representation of the aims of these studies

Figure 6.2: Rationale for the choice of the cores

Using these multifunctional initiators, growth of DMAEM-based star polymers by ATRP was studied and followed kinetically using the optimised reaction conditions determined in Chapter 5. All the experiments were carried out in DMF at 60 °C with the Cu(I)Br/HMTETA catalyst system. To study the synthesis of star polymers of different molecular weight, and to investigate the best conditions for controlled polymerisation, the [I]/[M], [Cat]/[M] and [Lig]/[M] ratios were varied from 1 to 2 %.

All the DMAEM-based star polymers synthesised were characterised by ^{1}H-NMR and GPC. In addition, the degradation of the alcohol-based star polymer was determined at basic pH using GPC. Hydrolysis of star polymers to liberate the polymer arms has been extensively employed by others (Angot *et al.* 1998; Deng and Chen 2004; Zhao *et al.* 2005) to enable estimation of the efficiency of the initiators used and the degree of control of the ATRP polymerisation. The regularity of arm length can also be estimated.

6.2. Methods

First it was necessary to synthesise multifunctional initiators and the methods used are described in the following Sections 6.2.1 and 6.2.2.

6.2.1. Synthesis of the DAB dendrimer-based multifunctional ATRP initiators with 4 and 8 functional groups

Both the DAB dendrimer-based multifunctional initiators (MuI-DAB-4 and MuI-DAB-8) were synthesised and purified using a procedure adapted from (Shemper *et al.* 2002) and (Lecolley *et al.* 2003) (Schemes 6.1 and 6.2). The method used to synthesise MuI-DAB-4 (Scheme 6.1) is described in detail and all the reaction conditions are summarised in Table 6.2. MuI-DAB-8 was synthesised using the same procedure (Scheme 6.2), but in this case the equivalences used were twice as much as for the initiator with 4 functional groups.

The DAB-Am-4 dendrimer (1.0 mL, 3.03 mmol, 1.0 eq), was dissolved in a round bottom-flask in anhydrous dichloromethane (5.0 mL), and cooled to 0 °C under N_2. Triethylamine (2.0 mL, 14.35 mmol, 4.7 eq) was added to the mixture, and then 2-bromoisobutyryl bromide (1.7 mL, 13.75 mmol, 4.5 eq) was added dropwise. The

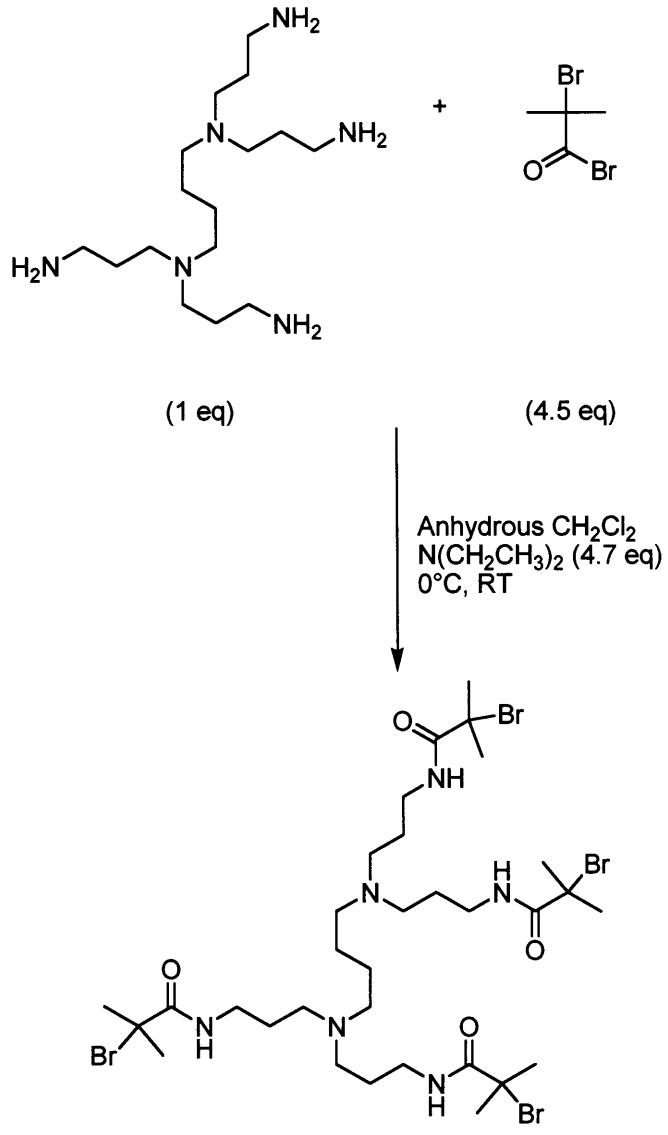

Scheme 6.1: Synthesis of MuI-DAB-4

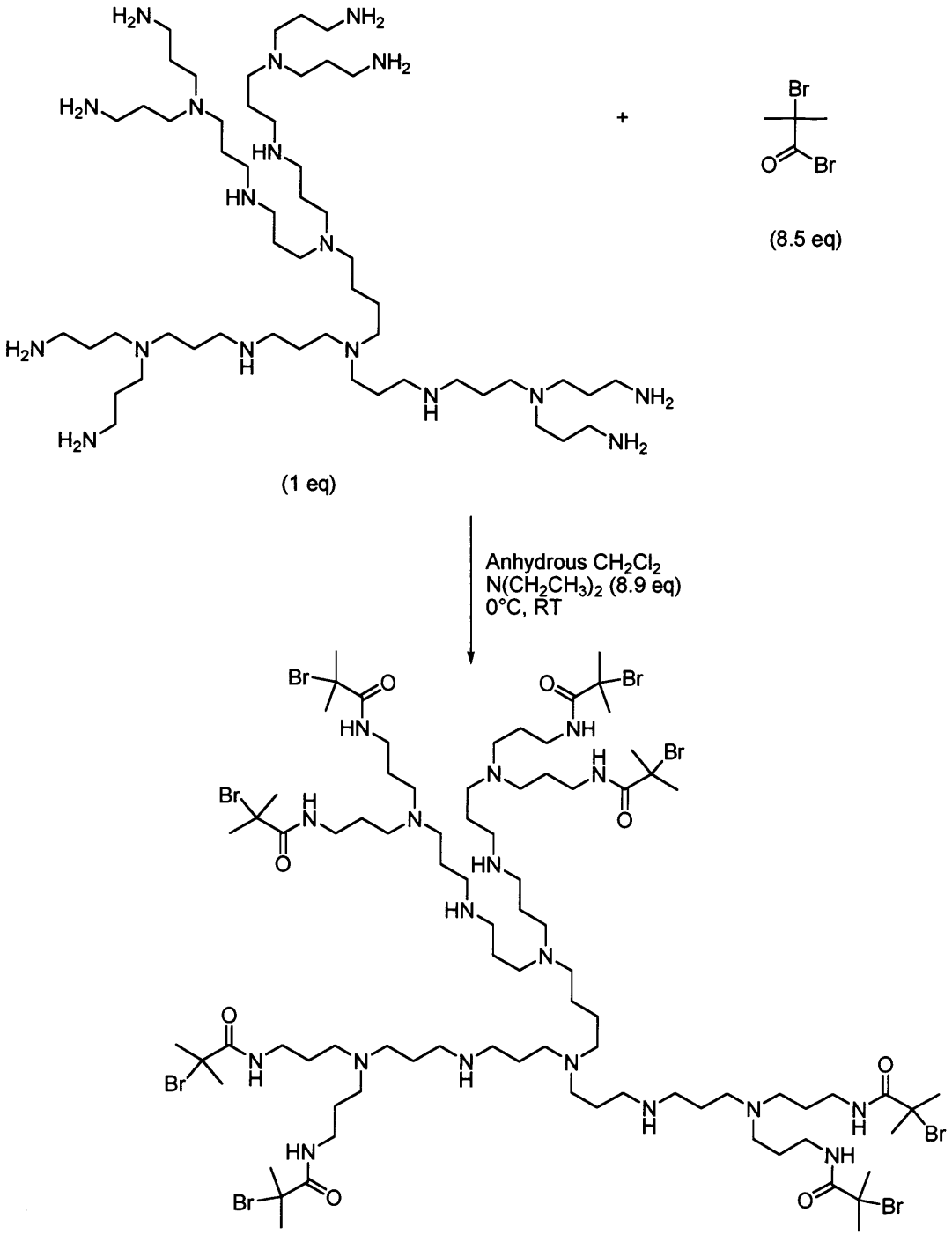

Scheme 6.2: Synthesis of MuI-DAB-8

Table 6.2: Conditions used for the synthesis of the multifunctional ATRP initiators (MuI)

MuI	Core	2-bromoisobutyryl bromide (eq)	Base (eq)	Solvent (%)	Yield (%)
MuI-DAB-4[a]	1 eq	4.5	4.7	20.0 v/v	85
MuI-DAB-8[b]	1 eq	8.5	8.9	20.0 v/v	88
MuI-ester-5[c]	1 eq	8.0	8.0	5.0 w/v	60
MuI-ester-8[d]	1 eq	16.0	16.5	3.3 w/v	40

[a]: DAB-Am-4 was used as the initial core reagent with $N(CH_2CH_3)_3$ as the base, in CH_2Cl_2; [b]: DAB-Am-8 was used as the initial core reagent with $N(CH_2CH_3)_3$ as the base, in CH_2Cl_2; [c]: Xylitol was used as the initial core reagent with DMAP as the base, in DMF; [d]: Tripentaerythritol was used as the initial core reagent with DMAP as the base, in DMF.

reaction was left for 1 h at 0 °C and then for 3 h at room temperature. The white precipitate formed during the reaction was then filtered off, and the organic phase washed with a sodium hydroxide aqueous solution (3 x 20 mL, pH = 14), dried over $MgSO_4$, filtered and the dichloromethane was then evaporated to yield an orange viscous oil in 85 %.

The product was characterised by EA, IR, ^{1}H-NMR and ^{13}C-NMR, and the results obtained are summarised below.

Key: the red letters are assigned to the protons of the compounds and carbon elements are labelled by the blue numbers.

Characterisation of the DAB dendrimer-based multifunctional initiator MuI-DAB-4

Yield: 85 %.

EA: $N_{Experimental}$ = 8.01 % ($N_{Theoretical}$ = 9.21 %); $H_{Experimental}$ = 6.80 % ($H_{Theoretical}$ = 6.63 %); $C_{Experimental}$ = 40.63 % ($C_{Theoretical}$ = 42.12 %);$Br_{Experimenal}$ = 32.66 % ($Br_{Theoretical}$ = 35.03 %).

IR: $\bar{\nu}$ (cm^{-1})* = wide band around 3 340, H-bonding with secondary amide ν_{N-H}; 2 970 and 2 920, ν_{C-H}; 1 656, $\nu_{C=O}$ (Amide I band); 1 532, ν_{C-N} and δ_{CNH} (Amide II band); 1 458, δ_{CH}; 1 393, δ_{CH} of aliphatic amines (–N-CH_2); 1 260, δ_{NH} and δ_{OCN} (Amide III band); 1 350-800, δ_{C-C} and δ_{CH}.

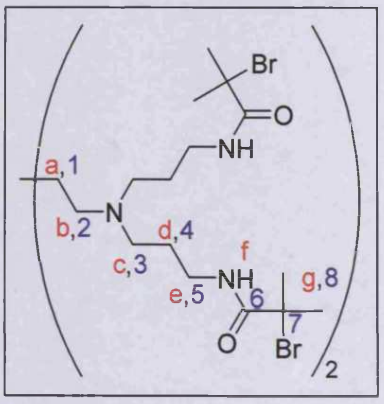

^{1}H-NMR ($CDCl_3$, ppm)**: δ = 7.36, bs, 4H, H_f; 3.30, q, 8H, H_e, $^3J_{ed}$ = 6.125 Hz and $^3J_{ef}$ = 12.025 Hz; 2.46, t, 8H, H_c, $^3J_{cd}$ = 6.375 Hz; 2.40, bs, 4H, H_b; 2.00, ss, 24H, H_g; 1.66, t, 8H, H_d, ^3J_d = 6.450 Hz; 1.40; bs, 4H, H_a.

^{13}C-NMR ($CDCl_3$, ppm): δ = 172.0, C_6;

---

* *Wavenumbers $\bar{\nu}$ are expressed in cm^{-1}. ν represents the stretching vibrations and δ, the bending vibrations.*

** *Where s is a singlet, bs is a broad singlet, d a doublet, t a triplet, q a quadruplet, and m a multiplet.*

77.0, C_2; 53.4, C_7; 51.9, C_3; 39.4, C_8; 32.5, C_4; 26.1, C_1.

Characterisation of the DAB dendrimer-based multifunctional initiator MuI-DAB-8

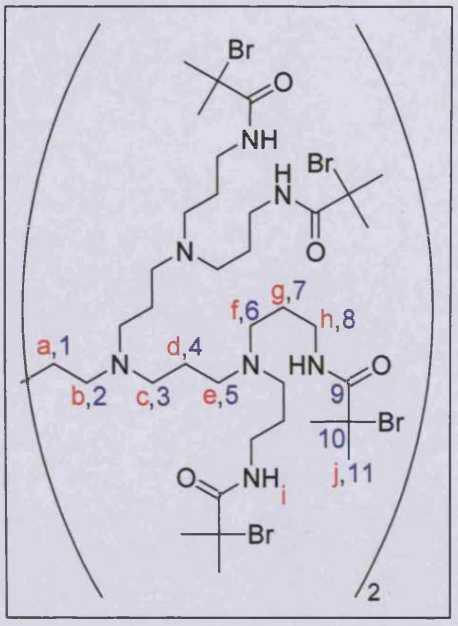

Yield: 88 %

EA: $N_{Experimental}$ = 9.17 % ($N_{Theoretical}$ = 9.97 %); $H_{Experimental}$ = 7.17 % ($H_{Theoretical}$ = 6.98 %); $C_{Experimental}$ = 42.46 % ($C_{Theoretical}$ = 44.01 %); $Br_{Experimenal}$ = 29.10 % ($Br_{Theoretical}$ = 32.53 %).

IR: $\bar{\nu}$ (cm^{-1}) = wide band around 3 343, H-bonding with secondary amide ν_{N-H}; 2 961 and 2 919, ν_{C-H}; 1 647, $\nu_{C=O}$ (Amide I band); 1 530, ν_{C-N} and δ_{CNH} (Amide II band); 1 460, δ_{CH}; 1 363, δ_{CH} of aliphatic amines (-N-CH_2); 1 260, δ_{NH} and δ_{OCN} (Amide III band); 1 350-800, δ_{C-C} and δ_{CH}.

^{1}H-NMR ($CDCl_3$, ppm): δ = 7.40, bs, 8H, H_i; 3.34, t, 16H, H_h, $^3J_{hg}$ = 5.80 Hz; 2.50, bs, 24H, H_e and H_f; 2.45, bs, 12H, H_b and H_c; 1.95, ss, 48H, H_j; 1.70, t, 16H, H_g, $^3J_{gh}$ = 6.30 Hz; 1.64, bs, 8H, H_d; 1.43, bs, 4H, H_a.

^{13}C-NMR ($CDCl_3$, ppm): δ = 170.9, C_9; 52.4, C_{10}; 50.9, C_2, C_3, C_5 and C_6; 38, C_8; 31.5, C_{11}; 25.2, C_1, C_4 and C_7.

6.2.2. Synthesis of the alcohol-based multifunctional ATRP initiators with 5 and 8 functional groups

The xylitol-based multifunctional initiator with 5 functionalised groups MuI-ester-5 was synthesised as described below (Scheme 6.3) using methods adapted from Shemper *et al.* (2002) and Lecolley *et al.* (2003). The MuI-ester-8 was synthesised using the same procedure (Scheme 6.4). In this last case, the equivalences used were higher than the one used for MuI-ester-5 (Table 6.2).

Scheme 6.3: Synthesis of MuI-ester-5

Scheme 6.4: Synthesis of MuI-ester-8

Xylitol (1.0 g, 6.57 mmol, 1 eq) and DMAP (6.4 g, 52.40 mmol, 8 eq) were dissolved in a round bottom-flask in anhydrous DMF (20 mL) cooled to 0 °C under N_2, and 2-bromoisobutyryl bromide (6.5 mL, 52.60 mmol, 8 eq) was then added dropwise. The reaction was allowed to proceed for 1 h at 0 °C and then at room temperature for 3 h. The white precipitate formed was then filtered off, and the organic phase evaporated. The residue was dissolved in fresh dichloromethane (20 mL), and then washed with a hydrochloric acid solution (4 x 10 mL, 0.5 N), a sodium bicarbonate aqueous solution (3 x 20 mL, pH ≈ 10), and finally double distilled water (3 x 20 mL). The organic phase was dried over $MgSO_4$, filtered and the dichloromethane evaporated. A white powder was obtained in 60 % yield.

The products were characterised by IR, ^{1}H-NMR and ^{13}C-NMR, and results obtained are presented below (key as above).

Characterisation of the xylitol-based multifunctional initiator MuI-ester-5

Yield: 60 %.

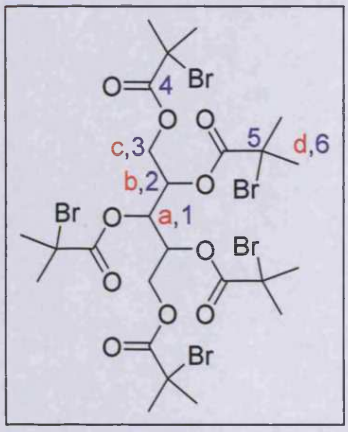

IR: $\bar{\nu}$ (cm^{-1}) = 2 966 and 2 900, ν_{C-H}; 1 741, $\nu_{C=O}$; 1 451 and 1 390, δ_{CH}; 1 259, ν_{C-O}; 1 350-800, δ_{C-C} and δ_{CH}.

^{1}H-NMR ($CDCl_3$, ppm): δ = 5.68, m, 1H, H_a, $^3J_{ab}$= 5.250 Hz; 5.46, m, 2H, H_b, $^3J_{ba}$= 5.650 Hz, $^3J_{bc}$= 3.225 Hz; 4.51- 4.21, doublet of quadruplet, 4H, H_c, $^3J_{bc}$= 3.000 Hz; 1.88, ss, 30H, H_d.

^{13}C-NMR ($CDCl_3$, ppm): δ = 170.5, C_4; 70.9, C_1; 69.9, C_2; 62.6, C_3; 55.1, C_5; 30.5, C_6.

Characterisation of the tripentaerythritol-based multifunctional initiator MuI-ester-8

Yield: 40 %.

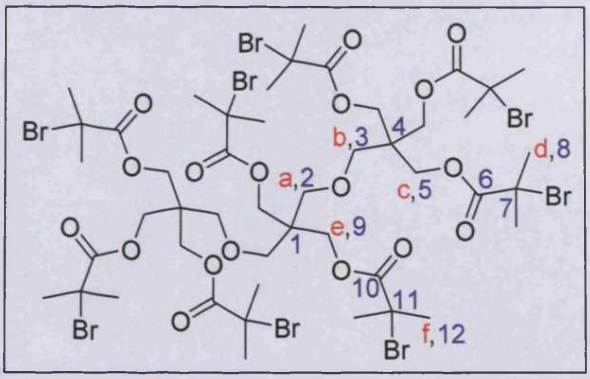

IR: $\bar{\nu}$ (cm^{-1}) = 2 971 and 2 901, ν_{C-H}; 1 735, $\nu_{C=O}$; 1 392, δ_{CH}; 1 268, ν_{C-O}; 1 350-800, δ_{C-C} and δ_{CH}.

^{1}H-NMR ($CDCl_3$, ppm): δ = 4.26, s, 16H, H_c and H_e; 3.55, bs, 8H, H_a and H_b; 1.94, s, 48H, H_f and H_d.

^{13}C-NMR ($CDCl_3$, ppm): δ = 169.9, C_{10} and C_6; 69.0, C_2; 68.0, C_3; 63.0, C_9; 62.5, C_5; 55.0, C_{11}; 54.0, C_7; 44.0, C_1; 43.0, C_4; 30.0, C_8 and C_{12}.

6.2.3. Synthesis of DMAEM star polymers by ATRP and studies on polymerisation kinetics

To synthesise the DMAEM star polymers, DMAEM was polymerised by ATRP initiated using the multifunctional initiators prepared above (DAB dendrimer- or alcohol-based cores bearing 4, 5 and 8 initiating moieties). The Cu(I)Br/HMTETA complex was used as catalyst (Scheme 6.5). The molar ratio ([I]/[M]) of the initiating moiety to monomer was varied from 1.0 % to 2.0 %, while the catalyst to monomer molar ratio ([Cat]/[M]) and the ligand to monomer molar ratio ([Lig]/[M]) were fixed either at 1.0 % or at 1.6 %. Table 6.3 summarises the reaction conditions for each ATRP experiment. All the syntheses were carried out using the reaction procedure described in detail below for the synthesis of the 5-arm DMAEM star polymer P 83 (Table 6.3).

Synthesis of the 5-arm DMAEM star polymer P 83 (Scheme 6.5, Table 6.3)

DMAEM (3.0 mL, 17.75 mmol), Cu(I)Br (41.2 mg, 278.00 µmol, [Cu(I)Br]/[DMAEM] = 1.6 %) and HMTETA (77.5 µL, 285.00 µmol, [HMTETA]/[DMAEM] = 1.6 %) were mixed in a round bottom-flask with a magnetic stirrer and purged with N_2 for 40 min. MuI-ester-5 (64.0 mg, 71.30 µmol, [I]/[M] = 2.0 %) was dissolved in DMF (3 mL) in a conical bottom flask and purged with N_2 for 40 min. At the end of the purge the initiator solution was carefully added using a N_2-purged syringe. The flask was then immediately placed at 60 °C in an oil-bath. Samples of the reaction mixture (0.1 mL) were carefully taken at different times throughout the reaction using a N_2-purged syringe. They were immediately frozen in liquid nitrogen to quickly stop the reaction, and later analysed by ^{1}H-NMR and GPC to determine the conversion and M_n. At the end of the reaction (24.5 h), the mixture was cooled to room temperature, and 20 mL of double distilled water was added. The polymer was then purified from unreacted monomer, residual catalyst and ligand, and solvent, by extensive dialysis (molecular weight cut-off 2 000 g.mol^{-1}) against double

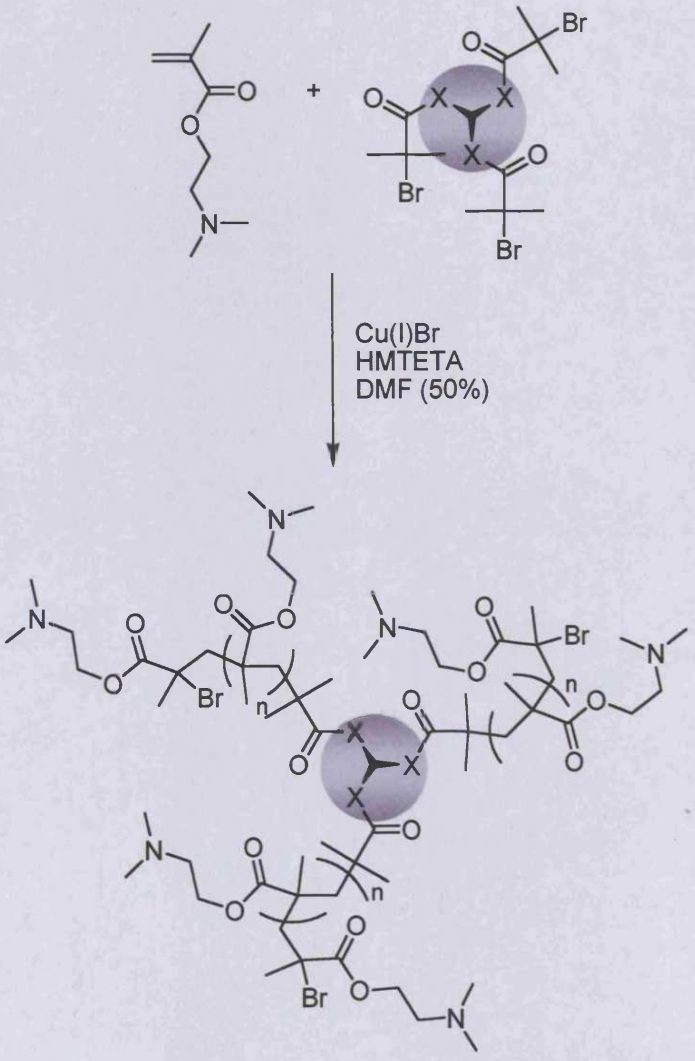

Scheme 6.5: Synthesis of DMAEM star polymers using ATRP and multifunctional initiators

Where X is either NH for DAB dendrimers-based multifunctional initiators (4 or 8 functional groups) or O for the alcohol-based multifunctional initiators (5 or 8 functional groups).

Table 6.3: Reaction conditions used for the synthesis of the DMAEM star polymers by ATRP using multifunctional initiators (MuI)

Identification	Multifunctional Initiator (MuI)	[MuI]/[M] (%)	[I]/[M] (%)	[Cat]/[M] (%)	[Lig]/[M] (%)	Time (h)
P 80	*MuI-ester-5*	0.2000	1.0	1.0	1.0	3.17
P 81	"	0.3000	1.5	1.0	1.0	5.00
P 82	"	0.4000	2.0	1.0	1.0	5.00
P 83	"	0.4000	2.0	1.6	1.6	24.50
P 84	MuI-ester-8	0.1250	1.0	1.0	1.0	3.17
P 85	"	0.1875	1.5	1.0	1.0	5.00
P 86	"	0.2500	2.0	1.0	1.0	4.50
P 87	"	0.2500	2.0	1.6	1.6	20.00
P 88	MuI-DAB-4	0.2500	1.0	1.0	1.0	29.00
P 89	"	0.3750	1.5	1.0	1.0	24.50
P 90	"	0.5000	2.0	1.0	1.0	22.00
P 91	"	0.5000	2.0	1.6	1.6	4.00
P 92	"	0.5000	2.0	1.6	1.6	51.00
P 93	MuI-DAB-8	0.1250	1.0	1.0	1.0	29.00
P 94	"	0.1875	1.5	1.0	1.0	24.50
P 95	"	0.2500	2.0	1.0	1.0	22.00
P 96	"	0.2500	2.0	1.6	1.6	4.00
P 97	"	0.2500	2.0	1.6	1.6	51.00

All reactions were carried out in DMF at 60 °C and catalysed by Cu(I)Br/HMTETA complex.

distilled water for 48 h. The aqueous polymer solution was then lyophilised for 2 days to yield white solid.

All the DMAEM star polymers were characterised by ^{1}H-NMR, ^{13}C-NMR and GPC. The key is the same as given above.

Characterisation of the DMAEM star polymer samples P 80-P 97 (Table 6.3)

^{1}H-NMR ($CDCl_3$, ppm): δ = 0.7 to 2.1, broad peaks, 5H, H_a and H_b; 2.2, bs, 6H, H_e; 2.6, bs, 2H, H_d; 4.1, bs, 2H, H_c.

^{13}C-NMR ($CDCl_3$, ppm): δ = 15, C_3; 17, C_1; 44, C_2; 45, C_7; 56, C_6; 62, C_5; 175, C_4.

GPC (THF, flow rate 1 mL/min, column calibrated with narrow PS standards): M_n ranging from 13 420 to 84 620 g.mol^{-1}, and M_w/M_n from 1.24 to 1.94.

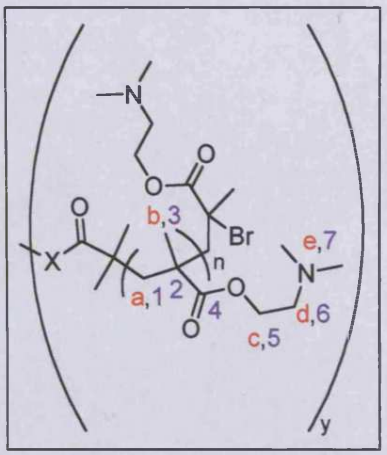

With X being either O (alcohol-based initiators) or NH (DAB dendrimer-based initiators) and y is 4, 5 or 8.

6.2.4. Chain extension reactions of DMAEM star polymers

Using previously synthesised DMAEM star polymers as macroinitiators (P 80 and P 84), chain extension reactions were conducted with a new batch of DMAEM and ATRP. The Cu(I)Br/HMTETA complex was again used as a catalyst (Scheme 6.6). The chain extension reaction of the 5-arm macroinitiators P 80 is described in detail below. The same procedure was applied for the chain extension of the 8-arm star PDMAEM P 84. The conditions of the chain extension reactions are summarised in Table 6.4.

Synthesis of the chain extended 5-arm DMAEM star polymer P 98 (Scheme 6.6. Table 6.4)

DMAEM (1.3 mL, 7.69 mmol), Cu(I)Br (11.0 mg, 76.70 μmol, [Cu(I)Br]/[DMAEM] = 1 %) and HMTETA (21.0 μL, 77.00 μmol, [HMTETA]/[DMAEM] = 1 %) were mixed in a round bottom-flask with a magnetic stirrer and purged with N_2 for 40 min. MaI-PDMAEM-5 P 80 (800.0 mg, M_w = 52 000 g.mol^{-1}, 15.40 μmol of macroinitiator, 77.00 μmol of initiating units, [MaI]/[M] = 1 %) was dissolved in DMF (1.3 mL) in a conical bottom flask and purged with N_2 for 40 min. At the end of

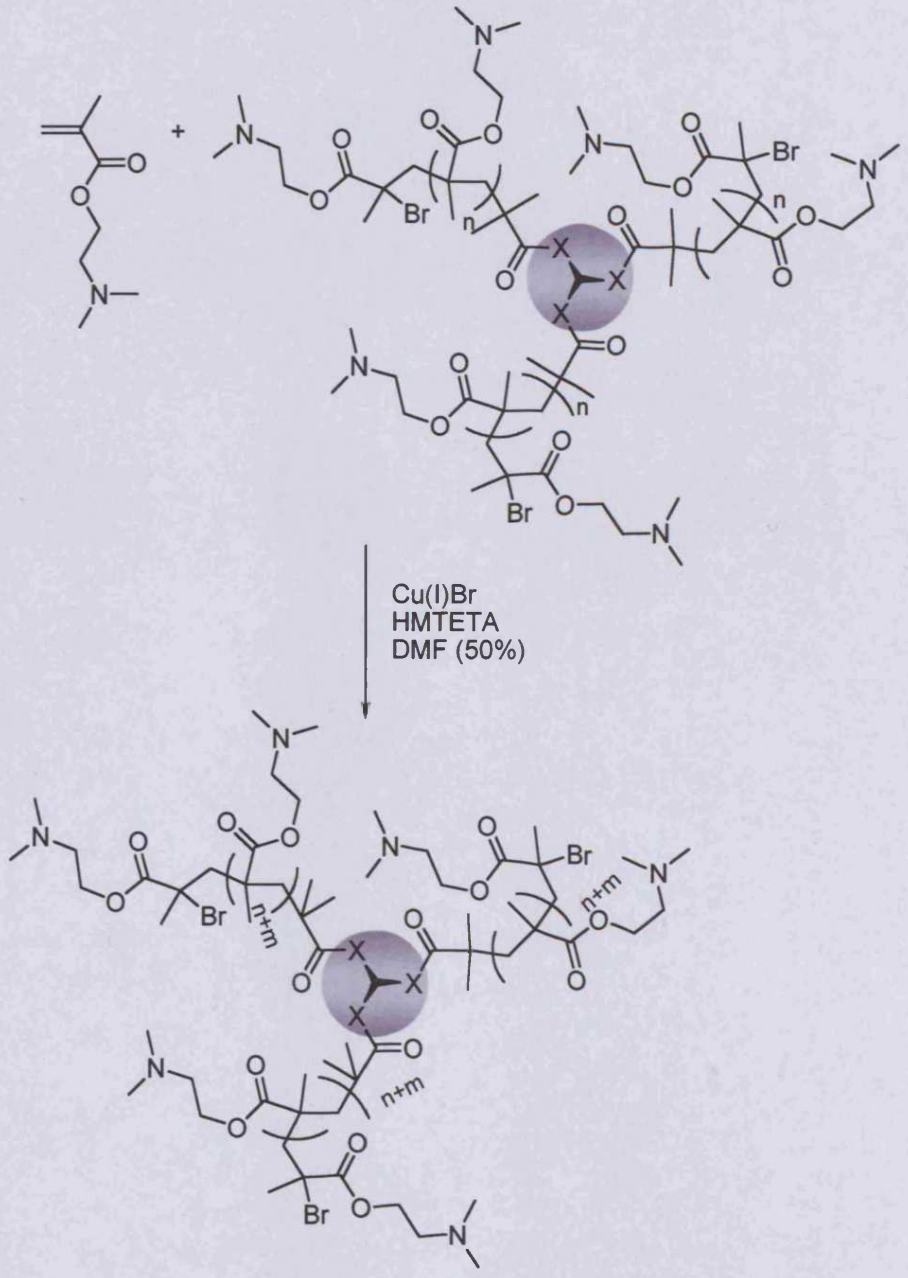

Scheme 6.6: Chain extension reaction of the DMAEM star polymers by ATRP

With X = NH for DAB dendrimers-based macroinitiators (4 or 8 arms) or X = O for the alcohol-based macroinitiators (5 or 8 arms).

Table 6.4: Reaction conditions used for chain extension of DMAEM star polymers by ATRP

Polymer	Identification of MaI used	M_n of MaI used ($g.mol^{-1}$)[c]	M_w/M_n of MaI used[c]	DMAEM (mL)	[MaI]/[M] (%)	Time (h)
P 98	P 80[a]	48 120	1.24	1.3	1	48
P 99	P 84[b]	84 620	1.38	1.2	1	48

All reactions were carried out at 60 °C in DMF (50 v/v %), and were catalysed by Cu(I)Br/HMTETA complex ([Cat]/[M] = 1 %; [Lig]/[M] = 1 % and [I]/[M] = 1 %); [a]: MaI-PDMAEM-5; [b]: MaI-PDMAEM-8; [c]: Determined by GPC, mobile phase THF, flow rate 1 mL/min, column calibrated with narrow PS standards.

the purge, the initiator solution was carefully added to the rest of the reagents, using a N_2-purged syringe and the flask was immediately placed at 60 °C in an oil-bath. At the end of the reaction (48 h), the mixture was cooled to room temperature and double distilled water (20 mL) was added. The polymer was then purified from unreacted monomer, residual catalyst, ligand, and solvent, by extensive dialysis (molecular weight cut-off 2 000 $g.mol^{-1}$) against double distilled water for 48 h. The aqueous polymer solution was finally lyophilised for 2 days to yield a white solid. Polymers were analysed by ^1H-, ^{13}C-NMR and GPC, and the results obtained are summarised below (key as above).

Characterisation of the chain extended DMAEM star polymer samples P 98-P 99 (Table 6.4)

^1H-NMR ($CDCl_3$, ppm): δ = 0.7 to 2.1, broad peaks, 5H, H_a and H_b; 2.2, bs, 6H, H_e; 2.6, bs, 2H, H_d; 4.1, bs, 2H, H_c.

^{13}C-NMR ($CDCl_3$, ppm): δ = 15, C_3; 17, C_1; 44, C_2; 45, C_7; 56, C_6; 62, C_5; 175, C_4.

GPC (THF, flow rate 1 mL/min, column calibrated with narrow PS standards): M_n ranging from 48 500 to 85 000 $g.mol^{-1}$, and M_w/M_n from 1.25 to 1.40.

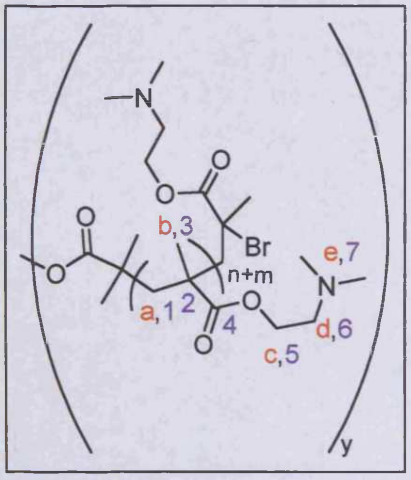

With y being either 5 or 8

6.2.5. Hydrolysis of the alcohol-based DMAEM star polymers

To study the degradation of the alcohol-based DMAEM star polymers, they were dissolved in 10 mL of THF (P 80, 160 mg, 5-arm or P 84, 265 mg, 8-arm) under nitrogen. Ethanol (3.6 mL) and an aqueous solution of KOH (18 M, 0.8 mL) were then added. The mixture was left for 48 h refluxing under nitrogen at 60°C. The solution was then concentrated using a rotavapor and neutralised with a concentrated HCl solution. The polymers (P 101 and P 102) obtained from the hydrolysis of P 80 or P 84, respectively were then recovered and purified by extensive dialysis against double distilled water and freeze-dried for 2 days to yield a white powder. These polymers were then characterised by GPC (THF, flow rate 1 mL/min, column

calibrated with narrow PS standards). The M_n were ranging from 12 920 to 13 300 $g.mol^{-1}$, and M_w/M_n from 1.21 to 1.37.

6.3. Results

Four multifunctional cores were successfully synthesised in good yield (ranging from 40 to 85 %, Table 6.2). All their composition and purity were confirmed by ^1H- and ^{13}C-NMR. EA of MuI-DAB-4 and MuI-DAB-8 showed up to 13 % errors between the experimental and theoretical values (up to 13 % errors for the MuI-DAB-4, and up to 10 % errors for the MuI-DAB-8). Even though, they all were used to polymerise DMAEM by ATRP.

The theoretical number-average molecular weight of the star polymers was determined using Equations 6.1 or 6.2, based on Equation 5.4 introduced in Chapter 5.

$$M_{n,theoretical} = \left(\frac{Conversion \times [M]_0}{[MuI]_0} \right) \times MW_{Monomer} + MW_{MuI} \quad \text{(Eq.6.1)}$$

Where: Molecular $weight_{MuI\text{-}ester\text{-}5}$ = 897.1 $g.mol^{-1}$; Molecular $weight_{MuI\text{-}ester\text{-}8}$ = 1564.3 $g.mol^{-1}$ Molecular $weight_{MuI\text{-}DAB\text{-}4}$ = 912.5 $g.mol^{-1}$; Molecular $weight_{MuI\text{-}DAB\text{-}8}$ = 1965.2 $g.mol^{-1}$.

$$M_{n,theoretical} = f \times \left(\frac{Conversion \times [M]_0}{[I]_0} \right) \times MW_{Monomer} + MW_{MuI} \quad \text{(Eq.6.2)}$$

Where f is the functionality of the multifunctional initiator (in our case f can be equal to 4, 5 or 8) and I is the initiating moiety with $[I] = f[MuI]$.

Tables 6.5 and 6.6 summarise the theoretical and actual values obtained for the star polymers synthesised in these studies (after extensive dialysis with ddH_2O of the product at the end of the reaction). The relationship between the conversion with time, and both M_n (both theoretical and experimental before dialysis of the product) and M_w/M_n with conversion of two typical experiments (P 82 and P 84) are shown in Figures 6.3 to 6.4.

It can be seen that the experimental values obtained for the M_n of the star polymers initiated with alcohol-based multifunctional initiators (P 80 to P 87) and after purification by dialysis, ranged from 84 620 to 18 495 $g.mol^{-1}$ (Table 6.5). These values were in agreement with those expected, even though they remained lower than

Table 6.5: Summary of the conversion, theoretical and experimental number-average molecular weight and polydispersity obtained for the DMAEM star polymers synthesised by ATRP and initiated by the alcohol-based multifunctional initiators MuI-ester-5 and MuI-ester-8

Identification	Initiator	Time (h)	Conversion (%)[e]	$M_{n,theoretical}$ (g.mol^{-1})[f]	$M_{n,experimental}$ (g.mol^{-1})[g]	M_w/M_n[g]
P 80[a]	MuI-ester-5	3.17	68	54 350	48 120	1.24
P 81[b]	"	5.00	66	35 480	22 500	1.26
P 82[c]	"	5.00	72	29 195	21 285	1.22
P 83[d]	"	24.5	76	30 770	18 495	1.38
P 84[a]	MuI-ester-8	3.17	72	92 120	84 620	1.38
P 85[b]	"	5.00	70	60 250	43 165	1.29
P 86[c]	"	4.50	76	49 355	33 320	1.40
P 87[d]	"	20.00	77	49 985	29 175	1.24

All reactions were carried out in DMF at 60 °C, and catalysed by Cu(I)Br/HMTETA complex. [a]: [I]/[M]= 1 %, [Cat]/[M]= 1 %, [Lig]/[M]= 1 %; [b]: [I]/[M]= 1.5 %, [Cat]/[M]= 1 %, [Lig]/[M]= 1 %; [c]: [I]/[M]= 2 %, [Cat]/[M]= 1 %, [Lig]/[M]= 1 %; [d]: [I]/[M]= 2 %, [Cat]/[M]= 1.6 %, [Lig]/[M]= 1.6 % with I being the initiating units or moieties (not the multifunctional initiator MuI); M being the monomer; Cat being the catalyst and Lig being the ligand; [e]: Determined by ^{1}H-NMR; [f]: Calculated with Eq.6.2; [g]: Determined by GPC (THF as mobile phase, 1 mL/min as flow rate and with columns calibrated with PS narrow-dispersed standards) after extensive dialysis of the final polymer at the end of the reaction.

Table 6.6: Summary of the conversion, theoretical and experimental number-average molecular weight and polydispersity obtained for the DMAEM star polymers synthesised by ATRP and initiated by the DAB dendrimer-based multifunctional initiators MuI-DAB-4 and MuI-DAB-8

Identification	Initiator	Time (h)	Conversion (%)[e]	$M_{n,theoretical}$ (g.mol^{-1})[f]	$M_{n,experimental}$ (g.mol^{-1})[g]	M_w/M_n[g]
P 88[a]	MuI-DAB-4	29.00	23	15 000	40 440	1.55
P 89[b]	"	24.50	58	25 230	50 700	1.80
P 90[c]	"	22.00	41	13 800	33 585	1.64
P 91[d]	"	4.00	40	13 490	44 320	1.85
P 92[d]	"	51.00	9	3 740	33 775	1.52
P 93[a]	MuI-DAB-8	29.00	9	13 000	13 420	1.84
P 94[b]	"	24.50	26	23 765	30 180	1.73
P 95[c]	"	22.00	60	39 700	32 865	1.94
P 96[d]	"	4.00	54	35 920	60 460	1.87
P 97[d]	"	51.00	9	7 625	33 330	1.61

All reactions carried out in DMF at 60 °C, and catalysed by Cu(I)Br/HMTETA complex. [a]: [I]/[M]= 1 %, [Cat]/[M]= 1 %, [Lig]/[M]= 1 %; [b]: [I]/[M]= 1.5 %, [Cat]/[M]= 1 %, [Lig]/[M]= 1 %; [c]: [I]/[M]= 2 %, [Cat]/[M]= 1 %, [Lig]/[M]= 1 %; [d]: [I]/[M]= 2 %, [Cat]/[M]= 1.6 %, [Lig]/[M]= 1.6 % with I being the initiating units or moieties (not the multifunctional initiator MuI); M being the monomer; Cat being the catalyst and Lig being the ligand; [e]: Determined by ^{1}H-NMR; [f]: Calculated with Eq.6.2; [g]: Determined by GPC (THF as mobile phase, 1 mL/min as flow rate and with columns calibrated with PS narrow-dispersed standards) after extensive dialysis of the final polymer at the end of the reaction.

(a)

(b)

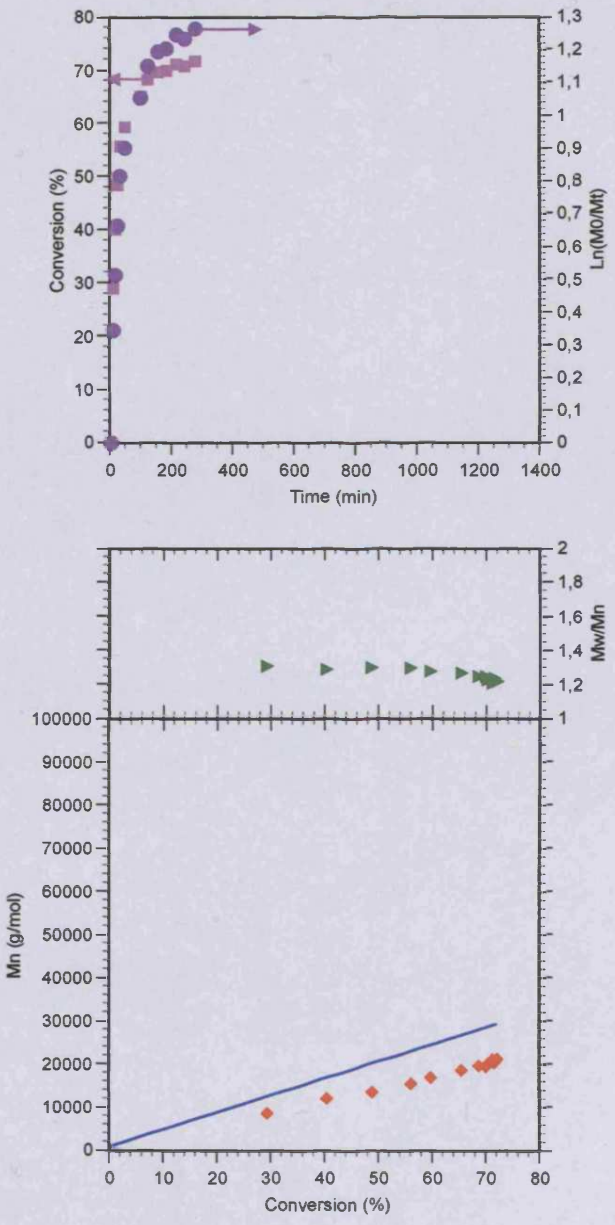

Figure 6.3*: Kinetic plots of the synthesis for the DMAEM-based star polymer initiated by MuI-ester-5 P 82, with [I]/[M] = 2 %, [Cat]/[M] = 1 %, [Lig]/[M] = 1 %

Panel (a) shows the evolution of conversion (■) and $Ln(M_0/M_t)$ (●) with time (min); Panel (b) shows the theoretical (—) and experimental (◆) number-average molecular weight and polydispersity (▶) against conversion (%).

*: The experimental M_n used for plotting part (b) of this Figure are the one measured during the experiment before dialysis of the final product, and thus does not correlate with figures presented in Table 6.5.

(a)

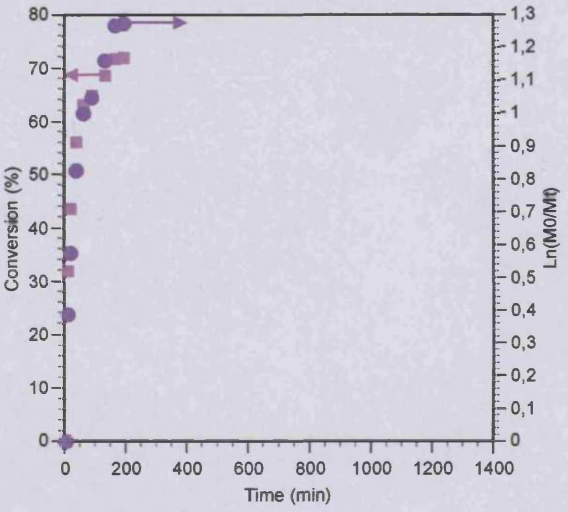

(b)

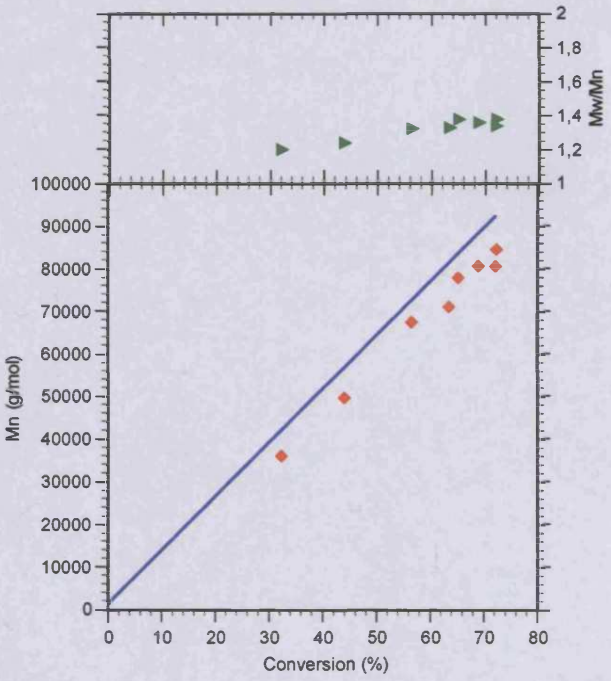

Figure 6.4*: Kinetic plots of the synthesis for the DMAEM-based star polymer initiated by MuI-ester-8 P 84, with [I]/[M] = 1 %, [Cat]/[M] = 1 %, [Lig]/[M] = 1 %

Panel (a) shows the evolution of conversion (■) and $Ln(M_0/M_t)$ (●) with time (min); Panel (b) shows the theoretical (—) and experimental (◆) number-average molecular weight and polydispersity (▶) against conversion (%).

---

*: The experimental M_n used for plotting part (b) of this Figure are the one measured during the experiment before dialysis of the final product, and thus does not correlate with figures presented in Table 6.5.

the theoretical M_n. Also, the polydispersity was never higher than 1.40, and monomer conversions reached 66 % after 5 h of reaction in general (P 80 - P 87, Table 6.5). Only in the case of P 82 (Table 6.5, MuI-ester-5 as initiator, [I]/[M] = 2 %, [Cat]/[M] = 1 %, [Lig]/[M] = 1 %) did the polydispersity decrease with conversion. In all cases, monomer conversion did not display first-order kinetics although it was shown that the experimental M_n increased linearly with conversion when the alcohol-based initiators were used (Figures 6.3 and 6.4).

In the case of reactions initiated using the DAB dendrimer-based cores (P 88 to P 97, Table 6.6), the experimental values obtained for M_n after extensive dialysis of the product against ddH_2O ranged from 60 460 to 13 420 $g.mol^{-1}$. These values were in general a lot higher than the theoretical M_n values. Moreover, polydispersity of these DMAEM star polymers was always higher than 1.52, and up to 1.94. In these experiments, monomer conversion was always lower than 60 % even after 22 h reaction (P 88 - P 97, Table 6.6) and reached a plateau at approximately 200 min, which consequently led to a plateau in the M_n and an increase in polydispersity (data not shown).

Figure 6.5 shows GPC traces obtained with time for experiment P 82 where the polymerisation was initiated by MuI-ester-5. Chromatograms followed a Gaussian bell shape, and neither tailing nor shoulder were seen with increasing the reaction time.

In a second step, the ability of the synthesised DMAEM star polymers P 80 (M_n = 48 120 $g.mol^{-1}$, M_w/M_n = 1.24, 5-arm alcohol-based star polymer of DMAEM) and P 84 (M_n = 84 620 $g.mol^{-1}$, M_w/M_n = 1.38, 8-arm alcohol-based star polymer of DMAEM) to re-initiate the polymerisation of a new batch of DMAEM monomer was studied. This was done as explained in Section 6.2.4 following Scheme 6.6. After 48 h reaction time, the obtained polymers P 98 and P 99 showed no increase in molecular weight compared to their macromolecular initiators P 80 and P 84, respectively. The experimental M_n and polydispersity were measured to be 48 500 $g.mol^{-1}$, M_w/M_n = 1.25 for P 98 and 85 000 $g.mol^{-1}$, M_w/M_n = 1.40.

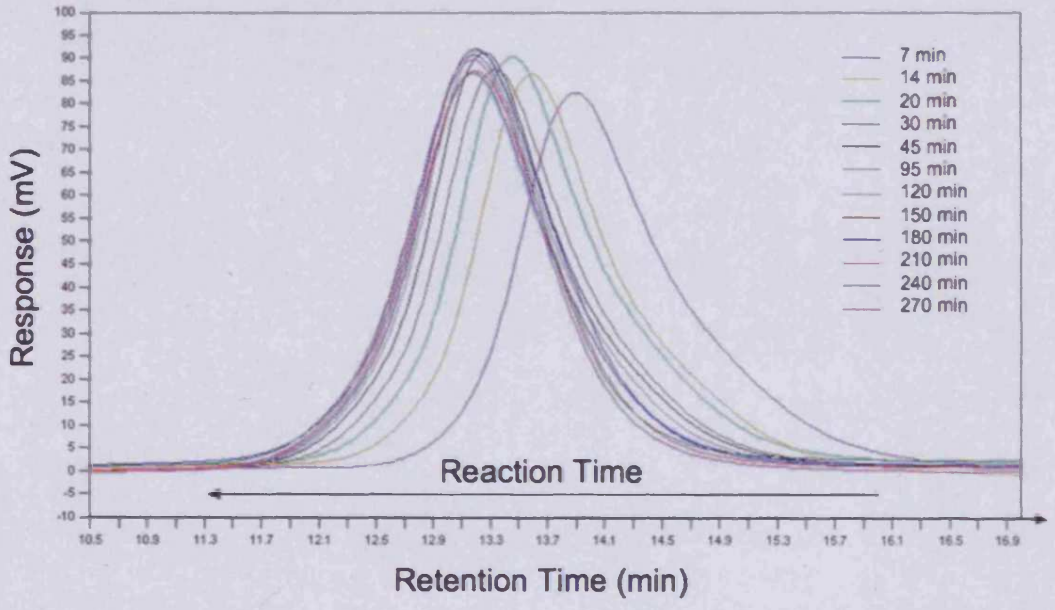

Figure 6.5: Change in molecular weight with time during the synthesis of the DMAEM-based star polymer initiated by MuI-ester-5, P 82 (Table 6.5)

Using [I]/[M] = 2 %, [Cat]/[M] = 1 %, [Lig]/[M] = 1 %.

Table 6.7: Expected and measured molecular weight characteristics of the DMAEM polymers obtained after hydrolysis of the DMAEM alcohol-based star polymers P 80 and P 84:

Polymer	$M_{n,theoritical}$ of alcohol-based DMAEM star polymer ($g.mol^{-1}$)[c]	$f_{theoritical}$	$M_{n,expected}$ of linear PDMAEM arms ($g.mol^{-1}$)[d]	$M_{n,experimental}$ of hydrolysed DMAEM-based star polymers ($g.mol^{-1}$)[c]	M_w/M_n[c]	$f_{calculated}$[e]
P 101[a]	92 120	8	11 320	12 920	1.37	7
P 102[b]	54 350	5	10 690	13 300	1.21	4

[a]: Product of the degradation of a 8-arm alcohol-based star polymer (P 84); [b]: Product of the degradation of a 5-arm alcohol-based star polymer (P 80); [c]: Determined by GPC (mobile phase THF, columns calibrated with narrow dispersed polystyrene standards); [d]: Calculated by dividing the theoretical M_n of the star polymer minus the molecular weight of the multifunctional initiator, by its functionality f (either 8 or 5 in these cases); [e]: Calculated with $f_{calculated} = (M_{n,theoretical\ of\ star} - \text{molecular weight}_{multifunctional\ initiator})/ M_{n,experimental\ arms}$.

Also, two alcohol-based star polymers (P 80 and P 84) were degraded by hydrolysis, and samples P 101 and P 102 were obtained. Table 6.7 summarises M_n and M_w/M_n determined by organic GPC in THF, before and after hydrolysis and it can be seen that the polymers P 101 and P 102 derived had a low polydispersity ($M_w/M_n \leq 1.37$). The measured molecular weight was consistent with the theoretical M_n values calculated by dividing the theoretical M_n of the DMAEM star polymer minus the molecular weight of the multifunctional initiator by its theoretical number of arms (either 8 or 5 in these cases). From the experimental results, calculated functionality values ($f_{calculated}$) of the star polymers P 80 and P 84 were estimated and it was seen that the theoretical 5-arm PDMAEM P 80 had 4 arms, while the theoretical 8-arm PDMAEM P 84 was made of 7 arms.

6.4. Discussion

The goal of this Chapter was the synthesis of DMAEM-based star polymers by ATRP using the core-first approach with multifunctional cores that could theoretically initiate ATRP.

Considering the results obtained in Chapter 5, multifunctional cores were designed and synthesised so that their initiating units or surface groups would be similar to the best linear ATRP initiator studied, namely, ethyl α-bromoisobutyrate.

The multifunctional initiators synthesised here were obtained in good yield with complete activation of the core surface groups, as confirmed by ^{1}H-NMR. Nevertheless, some errors were observed in the experimental EA of the synthesised DAB-based multifunctional initiators compared with their theoretical values, and it is thought to come from the impure DAB dendrimers commercially available used here as starting materials. For a deeper characterisation of the 4 multifunctional initiators, mass-spectra could have been used in order to confirm their composition and purity.

Of the 4 multifunctional initiators synthesised, the 2 ester-based ones proved their ability to initiate and sustain good ATRP properties using the conditions optimised in Chapter 5.

The library of DMAEM-based star polymers synthesised showed that the alcohol-based initiators were better ATRP initiators than DAB dendrimer-based cores. For the latter, there was a loss of activating species with time as conversion never displayed 1st order kinetics. There was a plateau in the experimental M_n and an increase in polydispersity with conversion (always higher than 1.50, which is considered too

high for an ATRP process as reviewed by Matyjaszewski and Xia (2001)). Even though no tailing or shoulder were observed in the GPC chromatograms, these observations suggest the existence in non negligible amount of:

- terminating reactions
- and/or transfer reactions,
- and/or contamination of the catalytic system that could happen through sampling of the reactions.

When these processes occur, the rate of polymerisation decreases and leads to "dead" polymers not able to reinitiate polymerisation. Also, the high experimental M_n in comparison with that expected theoretically, and the high polydispersity observed demonstrated the slow initiation ability of the synthesised DAB dendrimer-based initiators.

These results are not surprising as it is known that amide and amine groups strongly complex transition metals (reviewed by Matyjaszewski and Xia (2001)). It was previously concluded that the inactivation of the catalyst by complexation of copper with the amide groups (on monomers or like in our case on the initiators) and displacement of the terminal halogen atom by the amide groups are two side reactions occurring (Teodorescu and Matyjaszewski 1999 and 2000), leading to the loss of ATRP process, and uncontrolled FRP in our cases.

In the case of the alcohol-based initiators, although conversion did not display 1st order kinetics with time, M_n increased linearly with conversion and corroborated the expected M_n. Also, polydispersity either decreased or stayed in the acceptable range for ATRP polymerisation (reviewed by Matyjaszewski and Xia (2001)) (i.e. $\leq$ 1.50). As no tailing and shoulder were observed in the GPC chromatograms for these experiments, it was concluded that termination and/or transfer reactions were only occurring in negligible amounts, giving control over molecular weight and polydispersity. The small discrepancy observed in the theoretical and experimental M_n might be explained by errors in the GPC method used to determine the molecular weight characteristics of the star polymers. The GPC system used was calibrated with linear PS standards, which display a random coil conformation in comparison to the more globular 3-dimensional conformation of the star polymers. Therefore, the hydrodynamic volume of the synthesised DMAEM alcohol-based star polymers

would be expected to be lower than the linear PS standards used thus, leading to analytical errors.

It was thus concluded that the synthesised alcohol-based cores were efficient initiators for the ATRP of DMAEM, and that when used with the Cu(I)Br/HMTETA catalyst system in DMF at 60 °C were able to enable the synthesis of star polymers with predictable molecular weight and low polydispersity. These synthesised multifunctional alcohol-based initiators also showed better ATRP kinetic characteristics than the monofunctional ethyl α-bromoisobutyrate previously used in Chapter 5.

To verify the living character of the ATRP reactions, chain extension reactions of the DMAEM star polymers P 80 and P 84 were conducted as described in Scheme 6.6. However, no increase in molecular weight was observed.
As explained in Chapter 5, it is believed that the terminal bromine groups were displaced by substitution reaction with the tertiary amines of the pendant groups of the PDMAEM synthesised (Teodorescu and Matyjaszewski 1999, 2000 and reviewed by Matyjaszewski and Xia (2001)), leading to their quaternization, and the loss of the bromine-based initiating units needed for the subsequent chain extension attempted.

Hydrolysis of DMAEM alcohol-based star polymers was then conducted hoping to cleave the arms from the core. It should be noted that the procedure employed will not only cleave the linear arms from the core, but also hydrolyse the pendant groups of the repeating units on the backbone, theoretically leading to the isolation of linear poly(methacrylic acid). Scheme 6.7 represents the procedure of the degradation.
The main reason for this hydrolysis experiment was to prove that the synthesised star polymers could be biodegradable from their core when used in biological applications. As the resulting polymers were characterised by GPC in organic mobile phase, the variation in the chemical composition from DMAEM to methacrylic acid repeating units, was believed not to influence importantly the molecular weight information outcome. To be more precise, if molecular weight characterisation were done in an aqueous mobile phase, an important change in the hydrodynamic volume from the linear PDMAEM (bearing tertiary amino groups along the backbone) to

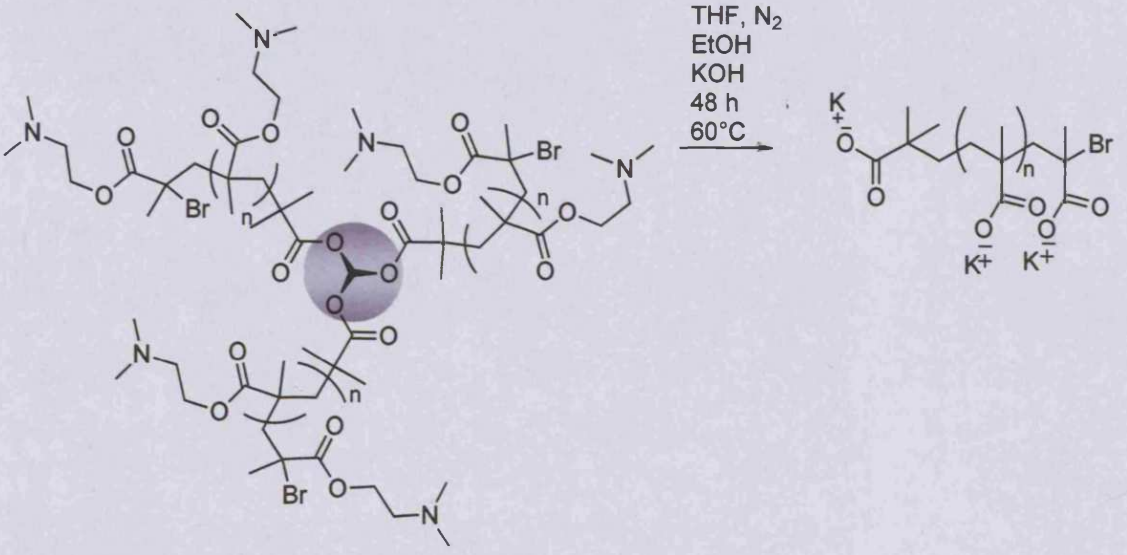

Scheme 6.7: Theoretical representation of the cleavage of the alcohol-based DMAEM star polymers (either 5 or 8 arms) through their ester bonds (of the core but also in the pendant groups of the repeating units)

linear poly(methacrylic acid) (bearing carboxylic acid groups along the polymer chain) was expected to be observed, not allowing the interpretation of the data. As here it was done in THF, and bearing this chemical change in mind, the molecular weight and the molecular weight distribution of the linear arms could be related to the composition and regularity of the star polymers. It was important to verify whether each alkyl halide fragments of the multifunctional initiator had participated equally in the ATRP process and whether the synthesised star polymer arms indeed had a low polydispersity. Use of biodegradable cores has been widely employed (Angot *et al.* 1998; Deng and Chen 2004; Zhao *et al.* 2005).

It is also important to mention that degradation conditions used here (Scheme 6.7) do not correspond to biodegradation that would happen in the body. The mechanism is based on a basic hydrolysis (pH > 7.4), to enable a full and rapid cleavage of the arms from the core. Nevertheless, it is believed that acidic hydrolysis of the ester bonds in intracellular compartments (where pHs can drop down to ~ 4.5) could permit the slow release of the arms of a high molecular-weight star-shaped carrier. If so, this would allow excretion via the porous glomerular membrane of the kidneys of initially star-shaped polymers with high molecular weight ($M_w \geq 40\,000$ g.mol^{-1}).

The calculated functionality of the star polymers (f) was determined to be smaller than the theoretical value (one unit smaller). Several explanations could be drawn from these figures, but the more probable one is coming from the changes occurring in the polymer after hydrolysis not only from the core (architectural change) but also along the main chain of the poly(ester) PDMAEM (chemical change), leading to errors in the calculation of star functionality.

6.5. Conclusions

In conclusion, using the core-first approach and ATRP, a library of DMAEM star polymers was synthesised. Four multifunctional initiators with 4, 5 or 8 initiating sites were synthesised, and the initiators used gave polymers that would be potentially biostable or biodegradable.

Full characterisation of the synthesised polymers here, by NMR, AFM, MALTI-TOF, SANS, etc should be done deeper for complete illustration of the synthesis of star-based polymers. It is believed that star-based polymers were synthesised with the

MuI-ester-4 and MuI-ester-8 compounds due to the good kinetics and GPC chromatograms profiles.

As expected, the alcohol-based multifunctional initiators were much more efficient for initiating and sustaining good CRP characteristics than their DAB dendrimer-based homologues (as amide groups are known to deactivate and generate the loss of control of ATRP process). They were also better than the linear homologue ethyl α-bromoisobutyrate described in Chapter 5.

Here hydrolysis was used was to cleave the arms from the core of the alcohol-based star polymers, and this procedure showed promise although the design of the experiment should always be carefully designed to enable data interpretation.

Nevertheless, the ATRP procedure used could be still further optimised for the design of more complex polymeric star structures with more than one type of monomer (either statistical or block copolymers).

In Chapter 7, several water-soluble polymers obtained by CTA-based FRP (Chapter 4), linear-based ATRP (Chapter 5) and star-based ATRP (Chapter 6) were selected and effects of molecular parameters, such as molecular weight, architecture, charge density, and amine substitution degree on cytotoxicity were studied.

7

Evaluation of *in vitro* Cytotoxicity of Polycations in B16F10 Cells: Effect of Charge Density, Molecular Weight, Polymerisation Technique, Architecture, Number of Arms and Core Chemistry

7.1. Introduction

In vitro cytotoxicity was assessed as a preliminary indicator of the potential of some of the polymers synthesised in these studies for further development as polymer therapeutics. Polymers designed for biomedical uses must be "biocompatible". The term **biocompatibility** has been defined (Guelcher and Hollinger 2005) as "the ability of a material to perform with an appropriate host response in a specific application". This means that biocompatibility is typically defined in terms of performance in relation to a specific application (Guelcher and Hollinger 2005). For drug delivery applications, two initial screening tests of biocompatibility have been widely used. The use of (i) *in vitro* cytotoxicity tests (Sgouras and Duncan 1990) and also (ii) blood-compatibility tests (e.g. by studying haemolytic activity and complement activation) (Sgouras and Duncan 1990; Duncan *et al.* 1991). These tests are useful as a first screen if the compounds are to be injected intravenously as drug delivery systems (reviewed by Duncan and Izzo (2005)).
In these tests, dextran has been usually used as a negative control, and PEI or PLL as positive reference controls. As already mentioned, PEG, PHPMA and PGA are water-soluble polymeric carrier the most widely tested clinically (reviewed by Duncan and Izzo (2005)). They show good biocompatibility in such assays.

Over the last decade, several groups have investigated the *in vitro* cytotoxicity and blood-compatibility of neutral polymers, polyanions and polycations. For example, the cytotoxicity of PEI (Fischer *et al.* 1999; Fischer *et al.* 2003; Kunath *et al.* 2003) (reviewed by Kircheis *et al.* (2001) and Neu *et al.* (2005)), polylysine (Morgan *et al.* 1988; Morgan *et al.* 1989; Choksakulnimitr *et al.* 1995; Brazeau *et al.* 1998; Fischer *et al.* 2003) (PLL), polyarginine (Morgan *et al.* 1988; Morgan *et al.* 1989), polyornithine (Morgan *et al.* 1988; Morgan *et al.* 1989), protamine (Morgan *et al.* 1988; Choksakulnimitr *et al.* 1995), polyhistine (Morgan *et al.* 1988), chitosans (Richardson *et al.* 1999; Kean *et al.* 2005), polyglutamic acid (Singh *et al.* 1992; Dekie *et al.* 2000), polyaspartic acid (Singh *et al.* 1992), polybrene (Singh *et al.* 1992), poly(vinylpyrrolidone bromide) (Fischer *et al.* 2003), and dextran sulfate (Choksakulnimitr *et al.* 1995), as well as PAMAM dendrimer (Roberts *et al.* 1996; Brazeau *et al.* 1998; Malik *et al.* 2000; El Sayed *et al.* 2002; Fischer *et al.* 2003; Jevprasesphant *et al.* 2003) and DAB dendrimer with either diaminobutane (Malik *et*

al. 2000; Zinselmeyer *et al.* 2002) or diaminoethane (Malik *et al.* 2000) (DAE) as core; was studied in relation to the effect of molecular weight and size (dendrimer generation), hydrophilic/hydrophobic balance, the type and density of charges, the overall chemical structure and the nature of the surface functional groups, and dendrimer conformation and flexibility (reviewed by Boas and Heegaard (2004), Wang *et al.* (2004b) and Duncan and Izzo (2005)).

The common purpose of the previously cited studies was to better understand the mechanism of action of these materials for a more secure and efficient design of biocarriers. Nevertheless, one of the limitations of these investigations comes from the fact that polymers that are being compared differ in more than one respect. For instance, and to make it simple, comparing the *in vitro* cytotoxicity of two generations of cationic dendrimers, would not be exclusively illustrating the effect of the molecular size, as the overall number of charges is also altered with the generation.

Here, the goal of the studies was to define the structure-biological activity relationship for a library of cationic poly(methacrylate)s with the hope that this would assist the design of safer and biocompatible polymeric carriers for drug delivery/ nanomedicine applications in the future. It was intended to strictly compare the effect of molecular parameters of the polymer on the *in vitro* cytotoxicity. Factors that were investigated included the effect of molecular weight, the charge density, the chemistry (amine substitution and core chemistry), the architecture (linear and star-based polymers), the number of arms of the star-based polymers, and also the polymerisation techniques employed for the synthesis of the polymers (FRP or ATRP).

7.1.1. Positive and negative reference controls

A high molecular weight branched PEI (750 000 $g.mol^{-1}$) and dextran (from 64 000 to 76 000 $g.mol^{-1}$) were used as positive and negative controls, respectively.

PEI has been widely used for wastewater treatment applications and in the paper industry. Linear PEI is commercially available as transfection reagent (e.g. ExGen500®, jetPEI®, and reviewed by Neu *et al.* (2005)). The high molecular weight

PEI used here (Figure 7.1, (a)) is highly branched and bears an exceptionally high charge density (Fischer *et al.* 2003). This leads to greater cytotoxicity than seen for low molecular weight PEI (Fischer *et al.* 2003; Kunath *et al.* 2003), and therefore only low molecular weight PEIs (from 5 000 to 25 000 $g.mol^{-1}$) have been developed as non-viral gene delivery vectors (reviewed by Neu *et al.* (2005)). PEI interacts electrostatically with DNA. It can also interact electrostatically with the negatively charged phospholipids head groups of cell membranes inducing loss of membrane integrity (Fischer *et al.* 2003; Moghimi *et al.* 2005).

Dextran (Figure 7.1, (b)) is a complex, branched and highly water-soluble polysaccharide produced by bacteria that is composed of α-D-(1-6) polyglucose (95 %) and α-(1-3) linkages that leads to the branching. Dextran (~ 70 000 $g.mol^{-1}$) has been used for more than 50 years as a plasma expander (reviewed by Thoren (1980)). Due to its chemical inertness and its high number of hydroxyl groups, it can also be conjugated to a variety of drugs and proteins to increase stability and decrease protein immunogenicity (reviewed by Mehvar (2000)).

7.1.2. Rationale for the choice of the polymers to be tested

Sixteen polymers synthesised in Chapters 4, 5 and 6 were selected for evaluation of cytotoxicity against B16F10 cells. Their cytotoxicity was compared with PEI (as a positive reference control) and dextran (as a negative reference control). Table 7.1 summarises the characteristics of the polymers used in these studies. The library was carefully chosen so that the influence of specific molecular parameters on the cytotoxicity could be investigated and compared (as depicted in Figure 7.2):

- the molecular weight
- the charge density (homopolymers of DMAEM or AEM against copolymers of amino-based methacrylate monomers with HPMA)
- the chemistry (amine substitution: primary, tertiary or quaternary- core of stars: DAB-based or ester-based)
- the architecture (linear or star-based polymers)
- the number of arms on the star (4, 5 or 8)
- the polymerisation techniques (FRP or ATRP catalysed with Cu(I)Br)

As the polymers synthesised here may be potentially useful for future conjugation to

(a)

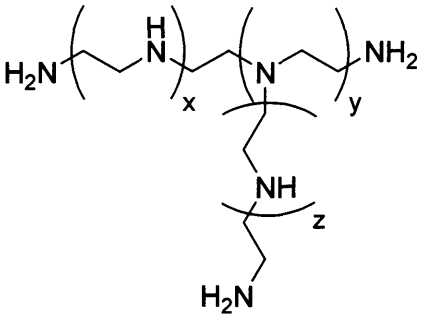

(b)

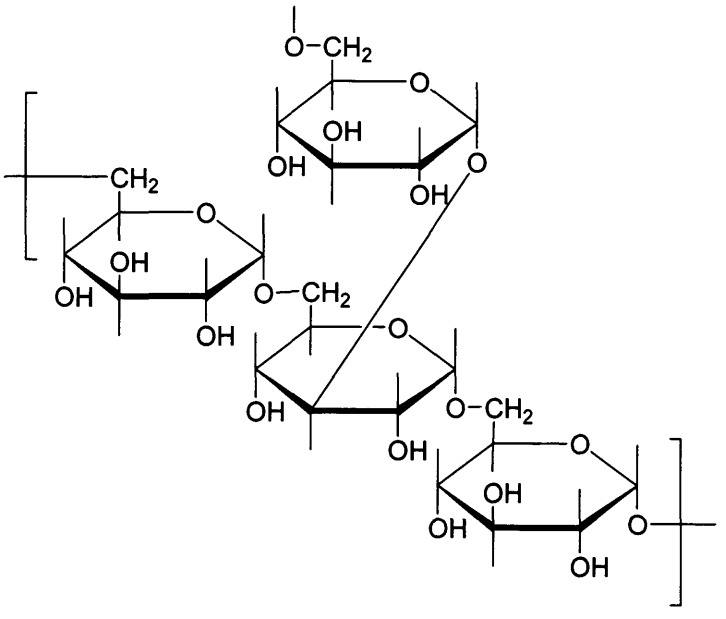

Figure 7.1: Reference polymers used for cytotoxicity tests. Panel (a) shows PEI and panel (b) dextran (taken from Mehvar (2000))

N.B: PEI has a theoretical ratio of primary to secondary to tertiary amines of 1:2:1 with a branching site every 3-3.5 nitrogen atoms.

Table 7.1: Physicochemical properties of the polycations evaluated using B16F10 cells

Polymer	Composition	Polymerisation Technique	Architecture	Core	Order of amines (°)	M_w (g.mol^{-1})	M_w/M_n
P 45	qAEM	CTA FRP	Linear	-	4	36 530	3.35
P 28	$AEM_{25}/HPMA_{75}$	CTA FRP	Linear	-	1/-	5 250	1.14
P 26	$AEM_{25}/HPMA_{75}$	CTA FRP	Linear	-	1/-	16 820	1.67
P 34	AEM	CTA FRP	Linear	-	1	15 450	1.80
P 38	$DMAEM_{25}/HPMA_{75}$	CTA FRP	Linear	-	3/-	5 360	1.80
P 36	$DMAEM_{25}/HPMA_{75}$	CTA FRP	Linear	-	3/-	19 500	2.70
P 40	DMAEM	CTA FRP	Linear	-	3	19 100	2.60
P 75	DMAEM	ATRP (linear)	Linear	-	3	8 120	1.23
P 65	DMAEM	ATRP (linear)	Linear	-	3	19 165	1.41
P 69	DMAEM	ATRP (linear)	Linear	-	3	29 675	1.68
P 68	DMAEM	ATRP (linear)	Linear	-	3	39 140	1.50
P 92	DMAEM	ATRP (star)	4-arm star	MuI-DAB-4	3	42 900	1.59
P 81	DMAEM	ATRP (star)	5-arm star	MuI-ester-5	3	24 500	1.33
P 97	DMAEM	ATRP (star)	8-arm star	MuI-DAB-8	3	40 200	1.63
P 87	DMAEM	ATRP (star)	8-arm star	MuI-ester-8	3	29 150	1.24
P 86	DMAEM	ATRP (star)	8-arm star	MuI-ester-8	3	44 620	1.28

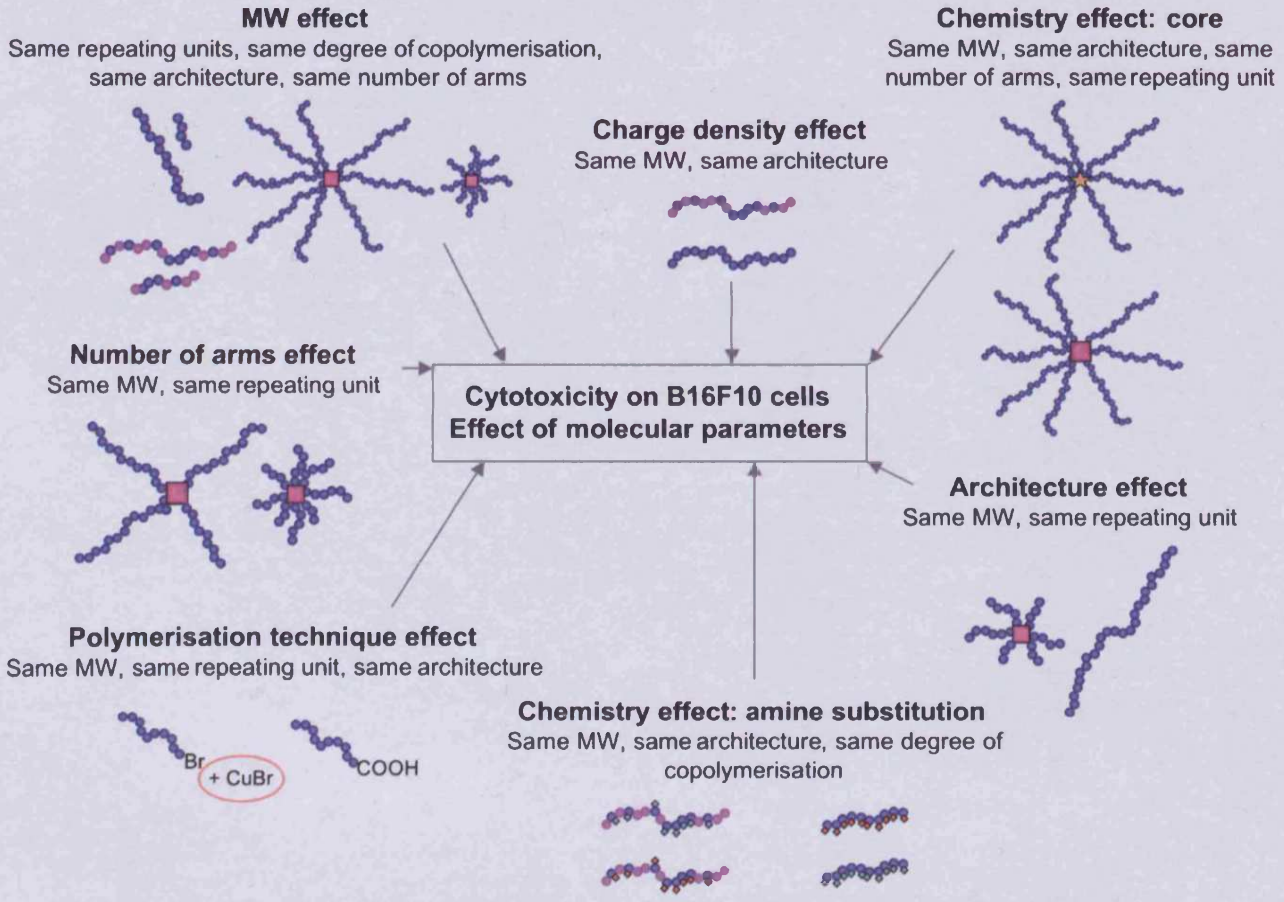

Figure 7.2: Rationale for the selection of cytotoxicity studies and choice of polymers

drugs (polymer-drug conjugates) or proteins (polymer-protein conjugates) or as gene delivery vectors (polyplexes), it was important to select polymers with a M_w lower than 40 000 $g.mol^{-1}$ when possible. It is essential that non-biodegradable polymers intravenously injected into the human body, are eventually eliminated and it is known that random coil polymers with a molecular weight greater than 40 000 $g.mol^{-1}$ are usually too bulky to pass through the kidney (Robinson *et al.* (1990) and reviewed by Duncan (2003b)).

7.1.3. Rationale for the choice of the cell line used: B16F10 cells

B16F10 murine melanoma cells were used for these studies as they have been widely used to study the cytotoxicity of novel polymers before (Malik *et al.* 2000; Wan *et al.* 2004; Duncan and Izzo 2005; Seib *et al.* 2007), to help optimise the design of polymer-drug conjugates (O'Hare *et al.* 1993; Seymour *et al.* 1994; Gianasi *et al.* 1999; Hreczuk-Hirst *et al.* 2001; Gianasi *et al.* 2002; Vicent *et al.* 2004a; Vicent *et al.* 2004b; Andersson *et al.* 2005; Veronese *et al.* 2005) and to study polymeric non-viral vectors as gene delivery systems (Fischer *et al.* 1999; Richardson *et al.* 2001; Howard *et al.* 2004; Lavignac *et al.* 2004; Wan *et al.* 2004). This permits comparison of the data obtained here with the past literature. In addition, these cells are also easy to grow, and compared to other cell lines, they have a fast doubling time (e.g. 10 h and ~ 48 h for seeding densities of $4 \cdot 10^4$ and 10^4 cells/mL, respectively).

7.1.4. Rationale for the choice of the cytotoxicity assay

Several non-radioactive methods are available to assess cytotoxicity. These include cell counting assays such as Coulter Counting® (Pruden and Winstead 1964), measurement of membrane permeability such as trypan blue exclusion (Cowan *et al.* 1984), measurement of metabolic activity using dyes such as MTT (Mosmann 1983; Sgouras and Duncan 1990) or sodium 3,3'-[1[(phenylamino)carbonyl]-3,4-tetrazolim]-*bis*-(4-methoxy-6-nitro) benzene sulfonic acid hydrate) (XTT), tetrazolium salt (Roehm *et al.* 1991), and assays that measure the release of lactate dehydrogenase (a cytosolic enzyme) LDH (Korovkin *et al.* 1963).

Here, the MTT assay was chosen to assess polymer cytotoxicity because of its rapidity, simplicity, and because it allows a quantitative screening that can easily be adapted to measure a wide range of polymer concentrations using 96-well plates

(Sgouras and Duncan 1990; Kean *et al.* 2005; Peng *et al.* 2005). It has also been widely used in our laboratory as a standardised protocol, so its use allows comparison with earlier studies. Finally, the small well volume of the plates used requires minimal amounts of polymer.

7.2. Methods

The general methods used for cell culture and the MTT assay have previously been described in Chapter 2 (Section 2.3.7, 2.3.8 and 2.3.9).

Before conducting the cytotoxicity tests, growth curves were obtained for the B16F10 cell line, at seeding densities of $4 \cdot 10^4$ cells/mL and $1 \cdot 10^4$ cells/mL. The doubling times were ~ 10 h and ~ 48 h, respectively at each seeding density (Chapter 2, Section 2.3.8; Figure 2.5). A seeding density of $1 \cdot 10^4$ cells/mL was used for these experiments. The polymers were added 24 h after subculture so cells were within their exponential growing phase. The polymer concentrations used ranged from 1 µg/mL to 10 mg/mL and cytotoxicity was assessed using a 77 h incubation time (72 h with the polymers alone and addition of MTT before a further 5 h incubation).

All cytotoxicity data are expressed as mean ± SEM. Statistical significance of $p < 0.05$ is indicated with * in the Figures. When only two groups were compared, a Student's t test for small sample size was used. If more than two groups were compared evaluation of significance was performed using one way Analysis Of Variance (ANOVA) followed by Bonferroni *post hoc* test.

In addition, the data were fitted using the Hill Equation to determine the IC_{50} values (described in Chapter 2, Section 2.3.9). IC_{50} values obtained in this way were compared with the values directly read from the graphs at 50 % of cell viability.

To enable comparison of the polycations, their **maximal charge to monomer ratio** was calculated (Tables 7.2 - 7.3, and Figure 7.5 of Section 7.3.1). It was defined as the ratio of the number of cationic charges by the molecular weight of the repeating unit of the polycation, assuming it was fully charged and without considering the counter ion. Table 7.2 summarises the chemical formula of the charged repeating unit, the polymer molecular weight, and the calculated maximal charge to monomer ratio.

Table 7.2: Chemical characteristics of the polycations used

Polycation types	Chemical formula of charged repeating unit[a];[b]	Molecular weight of the charged repeating unit ($g.mol^{-1}$)[a]	Maximal charge to monomer ratio[a]
PqAEM	$C_9H_{18}NO_2$	172.28	$5.80 \cdot 10^{-3}$
$PAEM_{25}HPMA_{75}$	$C_{27}H_{51}N_4O_8$	559.82	$1.79 \cdot 10^{-3}$
PAEM	$C_6H_{12}NO_2$	130.19	$7.68 \cdot 10^{-3}$
$PDMAEM_{25}HPMA_{75}$	$C_{29}H_{55}N_4O_8$	587.88	$1.70 \cdot 10^{-3}$
PDMAEM	$C_8H_{16}NO_2$	158.25	$6.32 \cdot 10^{-3}$

[a]: The repeating unit was considered charged and without counter ion; [b]: Where the molecular weight ($g.mol^{-1}$) equal to 12.01 for the element C, 1.01 for the element H, 14.01 for N and 16 for O.

Table 7.3: Polymer cytotoxicity in B16F10 cells expressed as IC_{50} values estimated by the Hill Equation

Polymer	Composition	Architecture	Core	Maximal charge to monomer ratio[a]	M_w (g.mol^{-1})	M_w/M_n	IC_{50} (µg.mL^{-1})[b]
P 45	qAEM	Linear[c]	NA	$5.80 \cdot 10^{-3}$	36 530	3.35	27.19 ± 13.26
P 28	$AEM_{25}/HPMA_{75}$	Linear[c]	NA	$1.79 \cdot 10^{-3}$	5 250	1.14	1872.00 ± 418.70
P 26	$AEM_{25}/HPMA_{75}$	Linear[c]	NA	$1.79 \cdot 10^{-3}$	16 820	1.67	2489.00 ± 342.50
P 34	AEM	Linear[c]	NA	$7.68 \cdot 10^{-3}$	15 450	1.80	7.39 ± 0.85
P 38	$DMAEM_{25}/HPMA_{75}$	Linear[c]	NA	$1.70 \cdot 10^{-3}$	5 360	1.80	10060.00 ± 3526.00
P 36	$DMAEM_{25}/HPMA_{75}$	Linear[c]	NA	$1.70 \cdot 10^{-3}$	19 500	2.70	600.70 ± 112.60
P 40	DMAEM	Linear[c]	NA	$6.32 \cdot 10^{-3}$	19 100	2.60	4.76 ± 1.12
P 75	DMAEM	Linear[d]	NA	$6.32 \cdot 10^{-3}$	8 120	1.23	6.04 ± 2.01
P 65	DMAEM	Linear[d]	NA	$6.32 \cdot 10^{-3}$	19 165	1.41	5.50 ± 0.73
P 69	DMAEM	Linear[d]	NA	$6.32 \cdot 10^{-3}$	29 675	1.68	4.41 ± 0.69
P 68	DMAEM	Linear[d]	NA	$6.32 \cdot 10^{-3}$	39 140	1.50	4.16 ± 0.88
P 92	DMAEM	4-arm star[e]	MuI-DAB-4	$6.32 \cdot 10^{-3}$	42 900	1.61	5.08 ± 1.42
P 81	DMAEM	5-arm star[e]	MuI-ester-5	$6.32 \cdot 10^{-3}$	24 500	1.33	2.90 ± 0.88
P 97	DMAEM	8-arm star[e]	MuI-DAB-8	$6.32 \cdot 10^{-3}$	40 200	1.52	4.72 ± 1.88
P 87	DMAEM	8-arm star[e]	MuI-ester-8	$6.32 \cdot 10^{-3}$	29 150	1.24	3.02 ± 0.90
P 86	DMAEM	8-arm star[e]	MuI-ester-8	$6.32 \cdot 10^{-3}$	44 620	1.28	5.14 ± 0.84
PEI	NA	Branched	NA	-	750 000	-	8.58 ± 0.53
Dextran	NA	-	NA	-	64 000-76 000	-	NA

[a]: Determined as explained in Section 7.2 and Table 7.2; [b]: Calculated using the Hill Equation model; [c]: Synthesised by CTA FRP; [d]: Synthesised by ATRP (linear); [e]: Synthesised by ATRP (star); NA: Not applicable.

The number of moles of positive charges per millilitres (mol/mL) was also calculated by dividing the mass concentration of the polymers (g/mL) by the molecular weight of their repeating units (g/mol) assuming it was fully charged and without considering a counter ion (Table 7.2).

7.3. Results

The cytotoxicity of the library of polymers is shown in Figures 7.3, 7.4 and 7.6 to 7.15. Briefly, and for all polymers, the B16F10 cell viability was concentration-dependent, with greater toxicity at higher polymer concentration (Figures 7.3, 7.4 and from 7.6 to 7.15). Table 7.3 summarises the calculated IC_{50} (mg/mL) for all polymers.

As expected, dextran was not toxic over the concentration range tested. In contrast, PEI had an IC_{50} of ~ 8.58 ± 0.53 μg/mL. From Table 7.3, it can be seen that all homopolymers of DMAEM (linear or star-shaped) displayed greater cytotoxicity than PEI. These polymers had IC_{50} values ranging from 2.90 ± 0.88 to 6.04 ± 2.01 μg/mL. Only the polymers P 28, P 26 (both $PAEM_{25}HPMA_{75}$) and P 38 ($PDMAEM_{25}HPMA_{75}$) were non-toxic with IC_{50} values ≥ 2 mg/mL.

7.3.1. Effect of charge density on the cytotoxicity

To study the effect of charge density, polymers were selected with minimal differences in molecular weight. The cytotoxicity of homopolymers of AEM (P 34, Table 7.3) and DMAEM (P 40, Table 7.3) were compared with either $AEM_{25}HPMA_{75}$ copolymer (P 26, Table 7.3) or $DMAEM_{25}HPMA_{75}$ copolymer (P 36, Table 7.3). All were linear polymers synthesised by FRP and they had a M_w of ~ 16 000 $g.mol^{-1}$ to ~ 19 000 $g.mol^{-1}$.

In Figures 7.3 and 7.4 it can be seen that the AEM homopolymer (P 34) was 337 times more toxic than its copolymer homologue (P 26). Also, the DMAEM homopolymer (P 40) was 126 times more toxic than P 36, its copolymer homologue. The IC_{50} values of the copolymers (P 26 and P 36) (IC_{50} ≥ 600.70 ± 112.60 μg/mL) were significantly different and higher than the IC_{50} of their homopolymers homologues (P 34 and P 40) (IC_{50} ≤ 7.39 ± 0.85 μg/mL).

Moreover, it was noted that the slopes of the curves [cell viability = f(polymer

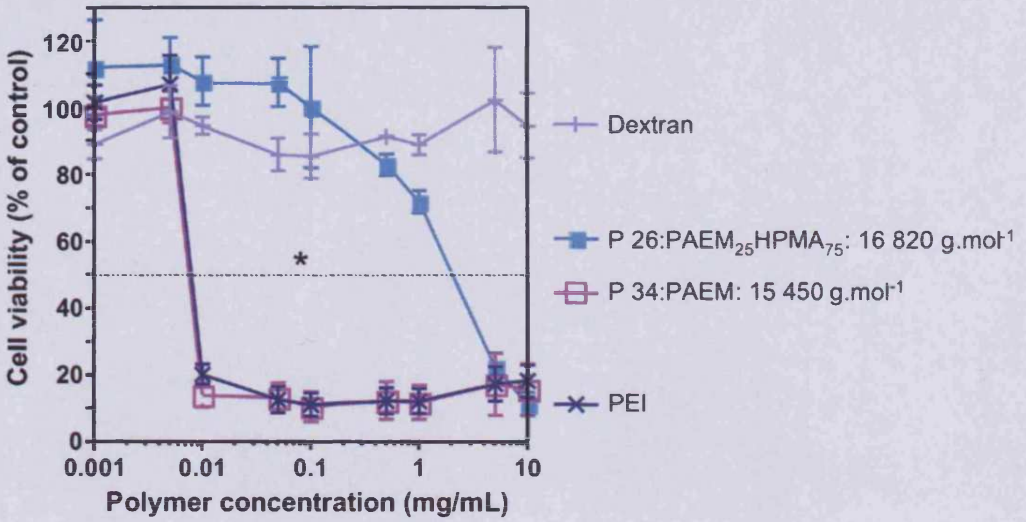

Figure 7.3: Effect of charge density on the cell viability of B16F10 cells: comparison of P 26 & P 34 with PEI & dextran

Where * represents the significant difference between P 26 and P 34 ($p < 0.05$)

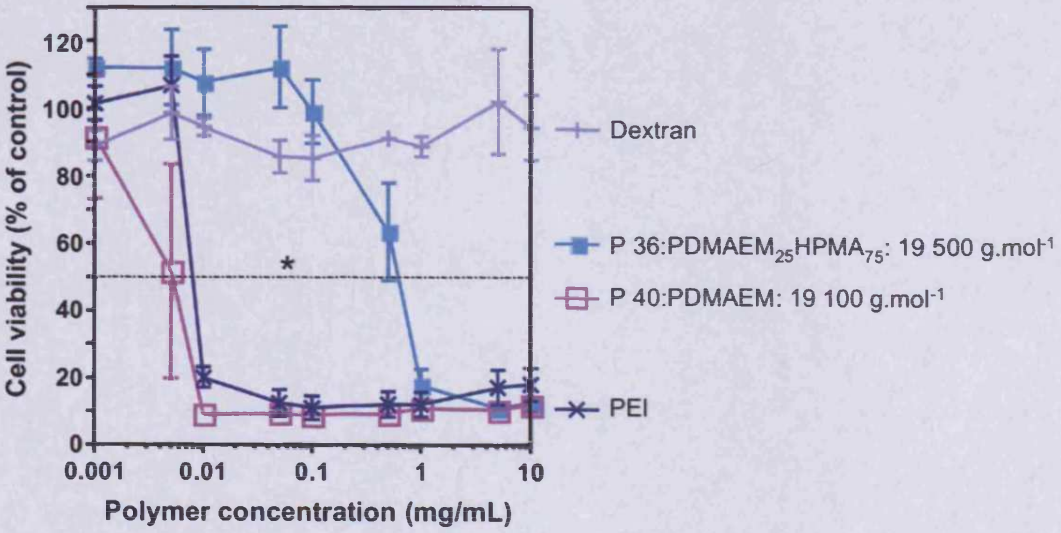

Figure 7.4: Effect of charge density on the cell viability of B16F10 cells: comparison of P 36 & P 40 with PEI & dextran

Where * represents the significant difference between P 36 and P 40 ($p < 0.05$)

concentration - mg/mL)] (Figures 7.3 and 7.4) for the homopolymers (P 34 and P 40) were steeper than those of their copolymer homologues (P 26 and P 36). Furthermore, the IC_{50} values of all the polymers tested increased with a decrease of the maximal charge to polymeric monomer ratio (Table 7.3 determined as explained in Section 7.2), and regardless of the other factors (molecular weight, architecture, etc).

The relative cytotoxicity of these polymers is shown schematically in Figure 7.5. It can be concluded that:

$PDMAEM_{25}HPMA_{75}$ and $PAEM_{25}HPMA_{75}$ > PqAEM > PDMAEM and PAEM

When cell viability for these polymers (P 26/P 34 and P 36/P 40) was plotted as a function of the number of moles of positive charges per mL (Figures 7.6 and 7.7), it was seen that the homopolymers of the amino-based methacrylate monomers (P 36 and P 40) were significantly different, and more toxic, than their copolymer homologues (P 26 and P 34). In the case of AEM, there was a 75-fold increase in cytotoxicity and for DMAEM, a 33-fold increase.

When cell viability was plotted as a function of the concentration of positive charges, both families of polymers show cytotoxicity as follows: at 0.1 μmol/mL of positive charges for homopolymers, whereas the copolymers were just starting to have an influence on the cell viability, but were not toxic yet.

7.3.2. Effect of molecular weight on cytotoxicity

To define the effect of molecular weight on the cytotoxicity samples P 36 and P 38, (both linear $DMAEM_{25}HPMA_{75}$ copolymers synthesised by FRP) were compared. As shown in Figure 7.8, only a marginal difference on the cell viability was observed when B16F10 cells were incubated with P 36 (M_w of 19 500 $g.mol^{-1}$) and P 38 (5 360 $g.mol^{-1}$). The lower molecular weight copolymer P 38 was slightly less toxic (IC_{50} = 10.06 ± 3.53 mg/mL) than the high molecular weight copolymer P 36 (IC_{50} = 0.60 ± 0.11 mg/mL).

Similar behaviour was observed for the four linear homopolymers of DMAEM P 75, P 65, P 69 and P 68, synthesised by ATRP and with M_w of 8 120, 19 165, 29 675 and

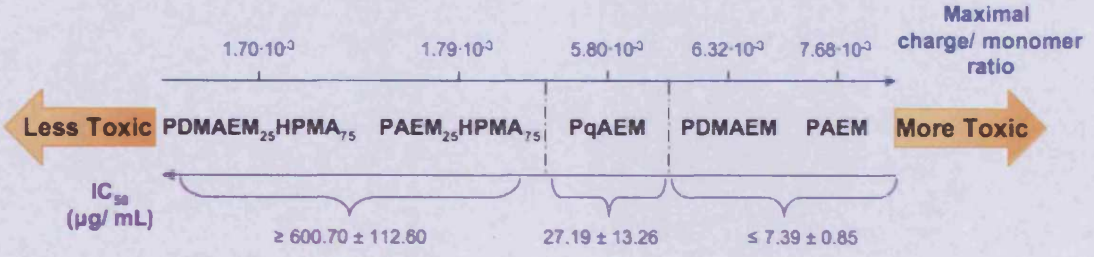

Figure 7.5: Classification of the toxicity of the polymers on their maximal charge per monomer ratio

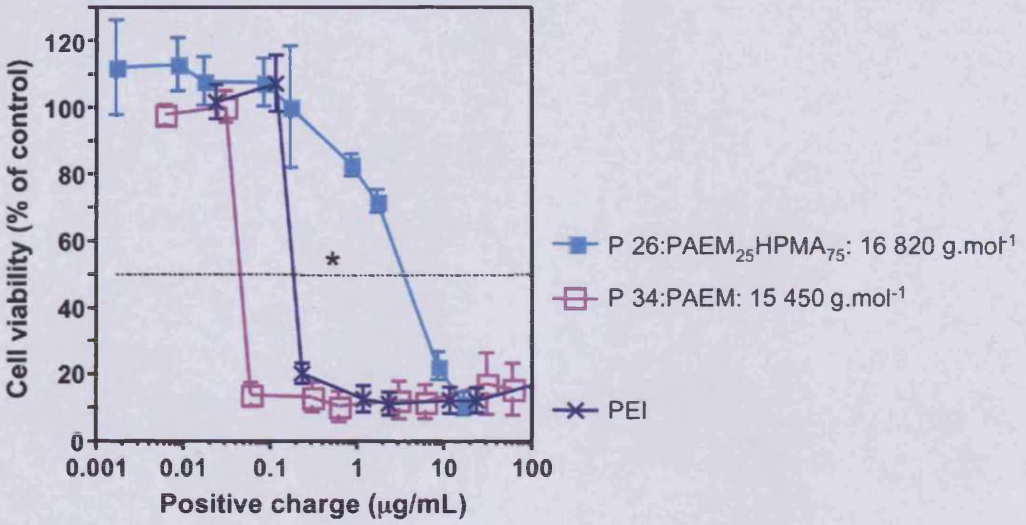

Figure 7.6: Effect of charge density on the cell viability of B16F10 cells: comparison of P 26 & P 34 with PEI as a function of the number of moles of positive charges per millilitres

Where * represents the significant difference between P 26 and P 34 ($p < 0.05$)

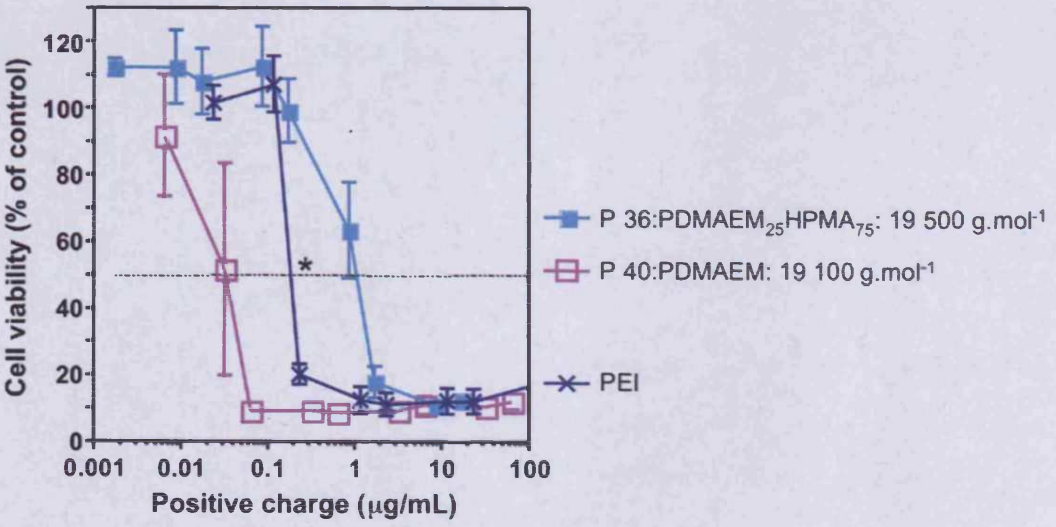

Figure 7.7: Effect of charge density on the cell viability of B16F10 cells: comparison of P 36 & P 40 with PEI as a function of the number of moles of positive charges per millilitres

Where * represents the significant difference between P 36 and P 40 ($p < 0.05$)

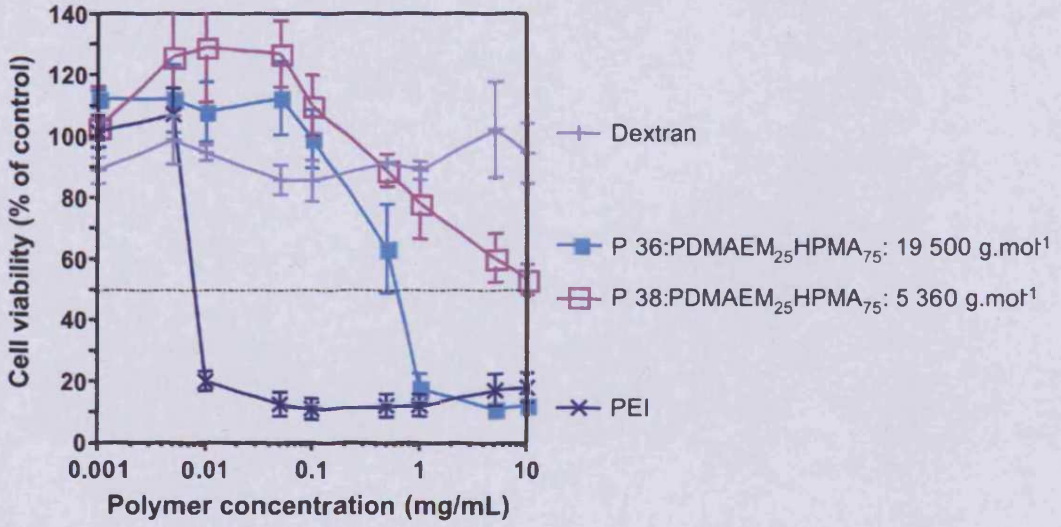

Figure 7.8: Effect of molecular weight on the cell viability of B16F10 cells: comparison of P 36 & P 38 with PEI & dextran

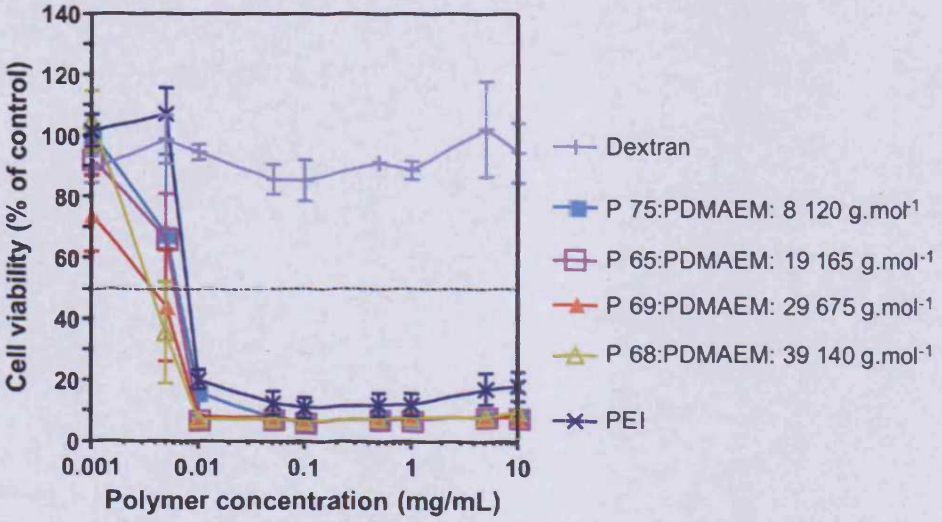

Figure 7.9: Effect of molecular weight on the cell viability of B16F10 cells: comparison of P 65, P 68, P 69 & P 75 with PEI & dextran

39 140 g.mol^{-1}, respectively (Figure 7.9). All polymers showed strong cytotoxicity (4.16 ± 0.88 ≤ IC_{50} ≤ 6.04 ± 2.01 μg/mL), with a very slight increase of the IC_{50} values with a decrease of the M_w (Table 7.3).

Figures 7.10 plot the concentration responses of P 26 against P 28 (both $AEM_{25}HPMA_{75}$ linear copolymers synthesised by FRP, M_w of 16 820 and 5 250 g.mol^{-1}, respectively). Figures 7.11 plot the concentration responses of P 86 against P 87 (both DMAEM-based 8-arm star polymers, with ester-based core, M_w of 44 620 and 29 150 g.mol^{-1}, respectively). In both cases no significant differences in toxicity were observed. Moreover, both copolymers of AEM with HPMA (P 26 and P 28) were relatively non-toxic with similar IC_{50} values (~ 2.00 mg/mL).

7.3.3. Effect of amine substitution on cytotoxicity

To determine the effect of the amine substitution on the cytotoxicity, polymers of the same architecture (all were linear) and the same molecular weight were compared:

- the AEM homopolymer P 34 (M_w = 15 450 g.mol^{-1}) and the DMAEM homopolymer P 40 (M_w = 19 100 g.mol^{-1});
- the $DMAEM_{25}HPMA_{75}$ copolymer P 36 (M_w = 19 500 g.mol^{-1}) and the $AEM_{25}HPMA_{75}$ copolymer P 26 (M_w = 16 820 g.mol^{-1});
- the $DMAEM_{25}HPMA_{75}$ copolymer P 38 (M_w = 5 360 g.mol^{-1}) and the $AEM_{25}HPMA_{75}$ copolymer P 28 (M_w = 5 250 g.mol^{-1});
- and the qAEM homopolymer P 45 (M_w = 36 530 g.mol^{-1}) and the DMAEM homopolymer P 68 (M_w = 39 140 g.mol^{-1})

In this way it was possible to compare of homo- or co-polymers having tertiary amines or primary amines, and quaternary amines or tertiary amines, respectively. The results obtained are shown in Figures 7.12 - 7.15. No significant differences were observed, nevertheless, in general it seems that polymers of DMAEM (either homo- or co-polymers) were slightly more toxic towards B16F10 cells than polymers of AEM or qAEM.

7.3.4. Effect of other parameters on cytotoxicity

Polymerisation technique:

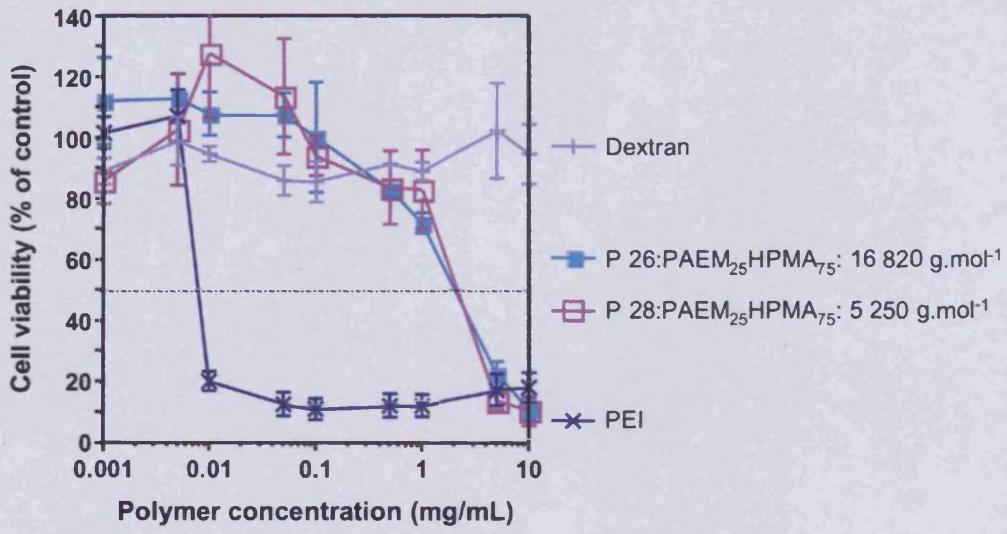

Figure 7.10: Effect of molecular weight on the cell viability of B16F10 cells: comparison of P 26 & P 28 with PEI & dextran

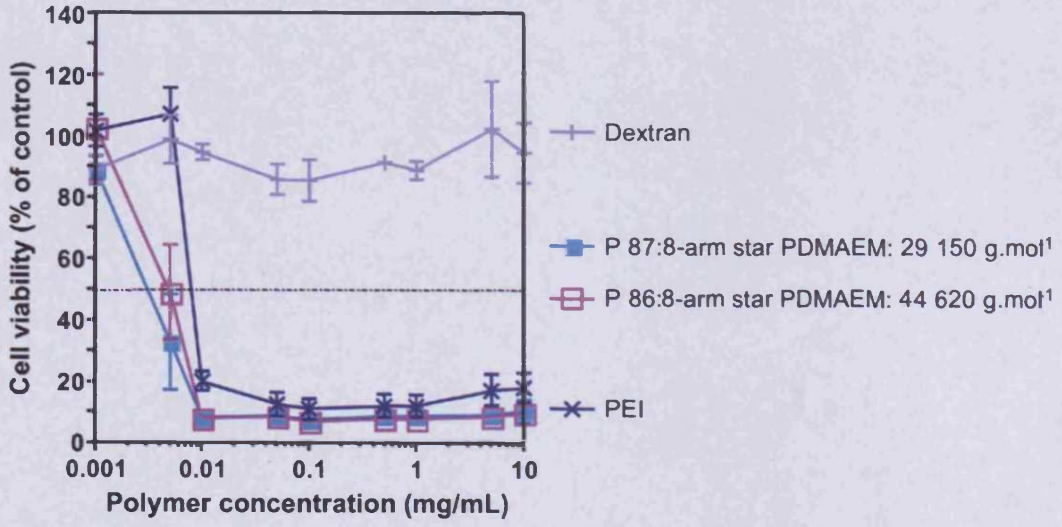

Figure 7.11: Effect of molecular weight on the cell viability of B16F10 cells: comparison of P 86 & P 87 with PEI & dextran

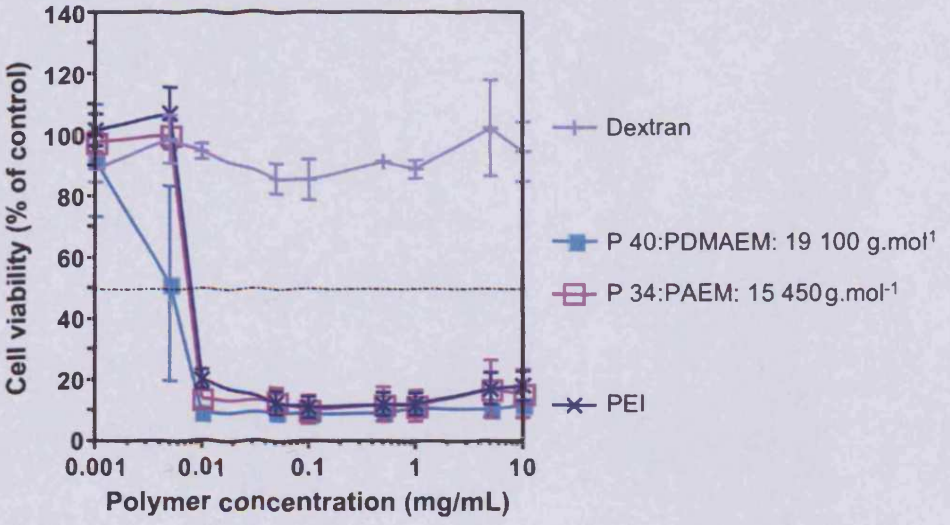

Figure 7.12: Effect of amine substitution on the cell viability of B16F10 cells: comparison of P 34 & P 40 with PEI & dextran

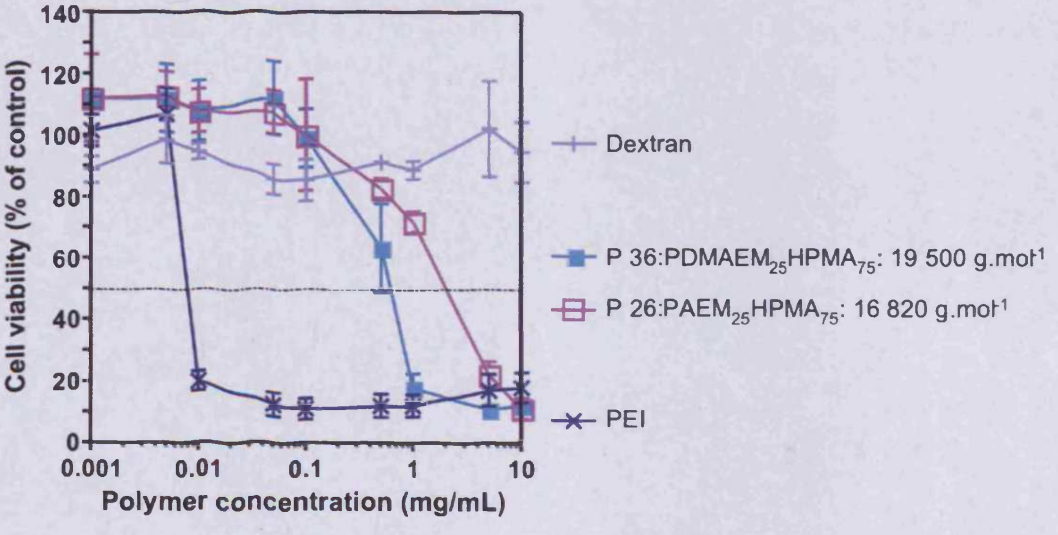

Figure 7.13: Effect of amine substitution on the cell viability of B16F10 cells: comparison of P 26 & P 36 with PEI & dextran

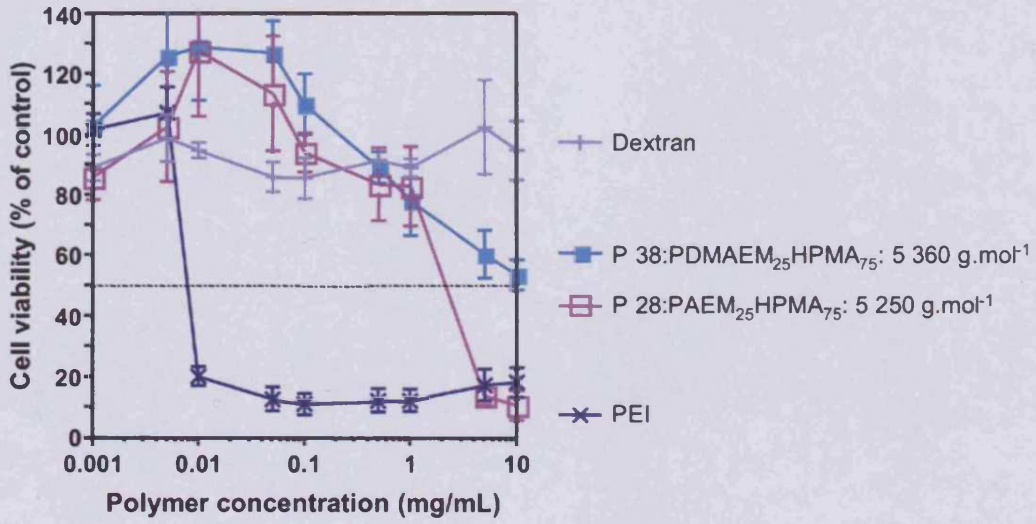

Figure 7.14: Effect of amine substitution on the cell viability of B16F10 cells: comparison of P 28 & P 38 with PEI & dextran

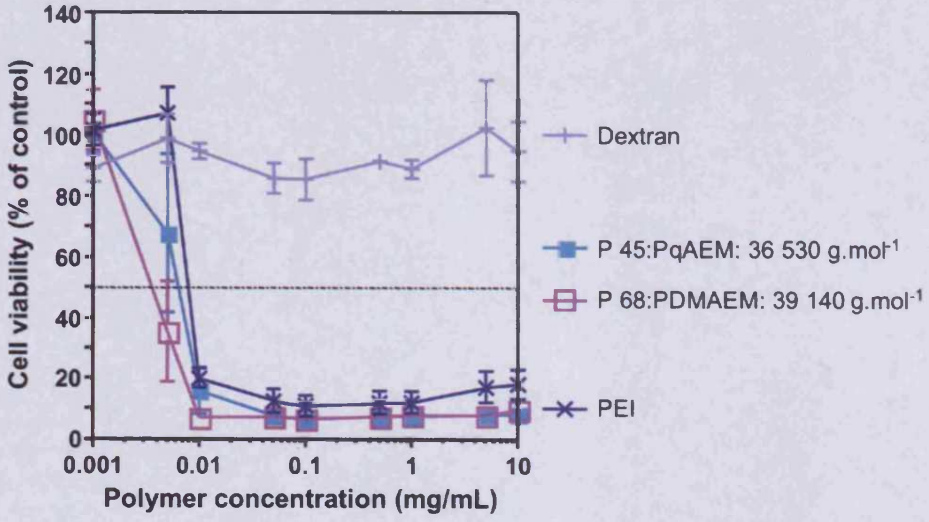

Figure 7.15: Effect of amine substitution on the cell viability of B16F10 cells: comparison of P 45 & P 68 with PEI & dextran

Before investigating the effect of the polymer architecture on the cytotoxicity, the linear PDMAEMs of similar molecular weight, but synthesised using different polymerisation techniques i.e. FRP or ATRP with the copper catalyst were compared. In this way it was possible to also examine the effect of any potential residual copper. When the concentration-dependent cytotoxicity of P 40 (PDMAEM, M_w = 19 100 g.mol^{-1}, synthesised by FRP, Table 7.3) and P 65 (PDMAEM, M_w = 19 165 g.mol^{-1}, synthesised by ATRP, Table 7.3) were compared, no significant difference in the IC_{50} values were seen (Table 7.3), the values being 4.76 ± 1.12 μg.mL^{-1} (P 40) and 5.50 ± 0.73 μg.mL^{-1} (P 65), respectively.

Architecture:

When the cytotoxicity of the linear homopolymers of DMAEM (P 69 and P 68, Table 7.3) was compared with star-shaped homopolymers of DMAEM (P 87 and P 86, Table 7.3), samples of approximately the same molecular weight (~ 30 000 to ~ 40 000 g.mol^{-1}), no significant difference in the IC_{50} values obtained was seen (they ranged from 3.02 ± 0.90 to 5.14 ± 0.84 μg/mL).

Number of arms on the star:

Comparison of DMAEM star-shaped polymers (P 92/P 97; P 81/P 87; and P 92/P 86, Table 7.3) with similar molecular weight but differing only in the number of arms, also showed no significant difference in the IC_{50} values obtained. In this case, they ranged from 2.90 ± 0.88 to 5.14 ± 0.84 μg/mL.

Core:

Finally, star-shaped polymers, which differed only in their cores were compared. The DMAEM 8-arm star polymer P 97 of M_w = 40 200 g.mol^{-1} and based on a DAB generation 1 core was compared with the DMAEM 8-arm star polymer P 86 of M_w = 44 620 g.mol^{-1} and having a tripentaerythritol core. Again no significant difference in the IC_{50} values obtained was found (4.72 ± 1.88 μg.mL^{-1} for P 97 and 5.14 ± 0.84 μg.mL^{-1} for P 86).

7.4. Discussion

The B16F10 cell viability assay proved to be a useful model for comparing the cytotoxicity of the polymer library designed here. Use of PEI and dextran as

reference polymers provided a useful calibration for the assay and allowed comparisons to be made with other polymers.

The most significant effect observed in these experiments, was the effect of the charge density on the cytotoxicity. For all other molecular parameters studied (molecular weight, amine substitution, architecture, number of arms on the star polymers, core chemistry and polymerisation technique), no significant differences in cytotoxicity were observed. This could be partially due to the fact that the homopolymers of DMAEM were too toxic for noticing any further variation.
One of the ideas to improve this study would be to synthesise of high and low molecular weight star-shaped copolymers of HPMA (75 %) with 25 % of either DMAEM or AEM, to be able to further study the influence of the architecture, molecular weight and amine substitution on the cell viability.

The cytotoxicity of polycations has been well documented and charge density directly correlates with increased cytotoxicity (Morgan *et al.* 1989; Choksakulnimitr *et al.* 1995; Fischer *et al.* 1999; Kean *et al.* 2005). Even though the mechanism of cytotoxicity caused by polycations is not yet fully understood, researchers generally agree that cytotoxicity is caused at least in part, by non specific adsorption of the polymer with the negatively charged phospholipids of the cell membrane by electrostatic interaction (Nevo *et al.* 1955; Karchalsky *et al.* 1959; Morgan *et al.* 1988; Morgan *et al.* 1989; Singh *et al.* 1992; Choksakulnimitr *et al.* 1995). Thus the higher the polymer charge density the stronger its affinity with the cell membrane will be, leading to more severe cell damage. A good example of this fact is PEI. Indeed, as already explained in Section 7.1.4, it is well known that high molecular weight PEI is cytotoxic and this is explained by its high charge density, since every third atom is a potentially protonable amino nitrogen (reviewed by Kircheis *et al.* (2001)).
All the DMAEM homopolymers when synthesised as low or high molecular weight linear polymers or as star polymers were the most toxic against B16F10 cells. In fact, they were even more toxic than PEI (Table 7.3). This might be explained by the fact that DMAEM homopolymer bears an amino group that can be protonated on each repeating unit (van de Wetering *et al.* 1998a). Thus, homopolymers of DMAEM are

not likely to be good candidates for further development as polymer therapeutics for cellular delivery of oligonucleotides, drugs or proteins.

Copolymerisation of the amino-based methacrylate monomers, such as AEM or DMAEM, with HPMA, causes a decrease in the overall positive charge density and a marked decrease in cytotoxicity was seen (at least 126 fold decrease). HPMA is well known to give inert homo- and copolymers, and they have already been widely developed as plasma expanders (Kopeček and Bazilova 1973; Sprincl *et al.* 1976) and as safe carriers for anticancer drugs, and proteins, etc (Duncan *et al.* 1986; Duncan *et al.* 1987; Vasey *et al.* 1999; Huang and Oliff 2001; Terwogt *et al.* 2001; Gianasi *et al.* 2002; Schoemaker *et al.* 2002; Seymour *et al.* 2002) and reviewed by Duncan (2003b)).

HPMA copolymers containing either AEM or DMAEM (25 %) were less toxic than their homopolymer homologues with a decrease of at least 125 times in cytotoxicity (Figures 7.3 and 7.4), and in these assays the IC_{50} values were always ≥ 2 mg.mL^{-1}. The use of the HPMA monomer to "dilute" the cationic residues in such copolymers, and to introduce more hydrophilicity along the backbone of the possible drug or gene delivery vector, is interesting and can be used to render the polycations more compatible, for example for gene delivery, without losing their potential ability to condense DNA fragments. This concept was for example applied by Seymour, Ulbrich and co-workers with the synthesis of HPMA/qAEM block copolymers for gene delivery applications (Koňák *et al.* 1998).

Moreover, it was also observed that the slope of the curves [cell viability = f(polymer concentration)] were steeper for the AEM or DMAEM homopolymers compared to their 75 % HPMA copolymer homologues (Figures 7.3 and 7.4). This was also observed by Kunath when comparing the cytotoxicity of low and high molecular weight PEI (Kunath *et al.* 2003). They concluded that a steeper slope in the cell viability curve was indicative of a smaller margin between the beginning of the metabolic down-regulation and the complete loss of metabolic activity when the cells were treated with high molecular weight PEI in their case, and in these studies, with the AEM or DMAEM homopolymers.

Furthermore, if the polymer is to be used as a gene delivery vector, it is important to consider both cytotoxicity effect and overall charge density. Indeed, the polycation should be designed such as it will have the least number of charged residues possible to minimise cytotoxicity, but still enough to enable condensation of the oligonucleotide/DNA to be delivered.

The fact that a significant difference in cytotoxicity was still visible when cell viability was plotted against the number of moles of positive charges/mL (Figures 7.6 and 7.7) confirmed that the cytotoxicity was directly linked to polymer charge density. However, at a concentration of 0.1 μmol/mL of positive charge, the homopolymers of AEM or DMAEM were strongly toxic, while their HPMA copolymer homologues were not yet toxic. This showed that factor(s) other than just charge density were influencing the cytotoxic behaviour. As polymers of similar molecular weight were selected for these experiments, a molecular weight effect can probably be discounted. It is interesting to consider other factors that might be important, and Figure 7.16 shows schematically the hypothesises described here.

First, and from a pure physicochemical point of view, the solution conformation of the four polymers studied (P 26 - P 34 and P 36 - P 40, Table 7.3) will differ. It can be expected that the homopolymers P 34 and P 40 will display a more extended shape in aqueous solution than the copolymers P 26 and P 36, which would be expected to adopt a more globular and compact shape. This could be verified by measuring the coil dimensions in solution (hydrodynamic radius R_h or radius of gyration R_g) by small angle neutron scattering (Paul *et al.* 2007), but these experiments were not done here.

Electrostatic cell membrane interactions will be affected by solution conformation and the extended homopolymers would present more positive residues to the cell surface than the more globular copolymers even though the total number of moles of positive charges would the same, leading to greater damage of the membrane. This hypothesis is in good agreement with the literature, where it has been shown that more globular polymeric structures such as higher generation PAMAM dendrimers show less cytotoxicity than more linear and flexible polymeric structures such as PLL and PEI (Fischer *et al.* 2003).

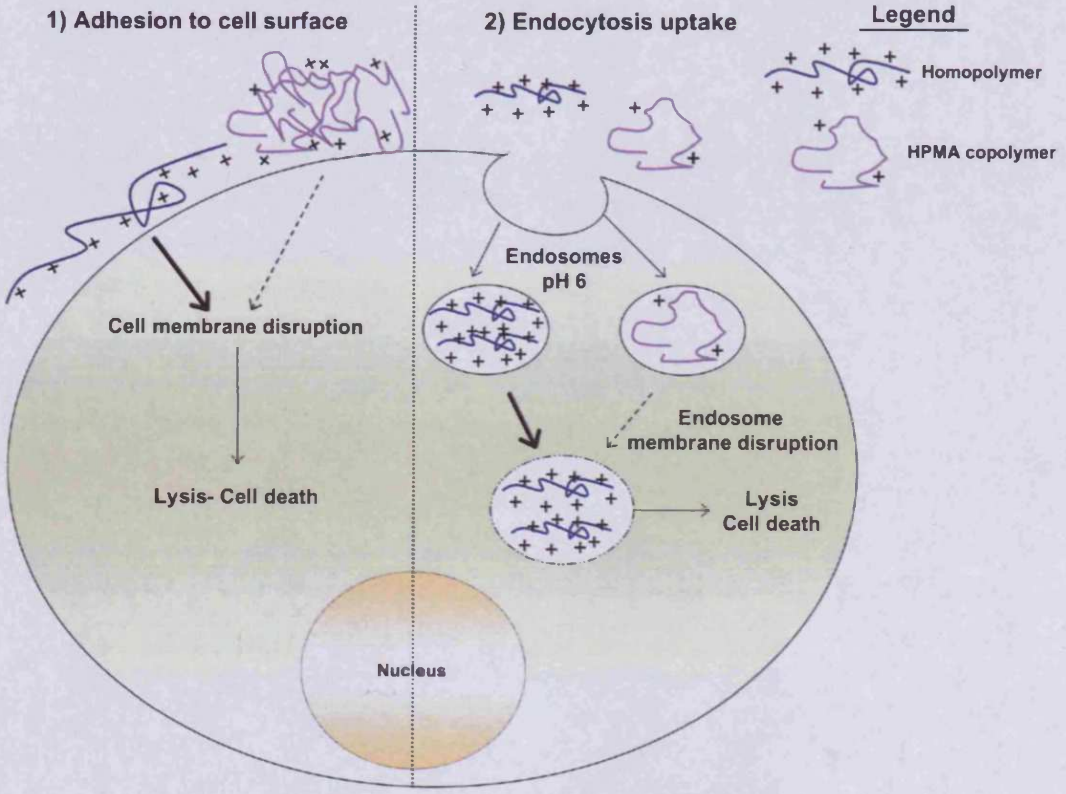

Figure 7.16: Schematic representation of the possible mechanisms of polycation-induced cell damage

Secondly, it is known that following membrane adsorption, polycations are taken up by endocytosis (Fischer *et al.* 2003). Considering the greater affinity of the linear homopolymers with the cell membrane, it is likely that a higher amount of homopolymer will be taken up by adsorptive endocytosis, leading to a higher intracellular concentration of polycation within the endosomes and lysosomes, which would itself induce greater cell damage and explain their stronger cytotoxic effects.

In fact, Ryser suggested that a three-point attachment on the cell membrane was necessary for polycations to elicit a biological response (Ryser 1967). He speculated that the activity of basic polymers decreases with increasing spacing between the reactive amino groups along the polymer chain. Here, the copolymers synthesised are statistical (Chapter 4) and thus they have on average a positive charge every four repeating units. This is obviously a much greater spacing than would be present in the homopolymers, leading to the decrease in cell adsorption, endocytosis, and cell damaging.

In conclusion, the charge density accessible to the cell surface and resulting from the number and the three-dimensional arrangement of the cationic residues is an important factor for cytotoxicity, and for the design of polymeric vectors.

By copolymerising either DMAEM or AEM with HPMA, not only the overall charge density of the copolymers was altered but also their three-dimensional arrangement and the number of attachment points accessible for the adsorption onto the negatively charged cell surface. The copolymers studied in these experiments, which showed low cytotoxicity at relatively high concentration of positive charges (up to ~ 0.1 μmol/mL - which could still be enough to efficiently condense DNA fragments to transfect) could be considered as good candidates for drug or gene delivery.

The effect of molecular weight on cytotoxicity has also been extensively studied (Morgan *et al.* 1988; Morgan *et al.* 1989; Singh *et al.* 1992; Choksakulnimitr *et al.* 1995; Roberts *et al.* 1996; Brazeau *et al.* 1998; Fischer *et al.* 1999; Malik *et al.* 2000; El Sayed *et al.* 2002; Zinselmeyer *et al.* 2002; Fischer *et al.* 2003; Kunath *et al.* 2003; Kean *et al.* 2005), and generally, higher molecular weight polymers are more toxic than their low molecular weight homologues. The number of attachment points by

which a polymer chain binds to the cell membrane (Ryser 1967), will obviously depends upon the length of the polymer, its conformation and the distribution of anionic domains on the cell surface. Thus higher molecular weight, flexible polycations will have the greatest potential to efficiently interact with the cell membrane, leading to greater cell damage. This trend was clearly observed in Figure 7.8, when the two copolymers of $DMAEM_{25}HPMA_{75}$ of 19 500 and 5 360 $g.mol^{-1}$ were compared (IC_{50} values of 0.601 ± 0.113 $mg.mL^{-1}$ and 10.060 ± 3.526 $mg.mL^{-1}$, respectively).

Moreover, it is important to discuss the nature of the amine, and this factor has already been discussed widely in the literature (Dekie *et al.* 2000; Fischer *et al.* 2003; Wang *et al.* 2004b). Generally it is agreed that primary and secondary amines are more toxic than tertiary amines, due to their lower basic character. However, in this study, a slightly more toxic response was observed for the tertiary amino-based polymers (samples P 40, P 68 and P 36 in Table 7.3). This might be explained, as those polymers are more lipophilic than the homo- and HPMA copolymers of AEM or qAEM (samples P 26, P 34 and P 45, Table 7.3). Indeed, the pK_a values of the DMAEM-based homopolymers and copolymers are slightly lower (pK_a = 7.6 and 7.8) than those of the AEM-based homopolymers and copolymers (pK_a = 8 and 8.5) (Chapter 3). This means that at all relevant pHs, the AEM-based polymers will be more charged. Thus they are expected to be more hydrophilic than their DMAEM-based polymer homologues.

Moreover, it is probable that DMAEM-based polymers, once adsorbed onto the cell membrane, would insert their hydrophobic pendant groups into the phospholipids bilayer inducing greater cell membrane changes, and thus greater cell damaging. The effect of varying the hydrophilic/hydrophobic balance of materials used in contact with biological environment, has been extensively studied, and it is proposed that introducing more hydrophilicity helps forming "stealth" compounds, which reduces the interaction between the material and the cell membrane, thus facilitate drug delivery and reduce their toxicity (reviewed by Wang *et al.* (2004b)). PEG is a good example of macromolecular compound used to form more hydrophilic stealth polymeric carrier (Harris and Chess 2003; Veronese and Pasut 2005).

Before discussing the effect of architecture on toxicity, it was important to consider the possibility that the copper catalyst used in ATRP for the synthesis of star polymers, might itself influence toxicity. The trace element copper plays an important role in cell metabolism, but it also exhibits toxicity at high concentrations that impairs cell function (Karash 1979; Rossi *et al.* 1996; Seth *et al.* 2004; Fotakis and Timbrell 2006).

The synthesis of star-shaped polymers was achieved by the mean of ATRP with Cu(I)Br as catalyst and HMTETA as ligand (Chapter 6). These star polymers were purified from copper by extensive dialysis against water, nevertheless, some copper could potentially still be trapped in the final product. The polymers synthesised are nitrogen atom-containing compounds, and it is well known that nitrogen compounds can complex with the transition metal copper (reviewed by Matyjaszewski and Xia (2001)).

However, the fact that no significant difference was observed when comparing the cytotoxicity of linear homopolymers of DMAEM synthesised by FRP or ATRP allows several conclusions to be drawn:

(i) The purification carried out by extensive dialysis of polymers synthesised by means of ATRP was efficient enough to remove the copper catalyst, and if present, the residual copper was low enough not to induce increased toxicity,

(ii) Alternatively, the linear PDMAEM was so toxic that it was impossible to see any effect attributable to the small concentration of residual copper trapped within the polymeric network.

As it is known that linear, more flexible polycations are more toxic than their more globular and rigid homologues (Singh *et al.* 1992; Choksakulnimitr *et al.* 1995; Brazeau *et al.* 1998; Fischer *et al.* 1999; Fischer *et al.* 2003) it was hoped that the star polymers would be less cytotoxic due to their more globular and rigid three-dimensional conformation. However, no significant difference was observed when linear homopolymers of DMAEM and star-shaped PDMAEM of the same molecular weight were compared (Table 7.3, linear samples P 69 and P 68 compared with star-shaped samples P 87 and P 86).

It is possible that the cytotoxicity of the DMAEM homopolymers is so high (after 72 h incubation) that it is difficult to see the effects of the structural conformation.

Comparison of the cytotoxicity of linear and star copolymers based on DMAEM and HPMA, of the same molecular weight and charge density, would have been interesting. Other interesting experiments might have been to study cytotoxicity using a shorter incubation period, or to test linear and star polymers of lower molecular weight.

Considering that more globular and rigid polycations show less toxicity than their more extended and flexible homologues (Singh *et al.* 1992; Choksakulnimitr *et al.* 1995; Brazeau *et al.* 1998; Fischer *et al.* 1999; Fischer *et al.* 2003), it is believed that increasing the number of arms on the star-based polymers (same molecular weight) would render the compounds more rigid and globular, thus leading to a decrease in cell damaging. In the present studies, the severe cytotoxicity of homopolymers of DMAEM does not permit to observe the influence of a change in the numbers of arms of the star-based polymers as shown in Section 7.3.4.3.

It is believed that the star-based polymers, such as P 97 (Table 7.3) having a DAB core would induce more toxic effects than those of similar molecular weight and number of arms with an ester-based core, such as P 86 (Table 7.3). Indeed, DAB is a diaminobutane-based dendrimer and showed dose- and generation-dependent cytotoxicity (Malik *et al.* 2000; Zinselmeyer *et al.* 2002) due to its internal tertiary amines.

However, in our studies, no significant differences were observed when comparing 2 star-based PDMAEM with same molecular weight, same number of arms, but different cores: P 97 and P 86 (Table 7.3) and this is probably due to the fact that the homopolymers of DMAEM display such a strong toxicity ($IC_{50} \leq 6.04 \pm 2.01$ $\mu g.mL^{-1}$) themselves.

7.4. Conclusions

Summarising the information gathered in the literature and from the results obtained in this set of experiments, a non-toxic polymeric carrier should be designed as follow:

- the polycation should preferably be a copolymer of a protonable amino-based monomer with an hydrophilic monomer such as HPMA.

Copolymerisation of those two types of monomer will, on a physico-chemical point of view, lower the charge density of the overall polymer without losing its positive charges; increase its overall hydrophilicity; make it more globular and less flexible; and lower its number of attachment points onto cell membranes. All these effects combined should reduce the intrinsic toxicity of the gene delivery vector (Ryser 1967; Morgan *et al.* 1989; Choksakulnimitr *et al.* 1995; Fischer *et al.* 1999; Fischer *et al.* 2003; Wang *et al.* 2004b; Kean *et al.* 2005),

- it should have a rigid and globular shape (Singh *et al.* 1992; Choksakulnimitr *et al.* 1995; Brazeau *et al.* 1998; Fischer *et al.* 1999; Fischer *et al.* 2003), which could be obtained by synthesising star-based polymers with a high number of arms,

- the smaller its molecular weight the less toxic should it be (Morgan *et al.* 1988; Morgan *et al.* 1989; Singh *et al.* 1992; Choksakulnimitr *et al.* 1995; Roberts *et al.* 1996; Brazeau *et al.* 1998; Fischer *et al.* 1999; Malik *et al.* 2000; El Sayed *et al.* 2002; Zinselmeyer *et al.* 2002; Fischer *et al.* 2003; Kunath *et al.* 2003; Kean *et al.* 2005), bearing in mind that the polymer should be big enough for passive targeting through the EPR effect (Matsumura and Maeda (1986); and reviewed by Duncan (2003b)) and for condensing the oligonucleotide fragments. Thus considering the point mentioned above, the star should preferably have a high number of arms of low molecular weight than a small number of arms of high molecular weight,

- the core of the star should preferably be an ester based core, which in comparison to DAB cores, should be less toxic towards biological components (Malik *et al.* 2000; Zinselmeyer *et al.* 2002),

- and finally the protonable amine residues should be tertiary amines rather than primary and secondary (Dekie *et al.* 2000; Fischer *et al.* 2003; Wang *et al.* 2004b).

8

General Discussion

8.1. General comments

This thesis has focused on the use of several radical polymerisation techniques for the synthesis of water-soluble polymers to be potentially used as carriers in the field of polymer therapeutics. From Chapter 3 to Chapter 6, the research has evolved from the use of conventional FRP to the use of ATRP, and it was attempted to step wisely synthesise polymers with an increasing control over molecular weight, polydispersity, composition and architecture. For each technique (FRP, CTA-mediated FRP, linear-based ATRP and star-based ATRP) and monomer studied, the first goal was to investigate possible reaction conditions and optimise them to be able to synthesise polymers with defined molecular weight, composition and architecture.

As this thesis finishes, it is interesting to note that polymer chemists working on the interface of chemistry and biology are devoted to the development of new polymeric carriers, where "uniformity" can carefully be controlled. Indeed, and as explained by Brocchini and co-workers, "differences in polymer molecular weight, morphology and chemical structure are known to display a wide range of differing biological and physicochemical properties" (Ali and Brocchini 2006). A uniform polymer is an homogeneous macromolecule in respect to its "molecular mass and constitution" (Hatada 1999; Hatada *et al.* 2004), therefore, with a narrow molecular weight distribution and a defined chemical structure regarding stereo-regularity, shape and chemical functionality. A lack of uniformity is considered to potentially lead to undesirable effects, if the polymer is to be administered or implanted in the patient, and therefore be in contact with the systemic circulation. Also determining the structure/property relationship for all non-uniform polymers to be in contact with the systemic circulation is not feasible, and this reduce their potential to enter clinical trials.

Synthetic polymer chemistry has therefore developed and improved several methodologies for the design of synthetic polymers where the degree of uniformity could be enhanced. These mainly encompass the CRP methods (ATRP, RAFT, and NMP) but also Ring Opening Polymerisation (ROP) techniques when a cyclic monomer is used (Ali and Brocchini 2006).

To a certain extent, this thesis aimed to enhance uniformity of polymeric constructs in respect to their composition, molecular weight, polydispersity and architecture, taking into account their potential uses in the field of polymer therapeutics. In parallel, it was hoped to develop polymers that would have a sufficiently good 'biocompatibility' and molecular weight properties (for these non-degradable polymers) that would allow, in the future, clinical use.

8.2. A critical view on the work done in this thesis

Some critical comments can be made as this thesis is coming to an end. The polymers synthesised in this work were chosen for their water-solubility character and thus their potential use as carriers in the field of polymer therapeutics. It was important to firstly develop the synthetic methods for the synthesis of polymers with different molecular weight, architecture and composition, and then to fully characterise them in order to finally be able to evaluate their cytotoxicity in relation to their molecular parameters.

Biodegradability

From a clinical point of view, it would have been interesting to focus on polymers, which are not only water-soluble but also biodegradable. In theory, the lack of biodegradability of the polymer might raise concern if longer-term clinical use is hoped. Almost all polymers used clinically are still non-biodegradable synthetic polymers such as PEG (Bukowski *et al.* 2002; Graham 2003; Veronese and Pasut 2005) and PHPMA (Vasey *et al.* 1999), and only polymers with a molecular weight below the renal threshold can thus be used to exclude progressive accumulation of the macromolecule within the body. Therefore, research on the field of polymer therapeutics converges on the design of new polymeric construct where the polymer would be biodegradable itself. The polymers being studied are for example PGA (Singer *et al.* 2003; Singer 2005; Singer *et al.* 2005; Vicent and Perez-Paya 2006), polymers based on lactide and glycolide (Ali and Brocchini 2006), dextrin (Hreczuk-Hirst *et al.* 2001; Ferguson *et al.* 2006; Hardwicke *et al.* 2007; Duncan *et al.* in press), and poly(acetal)s (Tomlinson *et al.* 2003; Vicent *et al.* 2004b).

Stimuli-responsive polymers

Moreover, scientists are nowadays interested in the development of bioresponsive

polymers, which conformation and architecture can be changed when an external stimuli is applied, such as NIPAAm-based polymers that find quite interesting applications in the field of polymer therapeutics (Cole *et al.* 1987; Takei *et al.* 1993b; a; Takei *et al.* 1994; Takei *et al.* 1995; Matsukata *et al.* 1996; Heath *et al.* 2007). It is thus appealing to work with these "smart" polymers, as they offer attractive points both from a polymer chemistry and polymer therapeutics point of view.

ATRP improvements

The choice of ATRP technique was made as it is a versatile technique, which allows the polymerisation of a wide range of monomers, using commercially available initiators, metal catalyst and ligands (reviewed by Matyjaszewski and Xia (2001)). Nevertheless, at the end of the reaction, it is important to remove the catalyst from the polymer, as it can cause aging of the polymer, coloration, and also can cause toxicological issues (Hansen *et al.* 2007). Several procedures have been developed for the successful removal of catalyst, and research is also developing other types of ATRP techniques where the amount of catalyst added can be reduced (http://www.chem.cmu.edu/groups/maty/about/research/02.html). Considering that polymers synthesised in this thesis could find a future use in a biomedical field, it is important to consider this improvement, not only for industrial synthesis but also and especially for toxicological matter.

8.3. Summary of the main findings of this work and selection of the lead polymer candidates to progress

Table 8.1 summarises all the polymers selected as best carriers from each Chapter.

This project started with the synthesis and the characterisation of a library of water-soluble homo- and copolymers by FRP in Chapter 3. The studies focused on the synthesis of amine-based poly(methacrylate)s, poly(methacrylamide)s and amine-based poly(acrylamide)s. The effect of the initiator to monomer molar ratios on molecular weight was investigated here, and the trend was found to be inversely dependant.

From all the polymers synthesised in Chapter 3, the sample P 23, a copolymer $PHPMA_{50}DMAEM_{50}$ of a weight-average molecular weight of 25 690 $g.mol^{-1}$ and a polydispersity of 2.09 was thought to be the best polymer to be used for future

Table 8.1: Summary of the "best" polymers synthesised in each Chapter for future use in the field of polymer therapeutics

	Polymerisation technique	Polymer selected	Composition	Architecture	M_w (g.mol^{-1})	M_w/M_n	IC_{50} (µg.mL^{-1})
Chapter 3	FRP	P 23	$PHPMA_{50}DMAEM_{50}$	Linear	25 690	2.09	ND
Chapter 4	CTA-mediated FRP	P 36	$PDMAEM_{25}HPMA_{75}$	Linear	19 500	2.70	600.70 ± 112.60
Chapter 5	Linear-based ATRP	P 69	PDMAEM	Linear	29 600	1.68	4.41 ± 0.69
"	"	P 73	PDMAEM	Linear	6 500	1.18	ND
Chapter 6	Star-based ATRP	P 82	PDMAEM	5-arm star-shaped, alcohol-based core	26 000	1.22	ND
Chapter 7	CTA-mediated FRP	P 38	$PDMAEM_{25}HPMA_{75}$	Linear	5 360	1.80	≥ 10000

ND: not determined

applications. It was selected due to its relatively low molecular weight, and the fact that it is a copolymer of the biocompatible hydrophilic HPMA monomer and contains amine residues for future conjugation to therapeutic drugs, targeting moieties or to be used as a non-viral gene delivery vector.

The use of thiol-based CTA in FRP was consecutively studied in Chapter 4. Here also, a library of water-soluble semitelechelic homo- and copolymers of methacrylate and methacrylamide was achieved. The studies focused on the evaluation of the effect of the CTA to monomer molar ratios on molecular weight and polydispersity. It was seen that molecular weight and polydispersity decreased when an increasing amount of CTA was used. The end-group characterisation was done through an indirect method, after activation of the carboxylic acid end-group with hydroxysuccinimide.
In general, the polymers synthesised in this Chapter were of lower molecular weight compared to the previous Chapter ($\leq$ 30 000 g.mol^{-1}). Keeping in mind their potential use in polymer therapeutics, the copolymer P 36 ($PDMAEM_{25}HPMA_{75}$, M_w = 19 500 g.mol^{-1} and M_w/M_n = 2.70) was chosen as the most promising one for future applications. In Chapter 7, the cytotoxicity of this copolymer on B16F10 cells was evaluated with an IC_{50} value of 0.6 $\pm$ 0.1 mg.mL^{-1}, and in general P 36 showed less toxic effects than the other polymers tested, due to its HPMA residues.

In Chapter 5, ATRP of DMAEM was optimised for the synthesis of well-defined linear amine-based poly(methacrylate)s. The catalytic system Cu(I)Br/HMTETA in DMF with the initiator ethyl α-bromoisobutyrate, showed the best results in terms of control of molecular weight and polydispersity. As expected, the polymers obtained here showed in general lower polydispersity than when PDMAEM was synthesised by FRP, CTA-mediated (Chapter 4) or not (Chapter 3). Although, it was seen in Chapter 7 that DMAEM-based homopolymers were quite toxic, it was thought that the most promising PDMAEM synthesised in these studies were samples P 69 (M_n = 17 620 g.mol^{-1}, M_w/M_n = 1.68) and P 73 (M_n = 5 500 g.mol^{-1}, M_w/M_n = 1.18) due to their narrow polydispersity and the good correlation of their molecular weight with the theoretical molecular weight expected by ATRP.

In Chapter 6, after the synthesis of multifunctional ATRP initiators, their efficiencies were determined with the star-based ATRP of DMAEM. A library of homopolymers

of DMAEM of different molecular weight and polydispersity was obtained. It was seen that the alcohol-based multifunctional initiators gave the best control of molecular weight and polydispersity. The DAB-dendrimer based multifunctional initiators was thought to play an undesirable role as ligand as the polymers derived from them showed much higher molecular weight than that expected.

Also, the idea of the synthesis of a degradable star-shaped polymer from its core was proven.

From the library of polymers synthesised, sample P 82 (5-arm star DMAEM-based polymer derived from the xylitol-based initiator) with a M_n of 21 285 $g.mol^{-1}$ and polydispersity of 1.22, was selected as the best candidate as it gave the best control over molecular weight, the lowest polydispersity, and showed possible degradation from its core.

Finally, in Chapter 7, the evaluation of cytotoxicity of selected polymers on B16F10 cells, in respect to molecular parameters (molecular weight, charge density, architecture, composition) was attempted, and it was seen that linear copolymers of HPMA of low molecular weight were the best candidates for future use in the field of polymer therapeutics, as they showed the lowest toxic effect towards the cell line studied.

8.4. Future opportunities for the synthesis of water-soluble polymers to be used as carriers for polymer therapeutics

Considering the results obtained in these studies and especially in Chapter 7, it is thought that the synthesis of star-shaped $DMAEM_{25}HPMA_{75}$ copolymers will be of great interest both from a polymer chemist point of view and for future polymer therapeutic applications.

Similarly to that observed when comparing linear homopolymers of DMAEM with their linear $DMAEM_{25}HPMA_{75}$ copolymer homologues, it is expected that a decrease in cytotoxicity would be observed when treating cells with these star-shaped $DMAEM_{25}HPMA_{75}$ copolymers.

Three kinds of star-shaped copolymers, with arms of heterogeneous composition, could be in theory synthesised by ATRP (Figure 8.1):

(i) star statistical copolymers

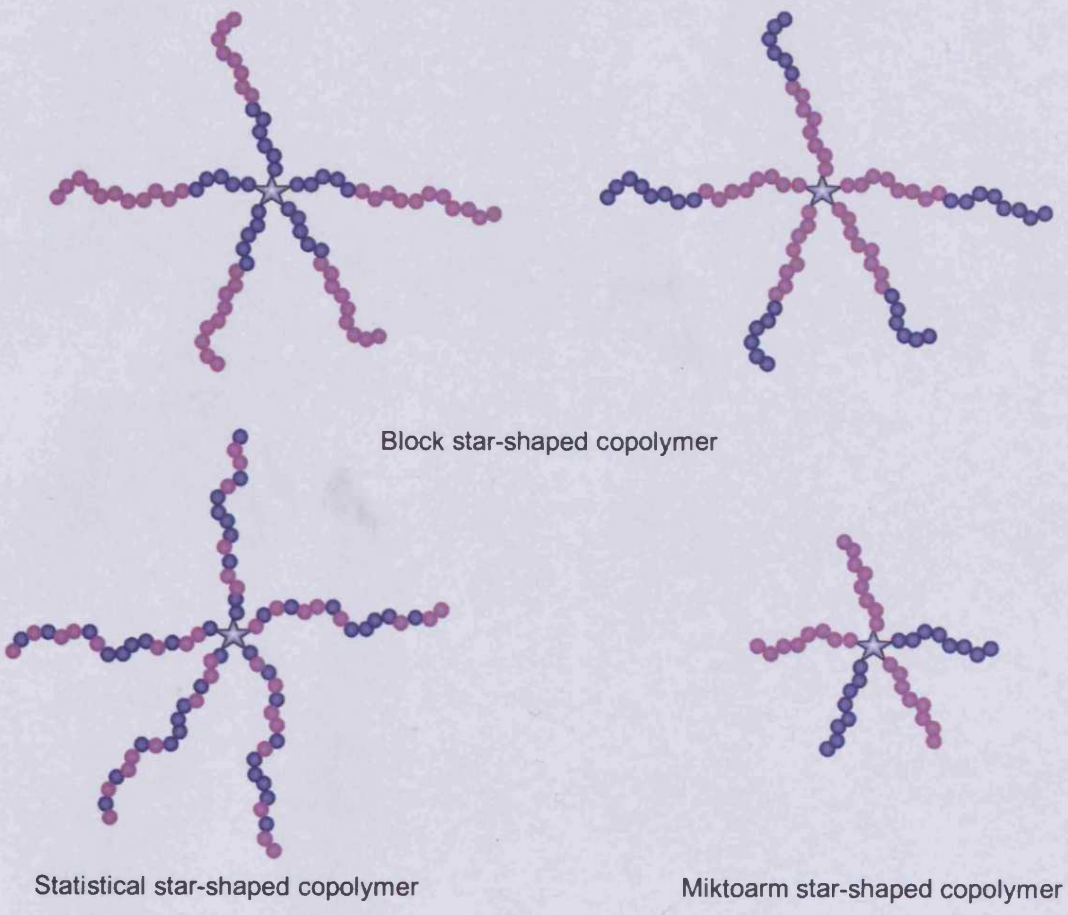

Figure 8.1: Schematic representation of the star-shaped copolymers that could be investigated as future perspective polymeric carriers

Where: ● represents the HPMA repeating unit and ● is DMAEM repeating unit

(ii) star block copolymers

(iii) star copolymers with different arms or miktoarms copolymers

For the obtention of star-shaped copolymer type (iii) through the core-first approach, the synthesis of multifunctional cores containing several types of initiating moieties needs to be first developed before running any ATRP experiments. These star-shaped polymers could alternatively be prepared by ATRP with the arm-first approach synthesis (Hadjichristidis 1999; Deng *et al.* 2007; Gao and Matyjaszewski 2007; Themistou and Patrickios 2007)

With the idea of optimising the reaction conditions and also to be able to compare the synthesised polymers regarding their architecture, it is believed that the synthesis of linear block copolymer (by sequential addition of monomer) using ATRP is important. HPMA has previously been polymerised by ATRP (Teodorescu and Matyjaszewski 2000; Save *et al.* 2002; Weaver *et al.* 2004), and thus conditions would have to be investigated and optimised for its copolymerisation with DMAEM.

All of these three types of star-shaped copolymers would certainly present different physicochemical and biological properties, and thus would be interesting to synthesised, characterised both from a physicochemical point of view and biological one, as they are attractive for future development of novel polymeric carriers.

8.5. Evaluation of the radius of gyration (R_g) of cationic linear and star-shaped polymers by SANS

One interesting future perspective of this thesis is the study and characterisation of the size and shape of the synthesised cationic polymers, in respect to their composition (charge density), their architecture (linear or star-shaped), under various pH conditions (fully protonated or neutral). This can be investigated using SANS technique, considered as a method of choice for studying polymer conformation in solution due to its sensitivity (Wang *et al.* 2001; Paul *et al.* 2007).

Preliminary SANS experiments were carried out in collaboration with Dr. A. Paul on the LOQ time-of-flight diffractometer on ISIS at Rutherford Appleton Laboratories, Chilton, Didcot, Oxfordshire, UK.

Briefly, scattering studies were carried out under physiologically relevant conditions and also under extremes of pH in order to map the maximum possible change in polymer conformation expected in response to solution environment. Polymer solutions were prepared in D_2O at 1 wt% concentration, at different pHs, using either a deuterated PBS buffer, or 0.1 M HCl deuterated solution, and subsequent adjustment of the pH by addition of small quantities of deuterated NaOH solution. Samples were placed in 2 mm path length quartz cells, mounted in a sample changer thermostatted to T ± 0.2 °C. Data were corrected for the scattering and transmission of the solvent and cell, and placed on an absolute intensity scale with reference to a well-characterised polymer standard. Data were modelled using the FISH analysis developed by R K Heenan at ISIS, which uses a least-squares iterative fitting process to define model parameters. A model for polydisperse Gaussian coil was employed to provide a fitted value for the radius of gyration, R_g.

Table 8.2 summarises the characteristics of the polymers studied (composition, architecture, molecular weight and polydispersity), as well as the R_g estimated.

It was seen that the linear quaternized PqAEM (P 45) was slightly larger that the standard linear polymer (P 40), consistent with elongation of the polymer chain caused by the increased charge on the amine groups. The $DMAEM_{25}HPMA_{75}$ copolymer is of a generally comparable size, slightly smaller than the fully quaternized polymer PqAEM (P 45).

At low pH when the star polymers are fully charged, the two star polymers show the same size, indicating that with the chains in an extended state there is no steric hindrance due to the central core. However, at high pH in the uncharged state the 8-arm star polymer is larger than the 4-arm star polymer, suggesting that the chains are less able to fully collapse due to crowding at the core for the 8-arm star polymer.

This marked variation of size for the star-shaped polymers when a change in pH occurs, is of great interest, and these stimuli-responsive star-shaped polymers could be finding attractive applications in biomedical field, where changes in pHs could trigger further changes in the polymer, and its environment.

Table 8.2: Summary of the radius of gyration R_g estimated by SANS of selected polymers synthesised in these studies, with different composition, architecture and molecular weight characteristics

Polymer identification	Composition	Architecture	M_w (g.mol^{-1})	M_w/M_n	Solution	pH	T (°C)	R_g (nm ± 0.2 nm)
P 40	DMAEM	linear	19 100	2.60	PBS	7.4	37	3.5
P 45	qAEM	linear	36 530	3.35	PBS	7.4	37	4.0
P 36	$DMAEM_{25}HPMA_{75}$	linear	19 500	2.70	PBS	7.4	37	3.8
P 92	DMAEM	4-arm star polymer	42 900	1.59	0.1M HCl	3	25	19.1
P 92	DMAEM	4-arm star polymer	42 900	1.59	0.1M HCl	12	25	6.1
P 97	DMAEM	8-arm star polymer	40 200	1.63	0.1M HCl	3	25	18.8
P 97	DMAEM	8-arm star polymer	40 200	1.63	0.1M HCl	12	25	10.6

In conclusion, SANS technique can be intelligently used to get some insights on the size, conformation and behaviour of polymers in solution, which could in the future, help to understand the processes taking part in more complicated mechanisms, such as in biological environment. The results presented here were only preliminary and further characterisation of the synthesised polymers with SANS is being considered.

References

A-

Abuchowski, A.; Kazo, G.M.; Verhoest, C.R., Jr.; Van Es, T.; Kafkewitz, D.; Nucci, M.L.; Viau, A.T. and Davis, F.F. (1984). Cancer therapy with chemically modified enzymes. I. Antitumor properties of polyethylene glycol-asparaginase conjugates. Cancer Biochemistry Biophysics 7(2): 175-186.

Abuchowski, A.; McCoy, J.R.; Palczuk, N.C.; van Es, T. and Davis, F.F. (1977a). Effect of covalent attachment of polyethylene glycol on immunogenicity and circulating life of bovine liver catalase. The Journal of Biological Chemistry 252(11): 3582-3586.

Abuchowski, A.; van Es, T.; Palczuk, N.C. and Davis, F.F. (1977b). Alteration of immunological properties of bovine serum albumin by covalent attachment of polyethylene glycol. The Journal of Biological Chemistry 252(11): 3578-3581.

Ali, M. and Brocchini, S. (2006). Synthetic approaches to uniform polymers. Advanced Drug Delivery Reviews 58(15): 1671-1687.

Andersson, L.; Davies, J.; Duncan, R.; Ferruti, P.; Ford, J.; Kneller, S.; Mendichi, R.; Pasut, G.; Schiavon, O.; Summerford, C.; Tirk, A.; Veronese, F.M.; Vincenzi, V. and Wu, G. (2005). Poly(ethylene glycol)-poly(ester-carbonate) block copolymers carrying PEG-peptidyl-doxorubicin pendant side chains: synthesis and evaluation as anticancer conjugates. Biomacromolecules 6(2): 914-926.

Angot, S.; Murthy, K.S.; Taton, D. and Gnanou, Y. (2000). Scope of the Copper Halide/Bipyridyl System Associated with Calixarene-Based Multihalides for the Synthesis of Well-Defined Polystyrene and Poly(meth)acrylate Stars. Macromolecules 33: 7261-7274.

Angot, S.; Shanmugananda, M.; Taton, D. and Gnanou, Y. (1998). Atom Transfer Radical Polymerization of Styrene Using a Novel Octafunctional Initiator: Synthesis of Well-Defined Polystyrene Stars. Macromolecules 31: 7218-7225.

Antony, P.; Kwon, Y.; Puskas, J.E.; Kovar, M. and Norton, P.R. (2004). Atomic force microscopic studies of novel arborescent block and linear triblock polystyrene-polyisobutylene copolymers. European Polymer Journal 40: 149-157.

B-

Baldrick, P. (2000). Pharmaceutical excipient development: the need for preclinical guidance. Regulatory Toxicology and Pharmacology 32(2): 210-218.

Barnes, C.P.; Sell, S.A.; Boland, E.D.; Simpson, D.G. and Bowlin, G.L. (2007). Nanofiber technology: Designing the next generation of tissue engineering scaffolds. Advanced Drug Delivery Reviews 59(14): 1413-1433.

Berger, K. and Brandrup, G. (1989). Transfer Constants to Monomer, Polymer, Catalyst, Solvent, and Additive in Free Radical Polymerization. In: Polymer Handbook (3rd

Edition). J. Brandrup and E.H. Immergut, Eds. New York, John Wiley & Sons. pp 81-151.

Billingham, N.C. and Jenkins, A.D. (1972). The Chemical Structure of Polymers. In: Polymer Science, A Materials Science Handbook. Jenkins, A.D. Ed. Amsterdam and London; American Elsevier Publishing Company, New York, vol. 1. pp 121-191.

Boas, U. and Heegaard, P.M. (2004). Dendrimers in drug research. Chemical Society Reviews 33(1): 43-63.

Boesel, L.F. and Reis, R.L. (2007). A review on the polymer properties of Hydrophilic, partially Degradable and Bioactive acrylic Cements (HDBC). Progress in Polymer Science. Available online 25.09.07. doi:10.1016/j.progpolymsci.2007.09.001

Bontempo, D.; Li, R.C.; Ly, T.; Brubaker, C.E.; Maynard, H.D. (2005). One-step synthesis of low polydispersity, biotinylated poly(N-isopropylacrylamide) by ATRP. Chemical Communications 37: 4702-4704.

Bos, G.W.; Kanellos, T.; Crommelin, D.J.; Hennink, W.E. and Howard, C.R. (2004). Cationic polymers that enhance the performance of HbsAg DNA in vivo. Vaccine 23(4): 460-469.

Bos, G.W.; Trullas-Jimeno, A.; Jiskoot, W.; Crommelin, D.J. and Hennink, W.E. (2000). Sterilization of poly(dimethylamino) ethyl methacrylate-based gene transfer complexes. International Journal of Pharmaceutics 211(1-2): 79-88.

Boussif, O.; Lezoualc'h, F.; Zanta, M.A.; Mergny, M.D.; Scherman, D.; Demeneix, B. and Behr, J.P. (1995). A versatile vector for gene and oligonucleotide transfer into cells in culture and in vivo: polyethylenimine. Proceedings of the National Academy of Sciences of the United States of America 92(16): 7297-7301.

Brazeau, G.A.; Attia, S.; Poxon, S. and Hughes, J.A. (1998). In vitro myotoxicity of selected cationic macromolecules used in non-viral gene delivery. Pharmaceutical Research 15(5): 680-684.

Brocchini, S. and Duncan, R. (1999). Pendent Drugs, Release from Polymers. In: Encyclopedia of Controlled Drug Delivery. Mathiowitz, E. Ed. New York, Wiley Interscience. pp 786-816.

Bukowski, R.; Ernstoff, M.S.; Gore, M.E.; Nemunaitis, J.J.; Amato, R.; Gupta, S.K. and Tendler, C.L. (2002). Pegylated interferon alfa-2b treatment for patients with solid tumors: a phase I/II study. Journal of Clinical Oncology 20(18): 3841-3849.

Bulmus, V.; Ding, Z.; Long, C.J.; Stayton, P.S. and Hoffman, A.S. (2000). Site-Specific Polymer-Streptavidin Bioconjugate for pH-Controlled Binding and Triggered Release of Biotin. Bioconjugate Chemistry 11: 78-83.

Bulmus, V.; Woodward, M.; Lin, L.; Murthy, N.; Stayton, P. and Hoffman, A. (2003). A new pH-responsive and glutathione-reactive, endosomal membrane-disruptive

polymeric carrier for intracellular delivery of biomolecular drugs. Journal of Controlled Release 93(2): 105-120.

C-

Chapman, A.P.; Antoniw, P.; Spitali, M.; West, S.; Stephens, S. and King, D.J. (1999). Therapeutic antibody fragments with prolonged in vivo half-lives. Nature Biotechnology 17(8): 780-783.

Chen and Min (2001). Swelling kinetics and stimuli-responsiveness of poly(DMAEMA) hydrogels prepared by UV-irradiation. Radiation Physics and Chemistry 61: 65-68.

Chen, Y.; Shen, Z.; Barriau, E.; Kautz, H. and Frey, H. (2006). Synthesis of multiarm star poly(glycerol)-block-poly(2-hydroxyethyl methacrylate). Biomacromolecules 7(3): 919-926.

Cherng, J.Y.; van de Wetering, P.; Talsma, H.; Crommelin, D.J. and Hennink, W.E. (1996). Effect of size and serum proteins on transfection efficiency of poly ((2-dimethylamino)ethyl methacrylate)-plasmid nanoparticles. Pharmaceutical Research 13(7): 1038-1042.

Chiefari, J.; Chong, B.Y.K.; Ercole, F.; Krstina, J.; Jeffery, J.; Le, T.P.T.; Mayadunne, R.T.A.; Meijs, G.F.; Moad, C.L.; Moad, G.; Rizzardo, E. and Thang, S.H. (1998). Living Free-Radical Polymerization by Reversible Addition-Fragmentation Chain Transfer: The RAFT Process. Macromolecules 31: 5559-5562.

Chiefari, J. and Rizzardo, E. (2002). Control of Free-Radical Polymerization by Chain Transfer Methods. In: Handbook of Radical Polymerization. Matyjaszewski, K. and Davis, T.P. Eds. Wiley-Interscience. pp 629-690.

Choksakulnimitr, S.; Masuda, S.; Tokuda, H.; Takakura, Y. and Hashida, M. (1995). In vitro cytotoxicity of macromolecules in different cell culture systems. Journal of Controlled Release 34: 233-241.

Cloninger, M.J. (2002). Biological applications of dendrimers. Current Opinion in Chemical Biology 6: 742-748.

Cole, C.A.; Schreiner, S.M.; Priest, J.H.; Monji, N. and Hoffman, A.S. (1987). N-isopropylacrylamide and N-acryloxysuccinimide copolymer- A thermally reversible, water-soluble, activated polymer for protein conjugation. ACS Symposium Series 350: 245-254.

Colombani, D. and Chaumont, P. (1996). Addition-fragmentation processes in free radical polymerization. Progress in Polymer Science 21: 439-503.

Corner, T. (1984). Free-Radical Polymerization. The synthesis of graft-copolymers. Advances in Polymer Science 62: 95-142.

Cowan, J.D.; Von Hoff, D.D.; Neuenfeldt, B.; Mills, G.M. and Clark, G.M. (1984). "Predictive value of trypan blue exclusion viability measurements for colony formation in a human tumor cloning assay. Cancer Drug Delivery 1(2): 95-100.

Cowie, J.M.G. (1991). Polymers: Chemistry & Physics of Modern Materials (2nd Edition). Chapman, E. & Hall, W. Eds. Nelson Thornes Ltd. Cheltenham, UK.

D-

Danhauser-Riedl, S.; Hausmann, E.; Schick, H.D.; Bender, R.; Dietzfelbinger, H.; Rastetter, J. and Hanauske, A.R. (1993). Phase I clinical and pharmacokinetic trial of dextran conjugated doxorubicin (AD-70, DOX-OXD). Investigational New Drugs 11(2-3): 187-195.

Darling, T.R. (2000). Comments on Living Polymerization: Rationale for Uniform Terminology. Journal of Polymer Science, Part A: Polymer Chemistry 38 (10): 1710-1752.

Darling, T.R.; Davis, T.P.; Fryd, M.; Gridnev, A.A.; Haddleton, D.M.; Ittel, S.D.; Matheson, R.R.; Moad, G. and Rizzardo, E. (2000). Living polymerization: Rationale for uniform terminology. Journal of Polymer Science Part A: Polymer Chemistry 38(10): 1706-1708.

Davis, F.F. (2002). The Origin of Pegnology. Advanced Drug Delivery Reviews 54: 457-458.

De Duve, C.; De Barsy, T.; Poole, B.; Trouet, A.; Tulkens, P. and Van Hoof, F. (1974). Lysosomotropic agents. Biochemical Pharmacology 23(18): 2495-2531.

Dekie, L.; Toncheva, V.; Dubruel, P.; Schacht, E.H.; Barrett, L. and Seymour, L.W. (2000). Poly-L-glutamic acid derivatives as vectors for gene therapy. Journal of Controlled Release 65(1-2): 187-202.

Deng, G. and Chen, Y. (2004). A Novel Way To Synthesize Star Polymers in One Pot by ATRP of N-[2-(2-Bromoisobutyryloxy)ethyl]maleimide and Styrene. Macromolecules 37: 18-26.

Deng, G.; Ma, D. and Xu, Z. (2007). Synthesis of ABC-type miktoarm star polymers by "click" chemistry, ATRP and ROP. European Polymer Journal 43: 1179-1187.

Denizot, F. and Lang, R. (1986). Rapid colorimetric assay for cell growth and survival. Modifications to the tetrazolium dye procedure giving improved sensitivity and reliability. Journal of Immunological Methods 89(2): 271-277.

De Santis, R.; Ambrosio, L. and Nicolais, L. (2000). Polymer-based composite hip prostheses. Journal of Inorganic Biochemistry 79(1-4): 97-102.

De Smedt, S.; Demeester, J. and Hennink, W.E. (2000). Cationic Polymer Based Gene Delivery Systems. Pharmaceutical Research 17(2): 113-126.

De Vries, P.; Bhatt, R.; Stone, I.; Klein, P. and Singer, J.W. (2001). Optimization of CT-2106: A water-soluble poly-L-glutamic acid (PG)- camptothecin conjugate with enhanced in vivo anti-tumor efficacy. Proceedings AACR-NCI-EORTC international conference. Abstract 100.

Dhal, P.K.; Holmes-Farley, S.R.; Mandeville, W.H. and Neenan, T.X. (2002). Polymeric Drugs. In: Encyclopaedia of Polymer Science and Technology (3rd Edition). Wiley-VCH, New York. pp 555-580.

Dufès, C.; Uchegbu, I.F. and Schatzlein, A.G. (2005). Dendrimers in gene delivery. Advanced Drug Delivery Reviews 57: 2177-2202.

Duncan, R. (1992). Drug-polymer conjugates: potential for improved chemotherapy. Anti-Cancer Drugs 3: 175-210.

Duncan, R. (2002). Polymer-drug conjugates: Targeting cancer. In: Biomedical aspects of drug targeting. Muzykantov, V. and Torchilin, V. Eds. Norwell, MA, USA. Kluwer Academic Publishers. pp 193-209.

Duncan, R. (2003a). Polymer-Drug Conjugates. In: Handbook of Anticancer Drug Development. Budman, D.R.; Calvert, A.H. and Rowinsky, E.K. Eds. Baltimore, MD, USA. Lippincott Williams and Wilkins. pp 239-260.

Duncan, R. (2003b). The Dawning Era of Polymer Therapeutics. Nature Reviews- Drug Discovery 2: 347-360.

Duncan, R. (2004). Nanomedicines in action. The Pharmaceutical Journal 273: 485-488.

Duncan, R.; Bhakoo, M.; Riley, M.L. and Tuboku-Metzger, A. (1991). Soluble polymeric drug carriers: haematocompatibility. In: Progress in Membrane Biotechnology. Gomez-Fernandez, J.; Chapman, D. and Packer, L. Eds. Basel, Switzerland. Birkhauser Verlag. pp 121-129.

Duncan, R.; Connors, T.A. and Meada, H. (1996). Drug targeting in cancer therapy: the magic bullet, what next? Journal of Drug Targeting 3(5): 317-319.

Duncan, R.; Gilbert, H.R.P.; Carbajo, R.J. and Vicent, M.J. (*in press*). Polymer Masked-Unmasked Protein Therapy (PUMPT): 1. Bioresponsive dextrin-trypsin and -MSH conjugates designed for α-amylase activation. Biomacromolecules.

Duncan, R. and Izzo, L. (2005). Dendrimer biocompatibility and toxicity. Advanced Drug Delivery Reviews 57(15): 2215-2237.

Duncan, R. and Kopeček, J. (1984). Soluble Synthetic Polymers as Potential Drug Carriers. Advances in Polymer Science 57: 51-101.

Duncan, R.; Kopečková-Rejmanova, P.; Strohalm, J.; Hume, I.; Cable, H.C.; Pohl, J.; Lloyd, J.B. and Kopeček, J. (1987). Anticancer agents coupled to N-(2-hydroxypropyl)methacrylamide copolymers. I. Evaluation of daunomycin and puromycin conjugates in vitro. British Journal of Cancer 55: 165-174.

Duncan, R.; Lloyd, J.B. and Kopeček, J. (1980). Degradation of side chains of N-(2-hydroxypropyl) methacrylamide copolymers by lysosomal enzymes. Biochemical and Biophysical Research Communications 94(1): 284-290.

Duncan, R.; Seymour, L.C.W.; Scarlett, L.; Lloyd, J.B.; Rejmanova, P. and Kopeček, J. (1986). Fate of N-(2-hydroxypropyl)methacrylamide copolymers with pendent galactosamine residues after intravenous administration to rats. Biochimica et Biophysica Acta 880: 62-71.

Dvořák, M.; Kopečková, P. and Kopeček, J. (1999). High-molecular weight HPMA copolymer-adriamycin conjugates. Journal of Controlled Release 60(2-3): 321-332.

E-

Elias, H.-G. (1997). An Introduction to Polymer Science. Weinheim, Wiley-VCH.

El Sayed, M.; Ginski, M.; Rhodes, C. and Ghandehari, H. (2002). Transepithelial transport of poly(amidoamine) dendrimers across Caco-2 cell monolayer. Journal of Controlled Release 81: 355-365.

Evans, M.D.; McLean, K.M.; Hughes, T.C. and Sweeney, D.F. (2001). A review of the development of a synthetic corneal onlay for refractive correction. Biomaterials 22(24): 3319-3328.

F-

Fagnani, R.; Hagan, M.S. and Bartholomew, R. (1990). Reduction of immunogenicity by covalent modification of murine and rabbit immunoglobulins with oxidized dextrans of low molecular weight. Cancer Research 50(12): 3638-3645.

Ferguson, E.L.; Schmaljohann, D. and Duncan, R. (2006). Polymer-phospholipase conjugates as novel anti-cancer agents: dextrin-phospholipase A2. Proceedings of the 33rd International Symposium on Controlled Release of Bioactive Materials, Vienna, Austria. Abstract 660.

Fischer, D.; Bieber, T.; Li, Y.; Elsasser, H.P. and Kissel, T. (1999). A novel non-viral vector for DNA delivery based on low molecular weight, branched polyethylenimine: effect of molecular weight on transfection efficiency and cytotoxicity. Pharmaceutical Research 16(8): 1273-1279.

Fischer, D.; Li, Y.; Ahlemeyer, B.; Krieglstein, J. and Kissel, T. (2003). In vitro cytotoxicity testing of polycations: influence of polymer structure on cell viability and hemolysis. Biomaterials 24: 1121-1131.

Folkman, J. and Shing, Y. (1992). Angiogenesis. The Journal of Biological Chemistry 267: 10931-10934.

Förster, S. and Konrad, M. (2003). From self-organizing polymers to nano- and biomaterials. Journal of Materials Chemistry 13(11): 2671-2688.

Fotakis, G. and Timbrell, J.A. (2006). Role of trace elements in cadmium chloride uptake in hepatoma cell lines. Toxicology Letters 164(2): 97-103.

G-

Gaertner, H.F. and Offord, R.E. (1996). Site-specific attachment of functionalized poly(ethylene glycol) to the amino terminus of proteins. Bioconjugate Chemistry 7(1): 38-44.

Ganachaud, F.; Monteiro, M.J.; Gilbert, R.G.; Dourges, M.-A.; Thang, S.H. and Rizzardo, E. (2000). Molecular Weight Characterization of Poly(*N*-isopropylacrylamide) Prepared by Living Free-Radical Polymerization. Macromolecules 33: 6738-6745.

Gao, H. and Matyjaszewski, K. (2007). Arm-first method as a simple and general method for synthesis of miktoarm star copolymers. Journal of the American Chemical Society 129(38): 11828-11834.

Gebelein, C.G. and Carraher, C.E. Jr. (1985). Bioactive Polymeric Systems. An Overview. In: Encyclopedia of Polymer Science and Engineering, Vol. 2. Gross L. Ed. New York, Plenum Press.

Gebhart, C.L. and Kabanov, A.V. (2001). Evaluation of polyplexes as gene transfer agents. Journal of Controlled Release 73(2): 401-416.

Georges, M.K.; Veregin, R.P.N.; Kazmaier, P.M. and Hamer, G.K. (1993). Narrow Molecular-Weight Resins by a Free-Radical Polymerization Process. Macromolecules 26(11): 2987-2988.

Georgiou, T.K.; Phylactou, L.A. and Patrickios, C.S. (2006). Synthesis, characterization, and evaluation as transfection reagents of ampholytic star copolymers: effect of star architecture. Biomacromolecules 7(12): 3505-3512.

Georgiou, T.K.; Vamvakaki, M.; Patrickios, C.S.; Yamasaki, E.N. and Phylactou, L.A. (2004). Nanoscopic cationic methacrylate star homopolymers: synthesis by group transfer polymerization, characterization and evaluation as transfection reagents. Biomacromolecules 5(6): 2221-2229.

Gianasi, E.; Buckley, R.G.; Latigo, J.; Wasil, M. and Duncan, R. (2002). HPMA copolymers platinates containing dicarboxylato ligands. Preparation, characterisation and in vitro and in vivo evaluation. Journal of Drug Targeting 10(7): 549-556.

Gianasi, E.; Wasil, M.; Evagorou, E.G.; Keddle, A.; Wilson, G. and Duncan, R. (1999). HPMA copolymer platinates as novel antitumour agents: in vitro properties, pharmacokinetics and antitumour activity in vivo. European Journal of Cancer 35(6): 994-1002.

Godwin, A.; Hartenstein, M.; Müller, A.H.E.; Brocchini, S. (2001). Narrow Molecular Weight Distribution Precursors for Polymer-Drug Conjugates. Angewandte Chemie International Edition 113(3): 614-617.

Goto, A.; Sato, K.; Tsujii, Y.; Fukuda, T.; Moad, G.; Rizzardo, E. and Thang, S.H. (2001). Mechanism and kinetics of RAFT-based living radical polymerizations of styrene and methyl methacrylate. Macromolecules 34(3): 402-408.

Graham, M.L. (2003). Pegaspargase: a review of clinical studies. Advanced Drug Delivery Reviews 55(10): 1293-1302.

Greco, F.; Vicent, M.J.; Gee, S.; Jones, A.T.; Gee, J.; Nicholson, R.I. and Duncan, R. (2007). Investigating the mechanism of enhanced cytotoxicity of HPMA copolymer-Dox-AGM in breast cancer cells. Journal of Controlled Release 117: 28-39.

Greenley, R.Z. (1989). Free radical copolymerization reactivity ratios. In: Polymer Handbook (3rd Edition). J. Brandrup and E.H. Immergut, Eds. New York, John Wiley & sons. pp 153-266.

Greenwald, R.B. (2001). PEG drugs: an overview. Journal of Controlled Release 74(1-3): 159-171.

Greenwald, R.B.; Gilbert, C.W.; Pendri, A.; Conover, C.D.; Xia, J. and Martinez, A. (1996a). Drug delivery systems: water soluble taxol 2'-poly(ethylene glycol) ester prodrugs-design and in vivo effectiveness. Journal of Medicinal Chemistry 39(2): 424-431.

Greenwald, R.B.; Pendri, A.; Conover, C.; Gilbert, C.; Yang, R. and Xia, J. (1996b). Drug delivery systems. 2. Camptothecin 20-O-poly(ethylene glycol) ester transport forms. Journal of Medicinal Chemistry 39(10): 1938-1940.

Greenwald, R.B.; Pendri, A.; Martinez, A.; Gilbert, C. and Bradley, P. (1996c). PEG thiazolidine-2-thione, a novel reagent for facile protein modification: conjugation of bovine hemoglobin. Bioconjugate Chemistry 7(6): 638-641.

Guelcher, S.A. and Hollinger, J.O. (2005). An Introduction to Biomaterials (biomedical Engineering Series). Neuman , M.R. Ed. New York, USA. Taylor & Francis, CRC Press.

Gunzler, H. and Gremlich, H.-U. (2002). IR Spectroscopy: An Introduction (1st Edition). Weinheim, Germany. WILEY-VCH Verlag GmbH.

Guo, W. and Lee, R.J. (1999). Receptor-Targeted Gene Delivery ViaFolate-Conjugated Polyethylenimine. The American Association of Pharmaceutical Scientists Journal 1(4): 1-7.

Guu, J.A.; Hiuse, G.H. and Juang, T.M. (2002). Synthesis and biological properties of antitumor-active conjugates of ADR with dextran. Journal of Biomaterials Science Polymer Edition 13: 1135-1151.

H-

Haag, R. and Kratz, F. (2006). Polymer Therapeutics: Concepts and Applications. Angewandte Chemie International Edition 45: 1198-1215.

Hacioğlu, B.; Berchtold, K.A.; Lovell, L.G.; Nie, J. and Bowman, C.N. (2002). Polymerization kinetics of HEMA/DEGDMA: using changes in initiation and chain transfer rates to explore the effects of chain-length-dependent termination. Biomaterials 23(20): 4057-4064.

Haddleton, D.M.; Edmonds, R.; Heming, A.M.; Kelly, E.J. and Kukulj, D. (1999). Atom transfer polymerisation with glucose and cholesterol derived initiators. New Journal of Chemistry 23: 477-480.

Hadjichristidis, N. (1999). Synthesis of miktoarm star (μ-star) polymers." Journal of Polymer Science Part A: Polymer Chemistry 37(7): 857-871.

Hadjichristidis, N.; Pitsikalis, M.; Pispas, S. and Iatrou, H. (2001). Polymers with complex architecture by living anionic polymerization. Chemical Reviews 101(12): 3747-3792.

Hansen, N.M.; Jankova, K. and Hvilsted, S. (2007). Fluoropolymer materials and architectures prepared by controlled radical polymerizations. European Polymer Journal 43: 255-293.

Hardwicke, J.; Moseley, R.; Schmaljohann, D.; Stephens, P.; Ferguson, E.; Duncan, R. and Thomas, D.W. (2007). Bioresponsive dextrin-EGF conjugates designed to promote tissue regeneration in impaired human wound healing. International Symposium on Polymer Therapeutics, ISPT07. Berlin, Germany. Abstract 44.

Harris, J.M. (1992). Poly(ethylene glycol) chemistry; Biotechnical and biomedical Applications. Katritzky, A.R. and Sabongi, G.J. Eds. New York, USA. Plenum Publishing Corporation.

Harris, J.M. and Chess, R.B. (2003). Effect of Pegylation on Pharmaceuticals. Nature Reviews Drug Discovery 2: 214-221.

Hatada, K. (1999). Trends in Polymer Science Uniform polymers. Progress in Polymer Science 24: 1405-1408.

Hatada, K.; Kitayama, T.; Ute, K. and Nishiura, T. (2004). Synthetic Uniform Polymers and Their Use for Understanding Fundamental Problems in Polymer Chemistry. Macromolecular Rapid Communications 25(16): 1447-1477.

Hawker, C. and Fréchet, J. (1990). Preparation of Polymers with Controlled Molecular Architecture: A New Convergent Approach to Dendritic Macromolecules. Journal of American Chemical Society 112: 7638-7647.

Hawker, C.J.; Hedrick, J.L.; Malmström, E.E.; Trollsås, M.; Mecerreyes, D.; Moineau, G.; Dubois, P. and Jérôme, R. (1998). Dual Living Free Radical and Ring Opening Polymerizations from a Double-Headed Initiator. Macromolecules 31(2): 213-219.

Hawthorne, D.G.; Moad, G.; Rizzardo, E. and Thang, S.H. (1999). Living radical polymerization with reversible addition-fragmentation chain transfer (RAFT): Direct ESR observation of intermediate radicals. Macromolecules 32(16): 5457-5459.

Heath, F.; Haria, P. and Alexander, C. (2007). Varying Polymer Architecture to Deliver Drugs. The American Association of Pharmaceutical Scientists Journal 9(2): E235-E240.

Heijl and Du Prez (2004). Fast, multi-responsive microgels based on photo-crosslinkable poly(2-(dimethylamino)ethyl methacrylate). Polymer 45: 6771-6778.

Heise, A.; Hedrick, J.L.; Trollsas, M.; Miller, R.D. and Frank, C.W. (1999). Novel starlike poly(methyl methacrylate)s by controlled dendritic free radical initiation. Macromolecules 32: 231-234.

Heise, A.; Nguyen, C.; Malek, R.; Hedrick, J.L.; Frank, C.W. and Miller, R.D. (2000). Starlike polymeric architectures by atom transfer radical polylmerization: templates for the production of low dielectric constant thin films. Macromolecules 33: 2346-2354.

Hobson, L.J. and Feast, W.J. (1999). Poly(amidoamine) hyperbranched systems: synthesis, structure and characterization. Polymer 40: 1279-1297.

Hoffman, A.S. (1987). Applications of thermally reversible polymers and hydrogels in therapeutics and diagnotics. Journal of Controlled Release 6: 297-305.

Hoffman, A.S. (1995). Intelligent Polymers in Medicine and Biotechnology. Artificial Organs 19(5): 458-467.

Hoffman, A.S. and Stayton, P.S. (2007). Conjugates of stimuli-responsive polymers and proteins. Progress in Polymer Science 32: 922-932.

Hong, K.; Uhrig, D. and Mays, J.W. (1999). Living anionic polymerization. Current Opinion in Solid State and Materials Science 4(6): 531-538.

Hoste, K.; De Winne, K. and Schacht, E. (2004). Polymeric prodrugs. International Journal of Pharmaceutics 277: 119-131.

Howard, K.A.; Dash, P.R.; Read, M.L.; Ward, K.; Tomkins, L.M.; Nazarova, O.; Ulbrich, K. and Seymour, L.W. (2000). Influence of hydrophilicity of cationic polymers on the biophysical properties of polyelectrolyte complexes formed by self-assembly with DNA. Biochimica et Biophysica Acta 1475(3): 245-255.

Howard, K.A.; Li, X.W.; Somavarapu, S.; Singh, J.; Green, N.; Atuah, K.N.; Ozsoy, Y.; Seymour, L.W. and Alpar, H.O. (2004). Formulation of a microparticle carrier for oral polyplex-based DNA vaccines. Biochimica et Biophysica Acta 1674(2): 149-157.

Hreczuk-Hirst, D.; Chicco, D.; German, L. and Duncan, R. (2001). Dextrins as potential carriers for drug targeting: tailored rates of dextrin degradation by introduction of pendant groups. International journal of pharmaceutics 230(1-2): 57-66.

Huang, P.S. and Oliff, A. (2001). Drug-targeting strategies in cancer therapy. Current Opinion in Genetics & Development 11: 104-110.

Hui, H.; Xiao-dong, F. and Zhong-lin, C. (2005). Thermo- and pH-sensitive dendrimer derivatives with a shell of poly(N,N-dimethylaminoethyl methacryalte) and study of their controlled drug release behavior. Polymer 46: 9514-9522.

J-

Jatzkewitz, H. (1954). Incorporation of physiologically-active substances into a colloidal blood plasma substitute. I. Incorporation of mescaline peptide into polyvinylpyrrolidone. Hoppe-Seyler's Zeitschrift fur physiologische Chemie 297(3-6): 149-156.

Jevprasesphant, R.; Penny, J.; Jalal, R.; Attwood, D.; McKeown, N.B. and D'Emanuele, A. (2003). The influence of surface modification on the cytotoxicity of PAMAM dendrimers. International Journal of Pharmaceutics 252(1-2): 263-266.

Jiang, X.; Xia, P.; Liu, W. and Yan, D. (2000). Atom transfer radical copolymerization of styrene and N-cyclohexylmaleinimide. Journal of Polymer Science, Part A: Polymer Chemistry 38: 1203-1209.

K-

Kabanov, A.V. (1999). Taking polycation gene delivery systems from *in vitro* to *in vivo*. Pharmaceutical Science & Technology Today 2(9): 365-372.

Kabanov, A.V. and Alakhov, V.Y. (1994). New approaches to targeting bioactive compounds. Journal of Controlled Release 28: 15-35.

Kabanov, A.V. and Kabanov, V.A. (1995). DNA Complexes with Polycations for the Delivery of Genetic Material into Cells. Bioconjugate Chemistry 6: 7-20.

Kabanov, A.V.; Sergeev, V.G.; Foster, M.S.; Kasaikin, V.A.; Levashov, A.V. and Kabanov, V.A. (1995a). Polyelectrolytes and oppositely Charged Surfactants in Organics Solvents: From Reversed Micelles to Soluble Polymer-Surfactant Complexes. Macromolecules 28: 3657-3663.

Kabanov, A.V.; Vinogradov, S.V.; Suzdaltseva, Y.G. and Alakhov, V.Y. (1995b). Water-Soluble Block Polycations as Carriers for Oligonucleotide Delivery. Bioconjugate Chemistry 6(6): 640-643.

Kakizawa, Y. and Kataoka, K. (2002). Block copolymer micelles for delivery of gene and related compounds. Advanced Drug Delivery Reviews 54(2): 203-222.

Kamei, S. and Kopeček, J. (1995). Prolonged blood circulation in rats of nanospheres surface-modified with semitelechelic poly[N-(2-hydroxypropyl)methacrylamide]. Pharmaceutical Research 12(5): 663-668.

Kamigaito, M.; Ando, T. and Sawamoto, M. (2001). Metal-catalyzed living radical polymerization. Chemical Reviews 101(12): 3689-3746.

Karasch, N. (1979). Trace Metals in Health and Disease: New Roles of Metals in Biochemistry, the Environmental and Clinical/Nutritional Studies. Kharasch, N. Ed. New York, Raven Press.

Karchalsky, A.; Danon, D. and Nevo, A. (1959). Interactions of basic polyelectrolytes with the red blood cell. II. Agglutination of red blood cells by polymeric bases. Biochimica et Biophysica Acta 33(1): 120-138.

Kasko, A.; Heintz, A. and Pugh, C. (1998). The effect of molecular weight architecture on the thermotropic behavior of poly(11-(4'-cyanophenyl-4"-phenoxy)undecyl acrylate) and its relation to polydispersity. Macromolecules 31: 256-271.

Kato, M.; Kamigaito, M.; Sawamoto, M. and Higashimura, T. (1995). Polymerization of Methyl-Methacrylate with the Carbon-Tetrachloride Dichlorotris(Triphenylphosphine)Ruthenium(II) Methylaluminum Bis(2,6-Di-Tert-Butylphenoxide) Initiating System - Possibility of Living Radical Polymerization. Macromolecules 28(5): 1721-1723.

Kean, T.; Roth, S. and Thanou, M. (2005). Trimethylated chitosans as non-viral gene delivery vectors: Cytotoxicity and transfection efficiency. Journal of Controlled Release 103(3): 643-653.

Kircheis, R.; Wightman, L. and Wagner, E. (2001). Design and gene delivery activity of modified polyethylenimines. Advanced Drug Delivery Reviews 53(3): 341-358.

Koňák, Č.; Mrkvičková, L.; Nazarova, O.; Ulbrich, K. and Seymour, L.W. (1998). Formation of DNA complexes with diblock copolymers of poly(N-(2-hydroxypropyl)methacrylamide) and polycations. Supramolecular Science 5(1-2): 67-74.

Kopeček, J. and Bazilova, H. (1973). Poly[N-(2-Hydroxypropyl)methacrylamide]. I-Radical Polymerization and copolymerization. European Polymer Journal 9: 7-14.

Kopeček, J.; Cifkova, I.; Rejmanova, P.; Strohalm, J.; Obereigner, B. and Ulbrich, K. (1981). Polymers Containing Enzymatically Degradable Bonds. Preliminary Experiments in vivo. Makromolekulare Chemie 182: 2941-2949.

Korovkin, B.F.; Eshina, E.F. and Predtechenskii, A.N. (1963). Colorimetric method of determining serum lactic dehydrase (lactate dehydrogenase) and its use in clinical practice. Laboratornoe delo 9: 17-20.

Kudelka, A.P.; Verschraegen, C.F.; Loyer, E.; Wallace, S.; Gershenson, D.M.; Han, J.; Ho, L.; Garzone, P.D.; Warner, M.; Bolton, M.G. and Kavanagh, J.J. (2002). Preliminary report of a phase I study of escalating dose PG-paclitaxel (CT-2103) and fixed dose cisplatin in patients with solid tumors. Proceedings of the American Society Of Clinical Oncology 21. Abstract 2146.

Kumazawa, E. and Ochi, Y. (2004). DE-310, a novel macromolecular carrier system for the camptothecin analogue DX-8951f: potent antitumor activities in various murine tumor models. Cancer Science 95(2): 168-175.

Kunath, K.; von Harpe, A.; Fischer, D.; Petersen, H.; Bickel, U.; Voigt, K. and Kissel, T. (2003). Low-molecular-weight polyethylenimine as a non-viral vector for DNA delivery: comparison of physicochemical properties, transfection efficiency and in vivo distribution with high-molecular-weight polyethylenimine. Journal of Controlled Release 89(1): 113-125.

L-

Lavignac, N.; Lazenby, M.; Foka, P.; Malgesini, B.; Verpilio, I.; Ferruti, P. and Duncan, R. (2004). Synthesis and endosomolytic properties of poly(amidoamine) block copolymers. Macromolecular Bioscience 4(10): 922-929.

Lecolley, F.; Waterson, C.; Carmichael, A.J.; Mantovani, G.; Harrisson, S.; Chappell, H.; Limer, A.; Williams, P.; Ohno, K. and Haddleton, D.M. (2003). Synthesis of functional polymers by living radical polymerisation. Journal of Materials Chemistry 13: 2689-2695.

Lee, J.H.; Kopečková, P.; Kopeček, J. and Andrade, J.D. (1990). Surface properties of copolymers of alkyl methacrylates with methoxy (polyethylene oxide) methacrylates and their application as protein-resistant coatings. Biomaterials 11(7): 455-464.

Lee, K.Y. and Yuk, S.H. (2007). Polymeric protein delivery systems. Progress in Polymer Science 32: 669-697.

Levy, Y.; Hershfield, M.S.; Fernandez-Mejia, C.; Polmar, S.H.; Scudiery, D.; Berger, M. and Sorensen, R.U. (1988). Adenosine deaminase deficiency with late onset of recurrent infections: response to treatment with polyethylene glycol-modified adenosine deaminase. The Journal of Pediatrics 113(2): 312-317.

Li, Y.; Tang, Y.; Narain, R.; Lewis, A.L. and Armes, S.P. (2005). Biomimetic Stimulus-Responsive Star Diblock Gelators. Langmuir 21: 9946-9954.

Li, C.; Yu, D.F.; Newman, R.A.; Cabral, F.; Stephens, L.C.; Hunter, N.; Milas, L. and Wallace, S. (1998). Complete regression of well-established tumors using a novel water-soluble poly(L-glutamic acid)-paclitaxel conjugate. Cancer Research 58(11): 2404-2409.

Li, Y.; Armes, S.P.; Jin, X. and Zhu, S. (2003). Direct synthesis of well-defined quaternized homopolymers and diblock copolymers via ATRP in protic media. Macromolecules 36: 8268-8275.

Limer, A.J.; Rullay, A.K.; San Miguel, V.; Peinado, C.; Keely, S.; Fitzpatrick, E.; Carrington, S.D.; Brayden, D. and Haddleton, D.M. (2006). "Fluorescently tagged star polymers by living radical polymerisation for mucoadhesion and bioadhesion. Reactive & Functional Polymers 66: 51-64.

Liu, S.-Q.; Yang, Y.-Y.; Liu, X.-M. and Tong, Y.-W. (2003). Preparation and Characterization of Temperature-Sensitive Poly(N-isopropylacrylamide)-b-poly(D,L-lactide) Microspheres for Protein Delivery. Biomacromolecules 4: 1784-1793.

Lu, Z.-R.; Kopečková, P. and Kopeček, J. (2000). Semitelechelic Poly[N-(2-hydroxypropyl)-methacrylamide] for Biomedical Applications. In: Polymeric Drugs & Drug Delivery Systems. Ottenbrite, R.M. and Kim, S.W. Eds. New York, USA. Taylor & Francis CRC Press. pp 1-14.

Lu, Z.-R.; Kopečková, P.; Wu, Z. and Kopeček, J. (1998). Functionalized Semitelechelic Poly[N-(2 hydroxypropyl)methacrylamide] for Protein Modification. Bioconjugate Chemistry 9: 793-804.

Lu, Z.-R.; Kopečková, P.; Wu, Z. and Kopeček, J. (1999). Synthesis of semitelechelic poly[N-(2-hydroxypropyl)methacrylamide] by radical polymerization in the presence of alkyl mercaptans. Macromolecular Chemistry and Physics 200: 2022-2030.

M-

Ma, P.X. (2008). Biomimetic materials for tissue engineering. Advanced Drug Delivery Reviews 60(2): 184-198.

MacLaughlin, F.C.; Mumper, R.J.; Wang, J.; Tagliaferri, J.M.; Gill, I.; Hinchcliffe, M. and Rolland, A.P. (1998). Chitosan and depolymerized chitosan oligomers as condensing carriers for in vivo plasmid delivery. Journal of Controlled Release 56: 259-272.

Maeda, H. (1994). Polymer conjugated macromolecular drugs for tumor-specific targeting. In: Polymer site-specific Pharmacotherapy. Domb, A.J. Ed. New York, UAS. John Wiley and Sons Ltd. pp. 95-116.

Maeda, H. (2001). The Enhanced Permeability and Retention (EPR) Effect in Tumor Vasculature: The Key Role of Tumor-Selective Macromolecular Drug Targeting. Advances in Enzyme Regulation 41: 189-207.

Maeda, H. and Konno, T. (1997). Metamorphosis of Neocarzinostatin to SMANCS: Chemistry, Biology, Pharmacology, and Clinical Effect of the First Prototype Anticancer Polymer Therapeutic. In: Neocarzinostatin: The Past, Present and Future of an Anticancer Drug. Maeda, H.; Edo, K. and Ishida, N. Ed. New York, USA. Springer-Verlag New York, Inc. pp 227-267.

Malik, N.; Wiwattanapatapee, R.; Klopsch, R.; Lorenz, K.; Frey, H.; Weener, J.W.; Meijer, E.W.; Paulus, W. and Duncan, R. (2000). Dendrimers: Relationship between structure and biocompatibility *in vitro*, and preliminary studies on the biodistribution of 125-I-labelled polyamidoamine dendrimers *in vivo*. Journal of Controlled Release 65: 133-148.

Malmström, E. and Hult, A. (1997). Hyperbranched Polymers: A Review. Journal of Macromolecular Science C37(3): 555-579.

March, J. (1992). Aliphatic Nucleophilic Substitution: Nitrogen Nucleophiles. In: Advanced Organic Chemistry: Reaction, Mechanisms and Structure. March, J. Ed. New York, John Wiley & Sons. pp 417-418.

Matsukata, M.; Aoki, T.; Sanui, K.; Ogata, N.; Kikuchi, A.; Sakurai, Y. and Okano, T. (1996). Effect of molecular architecture of poly(N-isopropylacrylamide)-trypsin conjugates on their solution and enzymatic properties. Bioconjugate Chemistry 7(1): 96-101.

Matsumura, Y. and Maeda, H. (1986). A new concept for macromolecular therapeutics in cancer chemotherapy: mechanism of tumoritropic accumulation of proteins and the antitumor agent Smancs. Cancer Research 46: 6387-6392.

Matyjaszewski, K. (1997). Controlled Radical Polymerization. Washington DC, American Chemical Society.

Matyjaszewski, K. (2002). From Atom Transfer Radical Addition to Atom Transfer Radical Polymerisation. Current Organic Chemistry 6: 67-82.

Matyjaszewski, K. (2003). Advances in Controlled/Living Radical Polymerization. Washington DC, American Chemical Society.

Matyjaszewski, K.; Miller, P.J.; Pyun, J.; Kickelbick, G. and Diamanti, S. (1999). Synthesis and characterization of star polymers with varying arm number, length, and composition from organic and hybrid inorganic/organic multifunctional initiators. Macromolecules 32: 6526-6535.

Matyjaszewski, K. and Xia, J. (2001). Atom transfer radical polymerization. Chemical Reviews 101(9): 2921-2990.

Mayadunne, R.T.A.; Jeffery, J.; Moad, G. and Rizzardo, E. (2003). Living Free Radical Polymerization with Reversible Addition-Fragmentation Chain Transfer (RAFT Polymerization): Approaches to Star Polymers. Macromolecules 36: 1505-1513.

McCarthy, T.D.; Karellas, P.; Henderson, S.A.; Giannis, M.; O'Keefe, D.F.; Heery, G.; Paull, J.R.; Matthews, B.R. and Holan, G. (2005). Dendrimers as drugs: discovery and preclinical and clinical development of dendrimer-based microbicides for HIV and STI prevention. Molecular Pharmaceutics 2(4): 312-318.

Mehvar, R. (2000). Dextrans for targeted and sustained delivery of therapeutic and imaging agents. Journal of Controlled Release 69: 1-25.

Mellman, I. (1996). Endocytosis and molecular sorting. Annual Review of Cell and Developmental Biology 12: 575-625.

Moghimi, S.M.; Hunter, A.C. and Murray, J.C. (2005). Nanomedicine: current status and future prospects. The FASEB Journal 19(3): 311-330.

Monji, N. and Hoffman, A.S. (1987). A novel immunoassay system and bioseparation process based on thermal phase separating polymers. Applied Biochemistry and Biotechnology 14(2): 107-120.

Morgan, D.M.; Clover, J. and Pearson, J.D. (1988). Effects of synthetic polycations on leucine incorporation, lactate dehydrogenase release, and morphology of human umbilical vein endothelial cells. Journal of Cell Science 91 (Pt 2): 231-238.

Morgan, D.M.; Larvin, V.L. and Pearson, J.D. (1989). Biochemical characterisation of polycation-induced cytotoxicity to human vascular endothelial cells. Journal of Cell Science 94 (Pt 3): 553-559.

Morgan, S.M.; Surbr, V.; Ulbrich, K.; Woodley, J.F. and Duncan, R. (1996). Evaluation of N-(2-hydroxypropyl)methacrylamide copolymer-peptide conjugates as potential oral vaccines. Studies on their degradation by isolated rat small intestinal peptidases on their degradation by isolated rat small intestinal peptidases and their uptake by adult rat small intestinal tissue in vitro. International Journal of Pharmaceutics 128: 99-111.

Mosmann, T. (1983). Rapid colorimetric assay for cellular growth and survival: application to proliferation and cytotoxicity assays. Journal of Immunological Methods 65(1-2): 55-63.

Mukherjee, A.; Trainer, P.; Monson, J. and Shalet, S. (2002). How to optimise pegvisomant treatment of acromegaly safely? Endocrine Abstracts 4: OC8.

N-

Nakagawa, Y.; Miller, P.J. and Matyjaszewski, K. (1998). Development of novel attachable initiators for atom transfer radical polymerization. Synthesis of block and graft copolymers from poly(dimethylsiloxane) macroinitiators. Polymer 39(21): 5163-5170.

Narrainen, A.P.; Pascual, S. and Haddleton, D.M. (2002). Amphiphilic Diblock, Triblock, and Star Block Copolymers by Living Radical Polymerization: Synthesis and Aggregation Behavior. Journal of Polymer Science Part A: Polymer Chemistry 40: 439-450.

Neu, M.; Fischer, D. and Kissel, T. (2005). Recent advances in rational gene transfer vector design based on poly(ethylene imine) and its derivatives. The Journal of Gene Medicine 7(8): 992-1009.

Nevo, A.; De Vries, A. and Karchalsky, A. (1955). Interaction of basic polyamino acids with the red blood cell. I. Combination of polylysine with single cells. Biochimica et Biophysica Acta 17(4): 536-547.

Nicolson, P.C. and Vogt, J. (2001). Soft contact lens polymers: an evolution. Biomaterials 22(24): 3273-3283.

O-

O'Brien, J.L. and Gornick, F. (1955). Chain transfer in the polymerization of methyl methacrylate. I. Transfer with monomer and thiols. The mechanism of termination reaction at 60°. Journal of American Chemical Society 77: 4757-4763.

Odian, G. (1991). Radical Chain Polymerization. In: Principles of Polymerization. New York, John Wiley & Sons, Inc. pp 198-355.

Oguma, T.; Morikawa, H.; Iwasaki, D. and Atsumi, R. (2005). Validation study of a method for assaying DE-310, a macromolecular carrier conjugate containing an anti-tumor camptothecin derivative, and the free drug in tumor tissue by high performance liquid chromatography/atmospheric pressure chemical ionization tandem mass spectrometry. Biomedical Chromatography 19(1): 19-26.

O'Hare, K.B.; Duncan, R.; Strohalm, J.; Ulbrich, K. and Kopečková, P. (1993). Polymeric drug-carriers containing doxorubicin and melanocyte-stimulating hormone: in vitro and in vivo evaluation against murine melanoma. Journal of Drug Targeting 1(3): 217-229.

Ohno, K.; Wong, B. and Haddleton, D.M. (2001). Synthesis of well-defined cyclodextrin-core star polymers. Journal of Polymer Science Part A-Polymer Chemistry 39(13): 2206-2214.

Omidi, Y.; Hollins, A.J.; Benboubetra, M.; Drayton, R.; Benter, I.F. and Akhtar, S. (2003). Toxicogenomics of Non-viral Vectors for Gene Therapy: A Microarray Study of Lipofectin- and Oligofectamine- induced Gene Expression Changes in Human Epithelial Cells. Journal of Drug Targeting 11(6): 311-323.

Otsu, T. and Yoshida, M. (1982). Role of Initiator-Transfer Agent-Terminator (Iniferter) in Radical Polymerizations - Polymer Design by Organic Disulfides as Iniferters. Makromolekulare Chemie-Rapid Communications 3(2): 127-132.

Otsu, T.; Yoshida, M. and Tazaki, T. (1982). A Model for Living Radical Polymerization. Makromolekulare Chemie-Rapid Communications 3(2): 133-140.

Oupický, D.; Howard, K.A.; Koňák, C.; Dash, P.R.; Ulbrich, K. and Seymour, L.W. (2000a). Steric stabilization of poly-L-Lysine/DNA complexes by the covalent attachment of semitelechelic poly[N-(2-hydroxypropyl)methacrylamide]. Bioconjugate Chemistry 11(4): 492-501.

Oupický, D.; Koňák, C.; Dash, P.R.; Seymour, L.W. and Ulbrich, K. (1999b). Effect of albumin and polyanion on the structure of DNA complexes with polycation containing hydrophilic nonionic block. Bioconjugate Chemistry 10(5): 764-772.

Oupický, D.; Koňák, C. and Ulbrich, K. (1999c). DNA complexes with block and graft copolymers of N-(2-hydroxypropyl)methacrylamide and 2-(trimethylammonio)ethyl methacrylate. Journal of Biomaterials Science 10(5): 573-590.

Oupický, D.; Koňák, C.; Ulbrich, K.; Wolfert, M.A. and Seymour, L.W. (2000b). DNA delivery systems based on complexes of DNA with synthetic polycations and their copolymers. Journal of Controlled Release 65(1-2): 149-171.

Oupický, D.; Ulbrich, K. and Rihova, B. (1999a). Conjugates of semitelechelic poly(n-(2-hydroxypropyl)methacrylamide) with enzymes for protein delivery. Journal of Bioactive and Compatible Polymers 14: 213-231.

P-

Painter, P.C. and Coleman, M.M. (1997). Molecular Weight and Branching. In: Fundamentals of Polymer Science. An Introductory Text (2nd Edition). Painter, P.C. and Coleman, M.M. Eds. Boca Raton, CRC Press LLC. pp 339-394.

Patten, T. and Matyjaszewski, K. (1998). Atom-transfer radical polymerization and the synthesis of polymeric materials. Advanced Materials 10: 901-915.

Paul, A.; Vicent, M.J. and Duncan, R. (2007). Using Small-Angle Neutron Scattering to Study the Solution Conformation of N-(2-Hydroxypropyl)methacrylamide Copolymer-Doxorubicin Conjugates. Biomacromolecules 8(5): 1573-1579.

Peng, L.; Wang, B. and Ren, P. (2005). Reduction of MTT by flavonoids in the absence of cells. Colloids and Surfaces B: Biointerfaces 45(2): 108-111.

Percec, V.; Barboiu, B.; Bera, T.K.; van der Sluis, M.; BGrubbs, R.B. and Fréchet, J.M.J. (2000). Designing functional aromatic multisulfonyl chloride initiators for complex organic synthesis by living radical polymerization. Journal of Polymer Science Part A: Polymer Chemistry 38: 4776-4791.

Petersen, H.; Fechner, P.M.; Martin, A.L.; Kunath, K.; Stolnik, S.; Roberts, C.J.; Fischer, D.; Davies, M.C. and Kissel, T. (2002). Polyethylenimine-graft-poly(ethylene glycol) copolymers: influence of copolymer block structure on DNA complexation and biological activities as gene delivery system. Bioconjugate Chemistry 13(4): 845-854.

Pruden, E.L. and Winstead, M.E. (1964). Accuracy Control of Blood Cell Counts with the Coulter Counter. The American Journal of Medical Technology 30: 1-35.

Q-

Qiu, L.Y. and Bae, Y.H. (2006). Polymer Architecture and Drug Delivery. Pharmaceutical Research 23(1): 1-30.

Quinn, J.F.; Rizzardo, E. and Davis, T.P. (2001). Ambient temperature reversible addition-fragmentation chain transfer polymerisation. Chemical Communications (11): 1044-1045.

Quirk, R.P.; Youngjoon, L. and Kim, J. (1999). Synthesis of Branched Polymers: An Introduction. Star and Hyperbranched polymers. Mishra, M.K.and Kobayashi, S. Eds. New York, Marcel Dekker. pp 1-25.

R-

Rajender Reddy, K.; Modi, M.W. and Pedder, S. (2002). Use of Peg-interferon alfa-2a (40 KD) (Pegasys) for the treatment of hepatitis C. Advanced Drug Delivery Reviews 54(4): 571-586.

Richardson, S.C.; Kolbe, H.V. and Duncan, R. (1999). Potential of low molecular mass chitosan as a DNA delivery system: biocompatibility, body distribution and ability to complex and protect DNA. International Journal of Pharmaceutics 178(2): 231-243.

Richardson, S.C.; Pattrick, N.G.; Man, Y.K.; Ferruti, P. and Duncan, R. (2001). Poly(amidoamine)s as potential nonviral vectors: ability to form interpolyelectrolyte complexes and to mediate transfection in vitro. Biomacromolecules 2(3): 1023-1028.

Ringsdorf, H. (1975). Structure and properties of pharmacologically active polymers. Journal of Polymer Science: Polymer Symposium 51: 135-153.

Ringsdorf, H. (2004). Hermann Staudinger and the Future of Polymer Research- Jubilees-Beloves Occasions for Cultural Piety. Angewandte Chemie International Edition 43: 1064-1076.

Roberts, J.C.; Bhalgat, M.K. and Zera, R.T. (1996). Preliminary biological evaluation of polyamidoamine (PAMAM) Starburst dendrimers. Journal of Biomedical Materials Research 30(1): 53-65.

Robinson, B.; Sullivan, F.; Borzelleca, J. and Schwarts, S. (1990). A Critical Review of the Kinetics and Toxicology of Polyvinylpyrrolidone (Povidone). Chelsea, Michigan, USA. Lewis Publishers Inc.

Roehm, N.W.; Rodgers, G.H.; Hatfield, S.M. and Glasebrook, A.L. (1991). An improved colorimetric assay for cell proliferation and viability utilizing the tetrazolium salt XTT. Journal of Immunological Methods 142(2): 257-265.

Rossi, A.; Poverini, R.; Di Lullo, G.; Modesti, A.; Modica, A. and Scarino, M. (1996). Heavy metal toxicity following apical and basolateral exposure in the human intestinal cell line Caco-2. Toxicology in vitro 10: 27-36.

Rungsardthong, U.; Deshpande, M.; Bailey, L.; Vamvakaki, M.; Armes, S.P.; Garnett, M.C. and Stolnik, S. (2001). Copolymers of amine methacrylate with poly(ethylene glycol) as vectors for gene therapy. Journal of Controlled Release 73: 359-380.

Ryser, H.J. (1967). A membrane effect of basic polymers dependent on molecular size. Nature 215(5104): 934-936.

S-

Sabbatini, P.; Brown, J.; Aghajanian, C.; Hensley, M.L.; Pezzulli, S.; O'Flaherty, C.; Lovegren, M.; Funt, S.; Warner, M.; Mitchell, P.; Bolton, M.G.; Spriggs, D. and Duggan, B. (2002). A phase I/II study of PG-paclitaxel (CT-2103) in patients (pts) with recurrent ovarian, fallopian tube, or peritoneal cancer. Proceedings of the American Society Of Clinical Oncology 21. Abstract 871.

Satchi-Fainaro, R.; Duncan, R. and Barnes, C.M. (2006). Polymer Therapeutics for Cancer: Current Status and Future Challenges. Advanced Polymer Science 193: 1-65.

Save, M.; Weaver, J. and Armes, S. (2002). Atom Transfer Radical Polymerization of Hydroxy-Functional Methacrylates at Ambient Temperature: Comparison of Glycerol Monomethacrylate with 2-Hydroxypropyl Methacrylate. Macromolecules 35: 1152-1159.

Schild, H.G. (1992). Poly(*N*-Isopropylacrylamide): Experiment, Theory and Application. Progress in Polymer Science 17: 163-249.

Schluep, T.; Cheng, J.; Khin, K.T. and Davis, M.E. (2006a). Pharmacokinetics and biodistribution of the camptothecin-polymer conjugate IT-101 in rats and tumor-bearing mice. Cancer chemotherapy and pharmacology 57(5): 654-662.

Schluep, T.; Hwang, J.; Cheng, J.; Heidel, J.D.; Bartlett, D.W.; Hollister, B. and Davis, M.E. (2006b). Preclinical efficacy of the camptothecin-polymer conjugate IT-101 in multiple cancer models. Clinical Cancer Research 12(5): 1606-1614.

Schmaljohann, D.; Oswald, J.; Jorgensen, B.; Nitschke, M.; Beyerlein, D. and Werner, C. (2003). Thermo-responsive Hydrogels for Controlled Cell Adhesion and Detachment. Biomacromolecules 4: 1733-1739.

Schoemaker, N.E.; van Kesteren, C.; Rosing, H.; Jansen, S.; Swart, M.; Lieverst, J.; Fraier, D.; Breda, M.; Pellizzoni, C.; Spinelli, R.; Grazia Porro, M.; Beijnen, J.H.; Schellens, J.H. and ten Bokkel Huinink, W.W. (2002). A phase I and pharmacokinetic study of MAG-CPT, a water-soluble polymer conjugate of camptothecin. British Journal of Cancer 87(6): 608-614.

Schulz, J.; Burris, H.A.; Redfern, C.; Mitchell, P.; Warner, M. and Bolton, M.G. (2002). Phase II study of CT-2103 in patients with colorectal cancer having recurrent disease after treatment with a 5-fluorouracil-containing regimen. Proceedings of the American Society Of Clinical Oncology 22. Abstract 1137.

Schwertschlag, U.S. (2007). Pharmacokinetics of a novel camptothecin conjugate (MER-1001) in the rat and dog. American Association for Cancer Research Annual Meeting: Proceedings, Los Angeles, CA., Philadelphia (PA): AACR.Abstract 4723.

Seib, F.P.; Jones, A.T. and Duncan, R. (2007). Comparison of the endocytic properties of linear and branched PEIs, and cationic PAMAM dendrimers in B16f10 melanoma cells. Journal of Controlled Release 117(3): 291-300.

Sershen, S. and West, J. (2002). Implantable, polymeric systems for modulated drug delivery. Advanced Drug Delivery Reviews 54(9): 1225-1235.

Seth, R.; Yang, S.; Choi, S.; Sabean, M. and Roberts, E.A. (2004). In vitro assessment of copper-induced toxicity in the human hepatoma line, Hep G2. Toxicology in vitro 18(4): 501-509.

Seymour, L.W.; Ferry, D.R.; Anderson, D.; Hesslewood, S.; Julyan, P.J.; Poyner, R.; Doran, J.; Young, A.M.; Burtles, S. and Kerr, D.J. (2002). Hepatic Drug Targeting: Phase I Evaluation of Polymer-Bound Doxorubicin. Journal of Clinical Oncology 20(6): 1668-1676.

Seymour, L.W.; Ulbrich, K.; Steyger, P.S.; Brereton, M.; Subr, V.; Strohalm, J. and Duncan, R. (1994). Tumour tropism and anti-cancer efficacy of polymer-based doxorubicin prodrugs in the treatment of subcutaneous murine B16F10 melanoma. British Journal of Cancer 70(4): 636-641.

Sgouras, D. and Duncan, R. (1990). Methods for the evaluation of biocompatibility of soluble synthetic polymers which have potential for biomedical use: 1- Use of the tetrazolium- based colorimetric assay (MTT) as a preliminary screen for evaluation ofin vitro cytotoxicity. Journal of Materials Science: Materials in Medicine 1(2): 61-68.

Shaffer, S.A.; Baker Lee, C.; Nudelman, E.; Kumar, A.; Coon, M.; Stone, I.; De Vries, P. and Singer, J.W. (2002). Metabolism of poly-L-glutamic acid (PG) paclitaxel (CT-2103); proteolysis by lysosomal cathepsin B and identification of intermediate metabolites. Proceedings of the American Association for Cancer Research 43, 2067.

Shemper, B.S.; Acar, E. and Mathias, L.J. (2002). Synthesis of Linear and Starlike Polymers from Poly(propylene glycol) Methacrylate Using Controlled Radical Polymerisation. Journal of Polymer Science, Part A: Polymer Chemistry 40: 334-343.

Shen, Y.; Zhu, S.; Zeng, F.; Pelton, R. (2000). Versatile Initiators for Macromonomer Syntheses of Acrylates, Methacrylates, and Styrene by Atom Transfer Radical Polymerization. Macromolecules 33: 5399-5404.

Shoemaker, S.G.; Hoffman, A.S. and Priest, J.H. (1987). Synthesis and properties of vinyl monomer/enzyme conjugates. Conjugation of L-asparaginase with N-succinimidyl acrylate. Applied Biochemistry and Biotechnology 15(1): 11-24.

Silverstein, R.M.; Bassler, C.G. and Morrill, T.C. (1981a). ^{13}C NMR Spectrometry. In: Spectrometric Identification of Organics Compounds. Silverstein, R.M. Ed. New York, John Wiley & Sons. pp 249-303.

Silverstein, R.M.; Bassler, C.G. and Morrill, T.C. (1981b). Proton Magnetic Resonance Spectrometry. In: Spectrometric Identification of Organic Compounds. Silverstein, R.M. Ed. New York, John Wiley & Sons. pp 181-247.

Singer, J.W. (2005). Paclitaxel poliglumex (XYOTAX, CT-2103): a macromolecular taxane. Journal of Controlled Release 109(1-3): 120-126.

Singer, J.W.; Baker, B.; De Vries, P.; Kumar, A.; Shaffer, S.; Vawter, E.; Bolton, M. and Garzone, P. (2003). Poly-(L)-glutamic acid-paclitaxel (CT-2103) [XYOTAX], a biodegradable polymeric drug conjugate: characterization, preclinical pharmacology, and preliminary clinical data. Advances in Experimental Medicine and Biology 519: 81-99.

Singer, J.W.; Shaffer, S.; Baker, B.; Bernareggi, A.; Stromatt, S.; Nienstedt, D. and Besman, M. (2005). Paclitaxel poliglumex (XYOTAX; CT-2103): an intracellularly targeted taxane. Anti-cancer Drugs 16(3): 243-254.

Singh, A.K.; Kasinath, B.S. and Lewis, E.J. (1992). Interaction of polycations with cell-surface negative charges of epithelial cells. Biochimica et Biophysica Acta 1120(3): 337-342.

Slater, T.F.; Sawyer, B. and Straeuli, U. (1963). Studies on Succinate-Tetrazolium Reductase Systems. Iii. Points of Coupling of Four Different Tetrazolium Salts. Biochimica et Biophysica Acta 77: 383-393.

Sludden, J.; Boddy, A.V.; Griffin, M.J.; Robson, L.; Todd, R.; Cassidy, J.; Bissett, D.; Main, M.; Brannan, M.D.; Elliott, S.; Verrill, M. and Calvert, H. (2001). Phase I and Pharmacological Study of CT-2103, a Poly(L-glutamic acid)-Paclitaxel Conjugate. Proceedings of the American Association for Cancer Research 42, 2883.

Solomon, D.H.; Rizzardo, E. and Cacioli, P. (1986). Polymerization process and polymers produced thereby. United States Patents 4581429. Commonwealth Scientific and Industrial Research Organization.

Sprincl, L.; Exner, J.; Sterba, O. and Kopeček, J. (1976). New types of synthetic infusion solutions. III. Elimination and retention of poly-[N-(2-hydroxypropyl)methacrylamide] in a test organism. Journal of Biomedical Materials Research 10(6): 953-963.

Subr, V.; Koňák, C.; Laga, R. and Ulbrich, K. (2006). Coating of DNA/poly(L-lysine) complexes by covalent attachment of poly[N-(2-hydroxypropyl)methacrylamide]. Biomacromolecules 7(1): 122-130.

Suzuki, F.; Daikuhara, Y.; Ono, N. and Takeda, Y. (1972). Studies on the mode of insulin: properties and biological activity of an insulin-dextran complex. Endocrinology 90(5): 1220-1230.

Svenson, S. and Tomalia, D.A. (2005). Dendrimers in biomedical applications-reflections on the field. Advanced Drug Delivery Reviews 57(15): 2106-2129.

T-

Tack, F.; Bakker, A.; Maes, S.; Dekeyser, N.; Bruining, M.; Elissen-Roman, C.; Janicot, M.; Brewster, M.; Janssen, H.M.; De Waal, B.F.; Fransen, P.M.; Lou, X. and Meijer, E.W. (2006a). Modified poly(propylene imine) dendrimers as effective transfection agents for catalytic DNA enzymes (DNAzymes). Journal of Drug Targeting 14(2): 69-86.

Tack, F.; Bakker, A.; Maes, S.; Dekeyser, N.; Bruining, M.; Elissen-Roman, C.; Janicot, M.; Janssen, H.M.; De Waal, B.F.; Fransen, P.M.; Lou, X.; Meijer, E.W.; Arien, A. and Brewster, M.E. (2006b). Dendrimeric poly(propylene-imines) as effective delivery agents for DNAzymes: dendrimer synthesis, stability and oligonucleotide complexation. Journal of Controlled Release 116(2): e24-e26.

Tack, F.; Bakker, A.; Maes, S.; Dekeyser, N.; Bruining, M.; Elissen-Roman, C.; Janicot, M.; Janssen, H.M.; De Waal, B.F.; Fransen, P.M.; Lou, X.; Meijer, E.W.; Arien, A. and Brewster, M.E. (2006c). Dendrimeric poly(propylene-imines) as effective delivery

agents for DNAzymes: toxicity, in vitro transfection and in vivo delivery. Journal of Controlled Release 116(2): e26-e28.

Takahashi, K.; Ajima, A.; Yoshimoto, T. and Inada, Y. (1984). Polyethylene glycol-modified catalase exhibits unexpectedly high activity in benzene. Biochemical and Biophysical Research Communications 125(2): 761-766.

Takashina, K.; Kitamura, K.; Yamaguchi, T.; Noguchi, A.; Noguchi, A.; Tsurumi, H. and Takahashi, T. (1991). Comparative pharmacokinetic properties of murine monoclonal antibody A7 modified with neocarzinostatin, dextran and polyethylene glycol. Japanese Journal of Cancer Research 82(10): 1145-1150.

Takei, Y.G.; Aoki, T.; Sanui, K.; Ogata, N.; Okano, T. and Sakurai, Y. (1993a). Temperature-responsive bioconjugates. 1. Synthesis of temperature-responsive oligomers with reactive end groups and their coupling to biomolecules. Bioconjugate Chemistry 4(1): 42-46.

Takei, Y.G.; Aoki, T.; Sanui, K.; Ogata, N.; Okano, T. and Sakurai, Y. (1993b). Temperature-responsive bioconjugates. 2. Molecular design for temperature-modulated bioseparations. Bioconjugate Chemistry 4(5): 341-346.

Takei, Y.G.; Aoki, T.; Sanui, K.; Ogata, N.; Sakurai, Y. and Okano, T. (1995). Temperature-modulated platelet and lymphocyte interactions with poly(N-isopropylacrylamide)-grafted surfaces. Biomaterials 16(9): 667-673.

Takei, Y.G.; Matsukata, M.; Aoki, T.; Sanui, K.; Ogata, N.; Kikuchi, A.; Sakurai, Y. and Okano, T. (1994). Temperature-responsive bioconjugates. 3. Antibody-poly (N-isopropylacrylamide) conjugates for temperature-modulated precipitations and affinity bioseparations. Bioconjugate Chemistry 5(6): 577-582.

Tang, G.P.; Zeng, J.M.; Gao, S.J.; Ma, Y.X.; Shi, L.; Li, Y.; Too, H.P. and Wang, S. (2003). Polyethylene glycol modified polyethylenimine for improved CNS gene transfer: effects of PEGylation extent. Biomaterials 24(13): 2351-2362.

Teodorescu, M. and Matyjaszewski, K. (1999). Atom Transfer Radical Polymerization of (Meth)acrylamides. Macromolecules 32: 4826-4831.

Teodorescu, M. and Matyjaszewski, K. (2000). Controlled polymerization of (meth)acrylamides by atom transfer radical polymerization. Macromolecular Rapid Communication 21: 190-194.

Terwogt, J.M.M.; Huinink, W.W.t.B.; Schellens, J.H.; Schot, M.; Mandjes, I.A.; Zurlo, M.G.; Rocchetti, M.; Rosing, H.; Koopman, F.J. and Beijnen, J.H. (2001). Phase I clinical and pharmacokinetic study of PNU166945, a novel water-soluble polymer-conjugated prodrug of paclitaxel. Anti-Cancer Drugs 12: 315-323.

Thanou, M. and Duncan, R. (2003). Polymer-protein and polymer-drug conjugates in cancer therapy. Current Opinion in Investigational Drugs 4(6): 701-709.

Thanou, M.; Florea, B.I.; Geldof, M.; Junginger, H.E. and Borchard, G. (2002). Quaternized chitosan oligomers as novel gene delivery vectors in epithelial cell lines. Biomaterials 23: 153-159.

Themistou, E. and Patrickios, C.S. (2007). Synthesis and characterization of amphiphilic star copolymers of 2-(dimethylamino)ethyl methacrylate and methyl methacrylate: Effects of architecture and composition. European Polymer Journal 43: 84-92.

Thoren, L. (1980). The dextrans--clinical data. Developments in Biological Standardization 48: 157-167.

Tomalia, D.A.; Baker, H.; Dewald, J.; Hall, M.; Kallos, G.; Martin, S.; Roeck, J.; Ryder, J. and Smith, P. (1985). A New Clas of Polymers: Starburst-Dendritic Macromolecules. Polymer Journal 17(1): 117-132.

Tomalia, D.A.; Naylor, A.M. and Goddard III, W.A. (1990). Starburst Dendrimers: Molecular-Level Control of Size, Shape, Surface Chemistry, Topology, and Flexibility from Atoms to Macroscopic Matter. Angewandte Chemie International Edition 29: 138-175.

Tomalia, D.A.; Reyna, L.A. and Svenson, S. (2007). Dendrimers as multi-purpose nanodevices for oncology drug delivery and diagnostic imaging. Biochemical Society transactions 35(Pt 1): 61-67.

Tomihata, K.; Suzuki, M.; Oka, T. and Ikada, Y. (1998). A new resorbable monofilament suture. Polymer Degradation and Stability 59: 13-18.

Tomlinson, R.; Heller, J.; Brocchini, S. and Duncan, R. (2003). Polyacetal-doxorubicin conjugates designed for pH-dependent degradation. Bioconjugate Chemistry 14(6): 1096-1106.

Trouet, A.; Deprez-de Campeneere, D. and De Duve, C. (1972). Chemotherapy through lysosomes with a DNA-daunorubicin complex. Nature: New biology 239(91): 110-112.

Tsunoda, S.; Kamada, H.; Yamamoto, Y.; Ishikawa, T.; Matsui, J.; Koizumi, K.; Kaneda, Y.; Tsutsumi, Y.; Ohsugi, Y.; Hirano, T. and Mayumi, T. (2000). Molecular design of polyvinylpyrrolidone-conjugated interleukin-6 for enhancement of in vivo thrombopoietic activity in mice. Journal of Controlled Release 68(3): 335-341.

Twaites, B.; de las Heras Alarcòn, C. and Alexander, C. (2005). Synthetic polymers as drugs and therapeutics. Journal of Materials Chemistry 15: 441-455.

Twentyman, P.R. and Luscombe, M. (1987). A study of some variables in a tetrazolium dye (MTT) based assay for cell growth and chemosensitivity. British Journal of Cancer 56(3): 279-285.

U-

Ueda, J.; Kamigaito, M. and Sawamoto, M. (1998). Calixarene-Core Multifunctional Initiators for the Ruthenium-Mediated Living Radical Polymerization of Methacrylates. Macromolecules 31: 6762.

UKCCCR (2000). UKCCCR guidelines for the use of cell lines in cancer research. British Journal of Cancer 82(9): 1495-1509.

V-

Vamvakaki, M.; Unali, G.; Bütün, V.; Boucher, S.; Robinson, K.; Billingham, N. and Armes, S. (2001). Effect of Partial Quaternization on the Aqueous Solution Properties of Tertiary Amine-Based Polymeric Surfactants: Unexpected Separation of Surface Activity and Cloud Point Behavior. Macromolecules 34(20): 6839-6841.

van de Wetering, P. (1999). Gene delivery with cationic polymers: Synthesis, characterization and biological evaluation of poly(2-(dimethylamino)ethyl methacrylate) and related polymers. PhD Thesis. Department of Pharmaceutics. Utrecht, Utrecht: 176.

van de Wetering, P.; Cherng, J.Y.; Talsma, H.; Crommelin, D.J. and Hennink, W.E. (1998a). 2-(Dimethylamino)ethyl methacrylate based (co)polymers as gene transfer agents. Journal of Controlled Release 53(1-3): 145-153.

van de Wetering, P.; Zuidam, N.J.; van Steenbergen, M.J.; van der Houwen, O.A.G.J.; Underberg, W.J.M. and Hennink, W.E. (1998b). A mechanistic study of the hydrolytic stability of poly(2-(dimethylamino)ethyl methacrylate). Macromolecules 31: 8063-8068.

van de Wetering, P.; Cherng, J.Y.; Talsma, H. and Hennink, W.E. (1997). Relation between transfection efficiency and cytotoxicity of poly(2-(dimethylamino)ethyl methacrylate)/plasmid complexes. Journal of Controlled Release 49(1): 59-69.

van de Wetering, P.; Moret, E.E.; Schuurmans-Nieuwenbroek, N.M.; van Steenbergen, M.J. and Hennink, W.E. (1999). Structure-activity relationships of water-soluble cationic methacrylate/methacrylamide polymers for nonviral gene delivery. Bioconjugate Chemistry 10(4): 589-597.

Vasey, P.A.; Kaye, S.B.; Morrison, R.; Twelves, C.; Wilson, P.; Duncan, R.; Thomson, A.H.; Murray, L.S.; Hilditch, T.E.; Murray, T.; Burtles, S.; Fraier, D.; Frigerio, E. and Cassidy, J. (1999). Phase I Clinical and Pharmacokinetics Study of PK1 (*N*-(2-Hydroxypropyl)methacrylamide Copolymer Doxorubicin): First Member of a New Class of Chemotherapeutic Agents-Drug-Polymer Conjugates. Clinical Cancer Research 5: 83-94.

Veronese, F.M. (2001). Peptide and protein PEGylation: a review of problems and solutions. Biomaterials 22(5): 405-417.

Veronese, F.M. and Pasut, G. (2005). PEGylation, successful approach to drug delivery. Drug Discovery Today 10(21): 1451-1458.

Veronese, F.M.; Schiavon, O.; Pasut, G.; Mendichi, R.; Andersson, L.; Tsirk, A.; Ford, J.; Wu, G.; Kneller, S.; Davies, J. and Duncan, R. (2005). PEG-Doxorubicin Conjugates: Influence of Polymer Structure on Drug Release, in Vitro Cytotoxicity, Biodistribution, and Antitumor Activity. Bioconjugate Chemistry 16: 775-784.

Viau, L.; Even, M.; Maury, O.; Haddleton, D.M. and Le Bozec, H. (2005). Synthesis of star-shaped metallo-polymeric chromophores by atom transfer radical polymerization. Comptes Rendus Chimie 8: 1298-1307.

Vicent, M.J. and Duncan, R. (2006). Polymer conjugates: nanosized medicines for treating cancer. TRENDS in Biotechnology 24(1): 39-47.

Vicent, M.J.; Manzanaro, S.; de la Fuente, J.A. and Duncan, R. (2004a). HPMA copolymer-1,5-diazaanthraquinone conjugates as novel anticancer therapeutics. Journal of Drug Targeting 12(8): 503-515.

Vicent, M.J. and Perez-Paya, E. (2006). Poly-L-glutamic acid (PGA) aided inhibitors of apoptotic protease activating factor 1 (Apaf-1): an antiapoptotic polymeric nanomedicine. Journal of Medicinal Chemistry 49(13): 3763-3765.

Vicent, M.J.; Tomlinson, R.; Brocchini, S. and Duncan, R. (2004b). Polyacetal-diethylstilboestrol: a polymeric drug designed for pH-triggered activation. Journal of Drug Targeting 12(8): 491-501.

Vistica, D.T.; Skehan, P.; Scudiero, D.; Monks, A.; Pittman, A. and Boyd, M.R. (1991). Tetrazolium-based assays for cellular viability: a critical examination of selected parameters affecting formazan production. Cancer Research 51(10): 2515-2520.

Vögtle, F. (2000). Dendrimers II: Architecture, Nanostructure and Supramolecular Chemistry.(Topics in Current Chemistry). Berlin Heidelberg New York. Springer-Verlag.

W-

Wagner, E. (2004). Strategies to improve DNA polyplexes for in vivo gene transfer: Will "artificial viruses" be the answer? Pharmaceutical Research 21: 8-14.

Wan, K.W.; Malgesini, B.; Verpilio, I.; Ferruti, P.; Griffiths, P.C.; Paul, A.; Hann, A.C. and Duncan, R. (2004). Poly(amidoamine) salt form: effect on pH-dependent membrane activity and polymer conformation in solution. Biomacromolecules 5(3): 1102-1109.

Wang, J.S.; Greszta, D. and Matyjaszewski, K. (1995). Atom-transfer radical polymerization (ATRP) - a new approach towards well-defined (co)polymers. Polymeric Materials Science Engineering 73: 416.

Wang, D.; Kopečková, P.; Minko, T.; Nanayakkara, V. and Kopeček, J. (2000). Synthesis of Starlike N-(2-Hydroxypropyl)methacrylamide Copolymers: Potential Drug Carriers. Biomacromolecules 1: 313-319.

Wang, D.; Lal, J.; Moses, D.; Bazan, G.C. and Heeger, A.J. (2001). Small angle neutron scattering (SANS) studies of a conjugated polyelectrolyte in aqueous solution. Chemical Physics Letters 348: 411-415.

Wang, D.; Li, W.; Pechar, M.; Kopečková, P.; Bromme, D. and Kopeček, J. (2004a). Cathepsin K inhibitor-polymer conjugates: potential drugs for the treatment of osteoporosis and rheumatoid arthritis. International Journal of Pharmaceutics 277(1-2): 73-79.

Wang, X.S.; Luo, N. and Ying, S.K. (1999). Synthesis of EPDM-g-PMMA through atom transfer radical polymerization. Polymer 40(16): 4515-4520.

Wang, J.S. and Matyjaszewski, K. (1995a). Controlled Living Radical Polymerization - Atom-Transfer Radical Polymerization in the Presence of Transition-Metal Complexes. Journal of the American Chemical Society 117(20): 5614-5615.

Wang, J.S. and Matyjaszewski, K. (1995b). Controlled/"Living" Radical Polymerization. Halogen Atom Transfer Radical Polymerization Promoted by a Cu(I)/Cu(II) Redox Process. Macromolecules 28: 7901-7910.

Wang, Y.X.; Robertson, J.L.; Spillman, W.B., Jr. and Claus, R.O. (2004b). Effects of the chemical structure and the surface properties of polymeric biomaterials on their biocompatibility. Pharmaceutical Research 21(8): 1362-1373.

Wang, P.; Sergeeva, M.V.; Lim, L. and Dordick, J.S. (1997). Biocatalytic plastics as active and stable materials for biotransformations. Nature Biotechnology 15(8): 789-793.

Wang, Y.S.; Youngster, S.; Grace, M.; Bausch, J.; Bordens, R. and Wyss, D.F. (2002). Structural and biological characterization of pegylated recombinant interferon alpha-2b and its therapeutic implications. Advanced Drug Delivery Reviews 54(4): 547-570.

Watson, P.; Jones, A.T. and Stephens, D.J. (2005). Intracellular trafficking pathways and drug delivery: fluorescence imaging of living and fixed cells. Advanced Drug Delivery Reviews 57(1): 43-61.

Weaver, J.; Bannister, I.; Robinson, K.; Brories-Azeau, X.; Armes, S.; Smallridge, M. and McKenna, P. (2004). Stimulus-Responsive Water-Soluble Polymers Based on 2-Hydroxyethyl Methacrylate. Macromolecules 37: 2395-2403.

Wei, C.; Lyubchenko, Y.L.; Ghandehari, H.; Hanes, J.; Stebe, K.J.; Mao, H.Q.; Haynie, D.T.; Tomalia, D.A.; Foldvari, M.; Monteiro-Riviere, N.; Simeonova, P.; Nie, S.; Mori, H.; Gilbert, S.P. and Needham, D. (2006). New technology and clinical applications of nanomedicine: highlights of the second annual meeting of the American Academy of Nanomedicine (Part I). Nanomedicine 2(4): 253-263.

Wiwattanapatapee, R.; Carreño-Gomez, B.; Malik, N. and Duncan, R. (2000). Anionic PAMAM Dendrimers Rapidly Cross Adult Rat Intestine *In Vitro*: A Potential Oral Delivery System? Pharmaceutical Research 17(8): 991-998.

Wu, X.Y.; Pelton, R.H.; Tam, K.C.; Woods, D.R. and Hamielec, A.E. (1993). Poly(*N*-isopropylacrylamide). I. Interactions with the sodium dodecyl-sulfate measured by conductivity. Journal of Polymer Science, Part A: Polymer Chemistry 31(4): 957-962.

X-

Xyloyiannis, M.; Padilla de Jesus, O.; Frechet, J. and Duncan, R. (2003). PEG-dendron architecture influences endocytic capture and intracellular trafficking. Proceedings of the 30th International Symposium on Controlled Release of Bioactive Materials.

Y-

Ydens, I.; Moins, S.; Degée, P.; Dubois, P. (2005). Solution properties of well-defined 2-(dimethylamino)ethyl methacrylate-based (co)polymers: a viscometric approach. European Polymer Journal 41: 1502-1509.

Yoo, M.; Heise, A.; Hedrick, J.L.; Miller, R.D. and Curtis, F.W. (2003). Photophysical Characterization of Conformational Rearrangements for Amphiphilic 6-Arm Star Block Copolymers in Selective Solvent Mixtures. Macromolecules 36: 268-271.

Young, R.J. and Lovell, P.A. (1991). Gel Permeation Chromatography. In: Introduction to Polymers (2nd Edition). Young, R.J. and Lovell, P.A. Eds. London, Chapman & Hall. pp 211-221.

Yurkovetskiy, A.; Papisov, M.; Fischman, A.J.; Hiller, A.; Yin, M.; Rolke, J.; Harrison, S.D.; Ball, R.; Sheridan, K.; Hollister, B.; Napier, C.; Schwertschlag, U.S.; Leone, P.B.; Olson, J.A. and Petter, R.C. (2007). MER-1001, a novel polymeric prodrug of camptothecin, is a potent inhibitor of LS174 and A2780 human tumor xenografts in a mouse model. American Association for Cancer Research Annual Meeting: Proceedings, Los Angeles, CA., Philadelphia (PA): AACR. Abstrat 781

Z-

Zalipsky, S. (1995). Functionalized poly(ethylene glycol) for preparation of biologically relevant conjugates. Bioconjugate Chemistry 6(2): 150-165.

Zeng, F.; Shen, Y.; Zhu, S.; Pelton, R. (2000a). Atom Transfer Radical Polymerization of 2-(Dimethylamino)ethyl Methacrylate in Aqueous Media. Journal of Polymer Science Part A: Polymer Chemistry 38: 3821-3827.

Zeng, F.; Shen, Y.; Zhu, S.; Pelton, R. (2000b). Synthesis and Characterization of Comb-Branched Polyelectrolytes. 1. Preparation of Cationic Macromonomer of 2-(Dimethylamino)ethyl Methacrylate by Atom Transfer Radical Polymerisation. Macromolecules 33: 1628-1635.

Zhang, X.; Xia, J.; Matyjaszewski, K. (1998). Controlled/"Living" Radical Polymerization of 2-(Dimethylamino)ethyl Methacrylate. Macromolecules 31(15): 5167-5169.

Zhao, Y.; Chen, Y.; Chen, C. and Xi, F. (2005). Synthesis of well-defined star polymers and star copolymers from dendrimer initiators by atom transfer radical polymerisation. Polymer 46: 5808-5819.

Zinselmeyer, B.H.; Mackay, S.P.; Schatzlein, A.G. and Uchegbu, I.F. (2002). The lower-generation polypropylenimine dendrimers are effective gene-transfer agents. Pharmaceutical research 19(7): 960-967.

Website addresses

http://www.wiley.co.uk/genmed/clinical.

http://www.chem.cmu.edu/groups/maty/about/research/02.html.

Appendix

Abstracts for poster presentations:

Dieudonné L., Schmaljohann, D. (2006). Synthesis of star polymers as polymer therapeutics. *Macro Group UK International Conference on Polymer Synthesis Warwick, UK.*

Dieudonné L., Pohl V., Jones A.J., Schmaljohann, D. (2006). Controlled synthesis strategies for the preparation of tailor-made polymer therapeutics. *Proceedings of the International Symposium of Controlled Release of Bioactive Materials*, **33**, 907.

Dieudonné L., Schmaljohann, D. (2005). Synthesis of amine-based polycations as models for novel gene delivery agents: systematic variation of structural parameters. *Proceedings of the International Symposium of Controlled Release of Bioactive Materials*, **32**, 401.

Dieudonné L., Schmaljohann, D. (2005). Synthesis and characterisation of amine-based polymers as models for novel gene delivery agents. *2nd Max Bergmann Symposium, focused on Polymer Science, Dresden, Germany.*

Abstracts for oral presentations:

Dieudonné L., Schmaljohann, D. (2006). Synthesis of star polymers as polymer therapeutics. *Postgraduate Research Day, Welsh School of Pharmacy, Cardiff University, Cardiff, Wales, UK.*

Dieudonné L., Schmaljohann, D. (2005). Designing novel polymer therapeutics: from free radical polymerisation to controlled polymerisation techniques. *EPSRC Platform Grant Seminar Series, Chemistry Department, Cardiff University, Cardiff, Wales, UK.*

Publications in progress:

Dieudonné L., Rickard J., Schmaljohann, D. Systematic variation of structural parameters of amine-based polycations as models for novel gene delivery agents: the use of Chain Transfer Agent in Free Radical Polymerisation.

Dieudonné L., Schmaljohann, D. Synthesis and characterisation of novel star-shaped poly(dimethylaminoethyl methacrylate) by Atom Transfer Radical Polymerisation with both stable and degradable multifunctional initiators.

Dieudonné L., Paul A., Schmaljohann, D. Characterisation of the solution behaviours of star-shaped polycations by Small Angle Neutron Scattering.